STUDY OF SOME HOMOGENEOUS AND ISOTROPIC COSMOLOGICAL MODELS IN THE PERSPECTIVE OF DYNAMICAL SYSTEM ANALYSIS

by

SOUMYA CHAKRABORTY

THIS THESIS IS SUBMITTED IN PARTIAL FULFILMENT OF THE REQUIREMENTS

FOR THE AWARD OF THE DEGREE OF

DOCTOR OF PHILOSOPHY IN SCIENCE

Department of Mathematics

Jadavpur University

Kolkata 700032, West Bengal, India

June, 2024

JADAVPUR UNIVERSITY
FACULTY OF SCIENCE
DEPARTMENT OF MATHEMATICS
KOLKATA- 700032, INDIA

CERTIFICATE FROM THE SUPERVISOR

This is to certify that the thesis entitled "**Study of some homogeneous and isotropic cosmological models in the perspective of dynamical system analysis**" submitted by **Soumya Chakraborty**, who got his name registered on March 22, 2021 (Index No.: 33/21/Maths./27) for the award of Ph.D. (Science) degree of Jadavpur University, is absolutely based upon his own work under my supervision and that neither this thesis nor any part of it has been submitted for either any degree/diploma or any other academic award anywhere before.

Subenoy Chakraborty

Prof. Subenoy Chakraborty
(Ph.D. thesis Supervisor)
Department of Mathematics
Jadavpur University
Kolkata- 700032, India
21/06/2024

Professor
DEPARTMENT OF MATHEMATICS
Jadavpur University
Kolkata – 700 032, West Bengal

DECLARATION BY THE AUTHOR

I hereby declare that the thesis is based on my own work carried out at the Department of Mathematics, Jadavpur University, Kolkata- 700032, India. Also, I declare that, no part of it has not been submitted for any degree/diploma/some other qualification at any other University.

All the figures presented in this thesis have been produced by the author using Mathematica and Matlab software. The thesis has been checked several times with extreme care to free it from all discrepancies and typos. Even then the vigilant readers may find some mistakes, and, several portions of this thesis may seem unwarranted or mistaken or incorrect. The author takes the sole responsibility for these unwanted errors which have resulted from his inadequate knowledge in the subject or escaped his notice.

Finally, I state that, to the best of my knowledge, all the assistance taken to prepare this thesis have been properly cited and acknowledged.

Soumya Chakraborty

Soumya Chakraborty

21/06/2024

To

My parents

Malati Chakraborty,

and

Sudarshan Chakraborty

ABSTRACT

The thesis consists of seven chapters. First chapter contains the introduction about dynamical system analysis while in next five chapters, my research works have been described. Recent observations suggest that the Universe is passing through a late stage accelerated expansion phase which standard cosmology fails to explain. Contemporary physicists seek to find an answer by fostering ingenious schemes. Their speculation ranges from the assumed existence of the 'dark energy' to the modification of the standard geometry of the spacetime.

This thesis considers both kind of approaches and investigates them in the light of dynamical systems theory. Precisely, the following attempts have been undertaken.

- In second chapter, self-interacting three-form field cosmological model has been studied using dynamical system approach. Possible bifurcation scenarios have been examined using Poincaré index theory to recognize possible cosmological phase transition.

- Third chapter contains three-form field dark energy model with baryonic matter which has been studied using dynamical system approach. Also global behavior and bifurcation analysis for this model has been studied.

- In the fourth chapter, we have studied a dynamical system analysis of cosmic evolution with coupled phantom dark energy with dark matter. In this chapter, cosmological phase transitions have been detected through bifurcation analysis which has been done by Poincaré index theory.

- In the fifth chapter, we have studied dynamical system analysis of the

universe with spatial curvature. Bouncing cosmological scenarios has been shown in this chapter also.

- In the sixth chapter, we have done discrete dynamical system analysis of quintessence dark energy scalar field model with exponential potential. The critical points are analyzed with center manifold theory and stability has been discussed using Schwarzian derivative.

Finally, the last chapter contains the brief discussion and future prospects of my work.

PREFACE

The work of this thesis has been carried out at the Department of Mathematics, Jadavpur University, Kolkata- 700032, India. The thesis is based on the following three published papers and two accepted papers:

- **CHAPTER 2** has been published as "*Dynamical system analysis of self-interacting three-form field cosmological model: stability and bifurcation*", **Soumya Chakraborty**, Sudip Mishra, Subenoy Chakraborty , **Eur.Phys.J.C 81** (2021) 5, 439.

- **CHAPTER 3** has been published as "*Dynamical system analysis of three-form field dark energy model with baryonic matter*", **Soumya Chakraborty**, Sudip Mishra, Subenoy Chakraborty, **Eur.Phys.J.C 80** (2020) 9, 852.

- **CHAPTER 4** has been published as "*A dynamical system analysis of cosmic evolution with coupled phantom dark energy with dark matter*", **Soumya Chakraborty**, Sudip Mishra, Subenoy Chakraborty, **Int.J.Mod.Phys.D 31**(2022) 01, 2150129.

- **CHAPTER 5** has been published as "*A dynamical system analysis of bouncing cosmology with spatial curvature*", **Soumya Chakraborty**, Sudip Mishra, Subenoy Chakraborty, **General Relativity and Gravitation** (accepted manuscript).

- **CHAPTER 6** has been published as "*Dynamical system analysis of quintessence dark energy model*", **Soumya Chakraborty**, Sudip Mishra, Subenoy Chakraborty, **Int.J.Geom.Meth.Mod.Phys** (accepted manuscript).

LIST OF PUBLISHED AND ACCEPTED PAPERS

1. S. Chakraborty, S. Mishra and S. Chakraborty, "Dynamical system analysis of self-interacting three-form field cosmological model: stability and bifurcation," Eur. Phys. J. C **81**, no.5, 439 (2021) doi:10.1140/epjc/s10052-021-09221-6.

2. S. Chakraborty, S. Mishra and S. Chakraborty, "Dynamical system analysis of three-form field dark energy model with baryonic matter," Eur. Phys. J. C **80**, no.9, 852 (2020) doi:10.1140/epjc/s10052-020-8427-3.

3. S. Chakraborty, S. Mishra and S. Chakraborty, "A dynamical system analysis of cosmic evolution with coupled phantom dark energy with dark matter," Int. J. Mod. Phys. D **31**, no.01, 2150129 (2022) doi:10.1142/S0218271821501297 [arXiv:2011.09842 [gr-qc]].

4. G. Mandal, S. Chakraborty, S. Mishra and S. K. Biswas, "A study of interacting scalar field model from the perspective of the dynamical systems theory," Phys. Dark Univ. **40**, 101210 (2023) doi:10.1142/S0218271821501297 [arXiv:2101.04496 [gr-qc]].

5. S. Chakraborty, S. Mishra and S. Chakraborty, "Dynamical system analysis of quintessence dark energy model," Int.J.Geom.Meth.Mod.Phys, https://doi.org/10.1142/S0219887824502505 (accepted manuscript) [arXiv:2406.10692 [gr-qc]].

6. S. Chakraborty, S. Mishra and S. Chakraborty, "A dynamical system analysis of bouncing cosmology with spatial curvature," Gen.Rel.Grav. (accepted manuscript).

ACKNOWLEDGMENTS

Writing this note of thanks and gratefulness is the finishing touch on my thesis. It has been an intensive time when I have learned about scientific arena and have accumulated experience in personal life. In this period, we all have encountered ups and downs in life due to the pandemic situation. It was really a tough time for me. In this period, I have witnessed the sufferings of known people around me due to Covid Pandemic. This thesis represents my hardwork and the helps of many people whithout whom I can't achieve my dream.

First of all I want to thank my advisor, Subenoy Chakraborty, D.Sc. Sir, you have been a great mentor for me. Without you, it was impossible for me to grow as a researcher. You have always encouraged me to research. I am grateful to you for your scoldings which helped me to correct my mistakes and I must say whithout this I would not be able to write this thesis. I am proud to be a student of a great teacher like you. I am also thankful to you for teaching me not only the General Relativity and Cosmology but also the values of life. I thank Kakima (Archana Chakraborty) for her love and blessings. Also I like to thank Dr. Sumanta Chakraborty for teaching the topics related to my research and helping me to draw research related plot by Mathematica when I was new.

Thank you Sudip da (Dr. Sudip Mishra) for your collaborations, help, advices and support. You have always helped me to understand the research related topics more clearly.

Thank you Sujoy da (Dr. Sujay Kr. Biswas) for your collaboration and help in my research.

Now I like to thank all the faculty and research scholars of the Department of Mathematics, Jadavpur University. Special thanks to Dr. Farook Rahaman, Dr. Anup Bandyopadhyay and Dr. Abhijit Lahiri. Sourav Da (Dr. Sourav Dutta), Dipanjana Di (Dr. Dipanjana Das), and Priti Di (Dr. Pritikana Bhandari) thank you for all of your support while I was new in LateX. Thank you Roshni Di (Dr. Roshni Bhaumik) for helping me all the time during course work and the time of thesis writing. Thank you Akash Da for fixing many problems which I have encountered in LateX. Thank you Subhajyoti Da (Dr. Subhajyoti Pal) for your help at the time of thesis writing. Thanks to Madhukrishna for providing many updates about national/international conferences. I also want to thank Gopal da (Dr. Gopal Sardar), Dipankar Da, Shriton for their helps. Special thanks to Bikram Da (Dr. Bikram Ghosh),

Subhayan Da (Dr. Subhayan Maity), Sudipto Da (Dr. Sudipto Bhattacharjee), Sourav Da (Dr. Sourav Haldar), and Abhijit Da (Dr. Abhijit Mandal).

I am grateful to all my teachers of my first school Sundarban Balika Vidyaniketan. Special mention to Shyamal Sir (Shyamal Das). Also I want to thank all the teachers of my school Sundarban Adarsha Vidyamandir. I convey my warmest regards to my tutors Narayan Babu, Rajashri Madam, Dipak Babu. Special thanks to my Mathematics teacher Srirup Babu. Thank you Sir for your encouragements.

Thanks to all my college friends Debarghya, Subhashis, Tapas, Anirban, Irphan, Avisek, Raja, Shilajit, Arghya, Palash, Bapan and Joydeep. A very special thanks to Anubhab who was my mess partner.

A special thanks to my family. Thakuma (Ganga Rani Chakraborty) thank you for your support. I want to thank my brother (Soumik Chakraborty) for whom I always feel proud. Words cannot express how grateful I am to you for always being by my side in my happiness and sadness. Now I would like to express my love and gratitude to Dipanwita (Dipanwita Palai) for her great support, care and love. I can't express my gratitude in words.

Above all I like to acknowledge the support of my parents Mamoni (Malati Chakraborty) and Bapi (Sudarshan Chakraborty). I would like to acknowledge the tremendous sacrifices that they made to ensure that I had an excellent education. I can't thank you enough Mamoni, first teacher of my life. I am grateful to you Bapi, you were my English and Mathematics teacher upto class VIII. I am unable to express my gratitude in words.

There are so many people to mention. I hope I haven't missed any.

This thesis is supported by Council of Scientific & Industrial Research (CSIR), Government of India, through Junior and Senior Research Fellowships.

Soumya Chakraborty

"Anyone who has never made a mistake has never tried anything new."

Albert Einstein

LIST OF FIGURES

LIST OF TABLES

CONTENTS

CHAPTER 1

INTRODUCTION

Some basic questions regarding the origin, structure, evolution, and the ultimate fate of the Universe have compelled people to investigate the evolution of the Universe from very beginning. 'Cosmology' is that branch of science which can provide the possible route map to find answers to the above questions. In other words, Cosmology is the study of the Universe as a whole. A cosmological model can be described by a mathematical formalism of the Universe in some particular averaging scale. Simply, it is structured mathematically as a differential manifold $\mathcal{M}$ in which the space-time geometry is determined by a Lorentzian metric g, and the matter source of the Universe is characterized by a family of fundamental observers whose congruence of world lines are four-velocity vector u. So, in notation, a cosmological model is described as triplet $(\mathcal{M}, g, u)$ [1].

Thus any cosmological model should be based on the following:
(1) Physical theories of gravity.
(2) Description of matter field of the Universe.
(3) Hypothesis on symmetries for solving the equation of gravity, and
(4) Topology or global structure of the Universe.

• **Cosmological Principle**

Cosmological principle is one of the fundamental pillars of modern cosmology. The principle states that at every epoch, the space-like hypersurface is assumed to be homogeneous and isotropic [2, 3] at a sufficiently large scale[1] (> 100 Mpc). The space-like hypersurfaces of the four dimensional manifold $\mathcal{M}$ constitute our universe, where slicing of space-like hypersurfaces defines the cosmic time t.

The term 'homogeneous' means uniformly distributed matter content throughout the Universe observed by co-moving observers. Although, the Universe is not exactly homogeneous at small scales, the presence of locally visible stars, galaxies, cluster of galaxies makes it inhomogeneous. But, on averaging over the cosmological scale, a co-moving observer will see the uniform spatial expansion of the Universe.

[1] where 1 Mpc $\simeq 3.26 \times 10^6$ light years $\simeq 3.08 \times 10^{19}$ km

On the other hand, isotropy confirms the phenomenon of the Universe to stay the same in all directions, *i.e.*, there is no preferred direction. In fact, spatial section of the manifold will remain unaltered under the rotation. Observations of Cosmic Microwave Background (CMB) suggest that the temperature ($\sim 2.73k$) of the Universe is same in all directions that is there exists isotropy of one part in 100,000 [4]. Simply, any inhomogeneity and anisotropy in the matter distribution of the universe can lead to anisotropy in radiation, and also in order to verify the homogeneity, one requires to test isometry from at least two different points separated by cosmic distances because isometry may be verified only from earth point of view, but homogeneity can not be verified from observations obtained from single location. In conclusion, for all observers (stars, galaxies etc.), isotropy implies the spatial homogeneity.

The main statement of Cosmological Principle (sometimes called as "Copernican Principle") is that we (earth) are not privileged observers. Although the principle has been challenged by several authors [5, 6, 7, 8, 9], nonetheless we shall follow the Cosmological Principle throughout our work as it is valid in the cosmic scales where it establishes the FLRW line element for the four dimensional space-time. In the next section (1.1), we have discussed the standard cosmological model and its failure. Then, various dark energy models as well as interacting dynamics and their physical consequences have been presented. A short discussion on dynamical system analysis and its applications in cosmology have been presented. Finally, cosmological models have been analyzed in the dynamical system perspective.

1.1 Standard Cosmological model and its failure

The modern relativistic cosmology is the four dimensional manifold ($\mathcal{M}$) of space-time geometry. Einstien's General Relativity (GR) is the mathematical basis of cosmology in which Einstein Field Equations (EFE) [10, 11] are the basic constituents relating the geometry of space-time to the energy momentum tensor of matter source as

$$G_{\mu\nu} \equiv R_{\mu\nu} - \frac{1}{2}Rg_{\mu\nu} = \kappa^2 T_{\mu\nu} \ . \tag{1.1}$$

Here, $G_{\mu\nu}$ is the Einstein tensor, and the quantity $T_{\mu\nu}$ in the right hand side of (1.1) is known as the stress energy tensor of the matter content of the universe, and $\kappa^2 = \frac{8\pi G}{c^4}$ is the coupling constant, where c represents the velocity of light [2]. G is the Newton's gravitational constant having value $G = 6.673 \times 10^{-11} Nm^2 kg^{-1}$. The geometry of the space-time metric is defined by the line element

$$ds^2 = g_{\mu\nu} dx^\mu dx^\nu \ , \tag{1.2}$$

where $g_{\mu\nu}$ is the metric tensor. The Ricci tensor $R_{\mu\nu}$ is the contracted Riemann tensor $R^\sigma_{\lambda\mu\nu}$ defined as $R_{\mu\nu} \equiv R^\sigma_{\mu\sigma\nu}$, and the Ricci scalar is found to be $R \equiv R^\mu_\mu = g^{\mu\nu} R_{\mu\nu}$.

[2] We assume the velocity of light $c = 1$ throughout the work

For different kinds of matter source term in EFE, the decomposition of stress-energy tensor with respect to time-like four- velocity vector u may be different. The symmetry of space-time (*i.e.*, Weyl postulate) forces the stress-energy tensor to be in perfect fluid form

$$T_{\mu\nu} = (p+\rho)u_\mu u_\nu + p g_{\mu\nu} \qquad \text{with} \quad u_\mu u^\mu = -1, \tag{1.3}$$

where p is the thermodynamic pressure and ρ is the energy density of the perfect fluid, and u^μ is the four-velocity vector of the co-moving observer. The ratio between the pressure and the energy density is termed as equation of state parameter of the fluid, which is expressed as

$$\omega = \frac{p}{\rho} \ . \tag{1.4}$$

Now, for stiff fluid is described by $\omega = 1$; for the non-relativistic matter (pressureless matter), $\omega = 0$, while for relativistic matter (*i.e.*, radiation), the value of equation of state parameter will be $\omega = 1/3$.

We now focus our attention on Friedmann-Lemaitre universe which is based on the Robertson-Walker metric. Assuming the validity of the cosmological principle at some cosmological scale, a four dimensional manifold with symmetry must possess the maximally spatial symmetric Robertson-Walker (RW) metric [12, 13, 14, 15] in that scale. The Friedmann-Lemaitre Robertson-Walker (FLRW) metric in co-moving coordinates (using spherical polar coordinates) takes the form

$$ds^2 = g_{\mu\nu}dx^\mu dx^\nu = -dt^2 + a^2(t)\left[\frac{dr^2}{1-Kr^2} + r^2 d\Omega^2\right] \ , \tag{1.5}$$

where $d\Omega^2 = d\theta^2 + \sin^2\theta d\phi^2$ is the metric on the unit 2-sphere. Here, K describes the spatial curvature of hypersurface, and it takes the value -1, 0, or, 1. For $K = -1$, the Universe is assumed to be open, while for $K = 1$, the Universe is closed, and the Universe is spatially flat for $K = 0$. The coordinate 't' measures the proper time along the world lines with the tangent vector u. The function $a(t)$ in the line element is called the scale factor that describes the expansion of the Universe. The matter sector in the Universe having the energy-momentum tensor (1.3) follows the conservation law

$$\dot{\rho} + 3\frac{\dot{a}}{a}(p+\rho) = 0 \ . \tag{1.6}$$

By substituting the line element (1.5) in (1.1), we get the Friedmann equation as

$$H^2 = \left(\frac{\dot{a}}{a}\right)^2 = \frac{\kappa^2}{3}\rho - \frac{K}{a^2} \ , \tag{1.7}$$

and the Raychaudhuri equation (acceleration equation) is (expressed in terms of scale factor)

$$\frac{\ddot{a}}{a} \ = \ -\frac{\kappa^2}{6}(\rho + 3p) \ , \tag{1.8}$$

where H, the Hubble scalar, measures the rate of expansion of the Universe (having the dimension of (time)$^{-1}$), $\kappa^2 = 8\pi G$, and an 'over-dot' denotes differentiation with respect to cosmic time t. However, we must note that only two of the above three equations (1.6),(1.7), and (1.8), are independent.

It should be noted that the Raychaudhuri equation (1.8) provides the conditions for accelerating or decelerating state of expansion of the Universe. One can easily check that for $\ddot{a} > 0$, the Universe will accelerate that means the Universe filled with the matter having energy density ρ and pressure p must follow the condition $\rho + 3p < 0$.

From (1.8), we have the condition $\rho + 3p > 0$ (which is called the strong energy condition) for matter field in decelerating phase of the Universe. Now, a normal matter always enjoys positive energy density and pressure ($\rho > 0$ and $p > 0$). Hence, a universe filled with normal matter satisfying the condition $\rho + 3p > 0$ (which implies $\ddot{a} < 0$ from equation (1.8)) must always produce decelerated expansion of the Universe. This conditions can be put in terms of the equation of state parameter as universe accelerates for $\omega < -\frac{1}{3}$ and decelerates for $\omega > -\frac{1}{3}$.

Here, equation (1.8) obtained from General Relativity predicts only decelerated expansion of universe for ordinary matter (such as dust, radiation etc) having equation of state parameter (ω) ranging from 0 to 1, and this model is termed as the Standard Cosmological Model (SCM). If the equation of state parameter is chosen as constant, then from the conservation equation (1.6), ρ can be obtained as

$$\rho \propto a^{-3(\omega+1)} \ . \tag{1.9}$$

So, for dust ($p_m = 0$) like ordinary non-relativistic matter fluid, we have

$$\rho_m \propto a^{-3} \ , \tag{1.10}$$

and for radiation like fluid (where $p_r = \frac{\rho_r}{3}$),

$$\rho_r \propto a^{-4} \ . \tag{1.11}$$

The density parameter Ω, which describes the dynamical effect of the matter density, is defined as

$$\Omega = \frac{\rho}{3H^2} \ . \tag{1.12}$$

So, the Friedmann equation (1.7) can be rewritten in terms of Ω as

$$\Omega(t) - 1 \quad = \quad \frac{K}{(aH)^2} \ , \tag{1.13}$$

which implies $\Omega(t) + \Omega_K = 1$, where $\Omega_K = -\frac{K}{a^2H^2}$ is the curvature parameter. This equation shows that the value of Ω determines the geometry of the 3-spaces t = constant and vice-versa:

$$\Omega(t)\begin{cases} > 1 \Longrightarrow \text{corresponds to closed 3 space } (K=+1) \\ = 1 \Longrightarrow \text{corresponds to flat 3 space } (K=0) \\ < 1 \Longrightarrow \text{corresponds to open 3 space } (K=-1) \end{cases}$$

In agreement with the present astronomical observations [16], the value of curvature parameter can be estimated very close to zero, *i.e.*, $\Omega_K \backsimeq 0$ and hence, from the Friedmann equation (1.7), we obtain the condition $\Omega \backsimeq 1$ [16]. The argument behind this observed flatness of universe is the existence of an inflationary phase of universe at very early times. More precisely, one can assume the spatially flat ($K = 0,\ \Omega = 1$) universe from the Big bang to the present phase. We will assume this flat nature throughout the thesis for this argument, and also for mathematical simplicity. For $K = 0$, using (1.9), the Friedmann equation (1.7) leads to

$$a(t) \propto t^{\frac{2}{3(\omega+1)}} \ . \tag{1.14}$$

So the scale factor $a(t)$ in terms of time t for different kinds of fluid can be written as

$$a(t) \propto t^{\frac{2}{3}} \tag{1.15}$$

for ordinary dust matter fluid, and

$$a(t) \propto t^{\frac{1}{2}} \tag{1.16}$$

for radiation respectively. The deceleration parameter q can be expressed as

$$q \ \equiv \ -\frac{a\ddot{a}}{\dot{a}^2} = -\frac{\ddot{a}}{aH^2} = -\left(1+\frac{\dot{H}}{H^2}\right) \ . \tag{1.17}$$

So, we have the restrictions for decelerating or accelerating universe in terms of q. The Universe will decelerate for $q > 0$ (*i.e.*, when $\ddot{a} < 0$ from acceleration equation) and will accelerate for $q < 0$ (*i.e.*, when $\ddot{a} > 0$).

1.1.1 Failure of standard cosmology: Introduction of DE model

In 1998, two Supernovae search teams, namely, Riess *et al.* [17] in the "High-redshift Supernovae Search Team" (HSST) and Perlmutter *et al.* [18] in the "Supernovae Cosmology Project Team" (SCPT), independently analyzed Supernovae type Ia (SNe Ia), and declared that the Universe is going through an accelerating phase. This discovery has brought a total surprise in Cosmology. Since then, many observations like Cosmic Microwave Background radiation (CMB) [16, 19, 20, 21, 22, 23, 24], Large Scale Structure of the Universe (LSS) [25, 26, 27], Baryon Acoustic Oscillation (BAO) [28, 29], weak lensing (WL) [30], and many others [31, 32, 33, 34, 35, 36, 37] have also shown that the Universe is expanding with ever

increasing speed. Standard cosmology asserts that the Universe is decelerating because it is filled with ordinary matter field which follows the strong energy condition

$$\rho + 3p \geq 0 \ . \tag{1.18}$$

Hence, it does not support the observations. So, if we consider Einstein's General Relativity to be the correct theory of gravity, the above observations demand the existence of a new kind of matter which violates the strong energy condition, that is,

$$\rho + 3p < 0 \ , \tag{1.19}$$

and as a result there is an accelerated expansion of the Universe. This new kind of matter is responsible for acceleration violating the strong energy condition, so it must have a large negative pressure (since the energy density of matter is positive). This type of matter is referred to as 'Dark Energy' (DE). Thus, one can conclude that the failure of SCM gives a new type of matter in this context. However, the nature of DE is completely unknown (except for its negative pressure) and is still an unresolved problem in modern cosmology [38, 39, 40, 41].

After formulating his general theory of relativity, Einstein wanted to model the universe using it. At that time, he was of the opinion that the Universe is static in nature. In order to get a static solution, he introduced cosmological constant (the famous Λ term) to his field equations to balance the attractive force of gravity. Later, when Hubble [42] observationally discovered that the universe is expanding, Einstein discarded this constant term from his field equations, and confessed it as the greatest blunder of his life. Recent observations have led people to reintroduce it into the gravitational equations as a dark energy candidate [43, 44]. Although, there are two severe problems related to the cosmological constant, namely, the cosmological constant problem [43, 45, 46] (where its value is so small to its predicted value using quantum field theory (QFT)) and the coincidence problem [47, 48] (why the energy densities of Λ and matter sector are of same order while they evolve so differently?), but recent observations [49] suggest that the cosmological constant is the best candidate for DE [43, 44] compared to other DE models. For a review of DE models, one can see Refs. [47, 50].

- **Dark Matter:**

Another mysterious component of matter speculated to be present in the universe is "Dark Matter" (see for a review [51]). The origin of dark matter has not been identified yet, but its existence can only be probed by gravitational effects on visible matter, although it interacts very weakly with standard model particles. From the data analysis of two fundamental observations depending on the behavior of the galactic rotation curve [52] observed by Zwicky [53, 54], and the mass discrepancy in the clusters of galaxies at a galactic and extra galactic scale indicate the existence of dark matter. The rotation curves of spiral galaxies [55, 56, 57] do not match with the expected ones as predicted by Newtonian and standard cosmology at the galactic/intergalactic scales. As a result, the behavior of galactic rotation curves and virial mass of clusters of galaxies are realized mainly by postulating the existence of invisible (dark) matter. This matter is cold, pressureless, and distributed in the spherical halo in the galaxies [58] known as Cold- dark- matter (CDM). There is another candidate for dark

matter called Hot Dark Matter (HDM) which is relativistic at the photon decoupling epoch and whose representative candidate is the neutrino. Many possible candidate for DM have been proposed in the literature. They are usually classified into two types — baroynic type DM such as in astrophysical candidates like black holes, neutron stars, and white dwarfs etc. and non-baryonic type CDM, namely, axion [59] and WIMPs (Weakly Interacting Massive Particles) (see Ref. [60] for an interpretation of DM from the point of view of particle physics) usually motivated by superstring theory. The latter is a good candidate for non-relativistic Cold Dark Matter [50]. Further, it is worthwhile to mention that detection of dark matter from space or from high-energy collisions of particles (see for instance [61, 62, 63, 64]) is being carried out at LHC.

1.1.1.1 Cosmological Constant: As Dark Energy

We stated earlier that standard cosmology provides only decelerating universe for normal matter and Einstein, in 1917, introduced a cosmological constant term [10] in the field equations to counter the attractive gravitational pull by other normal fluids. In other words, his main goal was to obtain a universe that satisfies Mach's Principle of relativity of inertia. So, he modified his field equations as

$$\widetilde{G}_{\mu\nu} = G_{\mu\nu} + \Lambda g_{\mu\nu} = \kappa^2 T_{\mu\nu}. \tag{1.20}$$

However, cosmological constant was not considered as a part of the stress-energy tensor $T_{\mu\nu}$ at first. But one may put the term $\Lambda g_{\mu\nu}$ in the right hand side of the field equations as a part of the source term for the stress-energy tensor and simply assume it ($\frac{\Lambda}{\kappa^2} = \rho_\Lambda$) as vacuum energy from the point of view of quantum field theory. Thus, ρ_Λ can take part in the dynamics of the Universe and the field equations (1.20) can be rewritten as

$$G_{\mu\nu} = \kappa^2 (T_{\mu\nu} - \rho_\Lambda g_{\mu\nu}) \ . \tag{1.21}$$

In the context of perfect fluid (1.3), from the above stress-energy composition, one obtains the energy density and the pressure of vacuum energy as

$$\rho_\Lambda = \frac{\Lambda}{\kappa^2}, \quad p_\Lambda = -\frac{\Lambda}{\kappa^2}$$

with the equation of state parameter

$$\omega_\Lambda \equiv \frac{p_\Lambda}{\rho_\Lambda} = -1 \ .$$

The important feature of cosmological constant is that it will be constant throughout the expansion of universe and this plays an important role in the dynamics of the Universe. This is considered to be the simplest candidate of dark energy. Now, Friedmann equation (1.7) changes in terms of the quantity ρ_Λ [65] as

$$H^2 \equiv \frac{\dot{a}^2}{a^2} \quad = \quad \frac{\kappa^2}{3}\left(-\frac{3K}{\kappa^2 a^2} + \rho_\Lambda + \rho\right), \tag{1.22}$$

and the acceleration equation becomes

$$\frac{\ddot{a}}{a} = -\frac{\kappa^2}{6}(-2\rho_\Lambda + \rho + 3p) \ . \tag{1.23}$$

Thus, by changing the above equations, we see that the cosmological constant can overcome the gravitational pull by other matter. Note that the equations of gravity remain unaltered, only a new component is added to the content of the Universe. The new component of stress-energy tensor has the nature of an ideal fluid having negative pressure. Let us note that Λ may take positive or negative values, though positive Λ is more acceptable for balancing the gravitational pull. So, it acts as gravitational repulsion. However, in string theory, sometime negative Λ is necessary to explain some theoretical issues. Introducing $\Omega_\Lambda = \frac{\Lambda}{3H^2}$, the first Friedmann equation can be written as

$$\Omega + \Omega_\Lambda - 1 = \frac{K}{a^2H^2} \ . \tag{1.24}$$

So, for a flat universe, $\Omega + \Omega_\Lambda = 1$, for an open universe, $0 < \Omega + \Omega_\Lambda < 1$, and for a closed universe, $\Omega + \Omega_\Lambda > 1$. Thus, it may be treated as a cosmic fluid with energy density ρ_Λ and pressure p_Λ.

1.2 Various Dark Energy models

The discovery of present accelerated expansion of the Universe have compelled to consider various dark energy component in the context of General Relativity. Though it has a mathematical explanation, the idea of DE is completely hypothetical. The universe is assumed to be largely dominated by DE. WMAP 5-year constraints [24] indicate that the sum of energy densities of radiation, baryons, and DM must not exceed 30 % of the total energy of the universe. Also, from the present observations bound the spatial curvature as $|\Omega_K^0| \lesssim 0.01$. This shows that there should still be needed to identify remaining 70 % of cosmic matter [50]. And this remaining part is assumed to be responsible for the present acceleration of the universe. The data collected from WMAP 5-yr constraint (WMAP+SN Ia+ BAO) have explored the constraint for present density of DE as

$$\Omega_{de} = 0.726 \pm 0.015. \tag{1.25}$$

The character of DE is completely unknown, and has never been detected or created in laboratory . Only it is characterized by its huge negative pressure which distinguishes DE from other constituents of the Universe. The equation of state parameter for any DE component should be

$$\omega_{de} < -\frac{1}{3}.$$

So, in one side it is mysterious, very less known to us. Another side is its interesting dynamics to provide the accelerating scenario of universe. However, motivated from the fact, many DE models have been extensively studied, among them ΛCDM is the simplest one where cosmological constant Λ is treated as DE component with equation of state '$\omega_\Lambda = -1$'

driving the late time acceleration of the universe. Though this model shows a good fit to a large number of observations, it suffers from several complexities in the cosmological point of view such as fine tuning, coincidence problem, cosmic age problem etc. which we shall discuss later.

The dynamically evolving DE can give the possible solutions of the two major problems with cosmological constant and thus dynamical dark energy model is assumed to be a viable alternative to cosmological constant. Various dynamical DE models based on scalar field have been reported in the literature:

(i) Quintessence [66, 67, 68, 69, 70, 71, 72, 73, 74, 75, 76, 77, 78],

(ii) K-essence [79, 80, 81, 82, 83, 84],

(iii) Tachyon [85, 86, 87, 88, 89, 90, 91]

(iv) Phantom [92]

(v) Chaplygin gas: perfect fluid models [93, 94, 95]

1.2.1 ΛCDM model:

In the ΛCDM concordance model, gravity theory from the General Relativity theory is assumed to be true where the constituents of the universe are the particles and fields of the standard model of particle physics, together with the Cold-Dark Matter (non-relativistic) and a Cosmological Constant (Λ). The action for the ΛCDM model is

$$S = \frac{1}{2\kappa^2}\int d^4x\sqrt{-g}(R-2\Lambda)+S_m, \tag{1.26}$$

where the Lagrangian density is a linear term in R plus Λ and S_m is the matter action. Although this model provides a very good fit to observations, it suffers from two major problems, namely, Cosmological Constant or fine tuning problem, and the coincidence problem.

- **Cosmological Constant Problem:**

To realize the present observed accelerated expansion of the Universe, one requires that the value of the Cosmological Constant is of the order of the present value of the Hubble parameter H_0 (observationally), *i.e.*,

$$\Lambda \approx H_0^2 = (2.1332h\times 10^{-42}\text{GeV})^2, \tag{1.27}$$

where h defines the uncertainty in the value of the present day Hubble (H_0) parameter[3]. This defines the energy density as

[3] H_0 $(= H(t = t_0))$ is the present value of the Hubble parameter usually written as $H_0 = 100h\ km\ sec^{-1}\ Mpc^{-1} = 2.1332h\times 10^{-2}$GeV. The observations of the Hubble Key Project constrain this value to be $h = 0.72\pm 0.08$ [96].

$$\rho_\Lambda = \frac{\Lambda}{8\pi G} \approx 10^{-47}\text{GeV}^4. \tag{1.28}$$

Now, from the particle physics point of view, if we consider this as the energy density coming from empty space (vacuum energy density), then by summing over all zero point energies for some field of mass m with momentum p upto a cut-off scale, the vacuum energy density reads

$$\rho_{vac} = \frac{1}{4\pi^2}\int_0^\infty p^2\sqrt{p^2+m^2}dp. \tag{1.29}$$

The vacuum energy is estimated to have a value $\rho_{vac} \simeq 10^{74}\text{GeV}^4$, so this is larger the 10^{121} orders of magnitude when compared to the observed value $\rho_\Lambda \simeq 10^{-47}\text{GeV}^4$.
This discrepancy in energy density is termed as the *Cosmological Constant problem* [43, 45, 46] in cosmology. It is a fact that the vacuum energy with the energy density of order $\rho_{vac} \simeq 10^{74}\text{GeV}^4$ already existed in the past, so, the Universe would have continued in an accelerated phase forever. This is in contradiction with the known evolutionary history of the Universe since it has undergone a decelerated phase of radiation and matter dominated eras [50].

- **Coincidence Problem:**

The Cosmological constant DE model faces another big problem from the observational point of view that the energy densities of both the dark energy and the matter are of the same order today even though they evolve differently in the expansion history of the universe since ρ_Λ = constant for Cosmological Constant while $\rho_r \propto a^{-4}$ for radiation and $\rho_m \propto a^{-3}$ for matter. This problem with the Cosmological Constant is referred to as the cosmological *Coincidence Problem* [47].

When the energy density for matter scales as $\rho_m \propto a^{-3}$, the crossover must have occurred at a cosmological time corresponding to the scale factor a_* given by

$$\rho_{m0}.a_*^{-3} = \rho_\Lambda \longrightarrow a_* = \left(\frac{\rho_\Lambda}{\rho_{m0}}\right)^{-\frac{1}{3}} \simeq 3^{-\frac{1}{3}} \simeq 0.7\ , \tag{1.30}$$

which corresponds to a redshift of $z_* \simeq 0.4$. At the earlier epochs of the cosmological evolution, the energy density of cosmological constant was less compared to the energy density of the other cosmic components. Thus, this is an unexpected coincidence between the appearance of Cosmological Constant and the present epoch which is termed as *coincidence problem* for the Cosmological Constant [65].

1.2.2 Dynamical Dark Energy model: Scalar field as DE

We have mentioned earlier that the lack of many orders of the observed energy density of the Cosmological Constant in comparison to the estimated value of vacuum energy has forced to introduce (theoretically) a new type of dynamically (time varying) evolving dark energy model which introduces the classical scalar field. Scalar field naturally arises in particle physics and string theory and this would be a good candidate for dark energy.

1.2.2.1 Quintessence:

The Quintessence scalar field (ϕ) moving in a self-interacting potential $V(\phi)$ can be described by a most general form of Lagrangian density in terms of a scalar and its four-derivative $p(\phi, \partial_\mu\phi)$. The action for the quintessence scalar field is given by

$$S = \int d^4x\sqrt{-g}\left[-V(\phi) - \frac{1}{2}(\nabla\phi)^2\right], \tag{1.31}$$

where $(\nabla\phi)^2 = g^{\mu\nu}\partial_\mu\phi\partial_\nu\phi$. Now, applying the least action principle to (1.31), we obtain the stress-energy tensor as

$$\begin{aligned} T_{\mu\nu} &= -\frac{2}{\sqrt{-g}}\frac{\delta S}{\delta g^{\mu\nu}} \\ &= \partial_\mu\phi\partial_\nu\phi - g_{\mu\nu}\left[-\frac{1}{2}g^{\alpha\beta}\partial_\alpha\phi\partial_\beta\phi + V(\phi)\right]. \end{aligned} \tag{1.32}$$

For a flat ($K = 0$) FLRW metric, the expression of the energy density ρ_ϕ and the pressure p_ϕ of a perfect fluid scalar field ϕ are given by

$$\rho_\phi = -T^0_0 = \frac{1}{2}\dot{\phi}^2 + V(\phi)\ , \tag{1.33}$$

$$p_\phi = T^i_i = \frac{1}{2}\dot{\phi}^2 - V(\phi)\ , \tag{1.34}$$

and then the equation of state parameter (ω_ϕ) for the quintessence scalar field takes the form

$$\omega_\phi = \frac{p_\phi}{\rho_\phi} = \frac{\frac{1}{2}\dot{\phi}^2 - V(\phi)}{\frac{1}{2}\dot{\phi}^2 + V(\phi)}\ . \tag{1.35}$$

In the flat FLRW Universe, the Friedmann equation (1.7) and the Raychaudhuri equation (1.8) respectively read as

$$H^2 = \frac{\kappa^2}{3}\left(\frac{1}{2}\dot{\phi}^2 + V(\phi)\right)\ , \tag{1.36}$$

$$\frac{\ddot{a}}{a} = -\frac{\kappa^2}{3}\left(\dot{\phi}^2 - V(\phi)\right)\ . \tag{1.37}$$

Now, for the flat FLRW space-time, varying the action (1.31) with respect to ϕ gives the evolution of scalar field ϕ as

$$\ddot{\phi} + 3H\dot{\phi} + \frac{dV}{d\phi} = 0\ . \tag{1.38}$$

The evolution of the scalar field ϕ is known as the Klein-Gordon equation. In fact the evolution equation (1.38) can also be obtained either from the energy conservation equation

$$\dot{\rho_\phi} + 3H(p_\phi + \rho_\phi) \quad = \quad 0 \ , \tag{1.39}$$

or from the equations (1.36) and (1.37). The continuity equation (1.39) gives the solution of energy density in terms of the equation of state parameter (ω_ϕ) for the scalar field

$$\rho_\phi \quad = \quad \rho_{\phi 0} \ exp\left[-\int 3(1+\omega_\phi)\frac{da}{a}\right] \ . \tag{1.40}$$

Equations (1.35) and (1.40) provide some important features of the scalar field model of DE. For the slow roll, *i.e.*, when the potential ($V(\phi)$) dominates over kinetic energy ($\frac{1}{2}\dot{\phi}^2$) of scalar field, it recovers the cosmological constant. So from equations (1.35) and (1.40),

$$\dot{\phi}^2 \ll V(\phi) \Longrightarrow \omega_\phi \simeq -1, \quad \rho_\phi = \text{constant}.$$

For the opposite case, *i.e.*, when the scalar field evolves very rapidly (in this case, the kinetic energy dominates over the potential energy) with time, DE behaves as a stiff fluid. From the equations (1.35) and (1.40), we have

$$\dot{\phi}^2 \gg V(\phi) \Longrightarrow \omega_\phi \simeq 1, \quad \rho_\phi \propto a^{-6}.$$

Thus, ω_ϕ of scalar field is no longer a constant rather it is evolving dynamically ranging from -1 to $+1$ throughout the expansion history of the universe and such a type of dynamic nature ($-1 \leq \omega_\phi \leq +1$) of the scalar field can solve the fine tuning problem. Also, from (1.37) we see that this kind of fluid gives acceleration ($\ddot{a} > 0$) when $\omega_\phi < -\frac{1}{3}$ which corresponds to $\dot{\phi}^2 < V(\phi)$. The model based on a canonical scalar field explaining the late time acceleration of universe is denoted by the name 'Quintessence'.

In an inflationary scenario, inflation will occur if the slow roll parameters ϵ, η satisfy the relations $\epsilon \ll 1$ and $|\eta| \ll 1$, where the slow roll parameters are described as $\epsilon = \frac{m_{pl}^2}{16\pi}\left(\frac{1}{V}\frac{dV}{d\phi}\right)^2$, $\eta = \frac{m_{pl}^2}{8\pi}\frac{1}{V}\frac{d^2V}{d\phi^2}$ [97]. However, since the Universe can have DM also during the evolution, it is not a completely trustworthy proof of inflation in the context of DE only. Nevertheless, they still can provide an accelerated expansion by defining the slow roll parameter ϵ as $\epsilon = -\frac{\dot{H}}{H^2}$ in terms of H and $\dot{H}$, and this includes the contribution of both DE and DM [47].

It should be mentioned that various quintessence potentials of the scalar field have been proposed in order to describe the present acceleration of the universe. Among them, the exponential, the inverse power law, and the hyperbolic types are most popular. The various type of quintessence potentials are shown in a tabular form in the table (1.1) [98, 99].

1.2.2.2 K-essence:

In the scalar field DE model, the quintessence potential can give rise to acceleration; modified kinetic energy of the scalar field is also modelled as a candidate of DE in order to produce the acceleration. The model K-inflation [79] was first used to describe the early inflation of the Universe where the acceleration is driven by the kinetic energy of the scalar field. Gradually

Table 1.1: The table shows different quintessence potentials of scalar field studied in the literature.

	Quintessence Potential ($V(\phi)$)	References
I	$V_0\ \exp(-\lambda\phi)$	Ratra & Peebles [70]; Wetterich [69];
II	$m^2\phi^2,\quad \lambda\phi^4$	Ferreira & Joyce [74].
III	$V_0/\phi^\alpha,\quad \alpha > 0$	Ratra & Peebles [70].
IV	$V_0\ \exp(\lambda\phi^2)/\phi^\alpha$	Brax & Martin. [100, 101]
V	$V_0\,(\cosh\lambda\phi - 1)^p$	Sahni & Wang [102].
VI	$V_0\ \sinh^{-\alpha}(\lambda\phi)$	Sahni & Starobinsky [103]; Lopez & Matos [104].
VII	$V_0\left(e^{\alpha\kappa\phi} + e^{\beta\kappa\phi}\right)$	T. Barreiro et al. [105].

this idea was conceived in Ref. [81] to describe the late time acceleration of the universe. Subsequently, this idea was extended to a more generalized version in Refs. [80, 82] and this is called the K-essence dark energy model. The most general action of this model is

$$S \;=\; \int d^4x\sqrt{-g}\;\; F(\phi, X), \tag{1.41}$$

where the Lagrangian density function $F(\phi, X)$ is a function of ϕ and the kinetic term $X :\equiv -\frac{1}{2}(\nabla\phi)^2 = -\frac{1}{2}\partial_\mu\phi\partial_\nu\phi$. Here, the Lagrangian density is described by the pressure $F(\phi, X)$. Since this model modifies kinetic energy term, so, $X \longrightarrow 0 \implies F(\phi, X) \longrightarrow 0$ (since Lagrangian density is vanish for this case). Now, one can expand the Lagrangian density in the neighbourhood of $X = 0$ as

$$F(\phi, X) \;=\; K(\phi)X + L(\phi)X^2 + ..., \tag{1.42}$$

neglecting the higher power terms of X. Then, we can redefine the the scalar field ϕ as follows:

$$\phi_{new} \;=\; \int^{\phi_{old}} d\phi\sqrt{\frac{L}{|K|}}, \tag{1.43}$$

and the Lagrangian takes the form

$$F(\phi, X) \;=\; f(\phi)(-X + X^2), \tag{1.44}$$

where $\phi \equiv \phi_{new},\quad X \equiv X_{new} = \left(\frac{L}{|K|}\right) X_{old}$ and $f(\phi) = \frac{K^2(\phi_{old})}{L(\phi_{old})}$.

In a flat ($K = 0$) FLRW universe, the pressure and the energy density for this K-essence model can be written as

$$p_\phi = F(\phi, X) \;=\; f(\phi)(-X + X^2)\ , \tag{1.45}$$

$$\rho_\phi = f(\phi)(-X + 3X^2). \tag{1.46}$$

The conservation equation remains the same as in (1.6), the Friedmann equation and the Raichudhuri equations modify as

$$H^2 = \frac{\kappa^2}{3} f(\phi)\left(-X + X^2\right) , \tag{1.47}$$

$$\frac{\ddot{a}}{a} = \frac{\kappa^2}{3}\left(-2X + 3X^2\right). \tag{1.48}$$

From the equations (1.45) and (1.46), we have the equation of state parameter for the K-essence model as

$$\omega_\phi \equiv \frac{p_\phi}{\rho_\phi} = \frac{1 - X}{1 - 3X}. \tag{1.49}$$

Equation (1.49) gives the conditions of DE in terms of X *i.e.,* for $\omega_\phi < -\frac{1}{3} \Longrightarrow X > \frac{2}{3}$ which gives the accelerated expansion of the universe since $\ddot{a} > 0$ (from the acceleration equation 1.48). On the other hand, when ω_ϕ behaves as a cosmological constant ($\omega_\phi = -1$), we get a condition for X as $X = \frac{1}{2}$ [47, 106].

1.2.2.3 Tachyon:

Rolling tachyon is also assumed to be a source of dark energy. It has an interesting feature that it has an equation of state parameter varying between -1 to 0 [107], thus showing a dynamic nature, which confirms rolling tachyon as a good candidate for DE. For suitable choice of the potential, the tachyon can give the accelerated scenario of the Universe and also may produce dark matter. Thus a tachyon based model could be viable to produce inflation [108, 109, 110] and dark energy [85, 111, 112, 113, 114, 115] depending upon the potential associated with the tachyonic field. The decay of D-branes producing pressureless gas having a finite energy density treated as classical dust has been reported in [87, 88, 89]. The action of the tachyon field [88, 90] is

$$S_\phi = -\int d^4x V(\phi)\sqrt{-det(g_{\alpha\beta} + \partial_\alpha\phi\partial_\beta\phi)} . \tag{1.50}$$

where $V(\phi)$ is the tachyon potential. The action (1.50) gives the energy momentum tensor as

$$T_{\mu\nu} = \frac{V(\phi)\partial_\mu\phi\partial_\nu\phi}{\sqrt{1 + g^{ab}\partial_a\phi\partial_b\phi}} - g_{\mu\nu}V(\phi)\sqrt{1 + g^{ab}\partial_a\phi\partial_b\phi} . \tag{1.51}$$

In a spatially flat FLRW universe, the pressure and the energy density of perfect fluid model take the forms

$$\rho_\phi = -T_0^0 = \frac{V(\phi)}{\sqrt{1-\dot{\phi}^2}} , \tag{1.52}$$

$$p_\phi = T_i^i = -V(\phi)\sqrt{1-\dot{\phi}^2} . \tag{1.53}$$

Further, for a flat FLRW Universe, the Friedmann equation (1.7) and the acceleration equation (Raichaudhury) equation (1.8) become

$$H^2 = \frac{\kappa^2}{3}\frac{V(\phi)}{\sqrt{1-\dot{\phi}^2}} , \tag{1.54}$$

$$\frac{\ddot{a}}{a} = \frac{\kappa^2}{3}\frac{V(\phi)}{\sqrt{1-\dot{\phi}^2}}\left(1-\frac{3}{2}\dot{\phi}^2\right) , \tag{1.55}$$

respectively, and the continuity equation for this case has the form

$$\frac{\ddot{\phi}}{1-\dot{\phi}^2} + 3H\dot{\phi} + \frac{1}{V}\frac{dV}{d\phi} = 0 . \tag{1.56}$$

Now, the equation of state parameter for this model will be

$$\omega_\phi \equiv \frac{p_\phi}{\rho_\phi} = \dot{\phi}^2 - 1 . \tag{1.57}$$

From the acceleration equation (1.55), the condition $\dot{\phi}^2 < 2/3$ refers to the acceleration of the Universe ($\ddot{a} > 0$). Also from Friedmann equation (1.54) and Raychaudhuri equation (1.55), we have the boundary $-1 < \dot{\phi}^2 < 1$ implying that the equation of state parameter ω_ϕ varies within the values -1 and 0.

1.2.2.4 Phantom:

Hoyle first introduced phantom field in his Steady State Theory. Then Caldwell used this to derive the accelerated expansion of the Universe. Phantom field with negative kinetic energy is produced from S-brane construction. The action for the phantom field minimally coupled to gravity [92, 116] is

$$S = \int d^4x\sqrt{-g}\left[\frac{1}{2}(\nabla\phi)^2 - V(\phi)\right] , \tag{1.58}$$

which when compared to the action (1.31), has an opposite sign in the kinetic term for the quintessence scalar field. The energy density (ρ_ϕ) and pressure (p_ϕ) for this phantom field are as follows:

$$\rho_\phi = -\frac{1}{2}\dot{\phi}^2 + V(\phi) \,, \tag{1.59}$$

$$p_\phi = -\frac{1}{2}\dot{\phi}^2 - V(\phi) \,. \tag{1.60}$$

We have the equation of state parameter for this kind of field as

$$\omega_\phi \equiv \frac{p_\phi}{\rho_\phi} = \frac{-\frac{1}{2}\dot{\phi}^2 - V(\phi)}{-\frac{1}{2}\dot{\phi}^2 + V(\phi)} \,. \tag{1.61}$$

From equation (1.61), we have the condition

$$2V(\phi) \gg \dot{\phi}^2 \Longrightarrow \omega_\phi < -1.$$

This shows that the equation of state parameter crosses the line $\omega_\phi = -1$ [16, 117] which confirms the present observations. This new type of scalar field bearing a negative kinetic energy term with the equation of state $\omega_\phi < -1$ responsible for the present accelerated expansion of the Universe.

1.2.3 Chaplygin gas

The perfect fluid model of dark energy namely "Chaplygin gas" has played an important role as a dark sector candidate since it has a possibility for the unification of dark energy and dark matter [93, 94, 95, 118, 119]. This was first introduced by Sergey Chaplygin in aerodynamics to find out the lifting force on a wing of an air plane. It has the following equation of state (EoS) [93]:

$$p = -\frac{A}{\rho} \,, \tag{1.62}$$

where A is a positive constant. This is the simplest form of the equation of state for the Chaplygin gas DE model. It has the ability to describe the late time acceleration of universe. In a flat, homogeneous and isotropic FLRW metric, the conservation equation (1.6) together with the EoS (1.62) gives the energy density of the Chaplygin gas as

$$\rho = \sqrt{A + \frac{B}{a^6}} \,, \tag{1.63}$$

where B is an arbitrary constant. Now, one can easily check the behavior of Chaplygin gas at early and late times respectively by the help of the solution (1.63). When 'a' takes small values, *i.e.*, at early times of the Universe, the Chaplygin gas mimics as a pressure less dust since from (1.63), we have

$$\rho \sim \frac{\sqrt{B}}{a^3} \,, \quad a \ll \left(\frac{B}{A}\right)^{\frac{1}{6}} \,, \quad p \sim -\frac{A}{\sqrt{B}}a^3 \,. \tag{1.64}$$

On the other hand, at late times, *i.e.*, for large values of a, we have the scenario:

$$\rho \sim \sqrt{A}, \quad p \sim -\sqrt{A}\,, \quad a \gg \left(\frac{B}{A}\right)^{\frac{1}{6}}\,, \tag{1.65}$$

which implies the relation $p = -\rho$, and thus Chaplygin gas behaves as cosmological constant at late times.

Further, if Chaplygin gas is treated as an ordinary scalar field ϕ with energy density ρ_ϕ and pressure p_ϕ, we can easily get the corresponding potential $V(\phi)$ for the Chaplygin gas by using equations (1.62) and (1.63) as follows:

$$\rho_\phi = \frac{1}{2}\dot{\phi}^2 + V(\phi) = \rho = \sqrt{A + \frac{B}{a^6}}\,, \tag{1.66}$$

$$p_\phi = \frac{1}{2}\dot{\phi}^2 - V(\phi) = p = -\frac{A}{\rho} = -\frac{A}{\sqrt{A + \frac{B}{a^6}}}\,. \tag{1.67}$$

Now, solving the equations (1.66) and (1.67), we obtain

$$\dot{\phi}^2 = \frac{B}{a^6\sqrt{A + \frac{B}{a^6}}}\,, \tag{1.68}$$

$$V(\phi) = \frac{1}{2}\left[\sqrt{A + \frac{B}{a^6}} + \frac{A}{\sqrt{A + \frac{B}{a^6}}}\right]\,. \tag{1.69}$$

Hence, for flat FLRW line element, the Friedmann equation, *i.e.*, $H^2 = \frac{\kappa^2}{3}\rho$ gives the following by using equation (1.68):

$$\frac{d\phi}{da} = \left(\frac{\sqrt{3}}{\kappa}\right)\frac{B}{a\sqrt{Aa^6 + B}}\,, \tag{1.70}$$

which implies

$$a^6 = \frac{4Be^{2\sqrt{3}\kappa\phi}}{A\left(1 - e^{2\sqrt{3}\kappa\phi}\right)^2}\,. \tag{1.71}$$

Now, using the equation (1.71) in (1.69), we obtain the explicit form of the potential

$$V(\phi) = \frac{\sqrt{A}}{2}\left(\cosh\sqrt{3}\kappa\phi + \frac{1}{\cosh\sqrt{3}\kappa\phi}\right), \tag{1.72}$$

which leads to equivalency between a minimally coupled scalar field and the Chaplygin gas [47].

- Generalized Chaplygin gas (GCG)

Generalized Chaplygin gas is described by the the equation of state[95]

$$p = -\frac{A}{\rho^{\alpha}} \tag{1.73}$$

with $A > 0$. The parameter α is assumed to be in the range $0 < \alpha < 1$. According to observational data at 95% confidence level, α can be restricted in the interval $0 < \alpha < 0.2$ [120]. In a similar way as we have derived the energy density for the CG case, we have the energy density for the GCG from (1.73) as

$$\rho = \left[A + \frac{B}{a^{3(1+\alpha)}}\right]^{1/(1+\alpha)}, \tag{1.74}$$

where B is an arbitrary constant. It also shows a similar behavior as the Chaplygin gas at early times and late times of the Universe depending on parameters involved. Note that it corresponds to pure chaplygin gas for $\alpha = 1$.

- **Modified Chaplygin gas (MCG)**

Benaoum further modified the CG [118, 119]

$$p = A\rho - \frac{B}{\rho^{\alpha}}, \tag{1.75}$$

known as the modified Chaplygin gas model, where $A > 0$, $B > 0$, and $0 \leq \alpha \leq 1$. The energy density in this MCG model can be obtained as

$$\rho = \left[\frac{B}{A+1} + \frac{C}{a^{3(A+1)(1+\alpha)}}\right]^{1/(1+\alpha)}, \tag{1.76}$$

where C is the arbitrary constant of integration. MCG has a huge impact in describing the evolution of the Universe in different phases from radiation dominated era to late ΛCDM [99]. Finally, it can be concluded that CG, GCG, and MCG unify the DE and DM.

1.3 Coupling between dark matter and dark energy

Modern cosmology has grown with two theoretical difficulties that can be summarized as "Dark Energy" and "Dark Matter" problems. The central issue of modern cosmology is the present acceleration of the Universe driven by dark energy. Observations from several independent astronomical sources reveal that almost 96% energy density of the total energy budget of the Universe is coming from the dark sectors in which DE contributes nearly 73%

and the rest 23% is DM. DE is modelled in the framework of Einstien's General Relativity theory when the Universe is assumed to be homogeneous and isotropic. The nature of DE is completely unknown to us except its huge negative pressure, which results in the late time acceleration. On the other hand, DM can be detected only through its gravitational effect. The observations from the behavior of galactic rotation curves and mass discrepancy in galactic clusters prove the existence of dark matter.

In the framework of GR, ΛCDM provides the best fit to several observations. But, it faces severe problems, namely, the fine tuning and the coincidence problem. Fine tuning problem can be resolved by introducing dynamically evolving DE model where scalar field DE models, namely, quintessence, phantom, tachyon etc is considered to be a good candidate which have been discussed earlier in details. Now, the main puzzling issue in modern cosmology is the coincidence problem. According to the coincidence problem, why we are living in a particular epoch having similar order of energy densities of DE and DM even though they evolve differently with cosmic evolution?

However DE has gravitationally repulsive force for which the Universe is accelerating, while DM shows its gravitational attractive nature and thus at the first sight, there does not seem to be any interaction between them in a standard approach. On the other hand, DE is assumed to be very homogeneously distributed in universe and the dark matter clumps around ordinary matter. The possibility of a weak or even a negligible dynamic interaction between two dark components in the dark sectors can not be excluded.

Further, cosmological models where dark matter (DM) and dark energy (DE) interacts with each other have gained significant attention with successive number of observational data. In fact, very latest observations indicate in favour of a non-zero interaction in the dark sector [121, 122, 123]. Thus, the interaction between DE and DM could be a major issue to be confronted in studying the physics of DE. However, the nature of these two components (DE and DM) are still unknown, and since there are no guiding principles to account for the interaction, so, this will necessarily be phenomenological (see Refs. [124, 125, 126, 58, 127, 128, 129, 130, 131, 132, 133, 134, 135].)

In the framework of field theory, it is natural to consider the inevitable interaction between the dark components. In fact, an appropriate interaction between DE and DM can provide a mechanism to alleviate the coincidence problem, phantom crossing, cosmic age problem [136, 137, 138, 139, 140, 141, 142, 143, 144, 145, 146], and also the transient nature of the deceleration parameter. Various DE models interacting with DM have been extensively studied in several works [125, 147, 148, 149, 150, 151, 152, 153, 154, 155, 156, 157, 158, 159, 160, 161, 162, 163]. Some interactions due to their mathematical simplicity are more realistics compared to others which have better physical justification. So, for a detailed study one may follow the Refs. [98, 164, 165, 166, 167, 168, 169, 170, 171, 172, 173, 174, 175, 176, 177].

The coupling models are well known for providing a possible solution to the cosmic coincidence problem [147], as well as yielding a physical explanation for measuring a DE phantom equation of state [178, 164]. It should be noted that there are other options apart from the above mentioned choices for explaining the cosmic coincidence and other cosmological conundrums. In particular, there is the LXCDM type of models (for detailed study see [179, 180]) where there exists an interaction between the vacuum energy and another DE component. In this case matter can be conserved and nevertheless the ratio between the DE and DM remains bounded in the entire cosmic history. Further, in this context one finds effective

quintessence and phantom like behaviors in Refs. [181, 182, 183].

A decisive test for achieving similar energy density of the dark components is to perform phase space analysis of the given cosmological model in the perspectives of dynamical system analysis. In this connection, note that the uncoupled models of scalar field, phantom field, etc. provide late time acceleration with $\mathcal{O}(\Omega_{de}) = 1$. In these cases, however, coincidence problem can not be alleviated. To alleviate the coincidence problem, one has to construct an interaction model in which the coupling leads to an accelerated scaling attractor satisfying [98]

$$\frac{\Omega_{DE}}{\Omega_{DM}} \approx \mathcal{O}(1) \text{ and } q < 0. \tag{1.77}$$

Now, it is easy to understand that any cosmological model suffering from coincidence problem can be realized as above in terms of the parameters involved giving rise to a possible solution of coincidence problem by reducing the choice of parameters to match Ω_{DE}/Ω_{DM} with observations.

We shall now concentrate on the dynamics of the Universe affected by introducing the interaction term in the dark sectors. Introducing DE and DM in the stress-energy tensor, the Einstein's field equations (1.1) take the form

$$R_{\mu\nu} - \frac{1}{2}Rg_{\mu\nu} = \kappa^2 \left(T^{(de)}_{\mu\nu} + T^{(dm)}_{\mu\nu}\right) . \tag{1.78}$$

Applying contracted Bianchi's identity on it, we have

$$\nabla_\mu \left(T^{\mu\nu}_{(de)} + T^{\mu\nu}_{(dm)}\right) = \nabla_\mu T^{\mu\nu}_{(de)} + \nabla_\mu T^{\mu\nu}_{(dm)} = 0, \tag{1.79}$$

where ∇_μ indicates the covariant derivative. In an interaction model, the total energy density of the dark sectors is conserved, however, they are not conserved separately. Hence the conservation equation is defined as

$$\nabla_\mu T^{\mu\nu}_{(i)} = Q^\nu_{(i)} , \tag{1.80}$$

where $Q^\nu_{(i)}$ is the four-vector of interaction indicating the transformation of energy-momentum tensor between the dark sectors, the subscript i is referred as $i = dm$ for dark matter component and $i = de$ for dark energy. As DE and DM are not separately conserved, from equation (1.79), the energy-momentum tensor $T^{\mu\nu}_{(de)}$ of DE transfers energy-momentum to or from the DM field $T^{\mu\nu}_{(dm)}$ such that

$$\nabla_\mu T^{\mu\nu}_{(de)} = -\nabla_\mu T^{\mu\nu}_{(dm)} = Q^\nu_{(i)} . \tag{1.81}$$

So, for DE and DM, we have

$$Q^\nu_{(dm)} = -Q^\nu_{(de)}.$$

In the spatially flat FLRW universe, the conservation equation for DM and DE read

$$\dot{\rho}_{dm} + 3H(1+\omega_{dm})\rho_{dm} = Q \ , \tag{1.82}$$
$$\dot{\rho}_{de} + 3H(1+\omega_{de})\rho_{de} = -Q \ . \tag{1.83}$$

Here, Q indicates the rate of energy density exchange between DM and DE, where

$$Q \begin{cases} > 0 \\ < 0 \end{cases} \implies \text{Energy exchange occurred} \begin{cases} DE \longrightarrow DM \\ DM \longrightarrow DE \end{cases}$$

We have mentioned that there are no guiding principles to choose the form of interaction in the dark sectors so any interaction model will necessarily be phenomenological, although some models give more realistic results than others, or are more convenient due to their mathematical simplicity. Various interaction models in terms of Q have been proposed in order to alleviate the coincidence problem. Linear and non-linear terms of Q are important amongst them.

The possible linear form of Q is $Q \equiv Q(H, \rho_{dm}, \rho_{de}, t)$. However, in view of coupling conservation equations (1.82), (1.83), the interaction Q can be thought to be the function of energy densities and other covariant quantities with unit of inverse of time, therefore, the time independent interaction will be required in place of the above term $Q = Hq(\rho_{dm}, \rho_{de})$. For this kind of factorization, the effect of coupling on the dynamics of energy densities ρ_{dm} and ρ_{de} become independent from the evolution of the Hubble scale H. These kinds of linear interactions are as follows:

$$Q = \alpha H \rho_{dm} \ [147,\ 151,\ 184,\ 185], \tag{1.84}$$
$$Q = \alpha H \rho_{de} \ [163,\ 186,\ 187], \tag{1.85}$$
$$Q = \alpha H(\rho_{dm} + \rho_{de}) \ [149,\ 152,\ 161], \tag{1.86}$$
$$Q = H(\alpha_{dm}\rho_{dm} + \alpha_{de}\rho_{de}) \ [163,\ 142,\ 188,\ 189,\ 190]. \tag{1.87}$$

Thus, linear interactions involve the linear form of ρ_{dm} and ρ_{de} or linear combination of both the energy densities.

Cosmological models with non-linear interactions (for a review, see [127], and references therein) have also gained much interest nowadays in the study of dark energy physics due to the fact that from the physical point of view the interaction should depend on both of their chemical or nuclear reactions also. The non-linear interaction is motivated by the structure formation of energy densities as [127]:

$$\rho_{dm} = \frac{r}{1+r}\rho, \quad \rho_{de} = \frac{1}{1+r}\rho, \quad r \equiv \frac{\rho_{dm}}{\rho_{de}}, \quad \rho = \rho_{dm} + \rho_{de} \ .$$

The general non-linear interaction term based upon the above can be formed as:

$$Q \propto H\rho_{de}^{m-n}\rho_{dm}^{n} \implies Q \propto H\rho_{de}^{m} r^{n} \ .$$

For different values of m and n, the interaction terms take the forms

$$Q \propto \frac{\rho_{dm}\rho_{de}}{\rho} , \tag{1.88}$$

$$Q \propto \frac{\rho_{dm}^2}{\rho}, \tag{1.89}$$

$$Q \propto \frac{\rho_{de}^2}{\rho}. \tag{1.90}$$

There are some interactions motivated from scalar tensor theories ([148, 191]) and also from local properties which have been shown in Ref. [125].

We have assumed here that in the equations (1.82) and (1.83), the dark components, *i.e.,* DM and DE are perfect fluids satisfying the barotropic equations of state, *i.e.,*

$$p_{dm} = \omega_{dm}\rho_{dm} , \tag{1.91}$$

$$p_{de} = \omega_{de}\rho_{de} . \tag{1.92}$$

Further, one can get the uncoupled form of equations (1.82) and (1.83) by introducing the effective equation of state parameters for both DM ($\equiv \omega_{dm,\ eff}$) and DE ($\equiv \omega_{de,\ eff}$) in the sense that the new system of equations represents the non-interacting scenario:

$$\dot{\rho}_{dm} + 3H\left(1 + \omega_{dm} - \frac{Q}{3H\rho_{dm}}\right)\rho_{dm} = 0 , \tag{1.93}$$

$$\dot{\rho}_{de} + 3H\left(1 + \omega_{de} + \frac{Q}{3H\rho_{de}}\right)\rho_{de} = 0 , \tag{1.94}$$

where the effective equation of state for both the dark components read as:

$$\omega_{dm,\ eff} = \omega_{dm} - \frac{Q}{3H\rho_{dm}} , \tag{1.95}$$

$$\omega_{de,\ eff} = \omega_{de} + \frac{Q}{3H\rho_{de}} . \tag{1.96}$$

It follows that

$$Q\begin{cases} > 0 \Longrightarrow \omega_{de,\ eff} > \omega_{de}, & \text{DE has less acceleration power} \\ < 0 \Longrightarrow \omega_{de,\ eff} < \omega_{de}, & \text{DE has more acceleration power} \end{cases}$$

However, concerning the late-time dynamics of the Universe, in general, one can neglect baryons due to its tiny presence as well as radiation too due to its very small percentage. For this, the Friedmann equation gives the constraint, $\Omega_{dm} + \Omega_{de} = 1$, and the total equation of state parameter is of the form

$$\omega_{tot} = \frac{p_{tot}}{\rho_{tot}} = \omega_{dm}\Omega_{dm} + \omega_{de}\Omega_{de} , \tag{1.97}$$

while the energy conservation equation for the total matter is

$$\dot{\rho_{tot}} + 3H(1+\omega_{tot})\rho_{tot} = 0. \tag{1.98}$$

1.4 Cosmological models from gravity modification

The most puzzling issue in modern cosmology is related to the present accelerating phase of the Universe leading to a new imbalance in the governing field equations. If General Relativity theory is the correct gravity theory in an averaging cosmological scale, the standard cosmological models intend to address such imbalance by introducing a new matter component (entitled as DE) in the energy-stress tensor (right hand side) of Einstein's field equation in that scale. The new matter source (DE) with a huge negative pressure is parameterized by the equation of state $\omega = \frac{p}{\rho}$ and hence, the GR equations change to the form

$$G_{\mu\nu} = \kappa^2(T_{\mu\nu} + T^{new}_{\mu\nu}).$$

Now, from the Friedmann equation and the acceleration equation, the condition for acceleration of the Universe is $\omega < -\frac{1}{3}$. Various DE models have been studied which satisfy this relation. Many of them have serious problems which forces us to think of other models.

On the other hand, a group of physicists have explored the second possibility and modify the geometric part (left hand side) of the Einstein's equations on very large scales ($r > H_0^{-1}$) have been introduced to justify the presently observed accelerating universe [192, 193, 194]. In this case, the field equations are modified as [98]

$$G_{\mu\nu} + G^{new}_{\mu\nu} = \kappa^2 T_{\mu\nu} \ .$$

It should be noted that at large scales, Einstein's theory of GR breaks down and a more general action is needed to describe the gravitational field. It is well known that the Einstein's field equations were first derived from the Hilbert action with a linear function of the Ricci scalar R (curvature scalar) in gravitational Lagrangian density. The action in GR can be presented as

$$S \ = \ \frac{1}{2\kappa^2}\int \sqrt{-g}\ d^4x\ R + \int \sqrt{-g}\ d^4x\ L_m \ . \tag{1.99}$$

However, there are no guiding principles to restrict the gravitational Lagrangian to the form in (1.99), rather several attempts have been taken to generalize the Einstein-Hilbert Lagrangian. As for example, the generalization may include the quadratic Lagrangians involving second order curvature invariants such as R^2, $R_{\mu\nu}R^{\mu\nu}$, $R_{\alpha\beta\mu\nu}R^{\alpha\beta\mu\nu}$, $\epsilon^{\alpha\beta\mu\nu}R_{\alpha\beta\nu\delta}R^{\nu\delta}{}_{\mu\nu}$, $C_{\alpha\beta\mu\nu}C^{\alpha\beta\mu\nu}$ etc. (see [195] and references therein). Thus, for modified gravity theories, the Ricci scalar R inside the action (1.99) should be transformed to an arbitrary function $f(R)$. These modified gravity theories include f(R)- gravity, Scalar tensor gravity, Einstein-Gauss-Bonnet gravity, Brane world gravity and many others [38, 39, 40, 41, 196, 197, 198, 199, 200, 201, 202, 203, 204, 205, 206, 207, 208, 209, 210, 211]. As of now a

number of works has been suggested in the context of $f(R)$ gravity [38, 41, 198, 208, 212, 213, 214, 215, 216, 217, 218].

1.4.1 $f(R)$ gravity and Cosmology

A more general modification of Einstein-Hilbert action in the gravitational Lagrangian (1.99) should be an involvement of an arbitrary function of R which is $f(R)$ first considered in [217] and it is then developed in [200, 201, 219]. Recently, several authors have explored their investigations of $f(R)$ modified theories of gravity explaining the accelerated expansion of the Universe [38, 214]. The most general action for the $f(R)$ gravity theory is

$$S = \frac{1}{2\kappa^2}\int d^4x\sqrt{-g}\; f(R) + S_m, \tag{1.100}$$

where $S_m = \int \sqrt{-g}\; d^4x\; L_m$, L_m is the matter Lagrangian, S_m indicates the action of the matter sector, and standard Einstein-Hilbert action is replaced by an arbitrary function of Ricci scalar R given by

$$R = g^{\mu\nu}\left(\partial_\lambda\Gamma^\lambda_{\mu\nu} - \partial_\nu\Gamma^\rho_{\mu\rho} - \Gamma^\sigma_{\sigma\nu}\Gamma^\sigma_{\mu\lambda} + \Gamma^\rho_{\mu\rho}g^{\mu\nu}\Gamma^\sigma_{\mu\nu}\right) \tag{1.101}$$

with the Christoffel symbol

$$\Gamma^k_{\mu\nu} = \frac{1}{2}g^{k\lambda}\left(\partial_\mu g_{\lambda\nu} + \partial_\nu g_{\lambda\mu} - \partial_\lambda g_{\mu\nu}\right)\ . \tag{1.102}$$

There are two possibilities in order to obtain the field equations from the given action (1.100) of $f(R)$ gravity– one is by varying the action (1.100) with respect to the metric tensor $g_{\mu\nu}$ defined as metric formalism where the Christoffel symbol (affine connection) $\Gamma^\alpha_{\beta\nu}$ depends on the metric $g_{\mu\nu}$. The second is the Palatini formalism [220] – different from the first approach. Here, $g_{\mu\nu}$ and $\Gamma^\alpha_{\beta\nu}$ are assumed to be independent variables when the action is varied. These two approaches give different field equations.

Now, in metric formalism, one obtains the field equation

$$f'(R)R_{\mu\nu} - \frac{1}{2}f(R)g_{\mu\nu} - \nabla_\mu\nabla_\nu f'(R) + g_{\mu\nu}\nabla^\alpha\nabla_\alpha f'(R) = \kappa^2 T^{\mathbf{m}}_{\mu\nu}\ , \tag{1.103}$$

where $f'(R) = \frac{\partial f(R)}{\partial R}$ and $T^{\mathbf{m}}_{\mu\nu}$ is the energy-momentum tensor arising from the matter action S_m. For the flat FLRW metric, the field equations (1.103) lead to the Friedmann equation

$$-18\left[4H^2\dot{H} + H\ddot{H}\right]f''(R) + 3\left[H^2 + \dot{H}\right]f'(R) - \frac{f(R)}{2} + \kappa^2\rho = 0, \tag{1.104}$$

where ρ is the total energy density of the matter field while the calculated Ricci scalar is given by

$$R = 6(2H^2 + \dot{H}). \tag{1.105}$$

It is worth mentioning that, motivated from the inflationary scenario, Starobinsky in 1980 [199] proposed an $f(R)$ model with $f(R) = R + \alpha R^2$ $(\alpha > 0)$ which provides an early accelerated expansion of the Universe due to the presence of the term αR^2. After the discovery of DE and DM, models based on $f(R)$ theories have been extensively studied in order to realize the late time acceleration of the Universe as an alternative theory of DE. Further, the model with Lagrangian density $f(R) = R - \frac{\alpha}{R^n}$, $(\alpha > 0, \quad n > 0)$ was proposed for DE in the metric formalism [41, 208, 212, 221, 222] (see the review [214] on $f(R)$ theories).

1.4.2 f(T) gravity and cosmology

Modified gravity theory is popular for explaining the acceleration of the Universe without need of dark energy. Several modified gravity theories have been proposed to address this fact. Among them, $f(T)$ gravity theory is the attractive one. Let us now start with the discussion of $f(T)$ gravity theory.

- **f(T) gravity:**

The torsion based gravity modified from the Teleparallel Equivalent of General Relativity (TEGR) allows us to construct the extension of gravity theory named as $f(T)$ gravity theory, where the Lagrangian is the torsion scalar T rather than the curvature scalar R. Here, in the underlying manifold $(\mathcal{M}, g_{\mu\nu})$, the basic dynamical object is the vierbein e^{μ}_{A} forming an orthonoraml basis[4] at each point x^{μ} of the manifold of tangent space which defines the metric tensor $g_{\mu\nu}$ as

$$g_{\mu\nu} = \eta_{AB} e^{A}_{\mu} e^{B}_{\nu} \tag{1.106}$$

on this manifold[5], where $\eta_{AB} = diag(+1, \ -1, \ -1, \ -1)$; $e_A.e_B = \eta_{AB}$. Also, torsion-less Levi-Civita connection with Einstein-Hilbert action replaces the curvature-less Weitzenböck connection defined as [249, 250]

$$\overset{\mathbf{w}}{\Gamma}{}^{\lambda}_{\nu\mu} \equiv e^{\lambda}_{A} \partial_{\mu} e^{A}_{\nu} \ , \tag{1.107}$$

where the gravitational field is described by the following torsion tensor

$$T^{\rho}_{\mu\nu} \equiv e^{\rho}_{A} \left(\partial_{\mu} e^{A}_{\nu} - \partial_{\nu} e^{A}_{\mu} \right) \ , \tag{1.108}$$

where $T^{\rho}_{\mu\nu} = \overset{\mathbf{w}}{\Gamma}{}^{\rho}_{\nu\mu} - \overset{\mathbf{w}}{\Gamma}{}^{\rho}_{\mu\nu}$. Moreover, the torsion scalar T is generalized from the contraction of torsion tensor as [250, 251, 252]

[4] e^{μ}_{A}, $(\mu = 0, 1, 2, 3)$ are components of the vierbein field $e_A(x^{\mu})$, $(A = 0, 1, 2, 3)$ in a coordinate basis, *i.e.*, $e_A = e^{\mu}_{A} \partial\mu$

[5] where Greek indices label the coordinate of manifold and Latin indices refers to tangent space.

$$T \equiv \frac{1}{4}T^{\rho\mu\nu}T_{\rho\mu\nu} + \frac{1}{2}T^{\rho\mu\nu}T_{\nu\mu\rho} - T^{\rho}_{\rho\mu}T^{\nu\mu}_{\nu} \ . \tag{1.109}$$

Now, one can extend T to a generalized function $T + f(T)$ as in $f(R)$ modified gravity theory. The action for this model is [211, 253]

$$S = \frac{1}{2\kappa^2}\int d^4x\ e\left[T + f(T)\right] \ , \tag{1.110}$$

where $e = det(e^A_\mu) = \sqrt{-g}$. It should be mentioned that for $f(T) = 0$ in equation (1.110), the general relativity is recovered, while for $f(T) =$ constant, GR is recovered with a cosmological constant (see for instance [254] and references therein).

- **f(T) cosmology:**

Let us consider the cosmological model of the Universe to be governed by $f(T)$ gravity theory. In this theory, the idea is the generalization of torsion scalar T to T plus $f(T)$ which is similar to the $f(R)$ theory as it is an extension of Ricci scalar R in Einstein-Hilbert action. In $f(T)$ gravity, the generalized action reads

$$S = \frac{1}{2\kappa^2}\int d^4x\ e\left[T + f(T)\right] + S_m \ , \tag{1.111}$$

where S_m is the matter action. We have the equation of motion from the variation of the action (1.111) with respect to the vierbein

$$\begin{aligned} e^{-1}\partial_\mu\left(ee^\rho_A S^{\mu\nu}_A\right)\left[1 + f'(T)\right] - e^\lambda_A T^\rho_{\mu\lambda}S^{\nu\mu}\left[1 + f'(T)\right] + \\ e^\rho_A S^{\mu\nu}_\rho \partial_\mu(T)f''(T) + \frac{1}{4}e^\nu_A\left[T + f(T)\right] = \frac{\kappa^2}{2}e^\rho_A\left[\overset{\mathbf{em}}{T}{}^\nu_\rho\right], \end{aligned} \tag{1.112}$$

where $\overset{\mathbf{em}}{T}{}^\nu_\rho$ on the r.h.s of the equation (1.112) indicates the usual energy-momentum tensor satisfying the perfect fluid model in equation (1.3). Let us now consider the opposite signature metric to describe the scenario of $f(T)$ cosmology. The common choice of vierbein considering the homogeneous and isotropic geometry is

$$e^\mu_A = \mathrm{diag}(1,\ a(t),\ a(t), a(t)) \ , \tag{1.113}$$

and this leads to flat FLRW background metric of the form

$$ds^2 = dt^2 - a^2(t)\delta_{ij}dx^i dx^j \ , \tag{1.114}$$

$a(t)$ is the scale factor. Now, for a perfect fluid model of the constituents of the Universe, using the vierbein (1.113) in the field equation (1.112), one obtains the background (Friedmann) equation as

$$H^2 = \frac{\kappa^2}{3}\rho_m - \frac{f(T)}{6} - 2f'(T)H^2 \tag{1.115}$$

and the acceleration equation as

$$\dot{H} = -\frac{\kappa^2}{2}\frac{(\rho_m + p_m)}{[1 + f'(T) - 12H^2 f''(T)]} , \tag{1.116}$$

where we have used the relation $T = -6H^2$ [255]. There are some recent works in $f(T)$ gravity and cosmology in references [256, 257, 258, 259].

1.4.3 f(R,T) gravity

Let us introduce another gravity theory which is a mixture of both R and T, namely, $f(R,T)$ gravity theory. This gravity theory is a modified gravity theory extended from the general relativity theory. This simple theoretical model is based on the replacement of Einstein-Hilbert action by an arbitrary function of Ricci scalar known as $f(R)$ gravity theory. Consequently, $f(T)$ gravity theory is also proposed as a modified theory of GR. These two models can successfully explain the present acceleration which we have discussed earlier in this section.

In $f(R,T)$ gravity, the gravitational Lagrangian is a function of the Ricci scalar R and the trace of the stress-energy tensor T. The most general action for this modified gravity theory is the following [260]:

$$S = \frac{1}{2\kappa^2}\int f(R,T)\sqrt{-g}d^4x + \int L_m\sqrt{-g}d^4x , \tag{1.117}$$

where $f(R,T)$ is an arbitrary function of R and T. Here, R is the Ricci curvature scalar and T is the trace of the stress-energy tensor [260] of matter $T_{\mu\nu}$ (or, sometimes T indicates the torsion of space-time [261, 262, 263]). L_m is the matter lagrangian density. The stress-energy tensor for the matter is given by [264]

$$T_{\mu\nu} = -\frac{2}{\sqrt{-g}}\frac{\delta\left(\sqrt{-g}L_m\right)}{\delta g^{\mu\nu}} \tag{1.118}$$

and the trace is $T = g^{\mu\nu}T_{\mu\nu}$. The model with $f(R,T)$ gravity can successfully provide an acceleration of the universe [265, 266].

1.5 Gravitational particle creation and Thermodynamics

In Cosmology, particle creation mechanism plays a crucial role in explaining many cosmic scenarios, mainly the present acceleration of the Universe without the need of DE. Let us

now present a brief review of particle creation mechanism from the thermodynamics point of view and how a cosmological model changes due to the effect of this mechanism.

We shall first discuss the terms related to thermodynamics, and its basic laws. In thermodynamics, a *system*[6] is described as any part of matter large enough to be described by macroscopic parameters. A *open system* can exchange matter as well as energy with the surroundings whereas a *closed system* can only exchange its energy with the surroundings, but not matter. For the case of an *isolated system*, neither matter nor energy can be exchanged with the surroundings. A *system* can be identified by its many properties such as mass, internal energy etc. Internal energy of a *system* is an *extensive* property which depends on the mass of the system whereas *intensive* property is mass independent. So, internal energy of a system depends upon the state of the system. Any thermodynamic state can be described as (P,V,T), where P is the pressure, V is the volume, and T is the temperature of the system. So, for a particular state, internal energy is definite. A thermodynamical system is said to be in *thermodynamical equilibrium* state when it satisfies the conditions of mechanical, chemical, and *thermal equilibrium* [7]. If any one of them fails, then it is in non-equilibrium state. In a thermodynamical equilibrium state, the equation of state is described as $f(P, V, T) = 0$ with the state parameters P,V, and T, and it reduces the number of independent parameters by one.

1.5.1 Thermodynamics at a glance

Let us start with the laws of thermodynamics that play very important role in constructing several cosmological models.

1.5.1.1 Zeroth law of thermodynamics:

This law is related to the thermal equilibrium of a system. The law states that if any system A is in thermal equilibrium with another system B and B is in thermal equilibrium with a third system C, then the systems A and C are in thermal equilibrium. That is according to Zeroth law, thermal equilibrium satisfy the transitive property.

1.5.1.2 First law of thermodynamics:

This law is related to the conservation of energy. That is, if heat flows in between two systems A and B, then according to the first law, the heat absorbed by A is equal to the transmission of heat by B, and this fact assigns the definition of 'temperature'. We have stated before that the internal energy of a system is a definite function of its state. The sate can be changed by a flow of heat in a system, and eventually, it increases the internal energy to perform work. Thus, when a particular process takes place, the energy conservation has the following form (for infinitesimal changes):

$$dE = dQ + dW \ , \tag{1.119}$$

[6] Usually, a system is a region within an arbitrary boundary.

[7] Note that thermodynamical and thermal equilibrium are different. Thermal equilibrium is related to heat only. This equilibrium describe the state in which two or more systems are communicate through a diathermic wall (which allows the transmission of heat only.)

where dE is the infinitesimal increment of internal energy, dQ is the heat flow into the system, and dW is the work done by the system on the environment (surroundings). Let us consider a system in a gaseous medium which has the state parameters p and V as the pressure and the volume respectively. For a 'quasi-static'[8] or 'adiabatic' condition with a particular pressure 'p', the increment of volume 'dV' is related to quantity 'dW' (work done by the system) as $dW = -pdV$, which implies that

$$dE = dQ - pdV \ , \tag{1.120}$$

and this is the mathematical formulation of the first law of thermodynamics.

1.5.1.3 Second law of Thermodynamics:

The second law of thermodynamics is based on the idea of 'entropy' ('S') changes in the system. As internal energy 'E' and heat 'H' are the functions of the system, entropy 'S' is also a function of system. Entropy depends on the mass of the system. The term 'entropy' was first introduced by Clausius and according to him, it measures the disorder of the system such that when gas expands in an empty space cannot be brought back to its original form with decreasing entropy. He also thought that " the energy of the universe is constant and the entropy of the universe tends to a maximum". When a system absorbs heat, the entropy increases, while it decreases for releasing heat. Now, for an irreversible process, the level of disorder always increases, and it tends to a maximum. So, entropy increases always for an irreversible process. Also, the change in entropy depends only on the initial state and the final state of the system. The change in entropy is described by the following relation:

$$dS = \frac{dQ}{T} \ , \tag{1.121}$$

where dQ is the heat flow into the system from environment and T is a particular temperature of the thermodynamic system. We put the statements of second law of thermodynamics of Clausius and Kelvin as:

Clausius statement: "There exists no thermodynamic transformation whose sole effect is to transfer heat from a colder reservoir to a warmer reservoir."

Kelvin statement: "There exists no thermodynamic transformation whose sole effect is to extract heat from a reservoir and to convert that heat entirely into work."

So, for an irreversible process, the second law of thermodynamics states that the entropy of a system is ever increasing (even it may be constant, but not decreasing) *i.e.*,

$$dS \geq 0 \ . \tag{1.122}$$

Now using (1.121) and (1.120), one arrives at

[8] Quasi-static process takes place so slowly that the system will always stay nearly in equilibrium.

$$TdS = dE + pdV \ , \tag{1.123}$$

which gives a mathematical derivation of the second law of thermodynamics.

1.5.2 Thermodynamics in FLRW Cosmology

When thermodynamics is considered, we naturally employ some thermodynamic variables, such as the entropy, temperature and some others, that often characterize the state of a cosmological model. Since the geometry of our universe is perfectly described by a FLRW universe, so we shall focus our discussions in such a universe. In particular, we shall consider the spatial flat case where the fluid distributions take perfect fluid orientation $T^{\alpha\beta} = (p + \rho)u^{\alpha}u^{\beta} + pg^{\alpha\beta}$.

in which p is the thermodynamic pressure and ρ is the energy density of the perfect fluid having four velocity vector u^{α}. The particle flow vector N^{α} is given by

$$N^{\alpha} = nu^{\alpha} \ , \tag{1.124}$$

where n is the particle number density. Considering the thermodynamically reversible process without dissipative phenomena in which the particle number is conserved because there are no unbalanced creation or annihilation processes, by (1.124), the covariant form of particle conservation is [267]

$$N^{\alpha}_{;\alpha} = 0 \iff \dot{n} + 3Hn = 0 \ , \tag{1.125}$$

that means $na^3 =$ co-moving const. Similarly, the perfect fluid follows the conservation law reads $T^{\alpha\beta}_{;\beta} = 0 \implies \dot{\rho} + 3H(\rho + p) = 0$. So clearly, when the particle creation is not allowed, then the basic equations remain unaltered. Now, let us see the effects of the main dynamical equations when the backgrund universe allows particle creation by the time varying gravitational field.

In an adiabatic (or isentropic) system the specific entropy (entropy per particle) is also conserved, so that $\dot{s} = 0$, so 's' is constant for each fluid particle. It should be mentioned that s is constant along fluid particle worldlines, and not throughout the fluid in general. The temperature is defined via Gibbs' equation

$$Tds = d\left(\frac{\rho}{n}\right) + pd\left(\frac{1}{n}\right) \ . \tag{1.126}$$

So, in thermodynamic equilibrium state, perfect fluids do not generate entropy and no frictional type heating, because their dynamics is reversible and without dissipation. On the other hand, a perfect fluid model is sufficient for many processes in cosmology and astrophysics, but real fluids behave irreversibly, and some processes in cosmology and astrophysics cannot be understood except as dissipative processes, requiring a relativistic theory of dissipative fluids. However, to model such processes, we require nonequilibrium or irreversible thermodynamics, and perhaps the most satisfactory approach to irreversible thermodynamics is via nonequilibrium kinetic theory [267].

Eckart, in 1940 [268], first extended the standard, or classical, irreversible thermodynamics from Newtonian to relativistic fluids. Now, for non-equilibrium, irreversible process of perfect fluid model can be applied to cosmology. Here, we consider the cosmic matter component to be characterized by the energy momentum tensor of a bulk viscous fluid [269]

$$T^{\alpha\beta} = \rho u^{\alpha} u^{\beta} + (p + \Pi) h^{\alpha\beta} , \tag{1.127}$$

and the particle flow vector N^{α} has the form (1.124). Here, $h^{\alpha\beta} = g^{\alpha\beta} + u^{\alpha}u^{\beta}$ is the spatial projection tensor, and the quantity Π is the dissipative term which denotes that part of the scalar pressure which is connected with entropy production. The dynamical effective pressure in presence of viscous fluid becomes $p_{eff} = p + \Pi$. Usually, Π is termed as the so-called bulk viscous pressure. In cosmological context, it has a significant role when particle number is not conserved and for this case, Π is called as creation pressure (here $p_c \equiv \Pi$) [270]

It is to be noted that there is a restriction $|\Pi| < p$ (correction to the thermostatic pressure) near to equilibrium. But this restriction can be neglected by using it as creation pressure (p_c). In irreversible thermodynamics, the entropy is no longer conserved, but grows, according to the second law of thermodynamics. So, for particle production/annihilation, the conservation of the particle flux vector satisfies $N^{\alpha}_{;\alpha} \neq 0$, that means

$$\dot{n} + 3Hn = n\Gamma , \tag{1.128}$$

where Γ describes the rate of particle creation or annihilation. That is, the creation of particles take place when $\Gamma > 0$, while particle annihilation occur for $\Gamma < 0$. For $\Gamma = 0$, the particle number is conserved.

Now, the Friedmann equations in a flat FLRW cosmology are essentially modified (including the creation pressure) as

$$H^2 = \frac{\kappa^2}{3}\rho, \tag{1.129}$$

$$2\dot{H} = \frac{\kappa^2}{3}(\rho + p + \Pi), \tag{1.130}$$

However, using (1.129) and (1.130), one can derive the conservation equation $\dot{\rho} + 3H(\rho + p + \Pi) = 0$.

Now using (1.128) in (1.126), the variation of the entropy is given as

$$nT\dot{s} = -3H\Pi - \Gamma(\rho + p), \tag{1.131}$$

which, for an adiabatic condition, turns out to be

$$\Pi = -\frac{\Gamma}{3H}(\rho + p). \tag{1.132}$$

Thus, for an adiabatic thermodynamical system, the dissipative pressure is determined by the particle creation rate. In this connection, one important thing to be pointed out is that,

sometimes, the expression (1.132) is written as $p_c = -\frac{\Gamma}{3H}(\rho + p)$ in terms of the creation pressure (p_c) which can be obtained in the framework of the so-called first-order non-equilibrium relativistic thermodynamics. But several authors have formulated relativistic second-order theories which circumvent some theoretical difficulties of the first order approach. (see [271] and references therein).

1.6 Dynamical system analysis

Dynamical system is a mathematical way out to realize the evolution of a point in physical state space. Using the dynamical systems tools, the evolution of any particle can be visualized in any space or state space (phase space) clearly. By the term 'state' of the system, one can realize position of a point, more precisely, the coordinate of a point in the system. For example, in a physical system in thermodynamics, the triplet (P, V, T) describes the state of a certain quantity of a gas, denoted here by $\mathbf{X}$, at any time t. Let us consider from now, $\mathbf{x}$ is the state (element) of the physical system and state space or phase space $\mathbf{X}$ is considered as the set of all states at an instant of time t in that system. Note that in Mathematics, Euclidean space $\mathbb{R}^n$ or its open subset can be treated as phase space. In this thesis, we closely follow Refs. [1, 272] to present dynamical system analysis. Interested readers may follow the famous books on dynamical systems [273, 274, 275, 276, 277, 278, 279] and also related articles [280, 281, 282]. The dynamical system is the evolution of any point $\mathbf{x}$ in space $\mathbf{X}$ which may be described by a system of Ordinary Differential Equations (ODEs)

$$\dot{\mathbf{x}} \equiv \frac{d\mathbf{x}}{dt} = \mathbf{f}(\mathbf{x}, t) \ , \tag{1.133}$$

where $t \in \mathbb{R}$ and $\mathbf{x} = (x_1, x_2, ..., x_n) \in \mathbb{R}^n$ at any point/ state in the phase space of the dynamical system (1.133). Here, 'over dot' denotes differentiation with respect to time 't'. Also, the function $\mathbf{f} : \mathbb{R}^{n+1} \longrightarrow \mathbb{R}^n$ can be interpreted as the vector field on $\mathbb{R}^n$ where $\mathbf{f} = (f_1, f_2, ..., f_n)$ is at least of class C^1 (continuously differentiable). Therefore, when a physical system evolves with time is referred to as a dynamical system. Dynamical system is of two types: continuous dynamical system and discrete dynamical system. Here, our study is only with the continuous dynamical system.

1.6.1 Autonomous System

Any system of differential equation is called an autonomous system of ordinary differential equations when $\mathbf{f}$ is explicitly time independent, *i.e.*, the dynamical system (1.133) is said to be autonomous if $\mathbf{f}$ on r.h.s is a function of $\mathbf{x}$ only and does depend on time t. Thus, the autonomous system of ODEs for the given dynamical system (1.133) can be rewritten as

$$\dot{\mathbf{x}} \equiv \frac{d\mathbf{x}}{dt} = \mathbf{f}(\mathbf{x}) \ , \quad \mathbf{x} \in \mathbb{R}^n. \tag{1.134}$$

The system can ne expressed as

$$\begin{aligned} \dot{x_1} &= f_1(x_1, x_2, ...x_n), \\ \dot{x_2} &= f_1(x_1, x_2, ...x_n), \\ &. \\ &. \\ \dot{x_n} &= f_1(x_1, x_2, ...x_n). \end{aligned} \tag{1.135}$$

1.6.1.1 Solution and orbit of an Autonomous System

The solutions of the system (1.134) can be expressed as a differentiable function $\psi : \mathbb{R} \longrightarrow \mathbb{R}^n$ satisfying $\dot{\psi}(t) = \mathbf{f}(\psi(t))$ for all $t \in \mathbb{R}$. This solution ψ represents a curve in $\mathbb{R}^n$ with tangent vector $\dot{\psi}(t)$ which is equal to $\mathbf{f}(\psi(t))$ (from (1.134)). The image of a solution in $\mathbb{R}^n$ is referred to as an orbit of the DE. The motion of state vector $\mathbf{x} \in \mathbb{R}^n$ along the orbit represents the evolution of the associated physical system in time. Thus, the DE reveals that the vector field $\mathbf{f}(\mathbf{x})$ is a tangent to the orbit and so, this can be realized as the velocity of the moving point in state space.

Now, we state (without proof) the existence and uniqueness of the solution of ODE with the given initial conditions $\mathbf{x} = \mathbf{x}_0$ at $t = t_0$. The theorem states that:
considering the system (1.134) with the initial conditions

$$\dot{\mathbf{x}} = \mathbf{f}(\mathbf{x}) \ , \quad \mathbf{x}(\mathbf{0}) = \mathbf{x}_0 \in \mathbb{R}^n \tag{1.136}$$

with $\mathbf{f} : \mathbb{R}^n \longrightarrow \mathbb{R}^n$ is of class C^1 and for all $\mathbf{x}_0 \in \mathbb{R}^n$ there exists an interval $(-\delta, \delta)$ and a unique function $\psi(\mathbf{x}_0) : (-\delta, \delta) \longrightarrow \mathbb{R}^n$ satisfies the relation

$$\dot{\psi}(t; \mathbf{x}_0) = \mathbf{f}(\psi(t, \mathbf{x}_0)) \ ; \quad \psi(0, \mathbf{x}_0) = \mathbf{x}_0. \tag{1.137}$$

Flow:

Let us assume the autonomous system of ODEs (1.134) is valid having solutions for all $t \in \mathbb{R}$. The flow of (1.134) can be defined as one parameter family of maps $\{\phi_t\}_{t\in\mathbb{R}}$ from $\mathbb{R}^n$ into itself such that

$$\phi_t(\mathbf{x}_0) = \psi(t; \mathbf{x}_0) \ , \quad \forall \ \ \mathbf{x}_0 \in \mathbb{R}^n \ , \tag{1.138}$$

where $\psi(t; \mathbf{x}_0)$ is the solution of the initial value problem (1.136). So, the flow ϕ_t is defined in terms of the solution functions $\psi(t; \mathbf{x}_0)$. Now, for a specific time t, the flow $\phi_t : \mathbb{R}^n \longrightarrow \mathbb{R}^n$ provides the state of the system $\psi = \phi_t(\mathbf{x}_0)$ for all initial states $\mathbf{x}_0$. On the other hand, an orbit $\psi(t; \mathbf{x}_0)$ passing through $\mathbf{x}_0$ can also be defined from the flow as

$$\psi(t; \mathbf{x}_0) = \{\mathbf{x} \in \mathbb{R}^n \mid \mathbf{x} = \phi_t(\mathbf{x}_0), \quad t \in \mathbb{R}\} \ . \tag{1.139}$$

Thus, we see that the ODEs (1.134) produce a flow and vice versa, *i.e.*, $\dot{\mathbf{x}} = \mathbf{f}(\mathbf{x}) \longleftrightarrow \{\phi_t\}_{t\in\mathbb{R}}$. It can also be seen that the flow of ODEs (1.134) can hold the group property.

Now, to achieve the qualitative behavior of the solutions of the system of differential equations which is our main goal in this thesis, we have to find out the flow of the given system since it is equivalent to the solutions. Thus, the flow of the system may be a powerful tool to analyze the qualitative behavior as the properties of flow can be derived by studying the vector field $\mathbf{f}$. For this, we have to find out the critical points of this system at first.

1.6.1.2 Critical Points of an Autonomous System

To get a qualitative idea about the solutions of ODEs (1.134), one has to find out the critical points (sometimes called equilibrium points or fixed points) of the system. A critical point of the system (1.134) is defined as a point (in phase space) $\mathbf{x} = \mathbf{x}_c \in \mathbb{R}^n$ for which

$$\mathbf{f}(\mathbf{x}_c) \quad = \quad \mathbf{0} \ , \tag{1.140}$$

or the zeros of the vector field $\mathbf{f}$ in the ODE $\dot{\mathbf{x}} = \mathbf{f}(\mathbf{x})$, or equivalently, one may define the critical point $\mathbf{x}_c$ as that which satisfies $\phi_t(\mathbf{x}_c) = x_c \quad \forall \ t \in \mathbb{R}$, where ϕ_t is the flow of the ODEs (1.134). The fixed point $\mathbf{x}_c$ in a physical system shows its equilibrium state because it does not change with time, *i.e.*, $\mathbf{f}(\mathbf{x}_c) = \mathbf{0}$ or equivalently, $\mathbf{x}_0$ is unchanged by the action of flow. Mathematically, in follows from equation (1.139) that the orbit through the equilibrium point is the point itself

$$\psi(t, \mathbf{x}_0) \quad = \quad \{\mathbf{x}_0\} \ . \tag{1.141}$$

• An orbit connecting different equilibrium points is referred to as a heteroclinic orbit. On the other hand, an orbit connecting equilibrium points to itself is called a homoclinic orbit.

In this thesis, we wish to apply the dynamical system approach to cosmological models using the known technique. In a cosmological model, there are governing equations which are highly nonlinear in nature and it is not quite possible to derive the solutions in analytic form. Therefore, one has to convert them to a system of ODEs or an autonomous system, and by finding the critical points of the system, the local properties of flow near the critical points can be realized by linearizing the system (ODEs) in the neighbourhood of the points. That is, the idea about the stability of the critical points and for that one must have the idea to linearize the system about the point. For that, we use the Hartman-Grobman theorem to relate the linear and non-linear differential equations.

A linear system of ODEs can be obtained from the system (1.134) by replacing the nonlinear function $\mathbf{f}(\mathbf{x})$ (on the r.h.s of (1.134)) as a linear function, *i.e.*, $\mathbf{f}(\mathbf{x}) = \mathbf{A}\mathbf{x}$, where $\mathbf{A}$ is a matrix of order $n \times n$. Therefore, the linear system of ODEs (for the non-linear system (1.134)) can be expressed as

$$\dot{\mathbf{x}} \quad = \quad \mathbf{A}\mathbf{x} \tag{1.142}$$

on $\mathbb{R}^n$ and the flow for the linear ODEs (1.142) is defined as

$$\phi_t(\mathbf{x}) \quad = \quad e^{At}\mathbf{x} \ \ \forall \ \ t \in \mathbb{R}, \quad \mathbf{x} \in \mathbb{R}^n. \tag{1.143}$$

1.6.2 Linear Stability Theory

Let $\mathbf{x} = \mathbf{x}_c$ be the critical point of the system (1.134). We shall now linearize the system around the critical point $\mathbf{x} = \mathbf{x}_c$ by using Taylor series expansion such that

$$\mathbf{f}(\mathbf{x}) \approx \mathbf{f}(\mathbf{x}_c) + \frac{\mathbf{f}'(\mathbf{x})}{1!}(\mathbf{x} - \mathbf{x}_c) + \frac{\mathbf{f}''(\mathbf{x})}{2!}(\mathbf{x} - \mathbf{x}_c)^2 + ... \tag{1.144}$$

i.e.,

$$\mathbf{f}(\mathbf{x}) \approx \mathbf{Df}(\mathbf{x}_c)(\mathbf{x} - \mathbf{x}_c), \tag{1.145}$$

where

$$\mathbf{Df}(\mathbf{x}_c) = \left(\frac{\partial f_i}{\partial f_j}\right)_{\mathbf{x}=\mathbf{x}_c}, \quad i = 1, 2, ..n; \quad j = 1, 2, ..n \tag{1.146}$$

is called as Jacobian of $\mathbf{f}(\mathbf{x})$ at $\mathbf{x}_c$. Now, we consider a perturbation near the critical point as $\mathbf{u} = \mathbf{x} - \mathbf{x}_c$. Let us assume that the perturbation $\mathbf{u}$ is very small, so we neglect the square and higher powers of it. Therefore, the system (1.134) can be expressed as

$$\dot{\mathbf{u}} = \mathbf{Df}(\mathbf{x}_c)\mathbf{u}. \tag{1.147}$$

Further, if we assume (1.134) is linear in form (when $\mathbf{f}$ is linear), it can be written as $\mathbf{f}(\mathbf{u}) = \mathbf{Au}$ (as in (1.142)) for $\mathbf{u} \in \mathbb{R}^n$. The derived linear dynamical system will be of the form

$$\dot{\mathbf{u}} = \mathbf{Au}. \tag{1.148}$$

Since $\mathbf{Df}(\mathbf{x}_c)$ is actually a $n \times n$ matrix with constant coefficients, ODE (1.147) represents a linear dynamical system. Now, for a linear dynamical system (1.148), the general solution with the initial conditions $\mathbf{u}(t_0) = \mathbf{u}_0$ will be

$$\mathbf{u}(t) = \mathbf{u}_0 e^{\mathbf{A}(t-t_0)}, \tag{1.149}$$

where the exponential matrix of $\mathbf{A}$ is given by

$$e^{\mathbf{A}(t-t_0)} = \sum_{N=0}^{\infty} \frac{\mathbf{A}^N (t-t_0)^N}{N!}. \tag{1.150}$$

$$\tag{1.151}$$

• Local behavior near the critical points

To get information about solutions near the critical points of the autonomous system, we have linearized the system near the points and then considering the eigenvalues (complex in

general) λ_i and the associated eigen vectors, we have the following three subspaces of $\mathbb{R}^n$:

The stable subspaces $E^s = \text{span } (e_1, e_2, ...e_s)$
The unstable subspaces $E^u = \text{span } (e_{s+1}, e_{s+2}, ...e_{s+u})$
The centre subspaces $E^s = \text{span } (e_{s+u+1}, e_{s+u+2}, ...e_{s+u+c})$,

where the eigenvectors $\{e_1, e_2, ...e_s\}$ in E^s is derived from the linearized Jacobian matrix corresponding to the eigenvalues λ_i having negative real parts form the stable subspaces in $\mathbb{R}^n$ whereas $\{e_{s+1}, e_{s+2}, ...e_{s+u}\}$ are the eigenvectors of $\mathbf{A}$ corresponding to the eigenvalues λ_i with positive real parts which form the unstable subspaces. Finally, the eigenvectors $\{e_{s+u+1}, e_{s+u+2}, ...e_{s+u+c}\}$ belonging to the eigenvalues having vanishing real parts. It is clear that

$$E^s \oplus E^u \oplus E^c \quad = \quad \mathbb{R}^n, \quad i.e., \quad s+u+c=n \tag{1.152}$$

Therefore, the union of three subspaces form the state space or phase space $\mathbb{R}^n$.

The linear ODE (1.148) on $\mathbb{R}^n$ provides the above three stable, unstable, and centre subspaces which describe the invariant set [9] (specifically subspaces). From the general solution (1.149), we see that the orbits passing through $\mathbf{u}_0$ remain in the same subspace for all $t \in \mathbb{R}$, and also we have

$$\mathbf{u}_0 \in E^s \implies \lim_{t\to+\infty} \mathbf{u}(t) = \lim_{t\to+\infty} \mathbf{u}_0 e^{\mathbf{A}(t-t_0)} = \mathbf{0}, \tag{1.153}$$

$$\mathbf{u}_0 \in E^u \implies \lim_{t\to-\infty} \mathbf{u}(t) = \lim_{t\to-\infty} \mathbf{u}_0 e^{\mathbf{A}(t-t_0)} = \mathbf{0}, \tag{1.154}$$

where $\mathbf{0}$ is a null vector assumed to be the origin in the state space $\mathbb{R}^n$. Equations (1.153) and (1.154) represent the asymptotic behavior of the orbits in the phase space of linear dynamical system. The orbits in the stable subspaces E^s are attracted to the origin while the orbits are repelled by the origin in the unstable subspaces E^u. In particular, if $s = n$ (*i.e.*, $E^s = \mathbb{R}^n$), all the orbits are attracted to the origin as $t \longrightarrow +\infty$ which is known as sink, while for $u = n$ (*i.e.*, $E^u = \mathbb{R}^n$), all are repelled by the origin as $t \longrightarrow -\infty$ which is referred to as source.

- **Hyperbolic and non-hyperbolic critical points:**

In the ODEs (1.134), *i.e.*, $\dot{\mathbf{x}} = \mathbf{f}(\mathbf{x})$ on $\mathbb{R}^n$, an equilibrium point $\mathbf{x} = \mathbf{x}_c$ is called hyperbolic type if all the eigenvalues of the linearized Jacobian matrix $\mathbf{Df}(\mathbf{x}_c)$ have non-zero real parts. On the other hand, if at least one of the eigenvalues has zero real part, the point is called non-hyperbolic critical point. Linear stability theory can be employed only on hyperbolic critical points to check their stability, but it fails to check the stability for non-hyperbolic critical points. However, center manifold theorem can be employed to check the stability for the non-hyperbolic one which will be discussed later.

- **Non-isolated critical points:**

[9] A set S is called an invariant set of the flow ϕ_t of the system (1.134) means that for all $t \in \mathbb{R}$, $\phi_{\mathbf{t}}(\mathbf{x}) \in S$, where $S \subset \mathbb{R}^n$.

We are interested another type of critical point, namely, non-isolated critical points which, sometimes, arising from the system of ODEs (1.134), are a curve of points (*i.e.*, set of points) or a line of critical points. This non-isolated critical points is called a *critical set or equilibrium set*. Mathematically, critical sets (set of points) S ($\in \mathbf{R}^n$) of points $\mathbf{x}_c$ satisfy the relation $\mathbf{f}(\mathbf{x}_c) = 0$ for every $\mathbf{x}_c \in S$. In the set of points, the linearized Jacobian matrix necessarily has one zero eigenvalue at each point $\mathbf{x}_c$ of the critical/equilibrium set, which follows that every critical point of a critical/equilibrium set is a non-hyperbolic critical point. The equilibrium set with exactly one vanishing eigenvalue (all other eigenvalues have $\mathrm{Re}(\lambda_i) \neq 0$) at each point is called a normally hyperbolic set. The stability of the normally hyperbolic set can, however, be determined by the signature of the eigenvalues in the remaining directions. Hence, for the negative eigenvalues, the set is an attractor, otherwise a repeller [1, 106].

• **Stable, unstable, and saddle-like critical points:**

Now, we are able to linearize the system around the critical points to realize the stability of the points. It is worthwhile to know the behavior of orbits near the critical points $\mathbf{x}_c$, *i.e.*, whether they are attracted or repelled by that point. First of all, we have to compute the eigenvalues of the linearized Jacobian matrix, then identify the following:

(1) If all the eigenvalues have negative real parts (in this case $E^s = \mathbb{R}^n$), then all the trajectories are attracted to the point $\mathbf{x}_c$ and the point is called a stable critical point or sink.

(2) If all the eigenvalues have positive real parts ($E^u = \mathbb{R}^n$), then all the trajectories emerge from the point $\mathbf{x}_c$ *i.e.*, they will be repelled by the point and the point is said to be an unstable critical point or source.

(3) When the eigenvalues have negative as well as positive real parts, then the point is called a saddle point.

It is very clear that critical points will show its nature if any one of the eigenvalues becomes positive, however, nothing can be concluded about its stability.

• **Stable, unstable, and center manifold:**

We have discussed earlier that the subspaces E^s, E^u, E^c arising from linearized ODE (1.147) are invariant subspaces. The behavior of orbits near the critical points of non-linear ODE (1.134) are equivalent to those in (1.147). This can be concluded from Hartman-Grobman theorem. Now, one can generalize the idea of stable, unstable, and centre subspaces for non-linear ODE derived from linear ODEs.

A stable manifold W^s of a critical point $\mathbf{x}_c$ is a differentiable manifold which is tangent to the stable subspaces E^s at $\mathbf{x}_c$ and all orbits in W^s are asymptotic to $\mathbf{x}_c$ as $t \longrightarrow +\infty$.

In a similar way, an unstable manifold W^u of critical point $\mathbf{x}_c$ is a differentiable manifold which is tangent to the unstable subspaces E^u at $\mathbf{x}_c$ such that all orbits in W^u are asymptotic to $\mathbf{x}_c$ as $t \longrightarrow -\infty$.

Lastly, a center manifold W^c (when neither all of eigenvalues are positive nor negative)

of equilibrium point $\mathbf{x}_c$ is a differentiable manifold which is tangent to the centre subspaces E^c at $\mathbf{x}_c$. Asymptotic behavior of the orbits in this center manifold cannot be determined by linearization.

• **Hartman-Grobman Theorem:**

The flow and ODE are equivalent. So, we obtain a nature of trajectory/orbit in the neighbourhood of critical points by finding the solution curve of ODE. The information of a non-linear system is completely determined from a linearized system (provided that the critical point is hyperbolic) by the Hartman-Grobman theorem which states that

"Let ϕ_t be a flow and $\mathbf{x}_c$ be a hyperbolic critical point of the non-linear ODE (1.134), there exists a neighbourhood $N_\delta(\mathbf{x}_c)$ of the point $\mathbf{x}_c$, where ϕ_t is topologically equivalent [10] to the flow of the linearized system (1.147) at $\mathbf{x}_c$."

Generally, a non-linear system cannot be rearranged as in matrix notation, the matrix form of a linear system is possible only for hyperbolic critical points. Keeping it in mind, using Hartman-Grobman theorem (as the flows arising from two system have same qualitative behavior), one can fully analyze the non-linear ODE by linearizing the system around at the hyperbolic critical points. So, by this theorem, wee see that non-linear flow of original non-linear ODE is equivalent to linear flow of linearized ODE. That is, the qualitative behavior of non-linear ODE is same as the linearized system. Therefore, it can be concluded that the stability of a point (hyperbolic) obtained from linearized ODE corresponds to the stability of the non-linear ODE. This is the importance of the Hartman-Grobman theorem.

1.6.2.1 2D autonomous system

Let us assume a 2-dimensional autonomous system

$$\dot{x} \;=\; P(x,y), \qquad \dot{y} = Q(x,y) \tag{1.155}$$

has a critical point (x_c, y_c) such that $P(x_c, y_c) = 0,\ \ Q(x_c, y_c) = 0$. From the earlier discussion, we have shown that the behavior of the phase path near the point (x_c, y_c) may be realized by linearizing the system. To do so, we have to perturb the system around the point and observe whether the perturbation grows or decays. Let the small perturbation be

$\eta(t) = x(t) - x_c, \quad \xi(t) = y(t) - y_c$, then $\dot{\eta}(t) = x(t), \quad \dot{\xi}(t) = y(t)$ since x_c and y_c are constants. Thus, we have $\dot{\eta}(t) = \dot{x} = P(x,y) = P(x_c + \eta(t),\ y_c + \xi(t))$ and using Taylor's theorem, $\dot{\eta}(t) = P(x_c, y_c) + \eta\frac{\partial P}{\partial x} + \xi\frac{\partial P}{\partial y} + O(\eta^2,\ \xi^2,\ \eta\xi)$. Since $P(x_c, y_c) = 0$, we have from the above:

$$\dot{\eta}(t) \;=\; \eta\frac{\partial P}{\partial x} + \xi\frac{\partial P}{\partial y} + O(\eta^2,\ \xi^2,\ \eta\xi). \tag{1.156}$$

Similarly,

[10] Let us assume flows ϕ_t and $\bar{\phi}_t$ are on $\mathbf{R}^n$. They are said to be topologically equivalent when there exists a homeomorphism $h : \mathbf{R}^n \longrightarrow \mathbf{R}^n$ which maps orbits of the flow ϕ_t onto orbits of $\bar{\phi}_t$, preserving their orientation.

$$\dot{\xi}(t) \;=\; \eta\frac{\partial Q}{\partial x} + \xi\frac{\partial Q}{\partial y} + O(\eta^2,\ \xi^2,\ \eta\xi). \tag{1.157}$$

Assuming the quadratic term in r.h.s to be small, we write (1.156) and (1.157) in matrix form as

$$\begin{pmatrix} \dot{\eta} \\ \dot{\xi} \end{pmatrix} \;=\; \begin{pmatrix} \frac{\partial P}{\partial x} & \frac{\partial P}{\partial y} \\ \frac{\partial Q}{\partial x} & \frac{\partial Q}{\partial y} \end{pmatrix} \begin{pmatrix} \eta \\ \xi \end{pmatrix}. \tag{1.158}$$

The system (1.158) is the linearized form and the matrix

$$J \;=\; \begin{pmatrix} \frac{\partial P}{\partial x} & \frac{\partial P}{\partial y} \\ \frac{\partial Q}{\partial x} & \frac{\partial Q}{\partial y} \end{pmatrix}_{(x_c,y_c)}. \tag{1.159}$$

is called the Jacobian matrix at (x_c, y_c).

For a 2D autonomous system, the stability of the critical point (x_c, y_c) depends on the eigenvalues $\lambda_1,\ \lambda_2$ arising from the linearized Jacobian matrix (1.159) as follows:

- (i) The equilibrium point shows stable nature for $\lambda_1 < 0,\ \lambda_2 < 0$.
- (ii) The point has unstable nature for $\lambda_1 > 0,\ \lambda_2 > 0$.
- (iii) The point is saddle-like in nature if any one of the eigenvalues is positive (or, $\lambda_1\lambda_2 < 0$).
- (iv) If two eigenvalues are complex conjugates $\lambda_1 = \alpha + i\beta,\ \lambda_2 = \alpha - i\beta$ with $\alpha > 0,\ \beta \neq 0$, the point will be an unstable spiral.
- (v) If two eigenvalues are complex conjugates $\lambda_1 = \alpha + i\beta,\ \lambda_2 = \alpha - i\beta$ with $\alpha < 0,\ \ \beta \neq 0$, the point will be a stable spiral.
- (vi) If the eigenvalues are purely imaginary *i.e.*, $\lambda_1 = i\beta,\ \lambda_2 = -i\beta$, then the point is a center.

- **Lyapunov stability theory:**

We have seen that negativity of eigenvalues of the linearized Jacobian matrix corresponds to local stability of the critical points. This linear stability theory is only applied for the case of hyperbolic critical points. For the case of non-hyperbolic critical points, linear stability fails to describe their local stability and in this case, center manifold theorem may be applied to check their stability, or one can predict the stability by finding out the Lyapunov functions. In this paragraph, we shall discuss the Lyapunov stability theory.

Let $\mathbf{x}_c$ be the critical point for ODEs $\mathbf{x} = \mathbf{f}(\mathbf{x})$. Let N be the neighbourhood of the point $\mathbf{x}_c$ and $V : \mathbb{R}^n \longrightarrow \mathbb{R}$ be a function of class C^1 such that $V(\mathbf{x}_c) = 0,\ \ V(\mathbf{x}) > 0\ \forall\ \mathbf{x} \in N - \{\mathbf{x}_c\}$.

Then

(1) if $\frac{d}{dt}V(\mathbf{x}) < 0 \ \ \forall \ \ \mathbf{x} \in N - \{\mathbf{x}_c\}, \quad \mathbf{x}_c$ is asymptotically stable.

(2) if $\frac{d}{dt}V(\mathbf{x}) \leq 0 \ \ \forall \ \ \mathbf{x} \in N - \{\mathbf{x}_c\}, \quad \mathbf{x}_c$ is stable.

(3) if $\frac{d}{dt}V(\mathbf{x}) > 0 \ \ \forall \ \ \mathbf{x} \in N - \{\mathbf{x}_c\}, \quad \mathbf{x}_c$ is unstable.

Now, a function V that satisfies the conditions of the theorem with $\frac{d}{dt}V(\mathbf{x}) \leq 0$ is called a Lyapunov function. Moreover, if V satisfies the conditions of the theorem with $\frac{d}{dt}V(\mathbf{x}) < 0$, then this is called a strict Lyapunov function. Therefore, in order to determine the stability of critical points, it is only required to identify the Lyapunov function in the neighbourhood of critical points. Thus, the existence of such Lyapunov function would guarantee the asymptotic stability and we don't need to solve ODEs explicitly.

- **Center manifold theorem:**

We have discussed the local stability (linear stability theory) properties of critical points by evaluating the eigenvalues of the linearized Jacobi matrix $\mathbf{Df}(\mathbf{x_c})$. This process can be applied only when the eigenvalues have non-zero real parts (*i.e.*, for hyperbolic type critical points). This theory is no longer valid when at least one of the eigenvalues have vanishing real parts. This type of critical points are called non-hyperbolic critical points. In this section, we shall discuss the stability of non-hyperbolic critical points. We have pointed out how to determine the stability of points having eigenvalues with zero real parts by finding the suitable Lyapunov functions using Lyapunov stability theory. However, it has a limitation that sometimes, it is not possible to find out proper Lyapunov functions for the system. So, Center Manifold theorem is an effective one to characterize the stability for these kind of points. This theorem allows us to simplify the system by reducing their dimensionality [280] (for a review see [279]).

We follow Perko [474] and Boehmer [609], for discussing the mathematical background of the center manifold theory. When Jacobian matrix corresponding to the given autonomous system at the equilibrium point has zero eigenvalue(s), linear theory fails to provide information on the stability of that equilibrium point. In this case, use of center manifold is interested because it reduce the dimension of the system near that equilibrium point so that stability of the reduced system can be investigated. There always exists an invariant local center manifold W^c passing through the fixed point to which the system could be restricted to study its behavior in the neighborhood of the fixed point. The stability of the reduced system determines the stability of the system at that point.

Let $x \in \mathbb{R}^p$ and $y \in \mathbb{R}^q$. An arbitrary dynamical system with zero eigenvalues in the Jacobian matrix can always be written in the following form

$$\begin{aligned} \dot{x} &= Ax + f(x, y), \\ \dot{y} &= Bx + g(x, y), \end{aligned} \tag{1.160}$$

where

$$\begin{aligned} f(0,0) = 0, \quad Df(0,0) = 0, \\ g(0,0) = 0, \quad Dg(0,0) = 0. \end{aligned} \tag{1.161}$$

Here we assume that the critical point is located at the origin and Df denotes the matrix of first derivatives of the vector valued function f. A is a $p \times p$ matrix having eigenvalues with zero real parts and B is an $q \times q$ matrix having eigenvalues with non-zero real parts.
It is noted that a dynamical system with zero eigenvalues can always be rewritten into the above form by linear shifting and matrix coordinate transformations. We will show this construction explicitly when we discuss the scalar field model below.

Definition. We call the space

$$W^c(0) = \{(x, y) \in \mathbb{R}^p \times \mathbb{R}^q | y = h(x), |x| < \delta, h(0) = 0, Dh(0) = 0\} \tag{1.162}$$

for δ sufficiently small, the center manifold for the system (1.160).

Next, we need to construct this center manifold explicitly. By differentiating the considering equation $y = h(x)$ with respect to the independent variable, we get $\dot{y} = Dh(x)\dot{x}$ where we used the chain rule. Eliminating $\dot{x}$ and $\dot{y}$ via (1.160), one arrives and the following quasilinear partial differential equation which h has to satisfy

$$\mathcal{N}(h(x)) = Dh(x)[Ax + f(x, h(x))] - Bh(x) - g(x, h(x)) = 0, \tag{1.163}$$

and the flow on the center manifold $W^p(0)$ is defined by the system of differential equations

$$\dot{x} = Cx + f(x, h(x)) \tag{1.164}$$

for all $x \in \mathbb{R}^p$ with $|x| < \delta$.

It is interesting to note that for a non-hyperbolic critical point having the eigenvalues of Jacobi matrix $\mathbf{Df(0)}$ with some positive or negative real parts, ideas of stability are realized by reducing the dimensions of dynamical systems. If we get p numbers of eigenvalues with positive real parts and q with negative real parts, then obviously, the number of eigenvalues with zero real parts will be $r(= n - p - q)$. It is clear that there exists a stable manifold of dimension q tangent to the stable subspace E^q whereas there exists a p-dimensional unstable manifold tangent to the unstable subspace E^p, and a r- dimensional center manifold also exists. All are invariant under the flow $\phi_{\mathbf{t}}$ of the non-linear system [106].

1.7 Analysis at Infinity

Consider the simple autonomous system in $\mathbb{R}$

$$\dot{x} = \frac{1}{x}, \quad x(1) = 1.$$

ZThe function $\mathbf{f}(x) = \frac{1}{x}$, defined over $(0, \infty)$ has no zero. However if the extended real number system is considered, then $x = \infty$ is a critical point and the solution $x(t) = \sqrt{2t - 1}$ suggests that ∞ is a stable critical point of the system, as $t \to \infty$ implies $x(t) \to \infty$.

There is a method due to Poincaré which addresses this kind of situation in more general set up. For the sake of simplicity, the entire discussion on Poincaré method [474] will be carried out for an autonomous system of dimension two. For higher dimensions, similar techniques are employed.

1.7.1 Poincaré projection

The Poincaré sphere [474] is the usual sphere $S^2 = \{(X, Y, Z) \in \mathbb{R}^3 \mid X^2 + Y^2 + Z^2 = 1\}$. The points in the sphere is projected in an one-one fashion onto $\mathbb{R}^2 = \{(x, y) \mid x, y \in \mathbb{R}\}$ as

$$x = \frac{Y}{Z}, \quad y = \frac{Y}{Z}, \tag{1.165}$$

The inverse of this projection map is

$$X = \frac{x}{\sqrt{1 + x^2 + y^2}}, \; Y = \frac{y}{\sqrt{1 + y^2 + z^2}}, \; Z = \frac{z}{\sqrt{1 + x^2 + z^2}}. \tag{1.166}$$

From (1.166), it can be easily seen that the critical points at infinity are spread out along the equator of the sphere, whereas the origin is mapped to the north pole.

1.7.2 Poincaré method

Given the dynamical system on $\mathbb{R}^2$,

$$\begin{aligned} \dot{x} &= M(x, y), \\ \dot{y} &= N(x, y) \end{aligned} \tag{1.167}$$

where M, N are polynomials, define

$$m = \max\{\text{degree}(M), \text{degree}(N)\}.$$

The system (1.167) can be written as

$$\frac{dy}{dx} = \frac{N(x, y)}{M(x, y)}.$$

or as

$$N(x, y)\, dx - M(x, y)\, dy = 0. \tag{1.168}$$

It follows from (1.165) that

$$dx = \frac{Z\, dX - X\, dZ}{Z^2}, \quad dy = \frac{Z\, dY - Y\, dZ}{Z^2}.$$

Therefore (1.168) can be written as

$$N(Z\, dX - X\, dZ) - M(Z\, dY - Y\, dZ) = 0 \tag{1.169}$$

where

$$M = M(x, y) = M\left(\frac{X}{Z}, \frac{Y}{Z}\right).$$

and

$$N = N(x, y) = N\left(\frac{X}{Z}, \frac{Y}{Z}\right).$$

are rational functions.

To eliminate Z from the denominators, one can multiply (1.169) by Z^m to obtain

$$ZN^*\,dX - ZM^*\,dY + (YM^* - XN^*)\,dZ = 0 \tag{1.170}$$

where

$$M^*(X,Y,Z) = Z^m M\left(\frac{X}{Z},\frac{Y}{Z}\right), \quad N^*(X,Y,Z) = Z^m N\left(\frac{X}{Z},\frac{Y}{Z}\right)$$

are polynomials in (X,Y,Z).

The equation (1.170) can be rewritten in the form of determinant equation as

$$\begin{vmatrix} dX & dY & dZ \\ X & Y & Z \\ M^* & N^* & 0 \end{vmatrix} = 0. \tag{1.171}$$

The flows of the system (1.170) in the sphere S^2 correspond to the flows of the system (1.165) in a one-one manner. The equator ($Z=0$) of S^2 contains the critical points at ∞ of the system (1.170).

When $Z=0$, the system (1.170) becomes

$$(YM^* - XN^*)\,dZ = 0.$$

For a critical point at ∞, if it is approached by the trajectories from the finite plane, then $dZ = 0$, consequently $YM^* - XN^* = 0$.

If

$$M(x,y) = M_0(x,y) + \cdots + M_m(x,y)$$

and

$$N(x,y) = N_0(x,y) + \cdots + N_m(x,y)$$

where M_j and N_j are homogeneous j-th degree polynomials in x and y, then

$$\begin{aligned} YM^* - XN^* &= Z^m Y M_1\left(\frac{X}{Z},\frac{Y}{Z}\right) + \cdots + Z^m Y M_m\left(\frac{X}{Z},\frac{Y}{Z}\right) \\ &\quad - Z^m X N_1\left(\frac{X}{Z},\frac{Y}{Z}\right) - \cdots - Z^m X N_m\left(\frac{X}{Z},\frac{Y}{Z}\right) \\ &= Z^{m-1} Y M_1(X,Y) + \cdots + Y M_m(X,Y) \\ &\quad - Z^{m-1} X N_1(X,Y) - \cdots - X N_m(X,Y) \\ &= Y M_m(X,Y) - X N_m(X,Y) \end{aligned} \tag{1.172}$$

for $Z=0$.

For $Z = 0$ also $X^2 + Y^2 = 1$. Therefore transforming (1.172) to the polar coordinates, one gets

$$\sin\theta M_m(\cos\theta, \sin\theta) - \cos\theta N_m(\cos\theta, \sin\theta) = 0.$$

These results [474] are summarized in the following

Theorem 1 *The critical points at infinity for the m-th degree polynomial system (1.165) occur at the points $(X, Y, 0)$ on the equator of the Poincaré sphere where $X^2 + Y^2 = 1$ and*

$$YM_m(X, Y) - XN_m(X, Y) = 0 \tag{1.173}$$

or equivalently at the polar angles θ_j and $\theta_j + \pi$ satisfying

$$G_{m+1}(\theta) \equiv \sin\theta M_m(\cos\theta, \sin\theta) - \cos\theta N_m(\cos\theta, \sin\theta) = 0. \tag{1.174}$$

This equation has at most $m + 1$ pair of roots θ_j and $\theta_j + \pi$ unless $G_{m+1}(\theta)$ is identically zero. If $G_{m+1}(\theta)$ is not identically zero, then the flow on the equator of the Poincaré sphere is counter-clockwise at the points corresponding to the polar angles? where $G_{m+1}(\theta) > 0$ and it is clockwise at the points corresponding to the polar angles θ where $G_{m+1}(\theta) < 0$.

The behavior of the flows of (1.172) in a neighborhood of any critical point at infinity can be obtained by projecting that neighborhood onto a plane tangent to S^2 at that point. Actually it is only necessary to project the hemisphere with $X > 0$ onto the plane $X = 1$ and to project the hemisphere with $Y > 0$ onto the plane $Y = 1$ in order to determine the behavior of the flow in the neighborhood of any critical point on the equator of S^2. This follows because the flow on S^2 defined by (1.172) is topologically equivalent at the antipodal points of S^2 if m is odd and it is topologically equivalent with the direction of the flow reversed, if m is even. For an example, if the critical point at infinity for the system (1.165) is $(\infty, 0)$; then one can project the flow on S^2 near that critical point defined by (1.172) onto the plane $X = 1$ by setting $X = 1$ and $dX = 0$ in (1.172). Similarly, for the critical point $(0, \infty)$ of the system (1.165), one can project the flow near $(0, \infty)$ defined by (1.172) onto the plane $Y = 1$ by setting $Y = 1$ and $dY = 0$ in (1.172).

These results [474] are summarized as follows

Theorem 2 *The flow defined by (1.172) in a neighborhood of any critical point of (1.172) on the equator of the Poincaré sphere S^2, except the points $(0, \pm 1, 0)$, is topologically equivalent to the flow defined by the system*

$$\begin{aligned} \pm\dot{y} &= yz^m M\left(\frac{1}{z}, \frac{y}{z}\right) - z^m N\left(\frac{1}{z}, \frac{y}{z}\right), \\ \pm\dot{z} &= z^{m+1} M\left(\frac{1}{z}, \frac{y}{z}\right), \end{aligned} \tag{1.175}$$

the signs being determined by the flow on the equator of S^2 as determined in the Theorem (1). Similarly, the flow defined by (1.172) in a neighborhood of any critical point of (1.172) on the equator of the Poincaré sphere S^2, except the points $(\pm 1, 0, 0)$, is topologically equivalent to the flow defined by the system

$$\begin{aligned} \pm\dot{x} &= xz^m N\left(\frac{x}{z}, \frac{1}{z}\right) - z^m M\left(\frac{x}{z}, \frac{1}{z}\right), \\ \pm\dot{z} &= z^{m+1} M\left(\frac{x}{z}, \frac{1}{z}\right), \end{aligned} \tag{1.176}$$

the signs being determined by the flow on the equator of S^2 as determined in the Theorem (1).

An example [474] demonstrating the application of the Poincaré method is as follows

Consider the autonomous system

$$\dot{x} = x,$$
$$\dot{y} = -y.$$

This system has $(0, 0)$ as the only finite critical point which is also a saddle point. According to the Theorem (1), the critical point at infinity for this system is determined by the solutions of

$$XN_1(X, Y) - YM_1(X, Y) = -2XY = 0.$$

Therefore, there are critical points on the equator of S^2 at $(\pm 1, 0, 0)$ and at $(0, \pm 1, 0)$. It is seen from the left hand side of the above expression that the flow on the equator of S^2 is clockwise for $XY > 0$ and counter-clockwise for $XY < 0$. According to the Theorem (2), the behavior in a neighborhood of the critical point $(1, 0, 0)$ is determined by the behavior of the system

$$-\dot{y} = yz\left(\frac{1}{z}\right) + z\left(\frac{y}{z}\right),$$
$$-\dot{z} = z^2\left(\frac{1}{z}\right)$$

or equivalently

$$\dot{y} = -2y,$$
$$\dot{z} = -z$$

near the origin. This system has a stable (improper) node at the origin. The y-axis consists of trajectories of this system and all the other trajectories come into the origin in tangent to the z-axis. This completely determines the behavior at the critical point $(1, 0, 0)$. The behavior at the antipodal point $(-1, 0, 0)$ is exactly the same as the behavior at $(1, 0, 0)$. There is also a stable (improper) node at $(-1, 0, 0)$, as $m = 1$ is odd in this example. Similarly, the behavior in a neighborhood of the critical point $(0, 1, 0)$ is determined by the behavior of the system

$$\dot{x} = 2x,$$
$$\dot{z} = z$$

near the origin. It can be inferred that this system has unstable (improper) nodes at $(0, \pm 1, 0)$.

Another example [474] of this method is in the following

Consider the following autonomous system

$$\dot{x} = x^2 + y^2 - 1,$$
$$\dot{y} = 5(xy - 1).$$

Since the circle $x^2 + y^2 = 1$ and the hyperbola $xy = 1$ do not intersect, there are no finite critical points of this system. The critical points at infinity are determined by

$$XN_2(X, Y) - YM_2(X, Y) = Y(4X^2 - Y^2) = 0$$

together with $X^2+Y^2=1$. Hence, the critical points at infinity are at $(\pm 1,0,0)$, $\pm\left(\frac{1}{\sqrt{5}},\frac{2}{\sqrt{5}},0\right)$ and $\left(\frac{1}{\sqrt{5}},-\frac{2}{\sqrt{5}},0\right)$. For $X=0$, the left hand side of the equation is negative while $Y>0$ and positive while $Y<0$. It indicates the direction of the flow on the equator of S^2. Then by using the Theorem (2), the behavior near each of the critical points $(1,0,0)$, $\left(\frac{1}{\sqrt{5}},\frac{2}{\sqrt{5}},0\right)$ and $\left(-\frac{1}{\sqrt{5}},-\frac{2}{\sqrt{5}},0\right)$ and $\left(\frac{1}{\sqrt{5}},-\frac{2}{\sqrt{5}},0\right)$ on S^2 is determined by the behavior of the system

$$\begin{aligned}\dot{y}&=4y-5z^2+yz^2-y^3,\\ \dot{z}&=-z-zy^2+z^3\end{aligned}$$

near the critical points $(0,0)$, $(2,0)$ and $(-2,0)$ respectively. For this system one has

$$D\mathbf{f}(0,0)=\begin{pmatrix}4&0\\0&-1\end{pmatrix}$$

and

$$D\mathbf{f}(\pm 2,0)=\begin{pmatrix}-8&0\\0&-5\end{pmatrix}.$$

By obtaining eigenvalues of the above two matrices, we can conclude that $(0,0)$ is a saddle point and $(\pm 2,0)$ are stable improper nodes for this system. Since $m=2$ is even in this example, the behavior near the antipodal points $-(1,0,0)$, $-\left(\frac{1}{\sqrt{5}},\frac{2}{\sqrt{2}},0\right)$, and $-\left(\frac{1}{\sqrt{5}},-\frac{2}{\sqrt{5}},0\right)$ is topologically equivalent to the behavior near $(1,0,0)$, $\left(\frac{1}{\sqrt{5}},\frac{2}{\sqrt{2}},0\right)$, and $\left(\frac{1}{\sqrt{5}},-\frac{2}{\sqrt{5}},0\right)$ respectively with the directions of the flow reversed. So $-(1,0,0)$ is a saddle point whereas $-\left(\frac{1}{\sqrt{5}},\pm\frac{2}{\sqrt{5}},0\right)$ are unstable (improper) nodes.

1.8 Bifurcation

Bifurcation theory is the mathematical study of changes in the topological structure of a given family such as the flows of an autonomous system. A bifurcation occurs when a very small and smooth changes made to the parameter values (also called the bifurcation value of the bifurcation parameters) of a system causes a sudden qualitative change in its topological behavior [699]. This concept was first introduced by Poincaré.

It is often useful to divide a bifurcation in one of the two following classes

• **Local bifurcations** A local bifurcation occurs when a parameter change cause the stability of a critical point to change.

• **Global bifurcations** Global bifurcations occur when 'larger' invariant sets, such as periodic orbits, collide with the equilibrium points. The effect is a change in the topology of the orbits in the phase space which cannot be confined to a small neighborhood, as is the case with local bifurcations. In fact, the changes in topology extend out to an arbitrarily large distance.

1.8.1 Local theory

Examples of local bifurcations include

• **Saddle-node bifurcation** The Saddle-node bifurcation is a local bifurcation in which two critical points of a dynamical system collide and annihilate each other.

• **Transcritical bifurcation** A transcritical bifurcation is a type of local bifurcation in which a fixed point exists for all values of a parameter and is never destroyed. However, such a fixed point interchanges its stability with another fixed point as the parameter is varied.

• **Pitchfork bifurcation** A pitchfork bifurcation is a particular type of local bifurcation where the system transits from one critical point to three critical points, hence the name 'Pitchfork'. Pitchfork bifurcations have two types, supercritical and subcritical.

• **Period-doubling bifurcation** A period doubling bifurcation in a discrete dynamical system is a local bifurcation in which a slight change in a parameter value leads to the system switching to a new behavior with twice the period of the original system.

• **Hopf bifurcation** A Hopf bifurcation is a local bifurcation where a system's stability switches and a periodic solution arises. To be more precise, it is a local bifurcation in which a critical point of a dynamical system loses its stability, as a pair of complex conjugate eigenvalues of the linearization matrix at that critical point crosses the complex plane imaginary axis.

• **Neimark-Sacker bifurcation** A Neimark-Sacker bifurcation (also called a secondary Hopf bifurcation) is a type of local bifurcation where the formation of a closed invariant curve happens from a critical point in a discrete dynamical systems, when the critical point changes its stability via a pair of complex eigenvalues with unit modulus. This type of bifurcation can be supercritical or subcritical, resulting in a stable or unstable closed invariant curve, respectively.

1.8.2 Global theory

Examples of global bifurcations include

• **Homoclinic bifurcation** Homoclinic bifurcation is a global bifurcation where a limit cycle collides with a saddle point. Homoclinic bifurcations can occur supercritically or subcritically.

• **Heteroclinic bifurcation** Heteroclinic bifurcation is a bifurcation of global type where a limit cycle collides with two or more saddle points. They involve a heteroclinic cycle. Heteroclinic bifurcations are of two types, resonance bifurcations and transverse bifurcations. Both types of bifurcations result in the change of stability of the heteroclinic cycle.

• **Infinite-period bifurcation** Infinite-period bifurcation is a type of global bifurcation where a stable node and saddle point simultaneously occur on a limit cycle. As the limit of a parameter approaches a certain critical value, the speed of the oscillation slows down and the period approaches infinity. The infinite-period bifurcation occurs at this critical value.

Beyond this critical value, two fixed points emerge continuously from each other on the limit cycle to disrupt the oscillation and form two saddle points.

• **Blue sky catastrophe** Blue sky catastrophe is a global bifurcation where a limit cycle collides with a non-hyperbolic cycle.

1.9 Criteria for stability corresponding to discrete dynamical system

In this section, we will establish some simple but powerful criteria for the local stability of fixed points [422]. Fixed (equilibrium) points may be divided into two types: hyperbolic and nonhyperbolic. A fixed point x^* of a map f is said to be hyperbolic if $|f'(x^*)| \neq 1$. Otherwise, it is nonhyperbolic. We will treat the stability of each type separately.

Definition 1.9.1 (Fixed points.) *A point $z \in \mathbb{R}^2$ is called a fixed point [421] of W if $W(z) = z$.*

1.9.1 Hyperbolic Fixed Points

The following result is the main tool for detecting local stability.

Theorem 3 *Let x^* be a hyperbolic fixed point of a map f, where f is continuously differentiable at x^*. The following statements then hold true [422]:*

1. *If $|f'(x^*)| < 1$, then x^* is asymptotically stable.*
2. *If $|f'(x^*)| > 1$, then x^* is unstable.*

1.9.2 Nonhyperbolic Fixed Points

The stability criteria for nonhyperbolic fixed points are more involved. They will be summarized in the next two results, the first of which treats the case when $f'(x^*) = 1$ and the second for $f'(x^*) = -1$.

Theorem 4 *Let x^* be a fixed point of a map f such that $f'(x^*) = 1$. If $f'(x)$, $f''(x)$, and $f'''(x)$ are continuous at x^*, then the following statements hold [422]:*

1. *If $f''(x^*) \neq 0$, then x^* is unstable (semistable).*
2. *If $f''(x^*) = 0$ and $f'''(x^*) < 0$, then x^* is aymptotically stable.*
3. *If $f''(x^*) = 0$ and $f'''(x^*) > 0$, then x^* is unstable.*

The preceding theorem may be used to establish stability criteria for the case when $f'(x^*) = -1$. But before doing so, we need to introduce the notion of the Schwarzian derivative.

Definition 1.9.2 *The Schwarzian derivative, Sf, of a function f is defined by [422]*

$$Sf(x) = \frac{f'''(x)}{f'(x)} - \frac{3}{2}\left[\frac{f''(x)}{f'(x)}\right]^2.$$

And if $f'(x^*) = -1$, then

$$Sf(x^*) = -f'''(x^*) - \frac{3}{2}\left[f''(x^*)\right]^2.$$

Theorem 5 *Let x^* be a fixed point of a map f such that $f'(x^*) = -1$. If $f'(x)$, $f''(x)$, and $f'''(x)$ are continuous at x^*, then the following statements hold [422]:*

1. *If $Sf(x^*) < 0$, then x^* is asymptotically stable.*
2. *If $Sf(x^*) > 0$, then x^* is unstable.*

Theorem 6 *Let $f : G \subset \mathbb{R}^2 \to \mathbb{R}^2$ be a C^1 map, where G is an open subset of $\mathbb{R}^2$, X^* is a fixed point of f, and $A = Df(X^*)$. Let $\rho(A)$ be the spectral radius of A defined as $\rho(A) = \max\{|\lambda_1|, |\lambda_2| : \lambda_1, \lambda_2$ are the eigen values of $A\}$. Then the following statements hold true:*

1. *If $\rho(A) < 1$, then X^* is asymptotically stable.*
2. *If $\rho(A) > 1$, then X^* is unstable.*
3. *If $\rho(A) = 1$, then X^* may or may not be stable.*

1.9.3 Center Manifolds

Consider the s-parameter map $F(\mu, u)$, $F : \mathbb{R}^s \times \mathbb{R}^k \to \mathbb{R}^k$, with $u \in \mathbb{R}^k$, $\mu \in \mathbb{R}^s$, where F is C^r $(r \geq 3)$ on some sufficiently large open set in $\mathbb{R}^k \times \mathbb{R}^s$. Let (u^*, μ^*) be a fixed point of F, *i.e.*,

$$F(\mu^*, u^*) = u^*.$$

The stability of hyperbolic fixed points of F is determined from the stability of the fixed points under the linear map

$$J = D_\mu F(\mu^*, u^*). \tag{1.177}$$

However, the situation is drastically different if one of the eigenvalues λ of J lies on the unit circle, that is, $|\lambda| = 1$. There are three separate cases in which the fixed point (u_0, μ_0) is non-hyperbolic.

1. J has one real eigenvalue equal to 1 and the other eigenvalues are off the unit circle.
2. J has one real eigenvalue equal to -1 and the other eigenvalues are off the unit circle.
3. J has two complex conjugate eigenvalues with modulus 1 and the other eigenvalues are off the unit circle.

Let us temporarily suppress the parameter μ. Then the map F can be written in the form

$$\begin{aligned} x &\longmapsto Ax + f(x, y), \\ y &\longmapsto By + g(x, y) \end{aligned} \tag{1.178}$$

where J in equation (1.177) has the form $J = \begin{pmatrix} A & 0 \\ 0 & B \end{pmatrix}$. Moreover, all of the eigenvalues of A lie on the unit circle, and all of the eigenvalues of B are off the unit circle. Furthermore,

$$\begin{aligned} f(0,0) &= 0, \quad g(0,0) = 0, \\ Df(0,0) &= 0, \quad Dg(0,0) = 0. \end{aligned}$$

Theorem 7 *There is a C^r-center manifold for system (1.178) that can be represented locally as [422]*

$$M_c = \left\{(x,y) \in \mathbb{R}^t \times \mathbb{R}^s : y = h(x), |x| < \delta, h(0) = 0, Dh(0) = 0, \text{ for a sufficiently small } \delta\right\}.$$

Furthermore, the dynamics restricted to M_c are given locally by the map

$$x \longmapsto Ax + f(x, h(x)), x \in \mathbb{R}^t. \tag{1.179}$$

This theorem asserts the existence of a center manifold, *i.e.,* a curve $y = h(x)$ on which the dynamics of System (1.178) is given by Equation (1.179). The next result states that the dynamics on the center manifold M_c determines completely the dynamics of the System (1.178).

Theorem 8 *The following statements hold.[422]*

1. If the fixed point $(0,0)$ of Equation (1.179) is stable, asymptotically stable, or unstable, then the fixed point $(0,0)$ of System (1.178) is stable, asymptotically stable, or unstable, respectively.

2. For any solution $(x(n), y(n))$ of the system (1.178) with an initial point (x_0, y_0) in a small neighborhood around the origin, there exists a solution $z(n)$ of Equation (1.179) and positive constants L, $\beta > 1$ such that

$$|x(n) - z(n)| \leq L\beta^n, \text{ and } |y(n) - h(z(n))| \leq L\beta^n \text{ for all } n \in \mathbb{Z}^+.$$

The question that still lingers is how to find the center manifold M_c or, equivalently, how to compute the curve $y = h(x)$. The first thing that comes to mind is to substitute for y in System (1.178) to obtain the system

$$\begin{aligned} x(n+1) &= Ax(n) + f(x(n), h(x(n))), \\ y(n+1) &= h(x(n+1)) \\ &= h\left[Ax(n) + f(x(n), h(x(n)))\right] \\ &= Bh(x(n)) + g(x(n), h(x(n))). \end{aligned}$$

Equating the two equations for $y(n+1)$ yields the functional equation

$$\mathcal{F}(h(x)) = h\left[Ax + f(x, h(x))\right] - Bh(x) - g(x, h(x)) = 0. \tag{1.180}$$

Solving Equation (1.180) is a formidable task, so at best one can hope to approximate its solution via power series. The next result provides the theoretical justification for our approximation.

Theorem 9 *Let $\psi : \mathbb{R}^t \to \mathbb{R}^s$ be a C^1-map with $\psi(0) = \psi'(0) = 0$. Suppose that $\mathcal{F}(\psi(x)) = \mathcal{O}(|x|^r)$ as $x \to 0$ for some $r > 1$ [422]. Then,*

$$h(x) = \psi(x) + \mathcal{O}(|x|^r) \text{ as } x \to 0.$$

1.10 Cosmology from the DSA perspective

We have achieved a set of non-linear governing equations, namely, Friedmann equation and the acceleration equation from the study of Einstein's General Relativity. The solutions of those equations make a huge impact on cosmology in understanding the origin, evolution, and the ultimate fate of our Universe. There are many ways to solve these analytically which have been reported in the literature. Dynamical system analysis (DSA), a mathematical branch, is one of the attractive approach to solve the system of ODEs. People are trying to solve cosmological problems with the help of dynamical system tools. Recently, many models incorporating DSA have been proposed (see some of them [1, 47, 149, 281, 282, 283, 284, 285, 286, 287] and references therein). In this thesis, we use dynamical system tools in some cosmological models to get some relevant idea of evolution of the Universe.

We have discussed the governing equations (Friedmann equation and Raychaudhuri equation) derived from the field equations in describing the evolution of the Universe. In this study, we assume that our Universe is filled with dark energy and dark matter (dark sector) and an interaction is possible between them atleast at a phenomenological level. As the evolution equations — Friedmann equation and Raychaudhuri equation are highly non-linear and the conservation equation of matter source are also complicated in presence of interaction, so, analytic solutions are not possible to obtain in that case. This has compelled us to find a new way to determine the solutions of the cosmological models.

We have already discussed DSA mathematically in detail. We know that many scientific disciplines use the dynamical system tools. Here, we focus only on the applications to physics, mainly in Cosmology. As the evolution equations are a system of second order differential equations, so it is hard to solve them analytically. So, we have to rewrite the Einstein's field equations for cosmological models in terms of dynamical system of autonomous system of ODEs. DSA is a powerful tool to sketch the picture of the Universe as a whole. First, we choose the phase variables (variables for autonomous system) in terms of the cosmological variables. There is no definite rule to choose such phase variables for converting the cosmological equations to an autonomous system of ODEs, however, one may follow the simple rules below to choose the phase variables:

- (1) The variables should be dimensionless.
- (2) The variables should be bounded in nature if possible, because only then a 'finite' analysis is possible. Otherwise one may have to resort to the techniques like the Poincaré map method.

However, dynamics of phase space reflects the same image as that of the cosmological model since the phase variables are framed from the cosmological variables. Also, it should be mentioned that there is an one to one correspondence between the exact solution of cosmological field equation and the point(state) in the phase space.

By analyzing the critical points extracted from the autonomous system, we get information regarding the dynamics of the Universe. To get an idea about the stability criteria of the critical points, one has to perturb the system around the points and for hyperbolic critical

points, first order perturbation is sufficient to get information about the qualitative behavior. To determine stability of the nonhyperbolic critical points, we use Center Manifold Theory. Therefore, the knowledge of critical points of the phase space derived from the ODEs for the given cosmological model is very important to achieve information about the dynamics of the Universe. In the study of Cosmology with the help of dynamical system tools, one must encounter the following scenarios.

- (1). **Early phases of the Universe:**

In cosmological studies, we know that the early phases of the Universe is likely to have an inflationary scenario and a radiation dominated era. In early inflationary scenario, the decelerating parameter is negative valued which indicates the initial accelerated phase of the Universe. On the other hand, to describe the radiation dominated era in the point of view of dynamical system analysis, one has to show that there exists a critical point in the phase space which is unstable in nature because all trajectories are emerging from that critical point. There exists a decelerating phase because deceleration parameter is positive valued. This phase will continue for a very small time interval.

- (2). **Intermediate phase of the Universe:**

After the inflation, radiation dominated era came and from that, the Universe transits into a matter dominated era. In this phase, the critical points should have a saddle-like nature. Some trajectories entering into the point and some are emerging from those points. The critical point in this phase shows a transient cosmological solution.

- (3). **Late-time accelerated expansion phase of universe:**

In the perspective of dynamical system, in order to describe the late time accelerated expansion of the Universe, there must be a critical point in the phase space derived from the cosmological model that has the nature of a stable sink. That is, all the trajectories entering into the point which is called an attractor. Many cosmological and astrophysical observations suggest that our universe is undergoing an accelerated phase at present which is mostly dominated by dark energy. Therefore, to describe a phenomenologically viable evolution of the Universe, one must find a heteroclinic orbit connecting to a matter dominated critical point to the DE dominated solution and such a trajectory describes a transition from DM to DE domination.

Therefore to describe a phenomenologically viable evolution of the Universe, one must find a heteroclinic orbit connecting a radiation dominated critical point to a matter dominated critical point further to a dark energy dominated critical point in the corresponding autonomous system and such a trajectory describes a transition from the radiation to the dark matter to the dark energy domination.

CHAPTER 2

DYNAMICAL SYSTEM ANALYSIS OF SELF-INTERACTING THREE-FORM FIELD COSMOLOGICAL MODEL: STABILITY AND BIFURCATION

2.1 Prelude

The series of observations for more than last two decades strongly confirm that our universe is currently going through a phase of accelerated expansion [587] preceding a smooth transition from decelerated era in recent past. There is a difference in opinion about the cause of this transition among the cosmologists. One group has preferred modification of the gravity theory while others are in favour of Einstein gravity with introduction of some exotic matter having large $-$ve pressure (known as dark energy (DE)). Observational evidences show that the cosmic fluid consists of 69% DE, 26% dark matter (DM) and rest is in the form of baryonic matter and radiation [613]. Although, the cosmological constant is the simplest choice for the DE candidate and is observationally most favourable one, still cosmologists search for dynamical DE models due to two severe drawbacks namely cosmological constant problem and cosmic coincidence problem of cosmological constant [614].

Initially, Cosmologists have chosen the dynamic DE in the form of perfect fluid with variable equation of state parameter of various forms (viz; quintessence, tachyon, phantom [580] and chameleon [616, 581] etc). Subsequently, some complicated fields namely spinors [601], vectors [573], and even higher order spin fields are chosen as DE candidate. A three-form field has been shown in Ref.[602, 603] as a possible DE candidate and the dynamical system analysis of the corresponding cosmological model has been studied in Ref. [609]. It has been shown that the dual of the three form fields is a scalar field and for non-quadratic potential, the kinetic term of the scalar field is non-canonical to have an equivalence with K-inflation model [610]. Further, a non-quadratic dependence on the three-form Faraday term is responsible for self-coupling nature of the scalar field [602]. For non-minimal coupling of the three form, the dual scalar field character of the three-form will no longer hold.

There are no observational/experimental evidences for the fundamental scalar particles. In fact, some higher form field are very much likely to be a candidate for DE and from cosmological point of view these field do not violet the cosmological principle. The higher form fields are very common in String theory. Hence, attempts have been made to use a vector field, a one-form field the DE candidate [489, 490, 491, 492]. However, most of the vector field models (also two-form fields) are not stable in nature [493]. However, it is found that three-form field models are very much stable [495, 494]. Hence, it is interesting to consider a three-form field as a candidate for DE. In recent past, it has been shown [494] that a three-form field as a DE candidate provides accelerating universe.

The present work deals with dynamical system analysis of the evolution equations of the Cosmological model with three form scalar field as the choice of DE while interacting DM in the form of dust. Although the choice of interaction is purely phenomenological but still the interaction term may resolve the coincidence problem as energy densities of DE and DM are comparable at stable fixed points.

Our present work has lots of differences with earlier works in [609, 486, 604]. In Ref.[609] the autonomous system [(19)-(21)] is identical to our autonomous system [2.22 – 2.24], but they have determined few critical points and have analyzed only one critical point by center manifold theory. On the other hand, we have determined all possible critical points both for interacting and non-interacting cases. For non-hyperbolic critical points center manifold theory has been used and global stability has been discussed with reference to bifurcation analysis using Poincaré index. In another work [486] the authors have similar autonomous system confined to a finite region. They have also analyzed few critical points from cosmological point of view. Some of our cosmic epochs are identical to them but we have procured other significant cosmic eras. They have not analyzed the critical points using center manifold theory and have not discussed global stability (as we have extensively done in our work), rather they have performed cosmological perturbations. In Ref.[604] the authors have 5D phase space as they have considered baryon and radiation as matter field in addition to interacting DE (three-form field) and DM. They have chosen various form of the interaction term and have analyzed some of the critical points in cosmological context. They have not employed center manifold theory nor have discussed global stability for any critical point. Therefore, present work is rich in dynamical system analysis and have studied various cosmic scenarios with reference to cosmic phase transition using bifurcation analysis [611, 488, 475].

This chapter is organized as follows: Basic equations for interacting 3-form field with DM in the form of dust has been formulated in Section 2.2. In Section 2.3 the above evolution equations are converted into an autonomous system by suitable choice of the dimensionless variables and critical points are determined. Also stability of the non-hyperbolic equilibrium points are discussed by formulating center manifold at the equilibrium points. Finally cosmological implications and conclusions are presented in Section 2.4.

2.2 Basic equations for Three-form field Cosmological model

The action of a three-form field $A_{\mu\nu\rho}$, minimally coupled to gravity is given by [609]

$$S_A = -\int d^4x\sqrt{-g}\left[\frac{1}{2\kappa^2}R - \frac{F^2}{48} - V\left(A^2\right)\right], \tag{2.1}$$

where R is the Ricci scalar and $V(A^2)$ is the potential of the three-form field $A_{\mu\nu\rho}$ having field strength tensor

$$F_{\mu\nu\rho\sigma} = 4\bigtriangledown_{[\mu}A_{\nu\rho\sigma]} \tag{2.2}$$

By notation, the square bracket indicates anti-symmetrization of the indices involved and $A^2 = A^{\mu\nu\rho}A_{\mu\nu\rho}$. Now, variation of the above action with respect to the metric tensor gives the usual Einstein field equations: $G_{\mu\nu} = \kappa^2 T\mu\nu$ with

$$T_{\mu\nu} = \frac{1}{6}F_{\mu\alpha\beta\gamma}F_{\nu}^{\alpha\beta\gamma} + 6V'(A^2)A_{\mu\alpha\beta}A_{\nu}^{\alpha\beta} - g_{\mu\nu}\left(\frac{1}{48}F_{\alpha\beta\gamma\rho}F^{\alpha\beta\gamma\rho} + V\left(A^2\right)\right) \tag{2.3}$$

while the equation of motion of the three form field is obtained by varying the action (2.1) with respect to $A^{\mu\gamma\rho}$ as

$$\bigtriangledown^{\alpha}F_{\alpha\mu\gamma\rho} = 12V'(A^2)A_{\mu\gamma\rho} \tag{2.4}$$

with $V'(A^2) = \frac{dV}{dA^2}$. As in the present work, we are considering homogeneous and isotropic FLRW space-time geometry, so the three-form field depends only on time. Hence, the evolution equation (2.4) gives $A_{0\mu\nu} = 0$, *i.e.,* a zero component of the three-form field is non-dynamical and spatial components are given by

$$A_{ijk} = a^3(t)\epsilon_{ijk}X(t). \tag{2.5}$$

The co-moving field X is related to the three field as $A^2 = 6X^2$ and the evolution equation (2.4) simplifies to

$$\ddot{X} = -3H\dot{X} - 3\dot{H}X - V_{,X} \tag{2.6}$$

where an over dot indicates differentiation with respect to the cosmic time 't' and a comma in the suffix denotes differentiation with respect to the corresponding variable. Further, the energy-density and thermodynamic pressure of the effective perfect fluid corresponding to the energy-momentum tensor (2.3) of the three-form field are given by

$$\rho_A = -T_0^0 = \frac{1}{2}\left(\dot{X} + 3HX\right)^2 + V(X), \tag{2.7}$$

$$p_A = T_i^i = -\frac{1}{2}\left(\dot{X} + 3HX\right)^2 - V(X) + XV_{,X} \tag{2.8}$$

with equation of state

$$\omega_A = \frac{p_A}{\rho_A} = -1 + \frac{XV_{,X}}{\rho_A}. \tag{2.9}$$

Now, in the context of series of recent observations the above three-form field (chosen as dark energy), interacting with dark matter (in the form of dust) is chosen as the matter context in the universe. So, the explicit form of the Einstein field equations in the background of homogeneous and isotropic space-time model are

$$3H^2 = \kappa^2(\rho_A + \rho_{DM}), \tag{2.10}$$
$$2\dot{H} = -\kappa^2\left[(\rho_A + p_A) + \rho_{DM}\right] \tag{2.11}$$

with energy conservation equations

$$\dot{\rho}_{DM} + 3H\rho_{DM} = Q, \tag{2.12}$$
$$\dot{\rho_A} + 3H(\rho_A + p_A) = -Q. \tag{2.13}$$

Here the two matter components are assumed to be interacting and Q represents arbitrary coupling. As a result of this coupling between the matter fields, the evolution equation (2.6) modifies to

$$\ddot{X} + 3H\dot{X} + 3\dot{H}X + \frac{dV}{dX} = -\frac{Q}{\dot{X} + 3HX}. \tag{2.14}$$

2.3 Autonomous system, Critical points and stability analysis

In the present work we shall consider interacting three-form field with exponential potential as

$$V(X) = V_0 e^{-\mu X}, \tag{2.15}$$

where μ is a dimensionless parameter and $V_0 > 0$. This type of potential is termed as runaway potential, *i.e.*, $\lim_{X\to\infty} V(X) = 0$ and $\frac{dV}{dX} < 0 \ \forall \ X$. The runaway potential will correspond to well-behaved evolution of the background [604].
Using the dimensionless variables (u, v, w, s) as defined in [609], viz;

$$u : = \frac{1}{\sqrt{6}H}(\dot{X} + 3HX), \tag{2.16}$$
$$v : = \frac{\sqrt{V}}{\sqrt{3}H}, \tag{2.17}$$
$$w : = \frac{2}{\pi}\tan^{-1}\frac{3X}{\sqrt{6}}, \tag{2.18}$$
$$s : = \frac{\sqrt{\rho_{DM}}}{\sqrt{3}H}. \tag{2.19}$$

The expression of equation of state parameter $\omega_X = p_X/\rho_X$ and the total equations of state parameters ω_{tot} can be written as [609],

$$\omega_X = -1 + \frac{XV_{,X}}{\rho_X} = -1 - \frac{1}{u^2+v^2}\sqrt{\frac{2}{3}}v^2\mu \ \tan\left[\frac{\pi w}{2}\right], \tag{2.20}$$
$$\omega_{tot} = \frac{p_{tot}}{\rho_{tot}} = \frac{p_X}{\rho_X + \rho_{DM}} = -u^2 - \frac{1}{3}v^2\left(3 + \sqrt{6}\mu \ \tan\left[\frac{\pi w}{2}\right]\right). \tag{2.21}$$

Thus the evolution equations in Section 2.2 can be converted to an autonomous system as follows [609]

$$u' = \frac{3}{2}u(1-u^2-v^2)+\sqrt{\frac{3}{2}}v^2\mu\left(1-u\tan\left[\frac{\pi w}{2}\right]\right)-\alpha\frac{(1-u^2-v^2)}{2u}, \tag{2.22}$$

$$v' = \frac{3}{2}v(1-u^2-v^2)-\sqrt{\frac{3}{2}}v\mu\left(u+(-1+v^2)\tan\left[\frac{\pi w}{2}\right]\right), \tag{2.23}$$

$$w' = \frac{6}{\pi}\cos^2\left[\frac{\pi w}{2}\right]\left(u-\tan\left[\frac{\pi w}{2}\right]\right) \tag{2.24}$$

where the interaction Q is chosen as $Q=\alpha\rho_{DM}H$ [604] and prime over a variable denotes differentiation with respect to $N=\ln\ a$. Hence, the first Friedmann equation gives constraint on the variables as

$$u^2+v^2+s^2=1 \tag{2.25}$$

(as s is not independent so the dynamical system is of $3D$ nature). The phase space is confined in a half cylinder of height 2 where $-1\leqslant u\leqslant 1$, $0\leqslant v\leqslant 1$, $-1\leqslant s\leqslant 1$ and $-1\leqslant w\leqslant 1$. Some non-hyperbolic critical points are already analyzed in [609]. In the present work, non-hyperbolic critical points are studied with a view to analyze bifurcation and Poincaré index. Cosmological evolutions are also examined near these critical points.

2.3.1 Non Interacting Model : $\alpha = 0$

Due to $\alpha=0$, the above autonomous system [2.22 − 2.24] simplifies to

$$u' = \frac{3}{2}u(1-u^2-v^2)+\sqrt{\frac{3}{2}}v^2\mu\left(1-u\tan\left[\frac{\pi w}{2}\right]\right), \tag{2.26}$$

$$v' = \frac{3}{2}v(1-u^2-v^2)-\sqrt{\frac{3}{2}}v\mu\left(u+(-1+v^2)\tan\left[\frac{\pi w}{2}\right]\right), \tag{2.27}$$

$$w' = \frac{6}{\pi}\cos^2\left[\frac{\pi w}{2}\right]\left(u-\tan\left[\frac{\pi w}{2}\right]\right). \tag{2.28}$$

As the critical points of the above system are enclosed by a half cylinder, so the only physically meaningful critical points are

$$P_1\left(1,0,\frac{1}{2}\right),\ P_2\left(-1,0,-\frac{1}{2}\right)\ \text{and}\ P_3(0,0,0)$$

and these critical points are same as in Ref.[609]. But the authors have analyzed only one critical point by using center manifold theory. But in this context we analyze the stability of all critical points by center manifold theory (for non-hyperbolic case) and Hartman-Grobman theorem (for hyperbolic case) and also discuss global stability with reference to bifurcation analysis using Poincaré index. The cosmological parameters, eigenvalues and the nature of critical points are presented in Table 2.1.

All the three critical points of the above autonomous system for non-interacting case has $v=0$ which corresponds to vanishing of the potential (as well as vanishing of the potential slope for the present choice of $V(X)$). Thus the three-form field behaves as a cosmological constant.

Table 2.1: The cosmological parameters, eigenvalues (λ_1, λ_2, λ_3) and the nature of critical points for the non-interacting model.

Critical Points	λ_1	λ_2	λ_3	ω_X	ω_{tot}	q	Nature of Critical points
$P_1 : (1, 0, \frac{1}{2})$	-3	0	-3	-1	-1	-1	nonhyperbolic
$P_2 : (-1, 0, -\frac{1}{2})$	-3	0	-3	-1	-1	-1	nonhyperbolic
$P_3 : (0, 0, 0)$	$\frac{3}{2}$	$\frac{3}{2}$	-3	-1	0	$\frac{1}{2}$	hyperbolic

Also for the first two critical points, *i.e.,* P_1 and P_2 there is no DM so the cosmological scenario purely corresponds to de Sitter phase [604, 486]. For the third critical point P_3, the evolution corresponds to non-interacting three form field (behaves as cosmological constant) with dark matter (DM) in the form of dust. Here DM dominates (three-form field DE is sub-dominant) the evolution and the resulting cosmic scenario represents the matter dominated era of evolution. This type of critical point is also obtained in [604] (see critical point (a) in Table 1 of Ref.[604]).

STABILITY ANALYSIS

We now investigate the stability of above nonhyperbolic critical points corresponding to this non interacting model. Most of the cases, the stability of non-hyperbolic critical points can be determined by center manifold (CM) theory. For this we first perform coordinate transformations so that the critical points moves to the origin.

2.3.1.1 Critical Point P_1

First we shift the critical point P_1 to the origin by using the coordinate transformation $u \to U + 1$, $v \to V$, $w \to W + \frac{1}{2}$, then the system of equations [2.26 – 2.28] changes to

$$U' = -3U - \frac{9}{2}U^2 - \frac{3}{2}U^3 - \frac{3}{2}V^2 - \frac{3}{2}UV^2 - \sqrt{\frac{3}{2}}\mu UV^2 - \sqrt{\frac{3}{2}}\pi\mu V^2 W + \text{higher order terms}, \tag{2.29}$$

$$V' = -\left(3 + \sqrt{\frac{3}{2}}\mu\right)UV - \frac{3}{2}U^2V - \left(\frac{3}{2} + \sqrt{\frac{3}{2}}\mu\right)V^3 + \sqrt{\frac{3}{2}}\pi\mu VW + \frac{\sqrt{3}}{2\sqrt{2}}\pi^2\mu VW^2 + \text{higher order terms}, \tag{2.30}$$

$$W' = -3W + \frac{3}{\pi}U - 3UW + \left(3 - \frac{3\pi}{2}\right)W^2 + \frac{\pi^2}{2}W^3 + \text{higher order terms}. \tag{2.31}$$

The Jacobian matrix at the origin corresponding to this autonomous system can be written as

$$J(P_1) = \begin{bmatrix} -3 & 0 & 0 \\ 0 & 0 & 0 \\ \frac{3}{\pi} & 0 & -3 \end{bmatrix}. \tag{2.32}$$

So the eigenvalues of the above matrix are $0, -3, -3$ and $[0, 1, 0]^T$ and $[0, 0, 1]^T$ are the eigenvectors corresponding to the eigenvalue 0 and -3 respectively. As Hartman-Grobman Theorem can not be used to analyze the nonhyperbolic critical point, we shall use center manifold theory (CMT). By center manifold theory there exist a continuously differentiable function h:$\mathbb{R}\to\mathbb{R}^2$ such that

$$h(V) = \begin{bmatrix} U \\ W \end{bmatrix} = \begin{bmatrix} a_1V^2 + a_2V^3 + \mathcal{O}\left(V^4\right) \\ b_1V^2 + b_2V^3 + \mathcal{O}\left(V^4\right) \end{bmatrix}. \tag{2.33}$$

Differentiating both side with respect to N yields

$$U' = (2a_1V + 3a_2V^2)V' + \text{higher order terms}, \tag{2.34}$$
$$W' = (2b_1V + 3b_2V^2)V' + \text{higher order terms}. \tag{2.35}$$

Comparing coefficients corresponding to power of V, we get $a_1 = -\frac{1}{2}$ and $a_2 = 0$; $b_1 = -\frac{1}{2\pi}$ and $b_2 = 0$, *i.e.,* the expression of center manifold can be written as

$$U = -\frac{1}{2}V^2 + \mathcal{O}\left(V^4\right), \tag{2.36}$$
$$W = -\frac{1}{2\pi}V^2 + \mathcal{O}\left(V^4\right). \tag{2.37}$$

The flow on the center manifold near the origin is determined by

$$\frac{dV}{dN} = -\sqrt{\frac{3}{2}}\mu V^3 + \mathcal{O}\left(V^4\right). \tag{2.38}$$

Here the stability of the vector field depends on the sign of μ. If $\mu > 0$ then $V' < 0$ for $V > 0$ and $V' > 0$ for $V < 0$. So for $\mu > 0$ the origin is a stable node. The vector field in UV-plane is shown in FIG.2.1(a) and the vector field near the origin in WV-plane is also same as of FIG.2.1(a). If $\mu < 0$ then $V' > 0$ for $V > 0$ and $V' < 0$ for $V < 0$. So for $\mu < 0$ the origin is a saddle node, *i.e.,* unstable in nature. The vector field in UV-plane near the origin is shown as in FIG.2.1(b) and the vector field near the origin in WV-plane is also the same as of FIG.2.1(b).

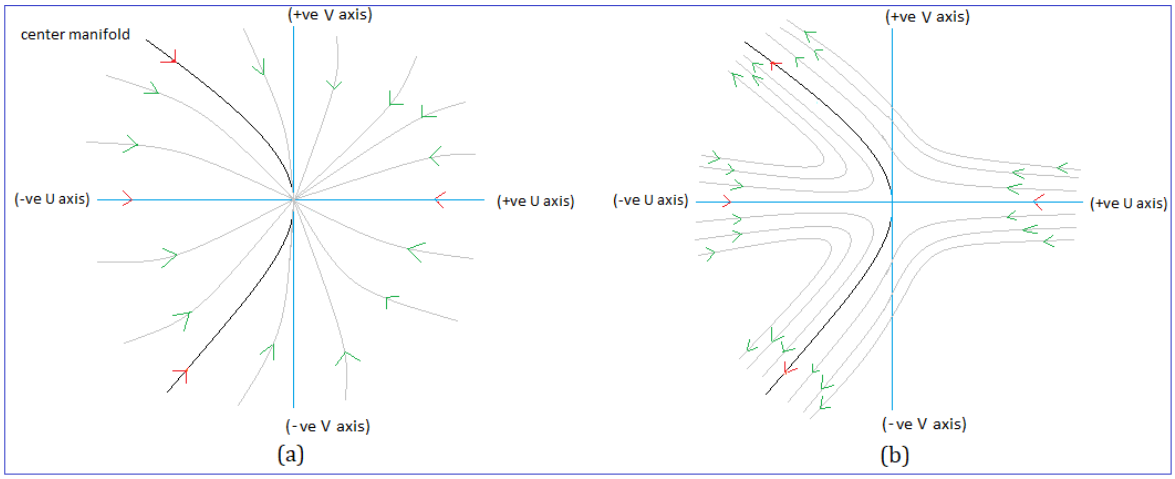

Figure 2.1: These figures show the vector field near the origin corresponding to the critical point P_1 in UV-plane. The phase plot (a) is for $\mu > 0$ and (b) is for $\mu < 0$.

If $\mu = 0$, the expression of center manifold is same with the equations (2.36) and (2.37) and the flow on the center manifold is determined by

$$\frac{dV}{dN} = -\frac{3}{8}V^5 + \mathcal{O}\left(V^6\right). \tag{2.39}$$

So the origin is a stable node and the flow near the origin is same as for $\mu > 0$ case (FIG.2.1).

2.3.1.2 Critical Point P_2

First, we shift the critical point P_2 to the origin by using the coordinate transformation $u \to U - 1$, $v \to V$, $w \to W - \frac{1}{2}$. The Jacobian matrix for the shifted autonomous system is same as of $J(P_1)$. So the set of eigenvalues and the corresponding eigenvectors of the Jacobian matrix are also same. Thus by center manifold theory, there exist a continuously differentiable function $h : \mathbb{R} \to \mathbb{R}^2$ such that

$$h(V) = \begin{bmatrix} U \\ W \end{bmatrix} = \begin{bmatrix} a_1V^2 + a_2V^3 + \mathcal{O}\left(V^4\right) \\ b_1V^2 + b_2V^3 + \mathcal{O}\left(V^4\right) \end{bmatrix}. \tag{2.40}$$

Differentiating both side with respect to N yields

$$U' = (2a_1V + 3a_2V^2)V' + \text{higher order terms}, \tag{2.41}$$

$$W' = (2b_1V + 3b_2V^2)V' + \text{higher order terms}. \tag{2.42}$$

Comparing coefficients corresponding to different power of V, we have $a_1 = \frac{1}{2}$ and $a_2 = 0$, $b_1 = \frac{1}{2\pi}$ and $b_2 = 0$. Then the center manifold is given by

$$U = \frac{1}{2}V^2 + \mathcal{O}\left(V^3\right), \tag{2.43}$$

$$W = \frac{1}{2\pi}V^2 + \mathcal{O}\left(V^3\right). \tag{2.44}$$

The flow on the center manifold near the origin is determined by

$$V' = \sqrt{\frac{3}{2}}\mu V^3 + \mathcal{O}\left(V^4\right). \tag{2.45}$$

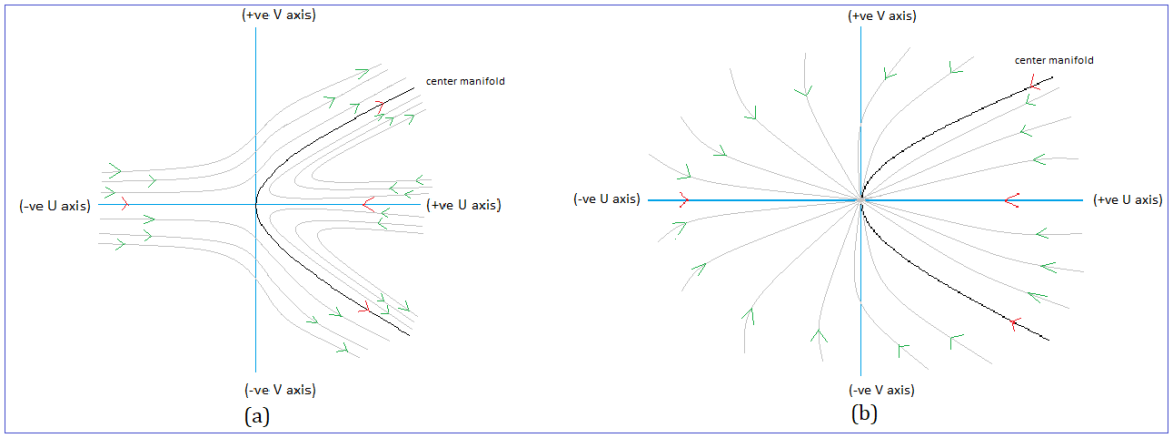

Figure 2.2: These figures show the vector field near the origin in UV-plane corresponding to the critical point P_2. The phase plot (a) is for $\mu > 0$ and the phase plot (b) is for $\mu < 0$.

Here the stability of the vector field depends on the sign of μ. If $\mu > 0$ then the origin is a saddle node, *i.e.,* unstable in nature and the vector field near the origin is shown as in FIG.2.2(a) and the flow on the center manifold in the WV-plane is also same as in (FIG.2.2(a)). If $\mu < 0$ then the origin is a stable node and the vector field near the origin is shown as in (FIG.2.2(b)) and the flow on the center manifold in WV-plane is also same as (FIG.2.2(b)). If $\mu = 0$ then the center manifold is same as of equations (2.43) and (2.44) and the flow on the center manifold is same as of equation (2.39), that is., the plot of the vector field near the origin is same as for $\mu < 0$ case (FIG.2.2(b)).

2.3.1.3 Critical Point P_3

The Jacobian matrix at P_3 for the autonomous system $[2.26 - 2.28]$ can be put as

$$J(P_3) = \begin{bmatrix} \frac{3}{2} & 0 & 0 \\ 0 & \frac{3}{2} & 0 \\ \frac{6}{\pi} & 0 & -3 \end{bmatrix} \tag{2.46}$$

The eigenvalues of the above Jacobian matrix are $\frac{3}{2}$, $\frac{3}{2}$ and -3. $[\frac{3\pi}{4}, 0, 1]^T$ and $[0, 1, 0]^T$ are the eigenvectors corresponding to the eigenvalue $\frac{3}{2}$ and $[0, 0, 1]^T$ is the eigenvector corresponding to the eigenvalue -3. Since the critical point P_3 is hyperbolic in nature, so we can analyze the stability of this critical point by Hartman-Grobman theorem. Since two eigenvalues are positive and one is negative, so the origin is a saddle node and the phase portrait near the origin is unstable in nature (FIG.2.3).

Poincaré index and Bifurcation Analysis

The index of an isolated critical point of a vector field is defined by the winding number of a small counter-clockwise oriented circle with center at that point. If we restrict ourselves on VW-plane, P_1 is stable node in nature for $\mu \geqslant 0$ and the index of $P_1|_{VW}$ is 1. On the other hand, P_1 is saddle for $\mu < 0$ and index of $P_1|_{VW}$ is -1. We get identical nature of P_1

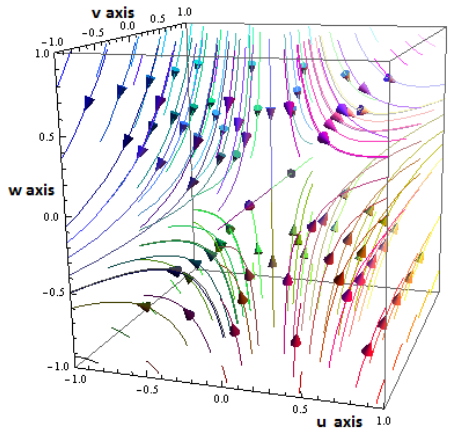

Figure 2.3: This figure shows the phase portrait near the origin corresponding to the equilibrium point P_3.

restricted on the UV-plane. On UW-plane, P_1 is stable node for all μ and the index is 1. Thus at $\mu = 0$ the system is structurally unstable in nature and bifurcation occurs.
If we restrict ourselves on VW-plane, P_2 is saddle in nature for $\mu > 0$ and the index of $P_2|_{VW}$ is -1. On the other hand, P_2 is stable node for $\mu \leqslant 0$ and index of $P_2|_{VW}$ is -1. We get identical nature of P_2 restricted on the UV-plane. On UW-plane, P_2 is stable node for all μ and the index is 1. Thus at $\mu = 0$ the system is structurally unstable in nature and bifurcation occurs.
The index of P_3 restricted on any plane is independent of μ. So in this case there is no bifurcation value.
Thus P_1 is stable for $\mu \geqslant 0$ and the universe undergoes an exponential de-sitter expansion near P_1. For $\mu < 0$, the universe goes away from P_1 as time evolves. On the other hand, P_2 is unstable in nature for $\mu > 0$ and stable for $\mu \leqslant 0$. So there may be a de-Sitter generic evolution of the universe from the neighborhood of P_2 towards P_1 for $\mu > 0$ and reverses the trajectory for $\mu < 0$. At $\mu = 0$, there may be a non-generic evolution from early time decelerating phase to late time accelerating phase. So a non-generic evolution of the universe may occur when μ passes through the bifurcation value.

2.3.2 Interaction Model : $\alpha \neq 0$

Now we shall study the stability analysis for interacting model with α as arbitrary parameter. For this case we consider the primary autonomous system [2.22 – 2.24]. The critical points for this autonomous system are:

$$P_4\left(1, 0, \frac{1}{2}\right), \quad P_5\left(-1, 0, -\frac{1}{2}\right), \quad P_6\left(\sqrt{\frac{\alpha}{3}}, 0, \frac{2}{\pi}\cos^{-1}\left[\sqrt{\frac{3}{\alpha+3}}\right]\right)$$
$$\text{and} \quad P_7\left(-\sqrt{\frac{\alpha}{3}}, 0, -\frac{2}{\pi}\cos^{-1}\left[\sqrt{\frac{3}{\alpha+3}}\right]\right).$$

There is also a line of critical point: $P_{l_c} = \left(u_c, \sqrt{\frac{3(1-u_c^2)}{3+\sqrt{6}u_c\mu}}, \frac{2}{\pi}\tan^{-1}u_c\right)$, where $u_c \in [-1, 0)\cup(0, 1]$ and which exists only for $\alpha = 3$. The cosmological parameters corresponding to

P_{l_c} are given by $\omega_X = -\left(\frac{\sqrt{3}+\sqrt{2}\mu u_c}{\sqrt{3}+\sqrt{2}\mu u_c^3}\right)$, $\omega_{tot} = -1$ and $q = -1$. Note that except line of critical points P_{l_c} all critical points are same as in Ref.[609]. But the authors have analyzed only one critical point by using center manifold theory. In this context we analyze the stability of all critical points by center manifold theory (for nonhyperbolic case) and Hartman-Grobman theorem (for hyperbolic case) for all possible values of the parameters α and μ and also discuss global stability with reference to bifurcation analysis using Poincaré index. The cosmological parameters, eigenvalues and the nature of critical points for this interacting model are presented in Table 2.2.

In the present interacting DE (in the form of three-form field) and DM (in the form of dust) cosmological model, the above autonomous system has four critical points of which top two (*i.e.,* P_4 and P_5) are identical in nature to the critical points P_1 and P_2 for the non-interacting case. The other two critical points namely P_6 and P_7 are quite interesting as they may stand for various cosmological scenarios [604, 486] with different choices of the interaction coupling parameter 'α'. Note that α should positive to have these critical points to be real and as a consequence there is a flow of matter from DM to DE (as speculated by recent observations for DE dominance). If α is very small (*i.e.,* close to zero) then the present model has DM dominance and the cosmic scenario corresponds to matter dominated era while DE (*i.e.,* 3-form field as cosmological constant) will dominate the evolution for $\alpha > 1$ and may be termed as LCDM model. In fact by adjusting α ($\alpha \approx 3$), it is possible to match recent Plank observation $\omega = -1.028 \pm 0.031$ [617]. Further there is a line of critical points given by $P_{l_c}=\left(u_c, \sqrt{\frac{3(1-u_c^2)}{3+\sqrt{6}u_c\mu}}, \frac{2}{\pi}\tan^{-1}u_c\right)$, with $u_c \in [-1,0)\cup(0,1]$ and it exists only for $\alpha = 3$. For this line of critical points the three form field behaves as a perfect fluid with equation of state parameter $\omega_X = -\left(\frac{\sqrt{3}+\sqrt{2}\mu u_c}{\sqrt{3}+\sqrt{2}\mu u_c^3}\right) < -1$, *i.e.,* a phantom fluid. However, interacting with DM, the resulting single fluid behaves as a cosmological constant. So effectively this line of critical points correspond to de Sitter era of evolution.

STABILITY ANALYSIS

We shall discuss the stability analysis of the critical point ($P_4 - P_7$) both for $\alpha = 3$ and $\alpha \neq 3$. The stability analysis for the line of critical point P_{l_c} is very complicated and laborious, so here we will not present the stability of this critical point.

2.3.2.1 Critical Point P_4

Case 1: $\alpha = 3$

At first we put $\alpha = 3$ in (2.22) and then shift the critical point P_4 to the origin by using the coordinate transformation $u \to U+1$, $v \to V$, $w \to W+\frac{1}{2}$. Then the system of equations

Table 2.2: Table shows the value of cosmological parameters, eigenvalues (λ_1, λ_2, λ_3) corresponding to the critical points and the nature of the critical points for the interaction model with interaction $Q = \alpha\rho_{DM}H$ where α is an arbitrary constant.

Critical Points	ω_X	ω_{tot}	q	λ_1	λ_2	λ_3	Nature of Critical point
$P_4 : (1, 0, \frac{1}{2})$	-1	-1	-1	$-3+\alpha$	0	-3	always non-hyperbolic
$P_5 : (-1, 0, -\frac{1}{2})$	-1	-1	-1	$-3+\alpha$	0	-3	always non-hyperbolic
$P_6 : \left(\sqrt{\frac{\alpha}{3}}, 0, \frac{2}{\pi}\cos^{-1}\left[\sqrt{\frac{3}{\alpha+3}}\right]\right)$	-1	$-\frac{\alpha}{3}$	$\frac{1}{2}(1-\alpha)$	$-\alpha+3$	$\frac{(-\alpha+3)}{2}$	-3	non-hyperbolic for $\alpha = 3$ and hyperbolic for $\alpha \neq 3$
$P_7 : \left(-\sqrt{\frac{\alpha}{3}}, 0, -\frac{2}{\pi}\cos^{-1}\left[\sqrt{\frac{3}{\alpha+3}}\right]\right)$	-1	$-\frac{\alpha}{3}$	$\frac{1}{2}(1-\alpha)$	$-\alpha+3$	$\frac{(-\alpha+3)}{2}$	-3	non-hyperbolic for $\alpha = 3$ and hyperbolic for $\alpha \neq 3$

(2.22 − 2.24) modifies to

$$U' = -6U^2 - \left(3 + \sqrt{\frac{3}{2}}\mu\right) UV^2 - \sqrt{\frac{3}{2}}\pi\mu V^2 W + \text{higher order terms}, \tag{2.47}$$

$$V' = -\left(3 + \sqrt{\frac{3}{2}}\mu\right) UV - \frac{3}{2}U^2 V - \left(\frac{3}{2} + \sqrt{\frac{3}{2}}\mu\right) V^3 + \sqrt{\frac{3}{2}}\pi VW\mu + \frac{\sqrt{3}}{2\sqrt{2}}\pi^2\mu VW^2 + \text{higher order terms}, \tag{2.48}$$

$$W' = -3W + \frac{3}{\pi}U - 3UW + \left(-\frac{3\pi}{2} + 3\right) W^2 + \frac{\pi^2}{2}W^3 + \text{higher order terms}. \tag{2.49}$$

The Jacobian matrix at the origin corresponding to the above autonomous system can be written as

$$J(P_4)|_{\alpha=3} = \begin{bmatrix} 0 & 0 & 0 \\ 0 & 0 & 0 \\ \frac{3}{\pi} & 0 & -3 \end{bmatrix}. \tag{2.50}$$

So the eigenvalues of the above matrix are 0, 0, −3; and $[1, 0, \frac{1}{\pi}]^T$ and $[0, 1, 0]^T$ are the eigenvectors corresponding to the eigenvalue 0 and $[0, 0, 1]^T$ is the eigenvector corresponding to the eigenvalue −3. Using the matrix of eigenvectors of the stability matrix of the system in U, V, W we introduce another set of new coordinates

$$\begin{bmatrix} U_T \\ V_T \\ W_T \end{bmatrix} = \begin{bmatrix} 1 & 0 & 0 \\ 0 & 1 & 0 \\ -\frac{1}{\pi} & 0 & 1 \end{bmatrix} \begin{bmatrix} U \\ V \\ W \end{bmatrix}. \tag{2.51}$$

In these coordinates, the system of equations is now in the correct form

$$\begin{bmatrix} U_T' \\ V_T' \\ W_T' \end{bmatrix} = \begin{bmatrix} 0 & 0 & 0 \\ 0 & 0 & 0 \\ 0 & 0 & -3 \end{bmatrix} \begin{bmatrix} U_T \\ V_T \\ W_T \end{bmatrix} + \begin{bmatrix} \text{non} \\ \text{linear} \\ \text{terms} \end{bmatrix}. \tag{2.52}$$

Thus by center manifold theory, there exist a continuously differentiable function $h : \mathbb{R}^2 \to \mathbb{R}$ such that $W_T = h(U_T, V_T) = aU_T^2 + bU_T V_T + cV_T^2 + \text{highe order terms}$, where $a, b, c \in \mathbb{R}$. We only concern about the nonzero coefficients of the lowest power terms in CMT as we analyze arbitrary small neighborhood of the origin. Now differentiating both sides of the expression of W_T with respect to N yields

$$\frac{dW_T}{dN} = \begin{bmatrix} 2aU_T + bV_T & bU_T + 2cV_T \end{bmatrix} \begin{bmatrix} \frac{dU_T}{dN} \\ \\ \frac{dV_T}{dN} \end{bmatrix}. \tag{2.53}$$

Comparing L.H.S. and R.H.S. of (2.53) we get, $a = \frac{3}{2\pi}$, $b = 0$ and $c = 0$, *i.e.*, the expression of the center manifold can be written as

$$W_T = \frac{3}{2\pi}U_T^2. \tag{2.54}$$

The flow on the center manifold near the origin is determined by

$$\frac{dU_T}{dN} = -6U_T^2 - (3+\sqrt{6}\mu)U_T V_T^2 + \text{higher order terms}, \tag{2.55}$$

$$\frac{dV_T}{dN} = -3U_T V_T + \left(\sqrt{6}\mu - \frac{3}{2}\right)U_T^2 V_T + \left(\frac{3}{2} + \sqrt{\frac{3}{2}}\mu\right)V_T^3 + \text{higher order terms}. \tag{2.56}$$

Now to analyze the stability of this critical point, we divide both sides of (2.55) by 6 and both sides of (2.56) by 3. Since we divided both sides of these equation by positive integers, so the direction of the vector field will be unchanged. We take $r^2 = U_T^2 + V_T^2$, then differentiating both sides with respect to N and using (2.55) and (2.56) yields $r' = -U_T r$. So r' depends on the sign of U_T. If $U_T > 0$ then $r' < 0$ and if $U_T < 0$ then $r' > 0$. So, the origin is a saddle node and hence the vector field near the origin is unstable in nature (FIG.2.4). Now we try to see the vector field near the origin for $\mu = -\sqrt{\frac{3}{2}}$ because for $\mu = -\sqrt{\frac{3}{2}}$ the coefficient of V^3 in equation (2.48) vanishes. The vector field in VW-plane near the origin for $\mu = -\sqrt{\frac{3}{2}}$ is shown as in FIG.2.5.

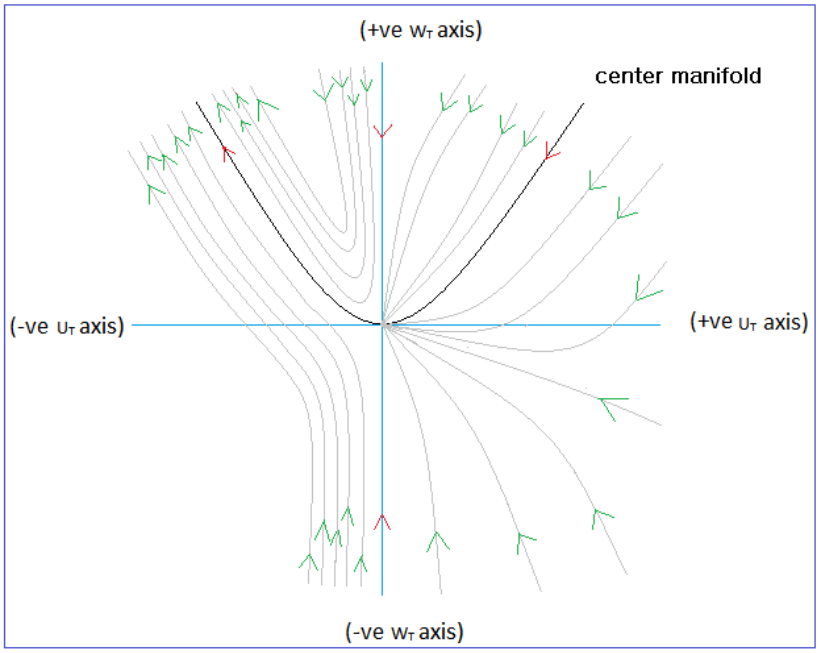

Figure 2.4: Projection of the vector field on $U_T W_T$-plane near the origin corresponding the critical point P_4 for $\alpha = 3$.

Case 2: $\alpha \neq 3$

After shifting the critical point P_4 to the origin and by using same transformation as above the autonomous system [2.22 – 2.24] changes to

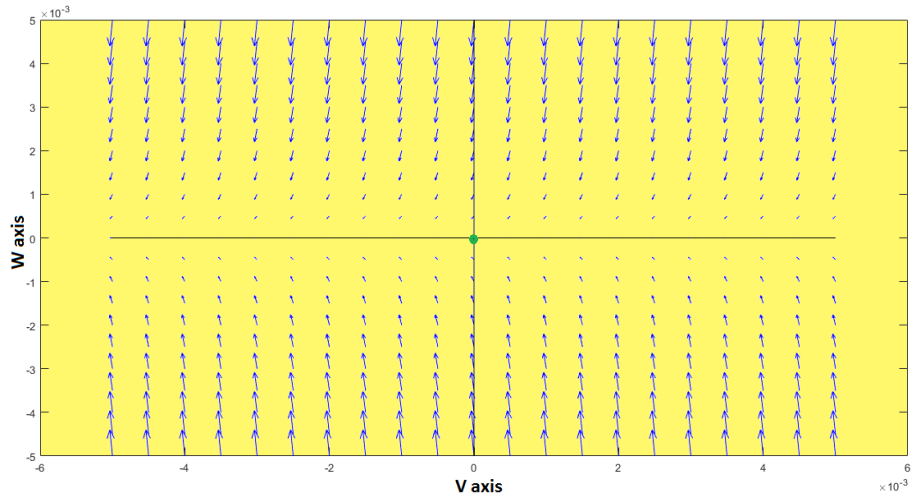

Figure 2.5: This figure shows the vector field near the origin in VW-plane corresponding to the critical point P_4 for $\left(\alpha = 3, \mu = -\sqrt{\frac{3}{2}}\right)$.

$$U' = (-3+\alpha)\,U - \left(\frac{9+\alpha}{2}\right)U^2 + \left(\frac{-3+\alpha}{2}\right)U^3 + \left(\frac{-3+\alpha}{2}\right)V^2 + \left(\frac{-3+\alpha}{2}\right)UV^2 - \sqrt{\frac{3}{2}}\mu UV^2 - \frac{\sqrt{3}}{\sqrt{2}}\pi\mu V^2 W + \text{higher order terms}, \tag{2.57}$$

$$V' = -\left(3+\sqrt{\frac{3}{2}}\mu\right)UV - \frac{3}{2}U^2V - \left(\frac{3}{2}+\sqrt{\frac{3}{2}}\mu\right)V^3 + \sqrt{\frac{3}{2}}\pi VW\mu + \frac{\sqrt{3}}{2\sqrt{2}}\pi^2\mu VW^2 + \text{higher order terms}, \tag{2.58}$$

$$W' = -3W + \frac{3}{\pi}U - 3UW + \left(-\frac{3\pi}{2}+3\right)W^2 + \frac{\pi^2}{2}W^3 + \text{higher order terms}. \tag{2.59}$$

The Jacobian matrix at the origin corresponding to the above autonomous system can be written as

$$J(P_4)|_{\alpha\neq 3} = \begin{bmatrix} -3+\alpha & 0 & 0 \\ 0 & 0 & 0 \\ \frac{3}{\pi} & 0 & -3 \end{bmatrix}. \tag{2.60}$$

So the eigenvalues of the above matrix are $-3+\alpha, 0, -3$ and $[\frac{\pi\alpha}{3}, 0, 1]^T$, $[0,1,0]^T$, $[0,0,1]^T$ are the corresponding eigenvectors, respectively. Then by using similar arguments which we have done for the critical point P_1, the center manifold can be expressed as

$$U = -\frac{1}{2}V^2 + \mathcal{O}\left(V^4\right), \tag{2.61}$$

$$W = -\frac{1}{2\pi}V^2 + \mathcal{O}\left(V^4\right). \tag{2.62}$$

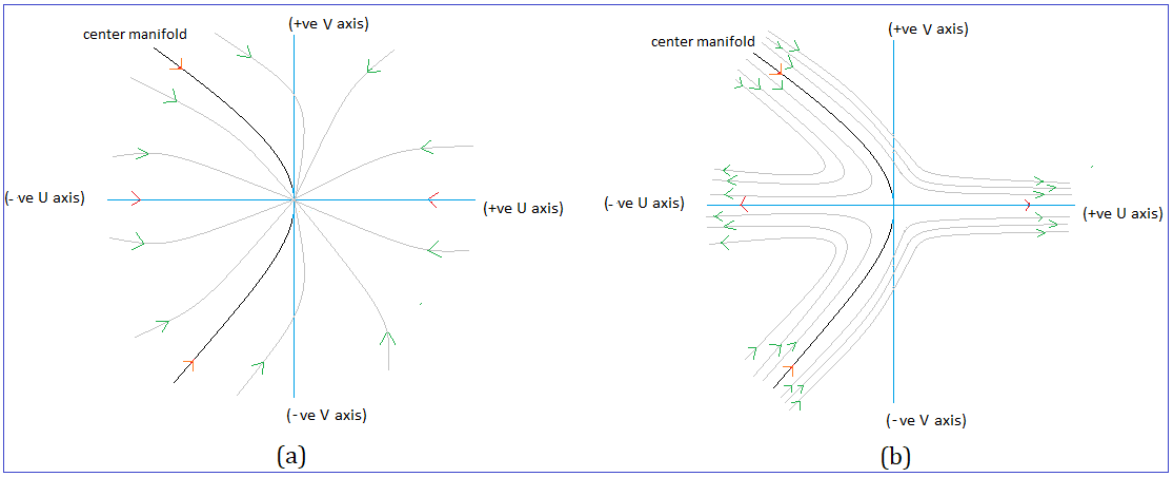

Figure 2.6: These figures show the vector field near the origin in UV-plane corresponding to P_4. The phase plot (a) is for $(\alpha < 3, \mu > 0)$ and (b) is for $(\alpha > 3, \mu > 0)$.

The flow on the center manifold near the origin is determined by

$$\frac{dV}{dN} = -\sqrt{\frac{3}{2}}\mu V^3 + \mathcal{O}\left(V^4\right). \tag{2.63}$$

For $\alpha \neq 3$, we get four different phase diagram near the origin depending on the values of α and μ. For $\mu > 0$ there arises two cases $\alpha > 3$ and $\alpha < 3$ and for $\mu < 0$ there also arises two cases $\alpha > 3$ and $\alpha < 3$.

Case (i): $\mu > 0$

For $\alpha < 3$ the origin is a stable node, *i.e.,* the vector field near the origin is stable in nature (FIG.2.6(a)). For $\alpha > 3$ the origin is a saddle node, *i.e.,* the vector field near the origin is unstable in nature (FIG 2.6(b)).

Case (ii): $\mu < 0$

In this case, the origin is a saddle node for $\alpha < 3$ (FIG 2.7(a)) and an unstable node for $\alpha > 3$ (FIG 2.7(b)), *i.e.,* for both of the cases the vector field near the origin is unstable in nature.

Case (iii): $\mu = 0$

If we calculate the center manifold for $\mu = 0$ then we can see that the center manifold is same as of equation (2.61) and (2.62) and the flow on the center manifold is determined by

$$\frac{dV}{dN} = -\frac{3}{8}V^5 + \mathcal{O}\left(V^6\right). \tag{2.64}$$

For $\alpha > 3$ the origin is a saddle node, *i.e.,* unstable in nature and for $\alpha < 3$ the origin is a stable node, *i.e.,* stable in nature and the vector field near the origin is same as for $\mu > 0$ case (FIG 2.6).

2.3.2.2 Critical Point P_5

Case 1: $\alpha = 3$

Similarly as above after putting $\alpha = 3$ in (2.22), we shift the critical point P_5 to the origin by using the coordinate transformation $u \to U - 1$, $v \to V$, $w \to W - \frac{1}{2}$. After using

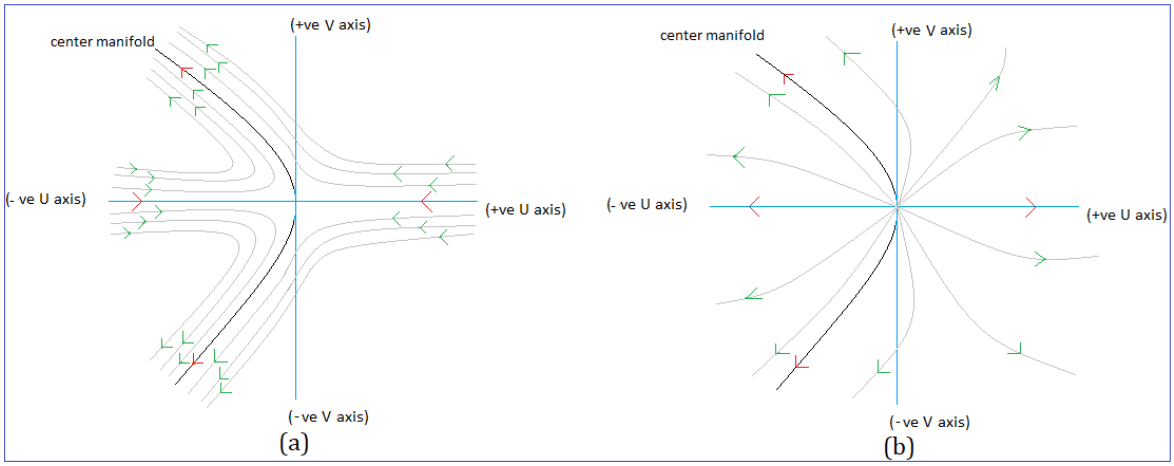

Figure 2.7: These figures show the vector field near the origin in UV-plane corresponding to P_4. The phase plot (a) is for $(\alpha < 3, \mu < 0)$ and (b) is for $(\alpha > 3, \mu < 0)$.

this shifting transformation, the Jacobian matrix at the origin corresponding to the modified autonomous system can be written as

$$J(P_5)|_{\alpha=3} = \begin{bmatrix} 0 & 0 & 0 \\ 0 & 0 & 0 \\ \frac{3}{\pi} & 0 & -3 \end{bmatrix}. \tag{2.65}$$

So the eigenvalues of the above matrix are $0,\ 0,\ -3$ and $[1, 0, \frac{1}{\pi}]^T$ and $[0, 1, 0]^T$ are the eigenvectors corresponding to the eigenvalue 0 and $[0, 0, 1]^T$ is the eigenvector corresponding to the eigenvalue -3. By computing the matrix of eigenvectors of the Jacobian matrix of the system in U, V, W; we introduce another set of new coordinates (U_T, V_T, W_T) in terms of (U, V, W) as follows

$$\begin{bmatrix} U_T \\ V_T \\ W_T \end{bmatrix} = \begin{bmatrix} 1 & 0 & 0 \\ 0 & 1 & 0 \\ -\frac{1}{\pi} & 0 & 1 \end{bmatrix} \begin{bmatrix} U \\ V \\ W \end{bmatrix}. \tag{2.66}$$

In these coordinates the system of equations is now in the correct form

$$\begin{bmatrix} U_T' \\ V_T' \\ W_T' \end{bmatrix} = \begin{bmatrix} 0 & 0 & 0 \\ 0 & 0 & 0 \\ 0 & 0 & -3 \end{bmatrix} \begin{bmatrix} U_T \\ V_T \\ W_T \end{bmatrix} + \begin{bmatrix} \text{non} \\ \text{linear} \\ \text{terms} \end{bmatrix}. \tag{2.67}$$

Thus by center manifold theory there exist a continuously differentiable function $h : \mathbb{R}^2 \to \mathbb{R}$ such that $W_T = h(U_T, V_T) = aU_T^2 + bU_TV_T + cV_T^2 + \text{higher order terms}$, where $a,\ b,\ c \in \mathbb{R}$. We only concern about the nonzero coefficients of the lowest power terms in CMT as we analyze arbitrary small neighborhood of the origin. Now differentiating both side with respect to N,

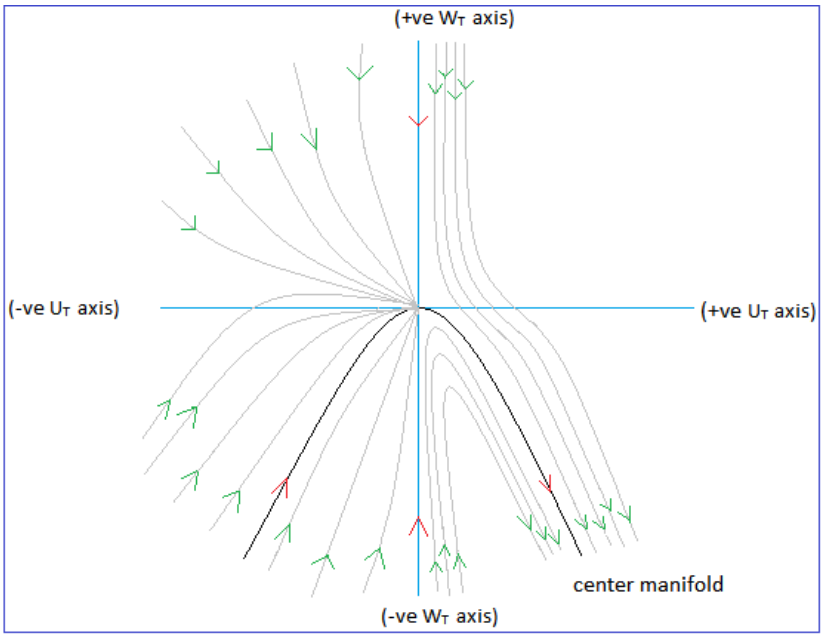

Figure 2.8: This phase plot shows the projection of the vector field on the $(U_T W_T)$-plane near the origin corresponding to P_5 for $\alpha = 3$.

we get

$$\frac{dW_T}{dN} = \begin{bmatrix} 2aU_T + bV_T & bU_T + 2cV_T \end{bmatrix} \begin{bmatrix} \frac{dU_T}{dN} \\ \\ \frac{dV_T}{dN} \end{bmatrix}. \tag{2.68}$$

Comparing L.H.S. and R.H.S. of (2.68) we get, $a = -\frac{3}{2\pi}$, $b = 0$ and $c = 0$, *i.e.*, the center manifold can be written as

$$W_T = -\frac{3}{2\pi} U_T^2. \tag{2.69}$$

The flow on the center manifold near the origin is determined by

$$\frac{dU_T}{dN} = 6U_T^2 + (-3 + \sqrt{6}\mu) U_T V_T^2 + \text{higher order terms}, \tag{2.70}$$

$$\frac{dV_T}{dN} = 3U_T V_T - \left(\sqrt{6}\mu + \frac{3}{2}\right) U_T^2 V_T - \left(\frac{3}{2} - \sqrt{\frac{3}{2}}\mu\right) V_T^3 + \text{higher order terms}. \tag{2.71}$$

Similarly to analyze the stability of this critical point, first we divide both sides of (2.70) by 6 and divide both sides of (2.71) by 3. Since we divided both sides of these equations by positive terms, so the direction of vector field will be unchanged. We take $r^2 = U_T^2 + V_T^2$, then differentiating both sides with respect to N and using (2.70) and (2.71) yields $r' = U_T r$. So r' depends on the sign of U_T. If $U_T > 0$ then $r' > 0$ and $r' < 0$ while $U_T < 0$. So the origin is a saddle node and hence the vector field near the origin is unstable in nature (FIG.2.8).

Now we try to see the vector field near the origin for $\mu = \sqrt{\frac{3}{2}}$ because for $\mu = \sqrt{\frac{3}{2}}$ the coefficient of V^3 in R.H.S. of the second equation of transformed autonomous vanishes. The

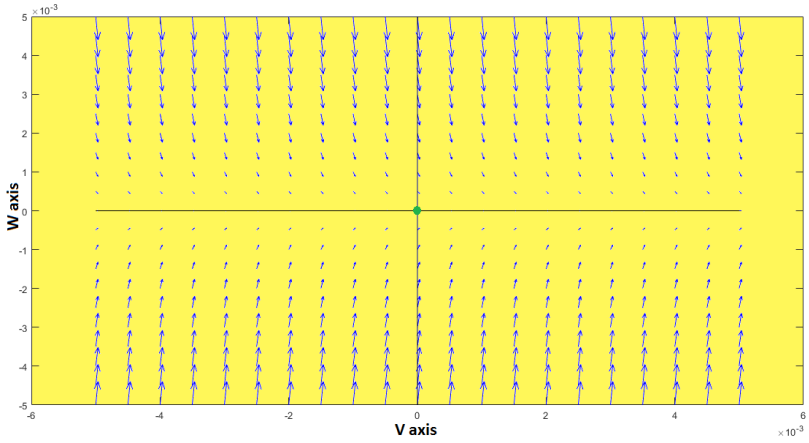

Figure 2.9: These figures shows the vector field near the origin in VW-plane corresponding to P_5 for $\left(\alpha = 3, \mu = \sqrt{\frac{3}{2}}\right)$.

vector field in VW plane near the origin for $\mu = \sqrt{\frac{3}{2}}$ is shown as in FIG.2.9.

Case 2: $\alpha \neq 3$

After shifting the critical point P_5 to the origin, by similar calculation we can easily see that the Jacobian matrix for the transformed autonomous system is same as of (2.60). Hence, we have the same eigenvalues and corresponding eigenvectors which already obtained for (2.60) and the center manifold near the origin can be written as

$$U = \frac{1}{2}V^2 + \mathcal{O}\left(V^4\right), \tag{2.72}$$

$$W = \frac{1}{2\pi}V^2 + \mathcal{O}\left(V^4\right). \tag{2.73}$$

The flow on the center manifold near the origin is determined by

$$\frac{dV}{dN} = \sqrt{\frac{3}{2}}\mu V^3 + \mathcal{O}\left(V^4\right). \tag{2.74}$$

For $\alpha \neq 3$ we get four different phase diagram near the origin depending on the values of α and μ. For $\mu > 0$ there arises two cases $\alpha > 3$ and $\alpha < 3$ and for $\mu < 0$ there also arises two cases $\alpha > 3$ and $\alpha < 3$.

Case (i): $\mu > 0$

The origin is a saddle node if α <3 (FIG.2.10(a)) and an unstable node if α >3 (FIG.2.10(b)), *i.e.,* the vector field near the origin is unstable in nature for both of the cases.

Case (ii): $\mu < 0$

For $\alpha < 3$ the origin is a stable node, *i.e.,* the vector field near the origin is stable in nature (FIG.2.11(a)). The origin is a saddle node if α >3; *i.e.,* the vector field near the origin is unstable in nature (FIG.2.11(b)).

Case (iii): $\mu = 0$

If we calculate the center manifold for $\mu = 0$ then the expression of center manifold is same as of equation (2.72) and (2.73) and the flow on the center manifold is determined by

$$\frac{dV}{dN} = -\frac{3}{8}V^5 + \mathcal{O}\left(V^6\right). \tag{2.75}$$

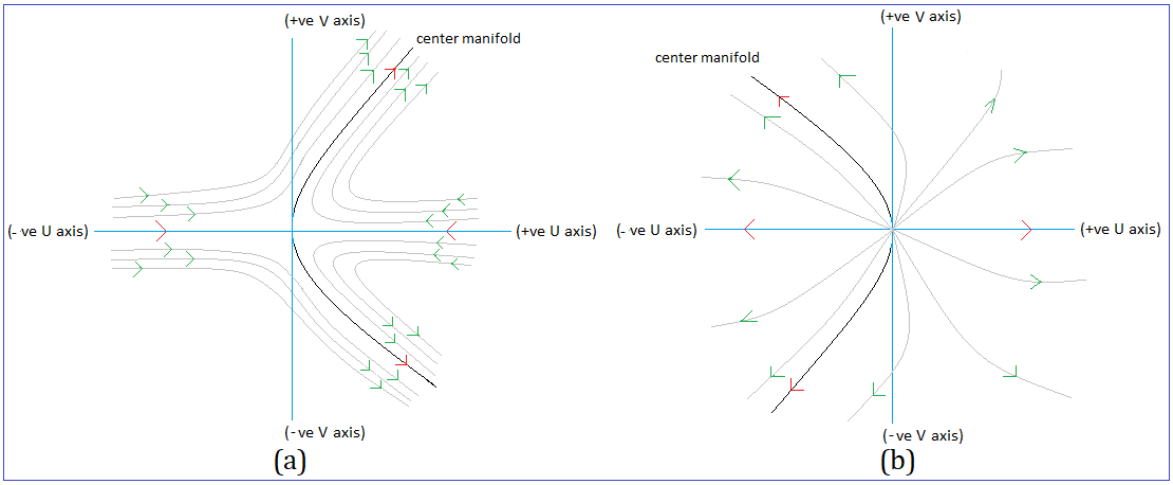

Figure 2.10: These figures show the vector field near the origin in UV plane for the critical point P_5. The phase plot (a) is for $(\alpha < 3, \mu > 0)$ and (b) is for $(\alpha > 3, \mu > 0)$.

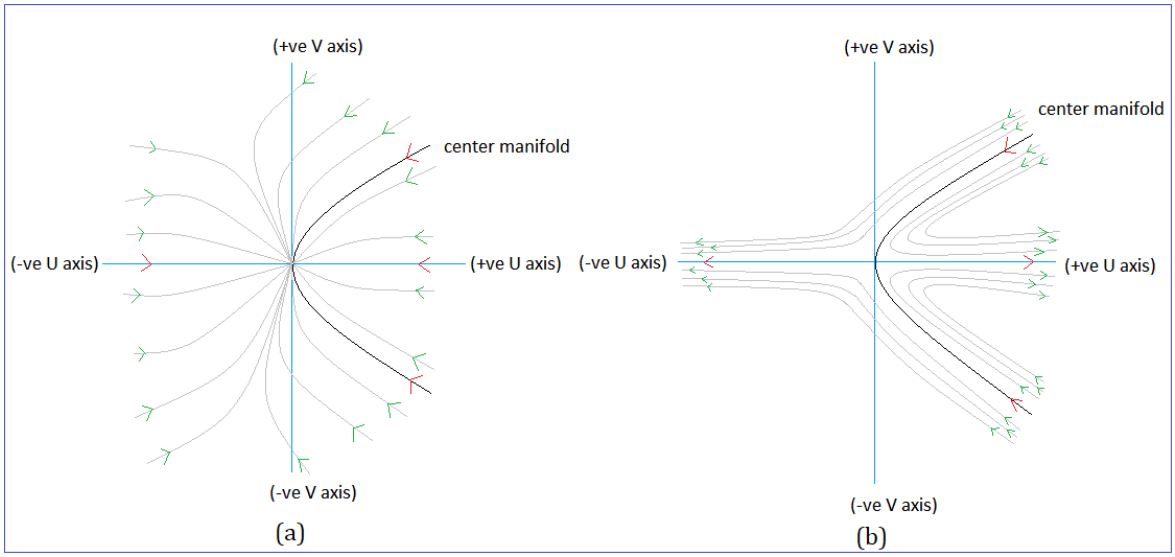

Figure 2.11: These figures show the vector field near the origin in UV plane for P_5. The phase plot (a) is for $(\alpha < 3, \mu < 0)$ and (b) is for $(\alpha > 3, \mu < 0)$.

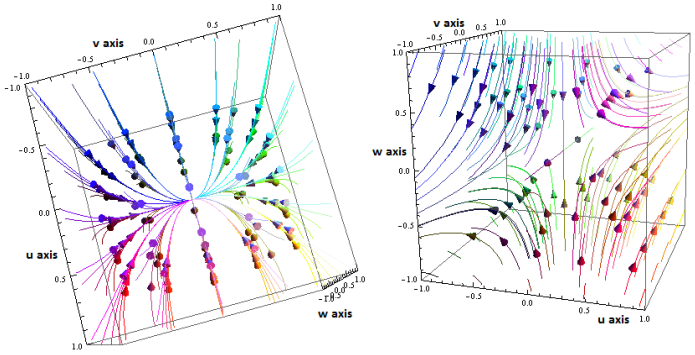

(a) (b)

Figure 2.12: These figures show the phase potrait near the origin corresponding to the critical point P_6. (a) is for $\alpha > 3$ (considering $\alpha = 4$) and (b) is for $\alpha < 3$ (considering $\alpha = 2$).

For α >3 the origin is a saddle node, *i.e.,* unstable in nature and for $\alpha < 3$ the origin is a stable node, *i.e.,* stable in nature and the flow near the origin is same as of the flow near the origin for $\mu < 0$ case (FIG.2.11).

2.3.2.3 Critical Point P_6

First we shift the critical point P_6 to the origin by using the coordinate transformation $u \to U + \frac{\alpha}{3}$, $v \to$V and $w \to W + \frac{2}{\pi}\cos^{-1}\left[\sqrt{\frac{3}{\alpha+3}}\right]$. Now the Jacobian matrix at the origin for the transformed autonomous system can be written as

$$J(P_6) = \begin{bmatrix} 3-\alpha & 0 & 0 \\ 0 & \frac{3-\alpha}{2} & 0 \\ \frac{18}{\pi(\alpha+3)} & 0 & -3 \end{bmatrix}. \tag{2.76}$$

The eigenvalues of the above Jacobian matrix are $(3-\alpha)$, $\frac{(3-\alpha)}{2}$ and -3. $[1, 0, \frac{18}{\pi(3+\alpha)(6-\alpha)}]^T$, $[0, 1, 0]^T$ and $[0, 0, 1]^T$ are the eigenvectors corresponding to the eigenvalues $(3-\alpha)$, $\frac{(3-\alpha)}{2}$ and -3 respectively. Since, the Jacobian matrix has nonzero real eigenvalues for $\alpha \neq 3$, so the critical point is hyperbolic and so we can analyze the stability of the critical point by Hartman-Grobman theorem [496]. For $\alpha > 3$ all eigenvalues are negative and hence the origin is a stable node and the phase portrait near the origin is asymptotically stable in nature (FIG.2.12(a)). For $\alpha < 3$ two eigenvalues are positive and one is negative and hence the origin is a saddle node and the phase portrait near the origin is unstable in nature (FIG.2.12(b)).

2.3.2.4 Critical Point P_7

If we determine the Jacobian matrix corresponding to the autonomous system [2.22 – 2.24] at the critical point P_7, then we will get the same Jacobian matrix as (2.76) and hence we have the same eigenvalues and corresponding eigenvectors. Since, the eigenvalues are nonzero, so we analyze the stability of this critical point by Hartman-Grobman theorem. The phase

portrait near the origin is shown as in FIG.2.12.

For $\alpha = 3$ the critical points P_6 and P_7 are non-hyperbolic. For this case, the stability analysis of those critical points is the same as Case 1 of the critical points P_4 and P_5 respectively.

Poincaré index and Bifurcation Analysis

For $\alpha < 3$ four critical points (P_4-P_7) appear to exist but at $\alpha = 3$ two critical points (P_6 and P_7) disappear. Again they appear for $\alpha > 3$. If we restrict ourselves on UW-plane, P_4 and P_5 are stable node in nature for $\alpha < 3$ and index of each $P_4, P_5|_{UW}$ is 1. On the UV-plane, for $\mu > 0$, P_4 is stable node for $\alpha < 3$ with index 1 and saddle for $\alpha > 3$ with index -1. For $\mu = 0$, the index of $P_4|_{UV}$ is 0 as the neighborhood has two hyperbolic sectors. On the VW-plane, for $\alpha \neq 3$, the index of $P_4|_{VW}$ is 1 for $\mu > 0$ and -1 for $\mu \leqslant 0$. For $\alpha = 3$, index of $P_4|_{VW}$ is -1 for $\mu \geqslant -\sqrt{\frac{3}{2}}$ and 1 for $\mu < -\sqrt{\frac{3}{2}}$.
Similarly on the UV-plane, for $\mu > 0$, P_5 is saddle for $\alpha < 3$ with index -1 and stable node for $\alpha > 3$ with index 1. For $\mu = 0$, the index of $P_5|_{UV}$ is 0 as the neighborhood has two hyperbolic sectors. For $\mu < 0$, P_5 is stable node for $\alpha < 3$ with index 1 and saddle for $\alpha > 3$ with index -1. For $\mu = 0$, the index of $P_5|_{UV}$ is 0 as the neighborhood has two hyperbolic sectors.On the VW-plane, for $\alpha \neq 3$, the index of $P_5|_{VW}$ is -1 for $\mu \geqslant 0$ and 1 for $\mu < 0$. For $\alpha = 3$, index of $P_4|_{VW}$ is 1 for $\mu > \sqrt{\frac{3}{2}}$ and -1 for $\mu \leqslant \sqrt{\frac{3}{2}}$. Again P_6 and P_7 are saddle for $\alpha < 3$ and stable node for $\alpha > 3$. So at $\alpha = 3$ and $\mu = 0, \pm\sqrt{\frac{3}{2}}$ the system is structurally unstable.
For $\alpha < 3$ and $\mu > 0$, P_4 is a stable node and P_5 is a saddle in nature. So generic de-Sitter evolution can be found from P_5 of index -1 plane to P_4 of index 1 plane. For $\mu < 0$, the generic evolution reverses its direction. At $\alpha < 3$ and $\mu = 0$ there may occur a non-generic evolution from P_6 or P_7 to P_4 or P_5 and the universe changes its phase from decelerating matter dominated era to phantom barrier. A similar non-generic evolution also can be found for $\alpha > 3$. At $\alpha = 3$ a de-Sitter generic evolution can be found from the plane of index -1 of P_5 to the plane of index 1 of P_4 for $\mu < -\sqrt{\frac{3}{2}}$ and the direction reverses for $\mu > \sqrt{\frac{3}{2}}$.

2.3.3 Interaction Model : $Q = 2u\rho_{DM}H$

For this interaction the autonomous system [2.26 – 2.28] modifies to

$$\dot{u} = \left(\frac{3}{2}u - 1\right)(1 - u^2 - v^2) + \sqrt{\frac{3}{2}}v^2\mu\left(1 - u\tan\left[\frac{\pi w}{2}\right]\right), \tag{2.77}$$

$$\dot{v} = \frac{3}{2}v(1 - u^2 - v^2) - \sqrt{\frac{3}{2}}v\mu\left(u + (-1 + v^2)\tan\left[\frac{\pi w}{2}\right]\right), \tag{2.78}$$

$$\dot{w} = \frac{6}{\pi}\cos^2\left[\frac{\pi w}{2}\right]\left(u - \tan\left[\frac{\pi w}{2}\right]\right). \tag{2.79}$$

The above autonomous system has the following three critical points:

$$P_8\left(1, 0, \frac{1}{2}\right), P_9\left(-1, 0, -\frac{1}{2}\right) \text{ and } P_{10}\left(\frac{2}{3}, 0, \frac{2}{\pi}\tan^{-1}\left[\frac{2}{3}\right]\right).$$

Note that in Ref.[609] the authors have not analyzed this model. So all critical points are new and here we analyze each critical points by center manifold theory (for non-hyperbolic case) and Hartman-Grobman theorem (for hyperbolic case) and also discuss global stability with reference to bifurcation analysis using Poincaré index. The cosmological parameters, eigenvalues and the nature of critical points are presented in Table 2.3.

Table 2.3: Table shows the value of cosmological parameters, eigenvalues (λ_1, λ_2, λ_3) and the nature of the critical points for the interaction model with interaction $Q = \alpha\rho_{DM}H$ where $\alpha = 2u$.

Critical Points	ω_X	ω_{tot}	q	λ_1	λ_2	λ_3	Nature of Critical point
$P_8 : (1, 0, \frac{1}{2})$	-1	-1	-1	-1	0	-3	always non-hyperbolic
$P_9 : (-1, 0, -\frac{1}{2})$	-1	-1	-1	-5	0	-3	always non-hyperbolic
$P_{10} : \left(\frac{2}{3}, 0, \frac{2}{\pi}\tan^{-1}\left[\frac{2}{3}\right]\right)$	-1	$-\frac{4}{9}$	$-\frac{1}{6}$	$\frac{5}{6}$	$\frac{5}{6}$	$-\frac{33}{13}$	always hyperbolic

The three critical points $P_8 - P_{10}$ for the second choice of the interaction are very similar to the previous ones. The critical points P_8 and P_9 are exactly identical to P_1 and P_2 (or P_4 and P_5). The critical point P_{10} represent a DE dominated era of evolution. Due to interaction of the three form field (*i.e.,* cosmological constant in the present context) with DM (in the form of dust) the resulting single fluid is in the quintessence era not closed to phantom divide line. This critical point may be termed as LCDM model.

STABILITY ANALYSIS

2.3.3.1 Critical Point P_8

First we shift the critical point P_8 to the origin by using the coordinate transformation $u \to U + 1$, $v \to V$, $w \to W + \frac{1}{2}$. If we determine the Jacobian matrix at the origin for the shifted autonomous system, we have the eigenvalues -1, 0 and -3 and $[1, 0, \frac{3}{2\pi}]^T$, $[0, 1, 0]^T$ and $[0, 0, 1]^T$ are the corresponding eigenvectors, respectively. Since, the critical point is non hyperbolic so we use center Manifold theory for analyzing the stability of the critical point. Proceeding in similar way for determining the center manifold, the center manifold can be expressed as

$$U = -\frac{1}{2}V^2 + \mathcal{O}\left(V^3\right), \tag{2.80}$$

$$W = -\frac{1}{2\pi}V^2 + \mathcal{O}\left(V^3\right). \tag{2.81}$$

The flow on the CM near the origin is determined by

$$V' = -\sqrt{\frac{3}{2}}\mu V^3 + \mathcal{O}\left(V^4\right). \tag{2.82}$$

Here the stability of the center manifold depends on the sign of μ. If $\mu > 0$ then the origin is a stable node and if $\mu < 0$ then the origin is a saddle node, *i.e.,* unstable in nature.

2.3.3.2 Critical Point P_9

We shift the critical point P_9 to the origin by the coordinate transformation $u \to U-1$,$v \to V$,$w \to W-\frac{1}{2}$. If we determine the Jacobian matrix at the origin for the shifted autonomous system, we get the eigenvalues -5, 0 and -3 and $[1,0,-\frac{3}{2\pi}]^T$, $[0,1,0]^T$ and $[0,0,1]^T$ are the corresponding eigenvectors respectively. Since the critical point is non-hyperbolic so we shall use center Manifold theory for analyzing the stability of the critical point. Proceeding in similar way for determining center manifold, the expression of center manifold can be written as

$$U = \frac{1}{2}V^2 + \mathcal{O}\left(V^3\right), \tag{2.83}$$

$$W = \frac{1}{2\pi}V^2 + \mathcal{O}\left(V^3\right). \tag{2.84}$$

The flow on the center manifold near the origin is determined by:

$$V' = \sqrt{\frac{3}{2}}\mu V^3 + \mathcal{O}\left(V^4\right). \tag{2.85}$$

The stability of the manifold depends on the sign of μ. If $\mu > 0$ then the origin is a saddle node; *i.e.,* unstable in nature and if $\mu < 0$ then the origin is a stable node; *i.e.,* asymptotically stable in nature.

2.3.3.3 Critical Point P_{10}

We shift the critical point P_9 to the origin by using the coordinate transformation $u \to U+\frac{2}{3}$, $v \to V$, $w \to W+\frac{2}{\pi}\tan^{-1}\left[\frac{2}{3}\right]$. Now the Jacobian matrix at the origin for the transformed autonomous system can be written as

$$J(P_{10}) = \begin{bmatrix} \frac{5}{6} & 0 & 0 \\ 0 & \frac{5}{6} & 0 \\ \frac{54}{13\pi} & 0 & -\frac{33}{13} \end{bmatrix}. \tag{2.86}$$

The eigenvalues of the above Jacobian matrix are $\frac{5}{6}$, $\frac{5}{6}$, and $-\frac{33}{13}$. The eigenvectors corresponding to the eigenvalue $\frac{5}{6}$ are $\left[1,0,\frac{324}{263}\right]^T$ and $[0,1,0]^T$; and $[0,0,1]^T$ is the eigenvector corresponding to the eigenvalue $-\frac{33}{13}$. Since the critical point is hyperbolic in nature, so by Hartman-Grobman theorem we can analyze the stability of this critical point. We can notice that two eigenvalues are positive and one is negative, so the origin is a saddle node and the phase portrait near the origin is unstable in nature.

Poincaré index and Bifurcation Analysis

Critical points P_8 and P_9 are sink (sum of index is 2) in nature when restricted on UW-plane. On the other hand, P_8 and P_9 swap their stability and indices (1 to -1 or -1 to 1) when the parameter μ passes through zero. Similar phenomenon can be found on the VW-plane.

Despite each of P_8 and P_9 changes its stability at $\mu = 0$, they together produce topological equivalent phase space for all μ. Since the phase space is confined in a finite region of space, there is a trajectory of non-generic evolution between P_8 and P_9 on UV or VW-plane. As there is no μ in the eigenvalues of (2.86), so qualitative behavior near P_{10} does not depend on μ. The Poincaré index of P_{10} restricted on uv-eigenplane is 1 and each on the two other planes is -1 and is independent of the sign of μ . But in cosmological point of view, near the critical point P_{10}, for $\mu > 0$, the comoving field behaves as a phantom field with runaway potential, whereas the field behaves as non-phantom with non-runaway potential when crosses the phantom barrier at $\mu = 0$ from positive to negative.

Now we consider a power-law potential as

$$V(X) = V_1 X^{-\lambda}$$

where λ is a dimensionless parameter and $V_1 > 0$. Then by using similar dimensionless variables [2.16-2.19] we have the following autonomus system

$$u' = \frac{3}{2}u(1-u^2-v^2) + \frac{3}{2}\lambda v^2\left(\cot\left[\frac{\pi w}{2}\right] - u\right) - \frac{\alpha}{2u}(1-u^2-v^2), \tag{2.87}$$

$$v' = \frac{3}{2}v(1-u^2-v^2) - \frac{3}{2}\lambda v\left(u\cot\left[\frac{\pi w}{2}\right] + v^2 - 1\right), \tag{2.88}$$

$$w' = \frac{6}{\pi}\cos^2\left[\frac{\pi w}{2}\right]\left(u - \tan\left[\frac{\pi w}{2}\right]\right). \tag{2.89}$$

We have two nonhyperbolic critical points R_1 and R_2 similar as P_1 and P_2 respectively corresponding to the non-interacting case, four nonhyperbolic critical points R_3, R_4, R_5 and R_6 similar as P_4, P_5, P_6 and P_7 repectively corresponding to the interacting case when $\alpha \neq 0$. Note that R_5 and R_6 are hyperbolic for $\alpha \neq 3$. Lastly, for $\alpha = 2u$ we have two nonhyperbolic critical points R_7 and R_8 similar as P_8 and P_9 respectively and one hyperbolic critical points R_9 is similar as of P_{10}. $\omega_X = p_X/\rho_X$ and the total equations of state parameters ω_{tot} corresponding to this model can be expressed as

$$\omega_X = -1 - \frac{\lambda v^2}{u^2+v^2}, \tag{2.90}$$

$$\omega_{tot} = -u^2 - (\lambda+1)v^2. \tag{2.91}$$

To avoid similar calculations we only state the stability of every critical points, value of Poincaré index and bifurcation value on the $\alpha - \lambda$ plane corresponding to each critical points in tabular form (Table 2.5) and the value of cosmological parameters corresponding to each critical points are shown as in Table 2.4.

2.4 Cosmological Implications and Conclusions

The present work deals with a cosmological model where the matter field in the context of recent observations is chosen as DE and DM interacting/non-interacting in nature. The three-form field acts as DE, interacting with CDM. Due to very complicated form of the evolution equations the present cosmological model has been studied by dynamical sytem

analysis, forming the autonomous system from the evolution equations by transformation with suitable dimensionless variables. There are two hyperbolic critical points (namely P_3 and P_{10}) and remaining eight critical points in $P_1 - P_{10}$ are non-hyperbolic in nature. Also there is a line of critical points P_{l_c} for the first choice of the interacting term and only for these critical points the three-form field behaves as perfect fluid with variable equation of state in phantom era. In the present work, non-hyperbolic critical points are mainly studied using center manifold theory and global stability has been examined through bifurcation scenarios using Poincaré index.

For the critical points (P_1, P_2), (P_4, P_5) amd (P_8, P_9), DM is absent and the cosmic matter is only the three-form field behaving as cosmological constant. So they represent the early inflationary era or the de Sitter phase. For critical point P_3 the three form field (*i.e.,* DE) is insignificant and cosmic evolution represents dust era due to dominance of DM. Similarly, for the critical point P_{10}, the three form field (*i.e.,* DE) has an edge over DM and there is accelerated expansion in the quintessence era and this can be termed as LCDM model. The remaining two critical points P_6 and P_7 have the same features-both of them represents the scaling cosmological solution with 'α' as the scaling parameter-for very small α (*i.e.,* α is positive but very close to zero) the present model corresponds to matter dominated era while late time accelerated era is represented for $\alpha > 1$.

For the power-law potential $V(X) = V_1 X^{-\lambda}$, the autonomous system [2.87-2.89] has nine equilibrium points R_i $(i = 1, 2, \ldots, 9)$, of which three are hyperbolic (R_5, R_6 and R_9) in nature while the remaining six are non-hypernbolic type. These equilibrium points are similar to the critical points P_i for the exponential potential form discussed earlier. The equilibrium points R_1, R_2, R_3, R_4, R_7 and R_8 correspond to de Sitter era of cosmic evolution. Here the universe is fully dominated by DE which behaves as cosmological constant. The remaining three equilibrium points (R_5, R_6 and R_9) represent cosmological scaling solution. R_9 still has DE dominance and the universe is in accelerating phase. The critical ppoints R_5 and R_6 correspond to matter dominated era of evolution for $\alpha < 1$, while they will also correspond to accelerated model of the universe for $\alpha > 1$.

As the phase space for the present model is confined to a finite region (given in Eq.2.25), so there should not be an critical point at infinity. Thus the critical points correspond to different cosmic scenarios (namely, inflationary era, matter dominated epoch and present accelerated phase) and stability analysis (using center manifold theory for non-hyperbolic equilibrium points) has been presented with existence of possible bifurcation at cosmic transition.

Table 2.4: Table shows the set of critical points corresponding to the autonomous system (2.87 − 2.89) and the value of cosmological parameters corresponding to each critical points:

Interaction	Critical points	ω_X	ω_{tot}	q
$Q=0$	$R_1\left(1,0,\frac{1}{2}\right)$	-1	-1	-1
	$R_2\left(-1,0,-\frac{1}{2}\right)$	-1	-1	-1
$Q=\alpha\rho_{DM}H$ where α is nonzero arbitrary constant	$R_3\left(1,0,\frac{1}{2}\right)$	-1	-1	-1
	$R_4\left(-1,0,-\frac{1}{2}\right)$	-1	-1	-1
	$R_5\left(\sqrt{\frac{\alpha}{3}},0,\frac{2}{\pi}\cos^{-1}\left[\sqrt{\frac{3}{\alpha+3}}\right]\right)$	-1	$-\frac{\alpha}{3}$	$\frac{1}{2}(1-\alpha)$
	$R_6\left(-\sqrt{\frac{\alpha}{3}},0,-\frac{2}{\pi}\cos^{-1}\left[\sqrt{\frac{3}{\alpha+3}}\right]\right)$	-1	$-\frac{\alpha}{3}$	$\frac{1}{2}(1-\alpha)$
$Q=2u\rho_{DM}H$	$R_7\left(1,0,\frac{1}{2}\right)$	-1	-1	-1
	$R_8\left(-1,0,-\frac{1}{2}\right)$	-1	-1	-1
	$R_9\left(\frac{2}{3},0,\frac{2}{\pi}\tan^{-1}\left[\frac{2}{3}\right]\right)$	-1	$-\frac{4}{9}$	$-\frac{1}{6}$

Table 2.5: Table shows the stability of every critical points corresponding to the autonomous system (2.87 − 2.89), value of Poincaré index and bifurcation value on the $\alpha - \lambda$ plane corresponding to each critical points.

Interaction	CPs	Stability	Poincaré Index	Bifurcation value (on the $\alpha - \lambda$ plane)
$Q = 0$	R_1	Stable node for $\lambda > 0$ and saddle node for $\lambda < 0$	1 for $\lambda > 0$ and 0 for $\lambda < 0$	$\lambda = 0$
	R_2	Stable node for $\lambda < 0$ and saddle node for $\lambda > 0$	1 for $\lambda < 0$ and 0 for $\lambda > 0$	$\lambda = 0$
$Q = \alpha\rho_{DM}H$ where α is nonzero arbitrary constant	R_3	For $\alpha = 3$, R_3 is a saddle node for any value of λ. If $\alpha \neq 3$, R_3 is a saddle node for $(\lambda > 0, \alpha > 3)$ and also for $(\lambda < 0, \alpha < 3)$. Further for $(\alpha < 3, \lambda > 0)$, R_3 is a stable node and unstable node for $(\lambda < 0, \alpha > 3)$.	0 for $\alpha = 3$ and any λ 0 for $\lambda > 0, \alpha > 3$ and $\lambda < 0, \alpha < 3$; 1 for $\alpha < 3, \mu > 0$ and $\alpha > 3, \lambda < 0$	$\lambda = 0$, $\alpha = 3$
	R_4	For $\alpha = 3$, R_4 is a saddle node for any value of λ. If $\alpha \neq 3$, R_4 is a saddle node for $(\lambda > 0, \alpha < 3)$ and also for $(\lambda < 0, \alpha > 3)$. Further for $(\alpha < 3, \lambda < 0)$ R_4 is a stable node and unstable node for $(\lambda > 0, \alpha > 3)$.	0 for $\alpha = 3$ and any λ 0 for $\lambda > 0, \alpha < 3$ and $\lambda < 0, \alpha > 3$; 1 for $\alpha < 3, \lambda < 0$ and $\alpha > 3, \lambda > 0$	$\alpha = 3$ line on $\alpha - \lambda$ plane.
	R_5	For $\alpha = 3$, R_5 is a stable node for $\lambda > 0$ and saddle node for $\lambda < 0$. Further R_5 is stable node $\alpha > 3$ and for any values of λ and saddle node for $\alpha < 3$.	1 for $\alpha = 3$ and $\lambda > 0$ 0 for $\alpha = 3$ and $\lambda < 0$ 1 for $\alpha > 3$ and any λ 0 for $\alpha < 3$ and any λ	$\alpha = 3$ line on $\alpha - \lambda$ plane.
	R_6	For $\alpha = 3$, R_6 is a stable node for $\lambda < 0$ and saddle node for $\lambda > 0$. Further R_6 is stable node $\alpha > 3$ and for any values of λ and saddle node for $\alpha < 3$.	1 for $\alpha = 3$ and $\lambda < 0$ 0 for $\alpha = 3$ and $\lambda > 0$ 1 for $\alpha > 3$ and any λ 0 for $\alpha < 3$ and any λ	$\alpha = 3$ line on $\alpha - \lambda$ plane.
$Q = 2u\rho_{DM}H$	R_7	Stable node for $\lambda > 0$ and saddle node for $\lambda < 0$.	1 for $\lambda > 0$ and 0 for $\lambda < 0$.	$\lambda = 0$
	R_8	Stable node for $\lambda < 0$ and saddle node for $\lambda > 0$.	1 for $\lambda < 0$ and 0 for $\lambda > 0$	$\lambda = 0$
	R_9	Always saddle node.	0 for any λ	N.A.

CHAPTER 3

DYNAMICAL SYSTEM ANALYSIS OF THREE-FORM FIELD DARK ENERGY MODEL WITH BARYONIC MATTER

3.1 Prelude

The cosmologists for the last two decades are tirelessly searching for a theory which shows the present accelerated expansion of the universe as predicted by a series of observational results [587]. Cosmologists are not unanimous over this issue rather they have two distinct opinions - one group is in favour of standard cosmology and they introduce some exotic matter (known as DE having large negative pressure) to explain this accelerated expansion while the other group prefers some modified gravity theory instead of Einstein gravity and they speculate that the extra geometric terms may responsible for this accelerated expansion [554].

In the context of the opinion of the first group the best candidate so far for DE is the cosmological constant which is simple in nature and observationally most favourable. But unfortunately, it has two severe drawbacks namely cosmological constant problem and cosmic coincidence problem [614]. As a result, several dynamic DE models in the form of perfect fluid with variable equation of state parameter (of various forms) come into picture (namely quintessence, tachyon, phantom [580] and chameleon [616, 581] etc). Also some complicated fields namely spinors [601], vectors [573], higher order spin field and three-form field [602, 603] are considered as DE (also one may refer [623, 619, 621, 620] on the p-form and their stability properties, the three-form inflation and the center manifold). Also other positive aspects of the three-form fields in the context of cosmology are to obtain dynamically the late-time acceleration, to describe the phantom like behaviour [618] and to produce non-Gaussianities [556].

In the present work the three-form field is chosen as DE candidate. It has been shown that the dual of the three-form field is a scalar field which has an equivalence with K-inflation model [610] if the potential is non-quadratic in form. The present cosmological model contains this three-form field with (interacting, non-interacting) baryonic matter in the form of dust and radiation. Due to complicated form of the Einstein field Equations, the evolution

equations are converted into an autonomous system by suitable choice of the dimensionless variables and non-hyperbolic equilibrium points are analyzed by Center manifold theory on the Hilbert space [551, 552, 553]. Bifurcation analysis [555] has been done to find the qualitative changes of global behavior due to different parameter values. The plan of this chapter is as follows: Section 3.2 deals with basic equations for the three form field, Einstein field equations and energy conservation equations of both types of fluids. Autonomous system is formed and critical points are determined in Section 3.3. Also stability analysis and possible bifurcation scenarios have been examined in this section. Finally, the summary of the present work is proposed in Section 3.4.

3.2 Basic Equations

For a three-form field $A_{\mu\nu\rho}$, the field strength tensor is given by

$$F_{\mu\nu\rho\sigma} = 4 \bigtriangledown_{[\mu} A_{\nu\rho\sigma]} \tag{3.1}$$

where square bracket indicates anti-symmetrization of the indices. The action of this three-form field is given by

$$S_A = \int d^4x\sqrt{-g}\left[\frac{F^2}{48} + V(A^2)\right] \tag{3.2}$$

where $V(A^2)$ is the potential of the field with $A^2 = A^{\mu\nu\rho}A_{\mu\nu\rho}$. The energy-momentum tensor corresponding to this action is given by

$$T_{\mu\nu} = \frac{1}{6}F_{\mu\alpha\beta\gamma}F_{\nu}^{\alpha\beta\gamma} + 6V'(A^2)A_{\mu\alpha\beta}A_{\nu}^{\alpha\beta} - g_{\mu\nu}\left(\frac{1}{48}F_{\alpha\beta\gamma\rho}F^{\alpha\beta\gamma\rho} + V(A^2)\right) \tag{3.3}$$

and the evolution equation of the three form field is obtained by varying the above action (3.2) with respect to $A^{\mu\nu\rho}$ as

$$\bigtriangledown^{\alpha}F_{\alpha\mu\nu\rho} = 12V'(A^2)A_{\mu\nu\rho} \tag{3.4}$$

where an over dash denotes differentiation with respect to the argument. The present cosmological model is considered in the background of homogeneous and isotropic flat Friedmann-Lemaître-Robertson-Walker (FLRW) space-time manifold having line element (choosing $c = 1$)

$$ds^2 = -dt^2 + a^2(t)\left[dr^2 + r^2\left(d\theta^2 + sin^2\theta d\phi^2\right)\right]. \tag{3.5}$$

So the three form field has only time dependence and the above evolution eqn.(3.4) results $A_{0\mu\nu} = 0$. Thus the spatial components of the three-form field can be written as

$$A_{ijk} = a^3(t)\epsilon_{ijk}X(t), \tag{3.6}$$

where ϵ_{ijk} is the three dimensional Levi-Civita symbol (with ϵ_{123}=1). So the scalars A^2 and X are related as $A^2 = 6X^2$ and the equation of motion (3.4) of the three-form field gives the evolution of the scalar field $X(t)$ as

$$\ddot{X} - 3H\dot{X} - 3\dot{H}X = -V_{,X} \tag{3.7}$$

where differentiation with respect to the cosmic time 't' is denoted by over dot in the above equation. Now from the expression (6.14) of the energy-momentum tensor for the three-form field, the explicit form of the energy-density and the pressure of the scalar field X are given by

$$\rho_{_X} = \frac{1}{2}\left(\dot{X}+3HX\right)^2 + V(X), \tag{3.8}$$

$$p_{_X} = -\frac{1}{2}\left(\dot{X}+3HX\right)^2 - V(X) + XV_{,X} \tag{3.9}$$

having equation of state parameter

$$\omega_{_X} = \frac{p_{_X}}{\rho_{_X}} = -1 + \frac{XV_{,X}}{\rho_{_X}}. \tag{3.10}$$

Thus if $V_{,X}$ $(= \frac{dV}{dX})$ is positive then the three-form field behaves as DE (*i.e.,* non-phantom) while the field behaves as phantom field if $V_{,X} < 0$.

Now for the present cosmological model the action integral for the whole system (assuming the three-form field to be minimally coupled to gravity) is given by

$$S_T = -\int d^4x\sqrt{-g}\left[\frac{1}{2\kappa^2}R - \frac{F^2}{48} - V(A^2)\right] + S_B, \tag{3.11}$$

where $\kappa^2 = 8\pi G$, R is the usual Ricci scalar and S_B, the standard action integral for the baryonic matter (in the form of dust and radiation) is given by

$$S_B = -\int d^4x\sqrt{-g}\;\rho_{_B} = \int d^4x\sqrt{-g}\;p_{_B}. \tag{3.12}$$

The last equality in the above expression for S_B holds upto a total derivative [622]. Here $\rho_{_B}$ and $p_{_B}$ are the energy density and thermodynamic pressure of the baryonic matter respectively. Now varying the action with respect to the metric tensor gives the usual Friedmann equations as

$$3H^2 = \kappa^2\left(\rho_{_A}+\rho_{_r}+\rho_{_d}\right), \tag{3.13}$$

$$2\dot{H} = -\kappa^2[(\rho_{_A}+p_{_A})+\rho_{_r}\left(1+\omega_{_r}\right)+\rho_{_d}], \tag{3.14}$$

where ρ_r, ρ_d are respectively the energy density of radiation and dust part of the matter and $\omega_r = \frac{1}{3}$ is the equation of state parameter for radiation. Also the energy conservation equations are (assuming three form field interacts with dust, the cold dark matter(CDM))

$$\dot{\rho_{_A}} + 3H(\rho_{_A}+p_{_A}) = -Q, \tag{3.15}$$

$$\dot{\rho_{_r}} + 4H\rho_{_r} = 0, \tag{3.16}$$

$$\dot{\rho_{_d}} + 3H\rho_{_d} = Q. \tag{3.17}$$

Now due to this interaction, the evolution of the scalar field X (*i.e.,* eqn. (3.7)) modifies to

$$\ddot{X} + 3H\dot{X} + 3\dot{H}X + \frac{dV}{dX} = -\frac{Q}{\dot{X}+3HX}. \tag{3.18}$$

In the present work, two possible choices for Q are taken as (i) $Q = \alpha\rho_d(\dot{X} + 3HX)$ and (ii) $Q = \alpha\rho_d H$, where α is the coupling parameter. Note that the above choices of Q are purely phenomenological and the only motivation of choosing such Q is the formation of the autonomous system (in Section 3.3 below) with the choices of the dimensionless variables (in eqn.(3.20)). Further, in order to derive the evolution equations (3.15) and (3.17) for the three-form field and dust, the interaction Lagrangian is of the form [622]

$$\mathcal{L}_{int} = -\sqrt{-g}\; f\left(X, \dot{X}, \rho_m, H\right), \tag{3.19}$$

where 'f' is an arbitrary function which will specify the particular model. Also 'f' depends only on the dynamical degrees of freedom of the fluids.

3.3 Formation of Autonomous System: Critical point and stability analysis

We now define a set of dimensionless variables as [604]

$$x \equiv \kappa X,\; y \equiv \frac{\kappa}{\sqrt{6}}(X' + 3X),\; z^2 \equiv \frac{\kappa^2 V}{3H^2},\; u^2 \equiv \frac{\kappa^2\rho_r}{3H^2},\; v^2 \equiv \frac{\kappa^2\rho_d}{3H^2},\; \lambda(x) \equiv -\frac{1}{\kappa}\frac{V_{,X}}{V}, \tag{3.20}$$

the equation of state parameter can be written in the form

$$\omega_{tot} = -y^2 - z^2(1 + \lambda(x)x) + u^2 \tag{3.21}$$

and the cosmic evolution equations (in the last section) can be written in an autonomous system as

$$x' = 3\left(\sqrt{\frac{2}{3}}y - x\right), \tag{3.22}$$

$$y' = -\frac{3}{2}\lambda(x)z^2\left(xy - \sqrt{\frac{2}{3}}\right) + \frac{3}{2}\left(\frac{4}{3}u^2 + v^2\right)y, \tag{3.23}$$

$$v' = -\frac{3}{2}v\left[1 + \lambda(x)xz^2 - \frac{4}{3}u^2 - v^2\right], \tag{3.24}$$

$$u' = -\frac{3}{2}u\left[\frac{4}{3} + \lambda(x)xz^2 - \frac{4}{3}u^2 - v^2\right], \tag{3.25}$$

where 'dash' over a variable denotes differentiation with respect to $N = \ln a$. Note that all the above dimensionless variables are not independent, rather due to first Friedmann equation (*i.e.,* eqn.(3.13)) they are constrained by the relation

$$y^2 + z^2 + u^2 + v^2 = 1 \tag{3.26}$$

and we have 4D phase space for the dynamical system.

In the present work for simplicity of calculation the potential of the scalar field X (*i.e.,* $V(X)$) is chosen as

$$V(X) = V_0 e^{-\mu x} \tag{3.27}$$

where $V_0(>0)$ and μ are constant parameters, so that $\lambda(X)$ is a non-zero constant. Also μ can be interpreted as the rate of decrease of the logarithm of the potential function. The properties of the critical points of the above autonomous system (3.22 - 3.25) are represented in the following lemmas.

Lemma 1 *Critical points can be located either on u-nullcline or on v-nullcline.*

Proof : Let us prove this by contradiction. We assume that both v and $u \neq 0$. Then from eqn.(3.24) and eqn. (3.25) we have

$$1 + R = 0 \qquad \text{and} \qquad \frac{4}{3} + R = 0$$

where $R = \lambda(x)xz^2 - \frac{4}{3}u^2 - v^2$. But it is not possible to exist any such R.

Lemma 2 *If $v = 0$ and $u \neq 0$, then either $y = 0$ or $\sqrt{\frac{2}{3}}\lambda(x)y \neq -2\sqrt{2}$ and $\lambda(x)y < 0$.*

Proof : If $v = 0$, then either $u = 0$ or $\frac{4}{3}(1-u^2) + \lambda(x)xz^2 = 0$. From eqn.(3.22) we have $x = \sqrt{\frac{2}{3}}y$. This implies

$$\frac{4}{3}(1-u^2) + \sqrt{\frac{2}{3}}\lambda(x)yz^2 = 0. \tag{3.28}$$

So either $y = 0$ or $z^2 = \frac{-2\sqrt{2}(1-u^2)}{\sqrt{3}\lambda(x)y}$. For $v = 0$, we also have the condition $u^2 + y^2 + z^2 = 1$. If $\sqrt{\frac{2}{3}}\lambda(x)y = -2\sqrt{2}$, then $z^2 = 1 - u^2$ which implies $y = 0$. This proves $\sqrt{\frac{2}{3}}\lambda(x)y \neq -2\sqrt{2}$ and $\lambda(x)y < 0$.

Lemma 3 *If $v = 0$, $u \neq 0$ and $y \neq 0$, then $(u^2-1)(y^2-1) = u^2y^2$.*

Proof : From eqn.(3.22) and eqn.(3.23) we have

$$-\frac{3}{2}\lambda(x)z^2(y^2-1) + 2u^2y = 0$$

Multiplying both side by y and using eqn.(3.28) we get $(u^2-1)(y^2-1) = u^2y^2$.

Lemma 4 *If $u = 0$ and $v \neq 0$, then either $y = 0$ or $y = -\sqrt{\frac{2}{3}}\lambda(x)z^2$.*

Proof : From eqn.(3.23) we have

$$\sqrt{\frac{3}{2}}v^2y = \lambda(x)z^2(y^2-1). \tag{3.29}$$

On the other hand, for $y \neq 0$, from eqn.(3.24) we have

$$v^2y = y + \sqrt{\frac{2}{3}}\lambda(x)y^2z^2 \tag{3.30}$$

Equating v^2y in eqn.(3.29) and eqn.(3.30) we can derive $y = -\sqrt{\frac{2}{3}}\lambda(x)z^2$.

Theorem 10 *1.* $x = \pm\sqrt{\frac{2}{3}}$ *are the critical points of the autonomous system (3.22-3.25).*

2. There is no critical point for which $u \neq 0$ *and* $v \neq 0$.

3. If $v = 0$ *and* $u \neq 0$, *then* $u = \pm 1$.

4. If $u = 0$ *and* $v \neq 0$, *then* $v = \pm 1$.

Proof : (1) Follows form eqn.(3.22) and eqn.(3.23) when u and v are both 0.
(2) Follows from lemma 1.
(3) If we consider the hypothesis of lemma 3, then from lemma 2 we can derive $\sqrt{\frac{2}{3}}\lambda(x)y = -2\sqrt{2}$ which is a contradiction to our hypothesis. So y must be 0. Then from the relation $u^2 + y^2 + z^2 = 1$, we have $z = \pm\sqrt{1-u^2}$. But due to eqn.(3.23), $z = 0$ which yields $u = \pm 1$.
(4) If $y = 0$, then $x = 0$. And eqn.(3.23) implies $z = 0$. Then the relation $y^2 + z^2 + v^2 = 1$ yields $v = \pm 1$.
If $y \neq 0$, then by lemma 4 we have $v = \pm\sqrt{1 - \frac{2}{3}\lambda^2(x)z^4 - z^2}$. But $y^2 + z^2 + v^2 = 1$ and eqn.(3.23) yield $z = 0$. So $v = \pm 1$.

3.3.1 NON-INTERACTING THREE-FORM FIELD

The vector fields of the autonomous system $(3.22 - 3.25)$ for non-interacting three-form field for exponential potential can be analyzed as follows. By taking exponential potential we will get $\lambda(x) = \mu$. The set of critical points, existence of critical points and the value of cosmological parameters are shown in Table 3.1 and the eigenvalues and the nature of critical points are shown in Table 3.2.

The first two critical points (*i.e.,* C_0, C_1) represent the evolution of the universe with barotropic matter and vanishing DE. In fact, the critical point C_0 describes the relativistic radiation era of evolution while C_1 represents the dust phase of evolution. The remaining three critical points namely $C_2 - C_4$ are fully dominated by DE and they correspond to de-Sitter phase.

STABILITY ANALYSIS

1. Critical Point C_0

The Jacobian matrix at the critical point C_0 can be put as

$$J(C_0) = \begin{bmatrix} -3 & \sqrt{6} & 0 & 0 \\ 0 & 2 & 0 & \mp\sqrt{6}\mu \\ 0 & 0 & \frac{1}{2} & 0 \\ 0 & 0 & 0 & 4 \end{bmatrix}. \tag{3.31}$$

The eigenvalues of $J(C_0)$ are -3, 2, $\frac{1}{2}$ and 4 (hyperbolic in character) with eigenvectors $[1,0,0,0]^T$, $\left[\frac{\sqrt{6}}{5},1,0,0\right]^T$, $[0,0,1,0]^T$ and $\left[\mp\frac{3\mu}{7},\mp\sqrt{\frac{3}{2}}\mu,0,1\right]^T$ respectively. So we can use Hartman-Grobman theorem for analyzing the stability of this critical point. As three eigenvalues are positive and one is negative, so the critical point C_0 is a saddle node and unstable in nature. For $\mu > 0$ the phase portrait in all possible 3D coordinate system near the origin are shown as in FIG. 3.1.

Table 3.1: Table shows the set of critical points, existence of critical points and the value of cosmological parameters corresponding to the autonomous system (3.22−3.25).

CPs	Existence	x	y	z	v	u	ω_{tot}	q
C_0	*all* μ	0	0	0	0	±1	1	2
C_1	*all* μ	0	0	0	±1	0	0	$\frac{1}{2}$
C_2	*all* μ	$\sqrt{\frac{2}{3}}$	1	0	0	0	-1	-1
C_3	*all* μ	$-\sqrt{\frac{2}{3}}$	-1	0	0	0	-1	-1
C_4	μ=0	$\sqrt{\frac{2}{3}}y_c$	$0 \leq y_c \leq 1$	$\sqrt{1-y_c^2}$	0	0	-1	-1

2. Critical Point C_1

The Jacobian matrix at the critical point C_1 can be put as

$$J(C_1) = \begin{bmatrix} -3 & \sqrt{6} & 0 & 0 \\ 0 & \frac{3}{2} & \mp\sqrt{6}\mu & 0 \\ 0 & 0 & 3 & 0 \\ 0 & 0 & 0 & -\frac{1}{2} \end{bmatrix}. \tag{3.32}$$

The eigenvalues of $J(C_1)$ are -3, $\frac{3}{2}$, 3 and $-\frac{1}{2}$ (hyperbolic in character) with eigenvectors $[1,0,0,0]^T$, $\left[\frac{2}{3}\sqrt{\frac{2}{3}},1,0,0\right]^T$, $\left[\mp\frac{2\mu}{3},\mp2\sqrt{\frac{2}{3}}\mu,1,0\right]^T$ and $[0,0,0,1]^T$ respectively. So we can use Hartman-Grobman theorem for analyzing the stability of this critical point. Since, two eigenvalues are positive and another two eigenvalues are negative, hence the critical point C_1 is unstable due to its saddle nature.

3. Critical Point C_2

The Jacobian matrix at the critical point C_2 can be put as

$$J(C_2) = \begin{bmatrix} -3 & \sqrt{6} & 0 & 0 \\ 0 & 0 & 0 & 0 \\ 0 & 0 & -\frac{3}{2} & 0 \\ 0 & 0 & 0 & -2 \end{bmatrix}. \tag{3.33}$$

The eigenvalues of $J(C_2)$ are -3, 0, $-\frac{3}{2}$ and -2 (non-hyperbolic in character) with eigenvectors $[1,0,0,0]^T$, $\left[\sqrt{\frac{2}{3}},1,0,0\right]^T$, $[0,0,1,0]^T$, and $[0,0,0,1]^T$ respectively. To apply Center

Table 3.2: Table shows the eigenvalues ($\lambda_1,\ \lambda_2,\ \lambda_3,\ \lambda_4$) of the Jacobian matrix corresponding to the critical points and the nature of all critical points for this non-interacting model:

Critical Points	λ_1	λ_2	λ_3	λ_4	Nature of Critical points
C_0	-3	2	$\frac{1}{2}$	4	hyperbolic
C_1	-3	$\frac{3}{2}$	3	$-\frac{1}{2}$	hyperbolic
C_2	-3	0	$-\frac{3}{2}$	-2	non-hyperbolic
C_3	-3	0	$-\frac{3}{2}$	-2	non-hyperbolic
C_4	-3	0	$-\frac{3}{2}$	-2	non-hyperbolic

Manifold Theory, we first transform the coordinate system ($x = X + \sqrt{2/3},\ y = Y + 1,\ v = V,\ u = U$) so that C_2 moves to the origin. As a result, the autonomous system (3.22 – 3.25) changes to

$$X' = -3X + \sqrt{6}Y, \tag{3.34}$$

$$Y' = \sqrt{6}\mu Y^2 + 3\mu XY + \frac{3}{2}V^2 + 2U^2 + \sqrt{\frac{3}{2}}\mu Y^3 + \frac{9}{2}\mu XY^2 + \frac{3}{2}\mu XU^2 + \frac{3}{2}\mu XV^2 + \frac{3}{2}\mu XY^3 + \frac{3}{2}\mu XYU^2 + \frac{3}{2}\mu XYV^2 + \sqrt{\frac{3}{2}}\mu U^2Y + \sqrt{\frac{3}{2}}\mu V^2Y + 2U^2Y + \frac{3}{2}V^2Y, \tag{3.35}$$

$$V' = -\frac{3}{2}V + \sqrt{6}\mu VY + 3\mu VXY + \frac{3}{2}\mu VXU^2 + \sqrt{\frac{3}{2}}\mu VU^2 + \frac{3}{2}\mu XV^3 + \sqrt{\frac{3}{2}}\mu V^3 + \frac{3}{2}\mu VXY^2 + \sqrt{\frac{3}{2}}\mu VY^2 + 2U^2V + \frac{3}{2}V^3, \tag{3.36}$$

$$U' = -2U + \sqrt{6}\mu UY + 2U^3 + \frac{3}{2}UV^2 + 3\mu UXY + \sqrt{\frac{3}{2}}\mu U^3 + \frac{3}{2}\mu UXY^2 + \sqrt{\frac{3}{2}}\mu UY^2 + \frac{3}{2}\mu XU^3 + \frac{3}{2}\mu UXV^2 + \sqrt{\frac{3}{2}}\mu UV^2. \tag{3.37}$$

Now, we can see that there is a linear term of Y in the R.H.S. of (3.34), so we have to introduce another set of new coordinates so that the Jacobian matrix (3.33) transforms into the diagonal form. By using the eigenvectors of the Jacobian matrix (3.33), we introduce the

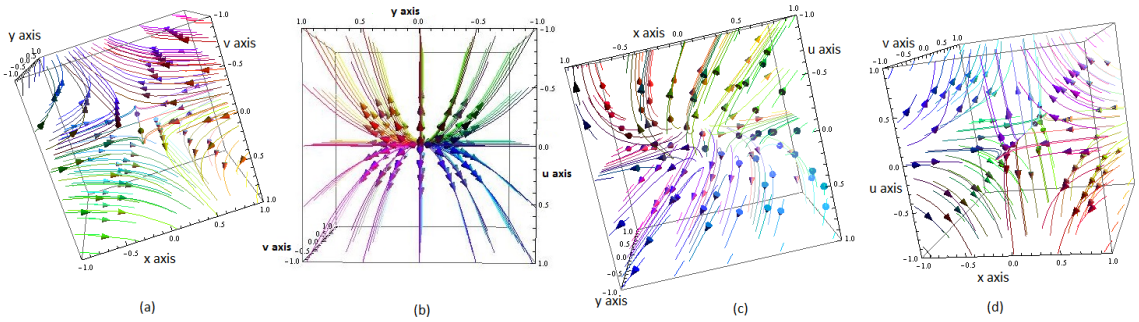

Figure 3.1: Panel of the figures show 3-dimensional phase plots corresponding to the critical point $C_0(0,0,0,1)$ for $\mu > 0$. In this panel (a) represents the phase portrait in $xyv-$coordinate system (saddle node), (b) represents the phase portrait in $yvu-$coordinate system (unstable node), (c) represents the phase portrait in $xyu-$coordinate system (saddle node), (d) represents the phase portrait in $xvu-$coordinate system (saddle node).

following coordinate system

$$\begin{bmatrix} X_T \\ Y_T \\ V_T \\ U_T \end{bmatrix} = \begin{bmatrix} 1 & -\sqrt{\frac{2}{3}} & 0 & 0 \\ 0 & 1 & 0 & 0 \\ 0 & 0 & 1 & 0 \\ 0 & 0 & 0 & 1 \end{bmatrix} \begin{bmatrix} X \\ Y \\ V \\ U \end{bmatrix} \tag{3.38}$$

and in these new coordinates the equations are transformed into

$$\begin{bmatrix} X_T' \\ Y_T' \\ V_T' \\ U_T' \end{bmatrix} = \begin{bmatrix} -3 & 0 & 0 & 0 \\ 0 & 0 & 0 & 0 \\ 0 & 0 & -\frac{3}{2} & 0 \\ 0 & 0 & 0 & -2 \end{bmatrix} \begin{bmatrix} X_T \\ Y_T \\ V_T \\ U_T \end{bmatrix} + \begin{bmatrix} non \\ lin \\ ear \\ terms \end{bmatrix}. \tag{3.39}$$

So by Center Manifold Theory there exists a continuously differentiable function $h : \mathbb{R} \to \mathbb{R}^3$ such that

$$h(Y_T) = \begin{bmatrix} X_T \\ V_T \\ U_T \end{bmatrix} = \begin{bmatrix} a_1 Y_T^2 + a_2 Y_T^3 + \mathcal{O}\left(Y_T^4\right) \\ b_1 Y_T^2 + b_2 Y_T^3 + \mathcal{O}\left(Y_T^4\right) \\ c_1 Y_T^2 + c_2 Y_T^3 + \mathcal{O}\left(Y_T^4\right) \end{bmatrix}. \tag{3.40}$$

Differentiating both sides with respect to N, we get

$$X_T' = (2a_1 Y_T + 3a_2 Y_T^2) Y_T' + \mathcal{O}\left(Y_T^3\right), \tag{3.41}$$
$$V_T' = (2b_1 Y_T + 3b_2 Y_T^2) Y_T' + \mathcal{O}\left(Y_T^3\right), \tag{3.42}$$
$$U_T' = (2c_1 Y_T + 3c_2 Y_T^2) Y_T' + \mathcal{O}\left(Y_T^3\right), \tag{3.43}$$

where $a_i, b_i, c_i \in \mathbb{R}$. We only concern about the nonzero coefficients of the lowest power terms in Center Manifold Theory as we analyze arbitrary small neighborhood of the origin. Comparing both sides the coefficients of the corresponding power of Y_T, we get the following

center manifold

$$X_T = -\frac{4\mu}{3}Y_T^2 + \left(-\frac{4\mu}{3} + \frac{20}{3}\sqrt{\frac{2}{3}}\mu^2\right)Y_T^3 + \mathcal{O}\left(Y_T^4\right), \tag{3.44}$$

$$V_T = 0, \tag{3.45}$$

$$U_T = 0. \tag{3.46}$$

This implies that one dimensional center manifold lies on the $(X_TY_T)-$ plane and tangent to the center subspace (Y_T axis) at the origin. The flow on the center manifold near the origin is determined by

$$\frac{dY_T}{dN} = 2\sqrt{6}\mu Y_T^2 + (2\sqrt{6}\mu - 4\mu^2)Y_T^3 + \mathcal{O}\left(Y_T^4\right). \tag{3.47}$$

The flow on the center manifold depends on the sign of μ. For both the cases $\mu > 0$ and $\mu < 0$, the origin is a saddle node and unstable in nature (FIG. 3.2). As the new coordinate system (X_T, Y_T, V_T, U_T) is topologically equivalent to the old one, hence the origin in the new coordinate system, *i.e.,* the critical point C_2 in the old coordinate system $(x,\ y,\ u,\ v)$ is a saddle node and unstable in nature.

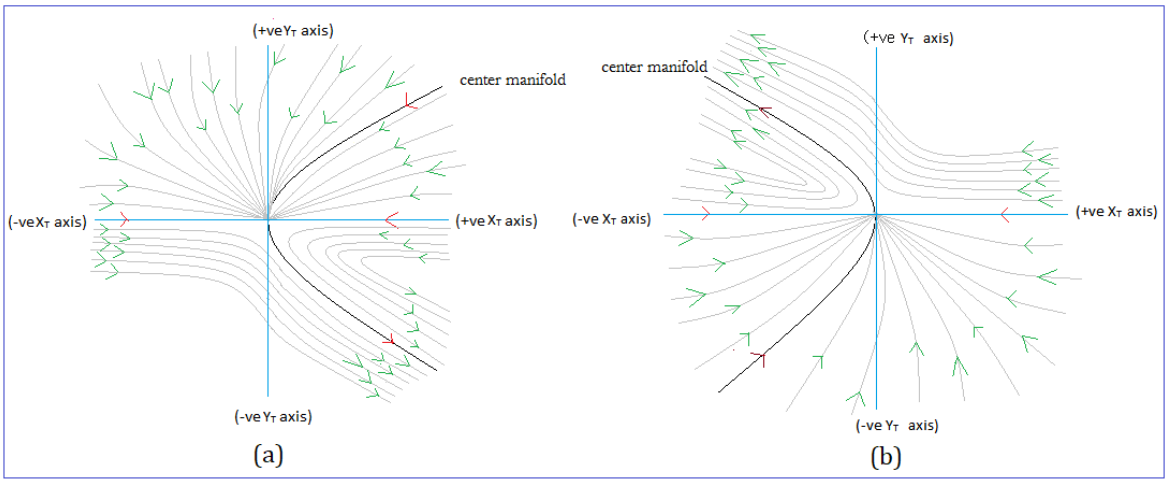

Figure 3.2: These figures show the vector field near the origin corresponding to the critical point C_2 in $(X_TY_T)-$plane. The phase plot (a) is for $\mu < 0$ and (b) is for $\mu > 0$.

4. Critical Point C_3

The Jacobian matrix at the critical point C_3, the corresponding eigenvalues and eigenvectors are same as for the critical point C_2. If we put forward similar argument as we have mentioned for the analysis of C_2 then we get the following center manifold

$$X_T = -\frac{4\mu}{3}Y_T^2 + \left(\frac{4\mu}{3} + \frac{20}{3}\sqrt{\frac{2}{3}}\mu^2\right)Y_T^3 + \mathcal{O}\left(Y_T^4\right), \tag{3.48}$$

$$V_T = 0, \tag{3.49}$$

$$U_T = 0 \tag{3.50}$$

and the flow on the center manifold is determined by

$$\frac{dY_T}{dN} = 2\sqrt{6}\mu Y_T^2 - (2\sqrt{6}\mu + 4\mu^2)Y_T^3 + \mathcal{O}\left(Y_T^4\right). \tag{3.51}$$

Since our interest only on the coefficient of the lowest power term of Y_T in the expression of the center manifold and also the flow on the center manifold, so the vector field near the origin is same as for the critical point C_2 (FIG.3.2). Hence, the critical point C_3 is unstable due to its saddle nature in the old coordinate system.

5. Critical Point C_4

The critical point C_4 exists only for $\mu = 0$. The Jacobian matrix at the critical point C_4 is same as of (3.33), so the eigenvalues and corresponding eigenvectors are also same. Since, the critical point C_4 is non-hyperbolic in nature so we can use center manifold theory. But here the equations of the center manifold are expressed by

$$X_T = 0, \tag{3.52}$$
$$V_T = 0, \tag{3.53}$$
$$U_T = 0 \tag{3.54}$$

and the flow on the center manifold is determined by

$$\frac{dY_T}{dN} = 0. \tag{3.55}$$

Since, from this information we can not determine the nature of the vector field near the origin, due to this reason we should try to define the stability of the vector field near the origin on each plane. The stability of the vector field on each plane is shown in Table 3.3.

3.3.2 Coupling Three-form field with dark matter

The existence of the coupling can be represented by the modified continuity equations (3.15) and (3.17), where ρ_d stands for energy density of dust, ρ_A is the energy density of three-form field and Q is the energy transfer between dark energy and dark matter.
Then the autonomous system changes due to eqn. (3.15) and eqn. (3.17) as follows

$$x' = 3\left(\sqrt{\frac{2}{3}}y - x\right), \tag{3.56}$$
$$y' = I - \frac{3}{2}\lambda(x)z^2\left(xy - \sqrt{\frac{2}{3}}\right) + \frac{3}{2}\left(\frac{4}{3}u^2 + v^2\right)y, \tag{3.57}$$
$$v' = -\frac{Iy}{v} - \frac{3}{2}v\left[1 + \lambda(x)xz^2 - \frac{4}{3}u^2 - v^2\right], \tag{3.58}$$
$$u' = -\frac{3}{2}u\left[\frac{4}{3} + \lambda(x)xz^2 - \frac{4}{3}u^2 - v^2\right], \tag{3.59}$$

where $I = \frac{\kappa Q}{\sqrt{6}(\dot{X}+3HX)H^2}$ and 'prime' denotes derivative with respect to $N = ln\ a$.

The properties of the critical points corresponding to the above autonomous system (depending on the choices of I) are presented in the form of lemmas as follows (we shall consider the relation $x = \sqrt{\frac{2}{3}}y$ due to eqn.(3.56)).

Table 3.3: Stability of the vector field on each coordinate plane for the critical point C_4:

Coordinate Plane	Stability
$X_TY_T - plane$	vector field is stable about Y_T axis
$X_TV_T - plane$	vector field near the origin is stable star
$X_TU_T - plane$	vector field near the origin is stable star
$Y_TU_T - plane$	vector field is stable about Y_T axis
$Y_TV_T - plane$	vector field is stable about Y_T axis
$U_TV_T - plane$	vector field near the origin is stable star

Lemma 5 *If u, v and y are non-zero, then $z = 0$ and the following relations must hold together*

1. $I = \frac{v^2}{2y}$,
2. $y^2 + u^2 + v^2 = 1$,
3. $4u^2 + 3v^2 = 4$.

Proof : (1) From eqn.(3.59), it is to be noted that $R = -\frac{4}{3}$. Then from eqn.(3.58), we have $I = \frac{v^2}{2y}$.
(2) The eqn.(3.57) and I yield

$$\sqrt{6}\lambda(x)z^2(y^2-1)y = 4u^2y^2 + 3v^2y^2 + v^2. \tag{3.60}$$

On the other hand, $R = -\frac{4}{3}$ yields

$$\sqrt{6}\lambda(x)yz^2 = 4u^2 + 3v^2 - 4 \tag{3.61}$$

So form eqn.(3.60) and eqn.(3.61) we have $y^2 + u^2 + v^2 = 1$.
(3) The result of (2) implies $z = 0$ due to relation (3.26). So from eqn.(3.61) we have $4u^2 + 3v^2 = 4$.

Lemma 6 *If only $u = 0$, then the following conditions must hold together*

1. $\lambda(x) = \sqrt{\frac{3}{2}}\frac{v^2}{z^2 y}$,
2. $I = -\frac{3}{2}\frac{v^2}{y}$,
3. $y^2 + v^2 + z^2 = 1$.

Proof : (1) From eqn.(3.58) , we have

$$Iy = -\frac{3v^2}{2}\left[1 + \sqrt{\frac{2}{3}}\lambda(x)yz^2 - v^2\right] \tag{3.62}$$

From eqn.(3.57), we have

$$Iy = \sqrt{\frac{3}{2}}\lambda(x)yz^2(y^2 - 1) - \frac{3}{2}y^2. \tag{3.63}$$

Eliminating Iy from (3.62) and (3.63) and using (3.26), we have $\lambda(x) = \sqrt{\frac{3}{2}}\frac{v^2}{z^2 y}$.
(2) Put the expression of $\lambda(x)$ in (3.58), we have $I = -\frac{3}{2}\frac{v^2}{y}$.
(3) Due to relation (3.26), we get $y^2 + v^2 + z^2 = 1$.

Corollary 1 *If only $u = 0$ and $I = \frac{v}{y}\alpha$, then $\alpha = -\frac{3v}{2}$ and critical points contain any real y,v and z with $y^2 + v^2 + z^2 = 1$.*

Lemma 7 *If only u and $z = 0$, then $I = -\frac{3}{2}v^2 y$ and critical points contain any real v and y with $v^2 + y^2 = 1$.*

Proof : From (3.57), we have

$$I = -\frac{3}{2}v^2 y. \tag{3.64}$$

From (3.58), we have

$$I = -\frac{3}{2}\frac{v^2(1 - v^2)}{y}. \tag{3.65}$$

From (3.64) and (3.65) we get $v^2 + y^2 = 1$ which also satisfies (3.26).

Corollary 2 *If only u, $z = 0$ and $I = \frac{v}{y}\alpha$, then $\alpha = -\frac{3}{2}vy^2$ and critical points contain any real v and y with $v^2 + y^2 = 1$.*

Lemma 8 *If $v = 0$ and $I = v\alpha$, then y must be 0 and $u = \pm 1$.*

Proof : From (3.58). we have $y = 0$. Then from (3.59), we have $u = \pm 1$ which satisfies (3.57) due to (3.26).

Lemma 9 *Consider $I = v^2\alpha$. Then if $v = 0$, then $z = 0$ and critical points contain any real u and y with $u^2 + y^2 = 1$.*

Proof : We consider $y \neq 0$. So from (3.57), we have

$$\sqrt{6}\lambda(x)yz^2(y^2-1) = 4u^2y^2. \tag{3.66}$$

From (3.59), we have

$$\sqrt{6}\lambda(x)yz^2 = 4u^2 - 4. \tag{3.67}$$

So eliminating $\sqrt{6}\lambda(x)yz^2$ from (3.66) and (3.67) we get $u^2+y^2=1$ and (3.26) yield $z=0$.

Corollary 3 *Consider $I = v^2\alpha$. If v, $u=0$ and $y\neq 0$, then $z=0$ which implies $y=\pm 1$. If v, $y=0$ and $u\neq 0$, then $z=0$ which implies $u=\pm 1$ and if v, u, $y=0$, then $z=\pm 1$.*

Lemma 10 *If $y=0$, then either $u=\pm 1$ or $v=\pm 1$ and $I=0$ at the critical points.*

Proof : From (3.58) and (3.59) we get at least one of u and v is 0. If $u=0$ then $v=\pm 1$ and if $v=0$ then $u=\pm 1$. For the both cases, (3.26) yields $z=0$. The eqn.(3.57) implies $I=0$ at the critical points.

*If y, u and v are 0, then $z=\pm 1$. In this case, $I=-\sqrt{\frac{3}{2}}\lambda(x)$.

Lemma 11 *If $z\neq 0$ and $y\neq 0$, then $u=0$ and $v\neq 0$, so lemma 6 can be applied.*

Proof : Let us assume v and $u\neq 0$. From (3.58), we have $I=\frac{v^2}{2y}$. From (3.59), we have $\sqrt{6}\lambda(x)yz^2 = 4u^2+3v^2-4$. Then from (3.57) we get $u^2+v^2+y^2=1$. So by (3.26), $z=0$ which contradicts to our hypothesis.
Now we consider only $v=0$. Then by lemmas 8 and 9, $z=0$ which contradicts to our hypothesis. So $u=0$ and lemma 6 can be applied.

Theorem 11

1. *There is no critical point with all non-zero coordinates for any I and $\lambda(x)$.*
2. *Any critical point can not contain both u and v non-zero coordinates.*
3. *critical points on the u-nullcline satisfy $z^2\lambda(x) = -\sqrt{\frac{2}{3}}I$.*
4. *On the v-nullcline the critical points form a right cylinder of height $2\sqrt{\frac{2}{3}}$ with circular base for $I=v^n\alpha$, $(n>1)$.*
5. *Origin is the only critical point on zy-plane.*

(1) If any critical point contains all non-zero coordinates then lemma 5 contradicts.
(2) If both u and v are non-zero, then y has to be non zero. Otherwise, theorem 10 contradicts. Now by lemma 5 z turns out to be 0 and $I=\frac{v^2}{2y}$. On the other hand, if we put the expression of I and $4u^2+3v^2=4$ in (3.57) we derive that $v^2+4y^2=0$ which implies both v and y are 0. But this contradicts our hypothesis.
(3) For u-nullcline, by lemma 6, we have $\lambda(x)=\sqrt{\frac{3}{2}}\frac{v^2}{z^2y}$. So $z^2\lambda(x)=-\sqrt{\frac{2}{3}}I$.
(4) For $n=1$, by lemma 8, we have $u=\pm 1$. Now the result true for $n=2$ by lemma 9. It is also should be note that the result is true for $n>2$ with exactly same argument as of $n=2$ in lemma 9
(5) Origin is a critical point. Now by lemma 11 we can derive that both u and v cant not be 0 in this case.

For two choices of Q, *i.e.*, (*a*) $Q=\alpha\rho_d(\dot{X}+3HX)$, (*b*) $Q=\alpha\rho_d H$; I becomes $\frac{\alpha}{2}v^2$, $\frac{\alpha v^2}{2y}$ respectively. Now for these two choices of Q we analyze the stability of the vector field near the origin for the autonomous system (3.56 – 3.59).

(a) $Q = \alpha\rho_d(\dot{X} + 3HX)$

For this choice of interaction the autonomous system (3.56 – 3.59) changes to

$$x' = 3\left(\sqrt{\frac{2}{3}}y - x\right), \tag{3.68}$$

$$y' = \frac{\alpha}{2}v^2 - \frac{3}{2}\mu z^2\left(xy - \sqrt{\frac{2}{3}}\right) + \frac{3}{2}\left(\frac{4}{3}u^2 + v^2\right)y, \tag{3.69}$$

$$v' = -\frac{\alpha vy}{2} - \frac{3}{2}v\left[1 + \mu xz^2 - \frac{4}{3}u^2 - v^2\right], \tag{3.70}$$

$$u' = -\frac{3}{2}u\left[\frac{4}{3} + \mu xz^2 - \frac{4}{3}u^2 - v^2\right]. \tag{3.71}$$

The critical points, existence of critical points and the value of cosmological parameters are shown in Table 3.4 and the eigenvalues and the nature of critical points are shown in Table 3.5.

In Table 3.4 there are six critical points of which the first four namely $P_0 - P_3$ are equivalent to the critical points C_0, $C_2 - C_4$ respectively in Table 3.1 from cosmological view point. The critical point P_4 describes the cosmic evolution due to interacting DE and CDM for $\alpha \neq \pm 3$. For $\alpha = \pm 3$, the matter is purely in the form of cosmological constant. So this critical point corresponds to scaling solution in cosmology. As long as the coupling parameter 'α' is restricted as $\alpha^2 < 3$ then CDM dominates over DE otherwise there is accelerated expansion. For critical point P_5 the DE in the form of a scalar field interacting with CDM. But here cosmic evolution is dominated by DE and is in the de-Sitter era of evolution.

STABILITY ANALYSIS

1. Critical Point P_0

The Jacobian matrix at P_0 is same as of (3.31). So the eigenvalues and the corresponding eigenvectors are also same. Since the critical point is hyperbolic, we can analyze the stability of this critical point by Hartman-Grobman theorem. The stability of this critical point is the same as the stability of C_0 (FIG.3.1).

2. Critical Point P_1

The Jacobian matrix at the critical point P_1 can be put as

$$J(P_1) = \begin{bmatrix} -3 & \sqrt{6} & 0 & 0 \\ 0 & 0 & 0 & 0 \\ 0 & 0 & -\frac{(3+\alpha)}{2} & 0 \\ 0 & 0 & 0 & -2 \end{bmatrix}. \tag{3.72}$$

To analyze the stability of the critical point P_1, we consider four choices of α:

(i) $\alpha \neq -3, 1, 3$;
(ii) $\alpha = -3$;
(iii) $\alpha = 1$;
(iv) $\alpha = 3$.

Table 3.4: Table shows the set of critical points, existence of critical points and the value of cosmological parameters corresponding to the autonomous system (3.68 - 3.71).

CPs	$Existence$	x	y	z	v	u	ω_{tot}	q
P_0	$\forall\mu$ *and* α	0	0	0	0	±1	1	2
P_1	$\forall\mu$ *and* α	$\sqrt{\frac{2}{3}}$	1	0	0	0	-1	-1
P_2	$\forall\mu$ *and* α	$-\sqrt{\frac{2}{3}}$	-1	0	0	0	-1	-1
P_3	$for\ \mu=0\ and\ all\ \alpha$	$\sqrt{\frac{2}{3}}y_c$	$0\leq y_c\leq 1$	$\sqrt{1-y_c^2}$	0	0	-1	-1
P_4	$\forall\mu$ *and for all* $\alpha\in[-3,0)\cup(0,3]$	$-\frac{\alpha}{3}\sqrt{\frac{2}{3}}$	$-\frac{\alpha}{3}$	0	$\pm\sqrt{1-\frac{\alpha^2}{9}}$	0	$-\frac{\alpha^2}{9}$	$\frac{1}{2}(1-\frac{\alpha^2}{3})$
P_5	$\alpha\leq-3\ and\ \frac{\alpha}{\sqrt{6}}<\mu<0$ *or,* $-3\leq\alpha<0\ and\ \mu<\frac{\alpha}{\sqrt{6}}$	$-\frac{3}{\alpha}\sqrt{\frac{2}{3}}$	$-\frac{3}{\alpha}$	$\pm\sqrt{\frac{1-\frac{9}{\alpha^2}}{1-\frac{\sqrt{6}\mu}{\alpha}}}$	$\pm\sqrt{\frac{\left(1-\frac{9}{\alpha^2}\right)\sqrt{6}\mu}{\sqrt{6}\mu-\alpha}}$	0	-1	-1

Table 3.5: Table shows the eigenvalues ($\lambda_1,\ \lambda_2,\ \lambda_3,\ \lambda_4$) of the Jacobian matrix for the autonomous system ($3.68-3.71$) corresponding to the critical points (P_0-P_4) and the nature of the critical points (P_0-P_4):

CPs	λ_1	λ_2	λ_3	λ_4	$Nature\ of\ CPs$
P_0	-3	2	$\frac{1}{2}$	4	hyperbolic
P_1	-3	0	$-\frac{(3+\alpha)}{2}$	-2	always nonhyperbolic for any α
P_2	-3	0	$\frac{(\alpha-3)}{2}$	-2	always nonhyperbolic for any α
P_3	-3	0	$-\frac{(3+\alpha y_c)}{2}$	-2	always nonhyperbolic for any α
P_4	-3	$3\left(1-\frac{\alpha^2}{9}\right)$	$\frac{3}{2}\left(1-\frac{\alpha^2}{9}\right)$	$-\frac{1}{2}\left(1+\frac{\alpha^2}{3}\right)$	nonhyperbolic for $\alpha=\pm3$ and hyperbolic for all $\alpha\in(-3,0)\cup(0,3)$

Case (i): $\alpha \neq -3, 1, 3$

For this case, the eigenvalues of the Jacobian matrix (3.72) are -3, 0, $-\frac{(3+\alpha)}{2}$, -2 (non-hyperbolic in nature) and $[1,0,0,0]^T$, $\left[1,\sqrt{\frac{3}{2}},0,0\right]^T$, $[0,0,1,0]^T$, $[0,0,0,1]^T$ are the corresponding eigenvectors, respectively. We put forward similar argument as we have mentioned for the analysis of C_2 then the center manifold is given by ($3.44-3.46$) and the flow on the center manifold is determined by (3.47). So the origin is a saddle node and unstable in nature (FIG.3.2). Hence, in this case the origin in the new coordinate system, *i.e.,* the critical point P_1 in the old coordinate system is a saddle node and unstable in nature.

Case (ii): $\alpha = -3$

In this case, the Jacobian matrix at the critical point P_1 can be put as

$$J(P_1)=\begin{bmatrix}-3 & \sqrt{6} & 0 & 0\\ 0 & 0 & 0 & 0\\ 0 & 0 & 0 & 0\\ 0 & 0 & 0 & -2\end{bmatrix}. \tag{3.73}$$

The eigenvalues of the above Jacobian matrix are -3, 0, 0, -2 (non-hyperbolic in nature). $[1,0,0,0]^T$ and $[0,0,0,1]^T$ are the eigenvectors corresponding to the eigenvalues -3 and -2 respectively, $\left[1,\sqrt{\frac{3}{2}},0,0\right]^T$ and $[0,0,1,0]^T$ are the eigenvectors corresponding to the eigenvalue 0. Since the algebraic multiplicity and the geometric multiplicity corresponding to each

eigenvalues are equal so we can transform the matrix (3.73) to its diagonal form. Similarly as above we shall take the same transformations so that P_1 moves to the origin and then introduce another transformation (3.38) (by using the eigenvectors of (3.73)) to make the Jacobian matrix (3.73) into the diagonal form. In these coordinates, our system of equations are transformed into

$$\begin{bmatrix} X_T' \\ Y_T' \\ V_T' \\ U_T' \end{bmatrix} = \begin{bmatrix} -3 & 0 & 0 & 0 \\ 0 & 0 & 0 & 0 \\ 0 & 0 & 0 & 0 \\ 0 & 0 & 0 & -2 \end{bmatrix} \begin{bmatrix} X_T \\ Y_T \\ V_T \\ U_T \end{bmatrix} + \begin{bmatrix} non \\ lin \\ ear \\ terms \end{bmatrix}. \tag{3.74}$$

So by Center Manifold Theory, there exists two continuously differentiable functions χ:$\mathbb{R}^2 \to \mathbb{R}$ and ϕ:$\mathbb{R}^2 \to \mathbb{R}$ such that

$$X_T = \chi(Y_T, V_T) = a_1 Y_T^2 + a_2 Y_T V_T + a_3 V_T^2 + \quad higher \quad order \quad terms, \tag{3.75}$$

$$U_T = \phi(Y_T, V_T) = b_1 Y_T^2 + b_2 Y_T V_T + b_3 V_T^2 + \quad higher \quad order \quad terms. \tag{3.76}$$

Now differentiating both sides with respect to N, we get

$$\frac{dX_T}{dN} = \begin{bmatrix} 2a_1 Y_T + a_2 V_T & a_2 U_T + 2a_3 V_T \end{bmatrix} \begin{bmatrix} \frac{dY_T}{dN} \\ \\ \frac{dV_T}{dN} \end{bmatrix}, \tag{3.77}$$

$$\frac{dU_T}{dN} = \begin{bmatrix} 2b_1 Y_T + b_2 V_T & b_2 U_T + 2b_3 V_T \end{bmatrix} \begin{bmatrix} \frac{dY_T}{dN} \\ \\ \frac{dV_T}{dN} \end{bmatrix}. \tag{3.78}$$

Comparing L.H.S. and R.H.S. of (3.77) and (3.78), we get $a_1 = -\frac{4\lambda}{3}$, $a_2 = 0$, $a_3 = 0$ and $b_i = 0$ for all i. Then the center manifold is given by

$$X_T = -\frac{4\mu}{3} Y_T^2 + \quad higher \quad order \quad terms, \tag{3.79}$$

$$U_T = 0. \tag{3.80}$$

The flow on the center manifold is determined by

$$\frac{dY_T}{dN} = 2\sqrt{6}\mu Y_T^2 + \left(2\sqrt{6}\mu - 4\mu^2\right) Y_T^3 + \left(\frac{3}{2} + \sqrt{6}\mu\right) V_T^2 Y_T + \text{higher order terms}, \tag{3.81}$$

$$\frac{dV_T}{dN} = \left(\frac{3}{2} + \sqrt{6}\mu\right) V_T Y_T + 3\sqrt{\frac{3}{2}}\mu V_T Y_T^2 + \left(\frac{3}{2} + \sqrt{\frac{3}{2}}\mu\right) V_T^3 + \text{higher order terms}. \tag{3.82}$$

Case (ii)(a): $\mu > 0$

In this case, the coefficient of lowest power terms of (3.81) and (3.82) are positive. Now divide both sides of (3.81) and (3.82) by $2\sqrt{6}\mu$ and $(\frac{3}{2} + \sqrt{6}\mu)$ respectively and since by dividing both sides any positive number there will no effect on the flow of the vector field Now let's take $r^2 = Y_T^2 + V_T^2$, in arbitrary small neighborhood of the origin. Differentiating both sides with respect to N, we get $r' = Y_T r$. For $Y_T < 0$ one has $r' < 0$ while $r' > 0$ for $Y_T > 0$. So for $\mu > 0$, the origin is a saddle node and unstable in nature (vector field near the origin is same as of FIG.3.2(b)).

Case (ii)(b): $\mu < -\frac{1}{2}\sqrt{\frac{3}{2}}$

Then the coefficient of lowest power terms of (3.81) and (3.82) are negative. We assume $2\sqrt{6}\mu = -\sigma^2$ and $(\frac{3}{2} + \sqrt{6}\mu) = -\gamma^2$ and divide (3.81) by σ^2 and (3.82) by γ^2 and we take $r^2 = Y_T^2 + V_T^2$, in arbitrary small neighborhood of the origin. Differentiating both sides with respect to N, we get $r' = -Y_T r$. For $Y_T < 0$ one has $r' > 0$ while $r' < 0$ for $Y_T > 0$. So for $\mu < -\frac{1}{2}\sqrt{\frac{3}{2}}$, the origin is a saddle node and unstable in nature (vector field near the origin is same as FIG.3.2(a)).

As for both of the subcases of this case, the origin is unstable due to its saddle nature, thus in the old coordinate system $(x,\ y,\ v,\ u)$ the critical point P_1 is a saddle node, *i.e.,* unstable in nature.

Case (iii): $\alpha = 1$

In this case, the eigenvalues of the Jacobian matrix are -3, 0, -2, -2 and $[1,0,0,0]^T$, $\left[1,\sqrt{\frac{3}{2}},0,0\right]^T$ are the eigenvectors corresponding to the eigenvalues -3 and 0 respectively, $[0,0,1,0]^T$ and $[0,0,0,1]^T$ are the eigenvectors corresponding to the eigenvalue -2. But for this case we will get the same vector field as Case-(i).

Case (iv): $\alpha = 3$

Then the eigenvalues of the Jacobian matrix are -3, 0, -3 and -2. $[1,0,0,0]^T$ and $[0,0,1,0]^T$ are the eigenvectors corresponding to the eigenvalue -3 and $\left[1,\sqrt{\frac{3}{2}},0,0\right]^T$ and$[0,0,0,1]^T$ are the eigenvectors corresponding to the eigenvalues 0 and -2 respectively. But for this case also we will get the same vector field as Case-(i).

3. Critical Point P_2

The Jacobian matrix at the critical point P_2 can be put as

$$J(P_2) = \begin{bmatrix} -3 & \sqrt{6} & 0 & 0 \\ 0 & 0 & 0 & 0 \\ 0 & 0 & \frac{(\alpha-3)}{2} & 0 \\ 0 & 0 & 0 & -2 \end{bmatrix}. \tag{3.83}$$

For avoiding similar calculation, we only state the expression of the center manifold and the flow on the center manifold. Here we also take four choices of α for analyzing the stability of this critical point:

$$\begin{aligned} (i)\ & \alpha \neq -3, -1, 3; \\ (ii)\ & \alpha = 3; \\ (iii)\ & \alpha = -1; \\ (iv)\ & \alpha = -3. \end{aligned}$$

Case (i) : $\alpha \neq -3, -1, 3$

The eigenvalues of the Jacobian matrix are -3, 0, $\frac{(\alpha-3)}{2}$, -2 and $[1,0,0,0]^T$, $\left[1,\sqrt{\frac{3}{2}},0,0\right]^T$, $[0,0,1,0]^T$ and $[0,0,0,1]^T$ are the corresponding eigenvectors, respectively. In this case, the

center manifold is same as (3.48 - 3.50) and the flow on the center manifold is determined by (3.51). So the origin is a saddle node and unstable in nature (FIG.3.2). Hence in the new coordinate system due to saddle nature of the origin, the critical point P_2 is a saddle node and unstable in nature.

Case (ii) : $\alpha = 3$

In this case, the center manifold is given by

$$X_T = -\frac{4\mu}{3}Y_T^2 + \quad higher \quad order \quad terms, \tag{3.84}$$

$$U_T = 0. \tag{3.85}$$

The flow on the center manifold is determined by

$$\frac{dY_T}{dN} = 2\sqrt{6}\mu Y_T^2 - \left(2\sqrt{6}\mu + 4\mu^2\right) Y_T^3 + \left(\frac{3}{2} - \sqrt{6}\mu\right) V_T^2 Y_T + \quad higher \quad order \quad terms, \tag{3.86}$$

$$\frac{dV_T}{dN} = \left(-\frac{3}{2} + \sqrt{6}\mu\right) V_T Y_T - 3\sqrt{\frac{3}{2}}\mu V_T Y_T^2 + \left(\frac{3}{2} - \sqrt{\frac{3}{2}}\mu\right) V_T^3 + \quad higher \quad order \quad terms. \tag{3.87}$$

Case (ii)(a) : $\mu > \frac{1}{2}\sqrt{\frac{3}{2}}$

In this case as above, divide both sides of (3.86) and (3.87) by $2\sqrt{6}\mu$ and $(-\frac{3}{2} + \sqrt{6}\mu)$ respectively and by taking $r^2 = Y_T^2 + V_T^2$, we can get $r' = Y_T r$. If $Y_T > 0$ then $r' > 0$ and $r' < 0$ while $Y_T < 0$. So the origin is a saddle node and unstable in nature (same as FIG.3.2(b)).

Case (ii)(b) : $\mu < 0$

In this case also by taking $r^2 = Y_T^2 + V_T^2$, we can get $r' = -Y_T r$ and as above we can determine that the origin is a saddle node and unstable in nature (same as FIG.3.2(a)).

As for both of the subcases, the origin is a saddle node, hence in the old coordinate system $(x,\ y,\ v,\ u)$ the critical point P_2 is a saddle node and unstable in nature.

Case (iii) $\alpha = -1$

In this case we will get the same eigenvalues and eigenvectors as in Case (iii) of the critical point P_1 and the center manifold is given by $(3.48 - 3.50)$ and the flow on the vector field near the origin is determined by (3.51).

Case (iv) $\alpha = -3$

In this case, we will get the same eigenvalues and eigenvectors as in Case (iv) of the critical point P_1 and the center manifold is given by $(3.48 - 3.50)$ and the flow on the vector field near the origin is determined by (3.51).

4. Critical Point P_3

The Jacobian matrix at the critical point P_3 can be put as

$$J(P_3) = \begin{bmatrix} -3 & \sqrt{6} & 0 & 0 \\ 0 & 0 & 0 & 0 \\ 0 & 0 & -\frac{(3+\alpha y_c)}{2} & 0 \\ 0 & 0 & 0 & -2 \end{bmatrix}, \tag{3.88}$$

the center manifold is same as (3.52 - 3.54) and the flow on the center manifold is determined by (3.55). So here we only define the stability near the origin on each coordinate plane which is shown in Table 3.6.

5. Critical Point P_4

The Jacobian matrix at the critical point P_4 can be put as

$$J(P_4) = \begin{bmatrix} -3 & \sqrt{6} & 0 & 0 \\ 0 & \left(1-\frac{\alpha^2}{9}\right)\left(\frac{3}{2}+\alpha\mu\sqrt{\frac{2}{3}}\right) & \mp\sqrt{6}\mu\left(1-\frac{\alpha^2}{9}\right)^{\frac{3}{2}} & 0 \\ 0 & \mp\sqrt{\left(1-\frac{\alpha^2}{9}\right)\left(\frac{\alpha^2\mu}{3}\sqrt{\frac{2}{3}}-\frac{\alpha}{2}\right)} & 3\left(1-\frac{\alpha^2}{9}\right)\left(1-\frac{\alpha\mu}{3}\sqrt{\frac{2}{3}}\right) & 0 \\ 0 & 0 & 0 & -\frac{1}{2}\left(1+\frac{\alpha^2}{3}\right) \end{bmatrix}. \tag{3.89}$$

The eigenvalues of $J(P_4)$ are -3, $3\left(1-\frac{\alpha^2}{9}\right)$, $\frac{3}{2}\left(1-\frac{\alpha^2}{9}\right)$ and $-\frac{1}{2}\left(1+\frac{\alpha^2}{3}\right)$ and the corresponding eigenvectors are $[1,0,0,0]^T$, $\left[\pm\frac{\sqrt{6}(k-n+p)}{m(6+k+n+p)}, \pm\frac{k-n+p}{2m}, 1, 0\right]^T$, $\left[\pm\frac{\sqrt{6}(k-n-p)}{m(6+k+n-p)}, \pm\frac{k-n+p}{2m}, 1, 0\right]^T$, and $[0,0,0,1]^T$ respectively; where $k = \left(1-\frac{\alpha^2}{9}\right)\left(\frac{3}{2}+\alpha\mu\sqrt{\frac{2}{3}}\right)$, $l = -\sqrt{6}\mu\left(1-\frac{\alpha^2}{9}\right)^{\frac{3}{2}}$, $m = -\sqrt{\left(1-\frac{\alpha^2}{9}\right)}\left(\frac{\alpha^2\mu}{3}\sqrt{\frac{2}{3}}-\frac{\alpha}{2}\right)$, $n = 3\left(1-\frac{\alpha^2}{9}\right)\left(1-\frac{\alpha\mu}{3}\sqrt{\frac{2}{3}}\right)$, $p = \frac{3}{2}\left(1-\frac{\alpha^2}{9}\right)$. The critical point P_4 is nonhyperbolic for $\alpha = \pm 3$ and for $\alpha = -3$ the critical point is same as P_1 and we have already analyzed the stability of this critical point and for $\alpha = 3$ the critical point is same as P_2 and we have already analyzed the stability of this critical point. So we have to analyze the stability of the critical point P_4 only when this is hyperbolic in nature and by Hartman-Grobman theorem we shall analyze the stability of this critical point. All eigenvalues of the above Jacobian matrix are negative only when $\alpha > 3$ or $\alpha < -3$ but this contradicts the existence of this critical point. So we have two positive and two negative eigenvalues and by Hartman-Grobman theorem we can say that the critical point P_4 is unstable due to its saddle nature.

If we try to analyze the stability of the critical point P_5 then we see that the values of $\frac{\partial f_1}{\partial x}$, $\frac{\partial f_1}{\partial y}$, $\frac{\partial f_2}{\partial x}$, $\frac{\partial f_2}{\partial y}$, $\frac{\partial f_2}{\partial v}$, $\frac{\partial f_3}{\partial x}$, $\frac{\partial f_3}{\partial y}$, $\frac{\partial f_3}{\partial v}$, $\frac{\partial f_4}{\partial u}$ are non-zero and without $\frac{\partial f_1}{\partial x}$, $\frac{\partial f_1}{\partial y}$ all other elements at this critical point contain complicated terms and this is very difficult to find the eigenvalues and corresponding eigenvectors of the Jacobian matrix. Due to this complicated calculation, we skip the stability analysis of this critical point.

(b) $Q = \alpha\rho_d H$

For this choice of interaction with exponential potential the autonomous system (3.56 -

3.59) changes to

$$x' = 3\left(\sqrt{\frac{2}{3}}y - x\right), \tag{3.90}$$

$$y' = \frac{\alpha}{2y}v^2 - \frac{3}{2}\mu z^2\left(xy - \sqrt{\frac{2}{3}}\right) + \frac{3}{2}\left(\frac{4}{3}u^2 + v^2\right)y, \tag{3.91}$$

$$v' = -\frac{\alpha v}{2} - \frac{3}{2}v\left[1 + \mu x z^2 - \frac{4}{3}u^2 - v^2\right], \tag{3.92}$$

$$u' = -\frac{3}{2}u\left[\frac{4}{3} + \mu x z^2 - \frac{4}{3}u^2 - v^2\right]. \tag{3.93}$$

The critical points, existence of critical points and the value of cosmological parameters are shown in Table 5.3 and the eigenvalues and the nature of critical points are shown in Table 3.8. The first three critical points $B_1 - B_3$ in Table 3.7 are cosmologically equivalent to the critical points $C_2 - C_4$ in Table 3.1. The critical point B_4 represents a scaling cosmological solution where DE is interacting with CDM. The CDM dominates the evolution for $-1 < \alpha < 0$, otherwise there is accelerated expansion due to dominance of DE. For $\alpha = -3$ the matter is purely in the form of cosmological constant.

STABILITY ANALYSIS

1. Critical Point B_1

The Jacobian matrix at the critical point B_1 is same as (3.72). So here we also take four choices of α (same as P_1) for analyzing the stability of this critical point.

Case (i): $\alpha \neq -3, 1, 3$

In this case, we have the same eigenvalues and corresponding eigenvectors of the Jacobian matrix. We put forward similar argument as we have mentioned for the stability analysis in case (i) of P_1, then the center manifold is given by (3.44 - 3.46) and the flow on the vector field near the origin is determined by the equation (3.47) (FIG.(3.2)).

Case (ii): $\alpha = -3$

In this case, we also get the same Jacobian matrix (3.73), so have the same eigenvalues and corresponding eigenvectors. We put forward similar argument as we have mentioned for the analysis in case (ii) of P_1, then we get the center manifold same as $(3.79 - 3.80)$ and the flow on the center manifold is determined by

$$\frac{dY_T}{dN} = 2\sqrt{6}\mu Y_T^2 + \left(2\sqrt{6}\mu - 4\mu^2\right)Y_T^3 + \left(\frac{3}{2} + \sqrt{6}\mu\right)V_T^2 Y_T + \textit{ higher order terms}, \tag{3.94}$$

$$\frac{dV_T}{dN} = \sqrt{6}\mu V_T Y_T + 3\sqrt{\frac{3}{2}}\mu V_T Y_T^2 + \left(\frac{3}{2} + \sqrt{\frac{3}{2}}\mu\right)V_T^3 + \textit{ higher order terms}. \tag{3.95}$$

Case (ii)(a): $\mu > 0$

Divide (3.94) and (3.95) by $2\sqrt{6}\mu$ and $\sqrt{6}\mu$ respectively and as the flow on the vector field is

not changed due to divide by positive number on the flow equation, we take $r^2 = Y_T^2 + V_T^2$, then we get $r' = Y_T r$. If $Y_T > 0$ then $r' > 0$ and $r' < 0$ while $Y_T < 0$. So the origin is a saddle node and unstable in nature (FIG.3.2(b)).

Case (ii)(b): $\mu < 0$

We put forward similar argument as we have mentioned above then we also obtain that the origin is a saddle node and unstable in nature (same as FIG.3.2(a)).

As for both of the subcases, the origin is unstable due to its saddle nature, thus in the old coordinate system (x, y, v, u) the critical point B_1 is a saddle node, *i.e.,* unstable in nature.

Case (iii): $\alpha = 1$

In this case the eigenvalues of the Jacobian matrix are -3, 0, -2, -2 and $[1,0,0,0]^T$, $\left[1,\sqrt{\frac{3}{2}},0,0\right]^T$ are the eigenvectors corresponding to the eigenvalues -3 and 0 respectively, $[0,0,1,0]^T$ and $[0,0,0,1]^T$ are the eigenvectors corresponding to the eigenvalue -2. But for this case we will get the same vector field as Case (i).

Case (iv): $\alpha = 3$

Then the eigenvalues of the Jacobian matrix are -3, 0, -3 and -2. $[1,0,0,0]^T$ and $[0,0,1,0]^T$ are the eigenvectors corresponding to the eigenvalue -3, $\left[1,\sqrt{\frac{3}{2}},0,0\right]^T$ and $[0,0,0,1]^T$ are the eigenvectors corresponding to the eigenvalues 0 and -2, respectively. But for this case also we will get the same vector field as Case (i).

2. Critical Point B_2

The Jacobian matrix at this critical point is also same as (3.72). Here four cases also arises. The Center manifold and the flow on the center manifold are shown in the Table 3.9. As for all possible cases in the new coordinate system (X_T, Y_T, V_T, U_T) the origin is a saddle node, *i.e.,* unstable in nature. Hence, in the old coordinate system (x, y, v, u) the critical point B_2 is a saddle node and unstable in nature.

3. Critical Point B_3

The Jacobian matrix at the critical point B_3 is same as (3.72). In this case also, we get the center manifold same as (3.52 – 3.54) and the flow on the center manifold is same as (3.55). So here we only define the stability of the vector field near the origin on each coordinate plane, shown in Table 3.10.

4. Critical Point B_4

The Jacobian matrix at B_4 can be put as

$$J(B_4) = \begin{bmatrix} -3 & \sqrt{6} & 0 & 0 \\ 0 & \left(1+\frac{\alpha}{3}\right)\left(3 \mp \sqrt{-2\alpha}\mu\right) & \mp\sqrt{6}\mu\left(1+\frac{\alpha}{3}\right)^{\frac{3}{2}} & 0 \\ 0 & \mp\sqrt{\frac{2}{3}}\mu\alpha\sqrt{\left(1+\frac{\alpha}{3}\right)} & \left(1+\frac{\alpha}{3}\right)\left(3 \pm \sqrt{-2\alpha}\mu\right) & 0 \\ 0 & 0 & 0 & -\frac{1}{2}(1-\alpha) \end{bmatrix}. \tag{3.96}$$

The eigenvalues of the above Jacobian matrix are -3, $\alpha+3$, $\alpha+3$ and $-\frac{1}{2}(1-\alpha)$. $[1,0,0,0]^T$, $[0,0,0,1]^T$ are the eigenvectors corresponding to the eigenvalues -3 and $-\frac{1}{2}(1-\alpha)$ respectively and $[\frac{\sqrt{6}(k-n)}{m(6+k+n)}, \frac{k-n}{2m}, 1, 0]^T$ be the eigenvector corresponding to the eigenvalue $\alpha+3$; where $k = \left(1+\frac{\alpha}{3}\right)\left(3\mp\sqrt{-2\alpha}\mu\right)$, $m = \mp\sqrt{\frac{2}{3}}\mu\alpha\sqrt{\left(1+\frac{\alpha}{3}\right)}$ and $n = \left(1+\frac{\alpha}{3}\right)\left(3\pm\sqrt{-2\alpha}\mu\right)$. We clearly see that this critical point is nonhyperbolic only when $\alpha = -3$ and the stability analysis for this case already studied for B_1. So here we analyze the stability of this critical point only when $\alpha \in (-3, 0)$. For this case the two eigenvalues are positive and another two are negative. So by Hartman-Grobman theorem we can say that the critical point B_4 is unstable due to its saddle nature.

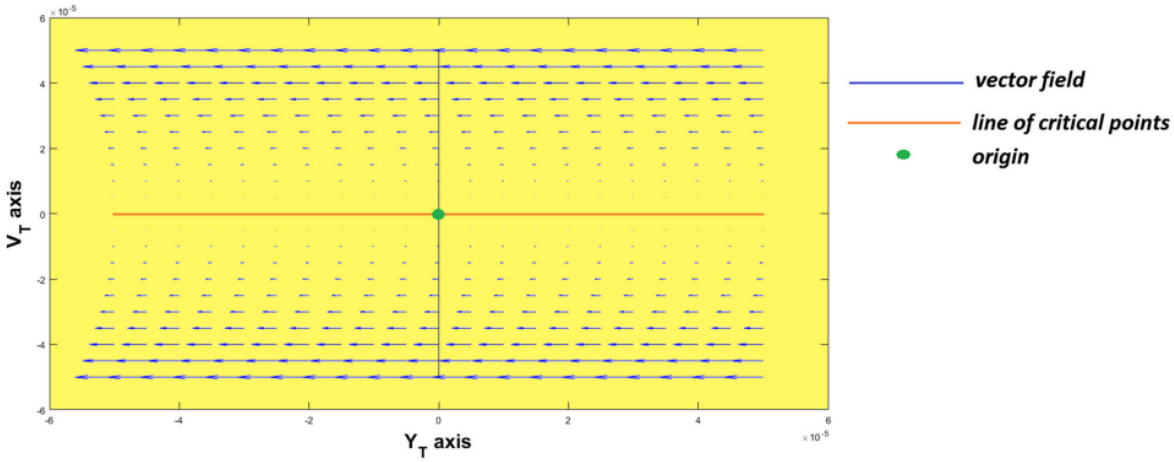

Figure 3.3: This figure shows the vector field near the origin in $Y_T V_T-$plane for $\alpha = -3$ corresponding to B_3. After applying shift-transformation and then matrix transformation, the line of critical points B_3 (in the old coordinate system (x, y, v, u)) is completely lying on the Y_T axis in the new coordinate system. We have considered $y_c = \frac{1}{2}$ to determine this vector field, that is, in this phase plot the origin corresponds to $\left(0, \frac{1}{2}, 0, 0\right)$ in the old coordinate system.

GLOBAL BEHAVIOR AND BIFURCATION ANALYSIS

For non-interacting model with exponential potential, we have five critical points (C_0-C_4) for various choices of μ. It is to be noted from matrix (3.32), that C_0 is saddle with one stable and three unstable eigen-directions. On the other hand, C_1 is saddle with two stable and two unstable eigen-directions. The stability of C_0 and C_1 do not depend on the parameter μ. At C_2 and C_3 the effective potential [603] reaches its extreme point in the dark energy dominated period. We can have global behavior of phase space and the main property of bifurcations on different nullclines. On the Y-nullcline, the vector field does not depend on μ. But on the center manifold of C_2 and C_3 the flow reverses its direction when μ passes through the value $\mu = 0$. But the vector fields remain topologically equivalent even after μ changes its sign. At $\mu = 0$, the stability is classified by considering the flow of the remaining eigen-directions. At $\mu = 0$, new non-isolated critical point C_4 appears to exist. C_4 is normally hyperbolic and stable in nature. It is to be noted that, for $\mu \neq 0$, C_2 and C_3 are saddle-node in nature. So there exists a non-generic de-Sitter evolution of the universe through only one trajectory (*i.e.,* invariant manifold) from past (C_2 or C_3) to future (C_3 or C_2). For $\mu > 0$, if

the trajectory starts near C_2 and ends asymptotically to C_3, then the three form field transit from phantom field to non-phantom field and reverse transition happens for $\mu < 0$. As C_4 is stable with de-Sitter phase, so there is a generic evolution near C_2 or C_3 towards C_4 at $\mu = 0$.

Next, we have considered the interaction $Q = \alpha(\rho_d)(\dot{X}+3HX)$. For exponential potential there exists three critical points $(P_0 - P_5)$ for various choices to μ. At $\alpha = \pm 3$, P_1 and P_2 change its stability. On the other hand, at $\mu = 0$, new non-isolated critical point P_3 appears to exist. P_3 is normally hyperbolic and on the Y-nullcline P_3 becomes stable node to saddle node when α becomes smaller than $-\frac{3}{y_c}$, $(y_c \neq 0)$ for any fixed y_c $(0 < y_c \leqslant 1)$. When α touches ± 3 and lies in $[-3, 0) \cup (0, 3]$, a new critical point P_4 appears to exist. P_1 and P_2 are the special case of P_4 at $\alpha = \pm 3$.
For interaction $Q = \alpha(\rho_d)yH$, at $\alpha \neq 3, -3$, both P_1 and P_2 are saddle node in nature. So there exists a non-generic de-Sitter evolution of the universe through the invariant manifold (3.86) from past P_2 to future P_3.

For the interaction $\alpha\rho_d H$, a new critical point B_4 appears to exist for $\alpha \in [-3, 0)$. This critical point changes its stability at -3 and $\mu = 0$. For $\mu \neq 0$, B_4 is saddle node in nature. So the evolution of the universe through the invariant manifold is performed as in the previous case.

Now, it is to be noted that at $\mu = 0$, the system associated with non-interacting model becomes structurally unstable. On the other hand, two new bifurcation values appear for the interacting model, namely $\alpha = -3, 3$. Moreover, at $\mu = 0$, the system associated with interacting model becomes structurally unstable. Also one may note that the potential becomes runaway to non-runaway through bifurcation value $\mu = 0$ [604]. On the other hand, if we neglect the contribution of matter and radiation, the fixed points at the extremum point of the effective potential [603] are same as in our non-interacting dynamical equation, *i.e.,* C_2 and C_3 which trigger non-generic evolution of the universe.

3.4 SUMMARY

The present work is an example where without making any attempt of solving the complicated coupled cosmic evolution equations (Einstein field equations), the cosmological interferences have been done using the technique of dynamical system analysis. The cosmic matter is chosen as three-form field (DE) interacting/non-interacting with baryonic matter (radiation with CDM). By suitable choice of the dimensionless variables the evolution equations are converted into an autonomous system for non-interacting case and for two suitable choices of the interaction. Out of total fifteen equilibrium points (presented in Tables 3.1, 3.4 and 3.7) the following sets of critical points (C_0, P_0), (C_2, P_1, B_1), (C_3, P_2, B_2), (C_4, P_3, B_3) are equivalent both cosmologically as well as from dynamical system analysis. It is to be noted that the set of critical points $(C_4, P_3.B_3)$ are essentially a line of critical points. The first set describes the radiation era of evolution while the remaining three sets correspond to accelerated expansion at the de-Sitter phase. The critical point C_1 describes the CDM dominated decelerated expansion. Although the critical point P_5 represents interacting DE and CDM but it also corresponds to de-Sitter phase. The most interesting critical points are P_4 and B_4 which are representing scaling cosmological solutions. Also the cosmic evolution representing these two critical points are observationally important as by choosing the coupling parameter α to be closed to ± 3 (for critical point P_4) / -3 (for B_4) the equation of state parameter agrees (within confidence limit) with the latest plank data [617].

The stability of the critical points are analysed by studying the eigenvalues of the Jacobian matrix for hyperbolic critical points while center manifold theory has been employed for non-hyperbolic critical points. The two parameters μ (in the potential) and α (coupling) on the system are found to be important for bifurcation analysis. Usually, it is speculated that at the bifurcation point there may be a cosmic phase transition.

Finally, the general nature of the critical points both for non-interacting and interacting cases have been presented in the form of lemmas and theorems. Lastly, one may note that the present work does not depend effectively on the choice of $V(X)$.

Table 3.6: Stability of the vector field on every coordinate plane for the critical point P_3.

Coordinate Plane	Stability
$X_TY_T - plane$	Vector field is stable about Y_T axis
$X_TV_T - plane$	Vector field near the origin is stable star (if $y_c = 0$ or $\alpha > -\frac{3}{y_c}$), vector field near the origin is a saddle node (if $\alpha < -\frac{3}{y_c}$), vector field is stable about V_T axis ($\alpha = -\frac{3}{y_c}$)
$X_TU_T - plane$	Vector field near the origin is stable star
$Y_TV_T - plane$	Vector field is stable about Y_T axis (if $y_c = 0$ or $\alpha > -\frac{3}{y_c}$), vector field is unstable about Y_T axis (if $\alpha < -\frac{3}{y_c}$), vector field near the origin for $\alpha = -\frac{3}{y_c}$ is parallel to V_T axis and the direction of the vector field is from negative V_T axis to positive V_T axis
$Y_TU_T - plane$	Vector field is stable about Y_T axis
$U_TV_T - plane$	Vector field near the origin is stable star (if $y_c = 0$ or $\alpha > -\frac{3}{y_c}$), vector field near the origin is a saddle node (if $\alpha < -\frac{3}{y_c}$), vector field is stable about V_T axis (for $\alpha = -\frac{3}{y_c}$)

Table 3.7: The set of critical points, existence of critical points and the value of cosmological parameters corresponding to the critical points for the autonomous system (3.90 - 3.93).

CPs	$Existence$	x	y	z	v	u	ω_{tot}	q
B_1	$\forall\ \mu\ and\ \alpha$	$\sqrt{\frac{2}{3}}$	1	0	0	0	-1	-1
B_2	$\forall\ \mu\ and\ \alpha$	$-\sqrt{\frac{2}{3}}$	-1	0	0	0	-1	-1
B_3	$\mu = 0\ and\ \forall\ \alpha$	$\sqrt{\frac{2}{3}}y_c$	$0 < y_c \leq 1$	$\sqrt{1-y_c^2}$	0	0	-1	-1
B_4	$\forall\ \mu\ and$ $\forall\alpha \in [-3, 0)$	$\pm\sqrt{-\frac{\alpha}{3}}\sqrt{\frac{2}{3}}$	$\pm\sqrt{-\frac{\alpha}{3}}$	0	$\pm\sqrt{1+\frac{\alpha}{3}}$	0	$\frac{\alpha}{3}$	$\frac{(1+\alpha)}{2}$

Table 3.8: Table shows the eigenvalues ($\lambda_1,\ \lambda_2,\ \lambda_3,\ \lambda_4$) of the Jacobian matrix for the autonomous system (3.90 - 3.93) corresponding to the above critical points and the nature of the critical points:

CPs	λ_1	λ_2	λ_3	λ_4	Nature of Critical points
B_1	-3	0	$-\frac{(3+\alpha)}{2}$	-2	nonhyperbolic
B_2	-3	0	$\frac{(\alpha-3)}{2}$	-2	nonhyperbolic
B_3	-3	0	$-\frac{(3+\alpha y_c)}{2}$	-2	nonhyperbolic
B_4	-3	$\alpha+3$	$\alpha+3$	$-\frac{1}{2}(1-\alpha)$	nonhyperbolic for $\alpha = -3$ and hyperbolic when $\alpha \in (-3, 0)$

Table 3.9: Center manifold, flow on the CM and the stability near the origin corresponding to the critical point B_2.

Case	*Center manifold*	*Flow on the center manifold*	*Stability*
$\alpha \neq -3, 1, 3$	$X_T = -\frac{4\lambda}{3}Y_T^2 + \mathcal{O}\left(Y_T^4\right)$, $V_T = 0$, $U_T = 0$.	$\frac{dY_T}{dN} = 2\sqrt{6}\mu Y_T^2 + \mathcal{O}\left(Y_T^3\right)$	Origin is a saddle node for both of the cases $\mu > 0$ *and* $\mu < 0$.
$\alpha = -3$	$X_T = -\frac{4\mu}{3}Y_T^2 + \mathcal{O}\left(Y_T^3\right)$, $U_T = 0$.	$\frac{dY_T}{dN} = 2\sqrt{6}\mu Y_T^2 + higher\ order\ terms$ $\frac{dV_T}{dN} = \sqrt{6}\mu V_T Y_T + higher\ order\ terms$	Origin is a saddle node for both of the cases $\mu > 0$ and $\mu < 0$.
$\alpha = 1, 3$	$X_T = -\frac{4\mu}{3}Y_T^2 + \mathcal{O}\left(Y_T^4\right)$, $V_T = 0$, $U_T = 0$.	$\frac{dY_T}{dN} = 2\sqrt{6}\mu Y_T^2 + \mathcal{O}\left(Y_T^3\right)$	Origin is a saddle node for both of the cases $\lambda > 0$ *and* $\lambda < 0$.

Table 3.10: Stability of the vector field on every coordinate plane for the critical point B_3.

Coordinate Plane	Stability
$X_T Y_T - plane$	Vector field is stable about Y_T axis
$X_T V_T - plane$	Vector field near the origin is stable star (if $\alpha > -3$), vector field near the origin a saddle node (if $\alpha < -3$), vector field is unstable about V_T axis(if $\alpha = -3$)
$X_T U_T - plane$	Vector field near the origin stable star
$Y_T V_T - plane$	Vector field is stable about Y_T axis (if $\alpha > -3$), vector field is unstable about Y_T axis (if $\alpha < -3$), vector field for $\alpha = -3$ is shown in FIG.3.3
$Y_T U_T - plane$	Vector field is stable about Y_T axis
$U_T V_T - plane$	Vector field near the origin is stable star (if $\alpha > -3$), vector field near the origin is a saddle node (if $\alpha < -3$)

CHAPTER 4

A DYNAMICAL SYSTEM ANALYSIS OF COSMIC EVOLUTION WITH COUPLED PHANTOM DARK ENERGY WITH DARK MATTER

4.1 Prelude

The unexpected accelerated expansion of the universe as predicted by recent series of observations is speculated by cosmologist as a smooth transition from decelerated era in recent past [640, 653, 654, 655, 656]. The cosmologists are divided in opinion about the cause of this transition. One group has the opinion of modification of the gravity theory while others are in favour introducing exotic matter component. Due to two severe drawbacks [666] of the cosmological constant as a DE candidate dynamical DE models namely quintessence field (canonical scalar field), phantom field [660, 661, 662, 663, 664, 665] (ghost scalar field) or a unifield model named quintom [657, 658, 659] are popular in the literature.

However, a new cosmological problem arises due to the dynamical nature of the DE although vacuum energy and DM scale independently during cosmic evolution but why their energy densities are nearly equal today. To resolve this coincidence problem cosmologists introduce interaction between the DE and DM. As the choice of this interaction is purely phenomenological so various models appear to match the observational prediction. Although these models may resolve the above coincidence problem but a non-trivial, almost tuned sequence of cosmological eras [667] appear as a result. Further, the interacting phantom DE models [668, 669, 670, 672, 673, 674, 688] deal with some special coupling forms, alleviating the coincidence problem.

Alternatively cosmologists put forward with a special type of interaction between DE and DM where the DM particles has variable mass, depending on the scalar field representing the DE [676]. Such type of interacting model is physically more sound as scalar field dependent varying mass model appears in string theory or scalar-tensor theory [677]. This type of interacting model in cosmology considers mass variation as linear [678, 676, 679], power law

[680] or exponential [681, 682, 683, 684, 685, 686, 687] on the scalar field. Among these the exponential dependence is most suitable as it not only solves the coincidence problem but also gives stable scaling behaviour.

In the present work, varying mass interacting DE/DM model is considered in the background of homogeneous and isotropic space-time model. Due to highly coupled nonlinear nature of the Einstein field equations it is not possible to have any analytic solution. So by using suitable dimensionless variables the field equations are converted to an autonomous system. The phase space analysis with non-hyperbolic equilibrium points by center manifold theory has been done for various choices for the mass function and for the scalar field potential. This chapter is organized as follows: Section 4.2 deals with basic equations for the varying mass interacting dark energy and dark matter cosmological model. Autonomous system is formed and critical points are determined in Section 4.3. Also stability analysis of all critical points for various choices of the involving parameters are shown in this section. Possible bifurcation scenarios [544, 611, 475] by Poincaré index theory and global cosmological evolution have been examined in Section 4.4. Finally, brief discussion and important concluding remarks of the present work is proposed in Section 4.5.

4.2 Varying mass interacting dark energy and dark matter cosmological model : Basic Equations

In the background of flat Friedmann-Lemaître-Robertson-Walker (FLRW) space-time with line element

$$ds^2 = -dt^2 + a^2(t)\, d\Sigma^2, \tag{4.1}$$

the Friedmann equations are

$$\begin{aligned} 3H^2 &= k^2(\rho_\phi + \rho_{_{DM}}), &(4.2)\\ 2\dot{H} &= -k^2(\rho_\phi + p_\phi + \rho_{_{DM}}), &(4.3) \end{aligned}$$

with t, the comoving time; $a(t)$, the scale factor; $d\Sigma^2$, the 3D flat space line element. Here $\kappa = 8\pi G$ is the coupling parameter, (ρ_ϕ, p_ϕ) are the energy density and thermodynamic pressure of the phantom scalar field ϕ (considered as DE) having expressions

$$\begin{aligned} \rho_\phi &= -\frac{1}{2}\dot{\phi}^2 + V(\phi),\\ p_\phi &= -\frac{1}{2}\dot{\phi}^2 - V(\phi), \end{aligned} \tag{4.4}$$

and $\rho_{_{DM}}$ is the energy density for the dark matter in the form of dust having expression

$$\rho_{_{DM}} = M_{_{DM}}(\phi) n_{_{DM}}, \tag{4.5}$$

where $n_{_{DM}}$, the number density [642] for DM satisfies the number conservation equation

$$\dot{n}_{_{DM}} + 3H n_{_{DM}} = 0. \tag{4.6}$$

In the present work we have considered interaction between dark matter and dark energy. Normally the interaction term is introduced by phenomenological choice. In particular, the

form of the interaction term is chosen so that either the problem is solvable or it is simplified to a great extend. Further mathematically one can see that the phenomenological choice of the interaction term 'Q' arises when we break up the conservation equation of the total matter (dark matter and dark energy) into their individual conservation form. Now differentiating (4.5) and using (4.6) one has the DM conservation equation as

$$\dot{\rho}_{DM} + 3H\rho_{DM} = \frac{d}{d\phi}\left\{\ln M_{DM}(\phi)\right\}\dot{\phi}\rho_{DM}, \tag{4.7}$$

which shows that mass varying DM (in the form of dust) can be interpreted as a barotropic fluid with variable equation of state : $\omega_{DM} = \frac{d}{d\phi}\left\{\ln M_{DM}(\phi)\right\}\dot{\phi}$. Now due to Bianchi identity, using the Einstein field equations (4.2) and (4.3) the conservation equation for DE takes the form

$$\dot{\rho}_{\phi} + 3H(\rho_{\phi} + p_{\phi}) = -\frac{d}{d\phi}\left\{\ln M_{DM}(\phi)\ \right\}\dot{\phi}\rho_{DM}. \tag{4.8}$$

or using (4.4) one has

$$\ddot{\phi} + 3H\dot{\phi} - \frac{\partial V}{\partial \phi} = \frac{d}{d\phi}\left\{\ln M_{DM}(\phi)\right\}\rho_{DM}. \tag{4.9}$$

The combination of the conservation equations (4.7) and (4.8) for DM (dust) and phantom DE (scalar) shows that the interaction between these two matter components depends purely on the mass variation, *i.e.*, $Q = \frac{d}{d\phi}\left\{\ln M_{DM}(\phi)\ \right\}\dot{\phi}\rho_{DM}$. So, if M_{DM} is an increasing function of ϕ, *i.e.*, $Q > 0$ then energy is exchanged from DE to DM while in the opposite way if M_{DM} is a decreasing function of ϕ. This type of interaction term is chosen in [**?**] also and according to that work, the presence of $\dot{\phi}$ in the interaction term is related to alleviate the H_0 tension. However, in our work of dynamical system analysis we have chosen this interaction for the simplicity of calculations. Further, combining equations (4.7) and (4.8), the total matter $\rho_{tot} = \rho_{DM} + \rho_{DE}$ satisfies

$$\dot{\rho}_{tot} + 3H(\rho_{tot} + p_{tot}) = 0 \tag{4.10}$$

with

$$\omega_{tot} = \frac{p_{\phi}}{\rho_{\phi} + \rho_{DM}} = \omega_{\phi}\Omega_{\phi}. \tag{4.11}$$

Here $\omega_{\phi} = \frac{p_{\phi}}{\rho_{\phi}}$ is the equation of state parameter for phantom field and $\Omega_{\phi} = \frac{\rho_{\phi}}{\frac{3H^2}{\kappa^2}}$ is the density parameter for DE.

4.3 Formation of Autonomous System : Critical point and stability analysis

In the present work the dimensionless variables can be taken as [642]

$$x : = \frac{\kappa\dot{\phi}}{\sqrt{6}H}, \tag{4.12}$$

$$y : = \frac{\kappa\sqrt{V(\phi)}}{\sqrt{3}H}, \tag{4.13}$$

$$z : = \frac{\sqrt{6}}{\kappa\phi} \tag{4.14}$$

together with $N = \ln a$ and the expression of the cosmological parameters can be written as

$$\Omega_\phi \equiv \frac{\kappa^2 \rho_\phi}{3H^2} = -x^2 + y^2, \tag{4.15}$$

$$\omega_\phi = \frac{-x^2 - y^2}{-x^2 + y^2} \tag{4.16}$$

and

$$\omega_{tot} = -x^2 - y^2. \tag{4.17}$$

For the scalar field potential we consider two well studied cases in the literature, namely the power-law

$$V(\phi) = V_0 \phi^{-\lambda} \tag{4.18}$$

and the exponential dependence as

$$V(\phi) = V_1 e^{-\kappa\lambda\phi}. \tag{4.19}$$

For the dark matter particle mass we also consider power-law

$$M_{_{DM}}(\phi) \quad = \quad M_0 \phi^{-\mu} \tag{4.20}$$

and the exponential dependence as

$$M_{_{DM}}(\phi) \quad = \quad M_1 e^{-\kappa\mu\phi}, \tag{4.21}$$

where $V_0, V_1, M_0, M_1 (> 0)$ and λ, μ are constant parameters. Here we shall study the dynamical analysis of this cosmological system for five possible models. In Model 1 (4.3.1) we consider $V(\phi) = V_0\phi^{-\lambda}, M_{_{DM}}(\phi) = M_0\phi^{-\mu}$, in Model 2 (4.3.2) we consider $V(\phi) = V_0\phi^{-\lambda}, M_{_{DM}}(\phi) = M_1 e^{-\kappa\mu\phi}$, in Model 3 (4.3.3) we consider $V(\phi) = V_1 e^{-\kappa\lambda\phi}, M_{_{DM}}(\phi) = M_0\phi^{-\mu}$, in Model 4 (4.3.4) we consider $V(\phi) = V_1 e^{-\kappa\lambda\phi}, M_{_{DM}}(\phi) = M_1 e^{-\kappa\mu\phi}$ and lastly in Model 5 (4.3.5) we consider $V(\phi) = V_2\phi^{-\lambda} e^{-\kappa\lambda\phi}, M_{_{DM}}(\phi) = M_2\phi^{-\mu} e^{-\kappa\mu\phi}$, where $V_2 = V_0V_1$ and $M_2 = M_0M_1$.

4.3.1 Model 1: Power-law potential and power-law-dependent dark-matter particle mass

In this consideration, the evolution equations in Section 4.2 can be converted to an autonomous system as follows

$$x' \quad = \quad -3x + \frac{3}{2}x(1 - x^2 - y^2) - \frac{\lambda y^2 z}{2} - \frac{\mu}{2}z(1 + x^2 - y^2), \tag{4.22}$$

$$y' \quad = \quad \frac{3}{2}y(1 - x^2 - y^2) - \frac{\lambda xyz}{2}, \tag{4.23}$$

$$z' \quad = \quad -xz^2, \tag{4.24}$$

where 'prime' over a variable denotes differentiation with respect to $N = \ln a$.

To obtain the stability analysis of the critical points corresponding to the autonomous system (4.22 – 4.24), we consider four possible choices of μ and λ as (i) $\mu \neq 0$ and $\lambda \neq 0$, (ii) $\mu \neq 0$ and $\lambda = 0$, (iii) $\mu = 0$ and $\lambda \neq 0$, (iv) $\mu = 0$ and $\lambda = 0$.

Case-(i) $\mu \neq 0$ and $\lambda \neq 0$

In this case, we have three critical points A_1, A_2 and A_3. First we determine the Jacobian matrix at these critical points corresponding to the autonomous system (4.22−4.24). Then we shall find the eigenvalues and corresponding eigenvectors of the Jacobian matrix. After that we shall obtain the nature of the vector field near the origin for every critical points. If the critical point is hyperbolic, we use Hartman-Grobman theorem and while the critical point is non-hyperbolic, we use Center Manifold Theory [636]. The set of all critical points with the value of cosmological parameters are shown in Table 4.1. The eigenvalues corresponding to the Jacobian matrix at each critical points A_1, A_2 and A_3 and their nature are shown in Table 4.2.

Table 4.1: The set of critical points corresponding to the autonomous system (4.22 − 4.24) with the values of cosmological parameters.

Critical Points	*Existence*	x	y	z	Ω_ϕ	ω_ϕ	ω_{tot}	q
A_1	For all λ and μ	0	0	0	0	Undetermined	0	$\frac{1}{2}$
A_2	For all λ and μ	0	1	0	1	-1	-1	-1
A_3	For all λ and μ	0	-1	0	1	-1	-1	-1

1. *Critical Point* A_1

The Jacobian matrix at the critical point A_1 can be put as

$$J(A_1) = \begin{bmatrix} -\frac{3}{2} & 0 & -\frac{\mu}{2} \\ 0 & \frac{3}{2} & 0 \\ 0 & 0 & 0 \end{bmatrix}. \tag{4.25}$$

The eigenvalues of $J(A_1)$ are $-\frac{3}{2}$, $\frac{3}{2}$ and 0 and $[1,0,0]^T$, $[0,1,0]^T$ and $[-\frac{\mu}{3},0,1]^T$ are the corresponding eigenvectors, respectively. Since, the critical point A_1 is nonhyperbolic in nature, so we use Center Manifold Theory to analyze the stability of this critical point. From the entries of the Jacobian matrix we can see that there is a linear term of z corresponding to the eqn.(4.22) of the autonomous system (4.22 − 4.24). But the eigen value 0 of the Jacobian matrix (4.25) is corresponding to (4.24). So we have to introduce another coordinate system $(X,\ Y,\ Z)$ in terms of $(x,\ y,\ z)$. By using the eigenvectors of the Jacobian matrix (4.25), we

Table 4.2: The set of eigenvalues of the Jacobian matrix corresponding to each critical points with their natures.

CPs	λ_1 λ_2 λ_3	*Nature of critical points*
A_1	$-\frac{3}{2}$ $\frac{3}{2}$ 0	Nonhyperbolic, behaves as stable node for $\mu < 0$ and saddle node for $\mu > 0$
A_2	-3 -3 0	Nonhyperbolic, behaves as stable node for $\lambda < 0$ and saddle node for $\lambda > 0$
A_3	-3 -3 0	Nonhyperbolic, behaves as stable node for $\lambda < 0$ and saddle node for $\lambda > 0$

introduce the following coordinate system

$$\begin{bmatrix} X \\ Y \\ Z \end{bmatrix} = \begin{bmatrix} 1 & 0 & \frac{\mu}{3} \\ 0 & 1 & 0 \\ 0 & 0 & 1 \end{bmatrix} \begin{bmatrix} x \\ y \\ z \end{bmatrix} \tag{4.26}$$

and in this new coordinate system the equations $(4.22 - 4.24)$ are transformed into

$$\begin{bmatrix} X' \\ Y' \\ Z' \end{bmatrix} = \begin{bmatrix} -\frac{3}{2} & 0 & 0 \\ 0 & \frac{3}{2} & 0 \\ 0 & 0 & 0 \end{bmatrix} \begin{bmatrix} X \\ Y \\ Z \end{bmatrix} + \begin{bmatrix} non \\ linear \\ terms \end{bmatrix}. \tag{4.27}$$

By Center Manifold Theory there exists a continuously differentiable function $h : \mathbb{R} \to \mathbb{R}^2$ such that

$$h(Z) = \begin{bmatrix} X \\ Y \end{bmatrix} = \begin{bmatrix} a_1 Z^2 + a_2 Z^3 + a_3 Z^4 + \mathcal{O}\left(Z^5\right) \\ b_1 Z^2 + b_2 Z^3 + a_3 Z^4 + \mathcal{O}\left(Z^5\right) \end{bmatrix}. \tag{4.28}$$

Differentiating both side with respect to N, we get

$$X' = (2a_1 Z + 3a_2 Z^2 + 4a_3 Z^3)Z' + \mathcal{O}(Z^4), \tag{4.29}$$
$$Y' = (2b_1 Z + 3b_2 Z^2 + 4b_3 Z^3)Z' + \mathcal{O}(Z^4), \tag{4.30}$$

where $a_i, b_i \in \mathbb{R}$. We only concern about the non-zero coefficients of the lowest power terms in CMT as we analyze the stability in arbitrary small neighbourhood of the origin. Comparing

coefficients corresponding to power of Z we get, $a_1 = 0$, $a_2 = \frac{2\mu^2}{27}$, $a_3 = 0$ and $b_i = 0$ for all $i \in \mathbb{N}$. So the expression of the center manifold is given by

$$X = \frac{2\mu^2}{27}Z^3, \tag{4.31}$$
$$Y = 0, \tag{4.32}$$

and the flow on the Center manifold is determined by

$$Z' = \frac{\mu}{3}Z^3 + \mathcal{O}(Z^5). \tag{4.33}$$

The flow on the center manifold depends on the sign of μ. If $\mu > 0$ then $Z' > 0$ for $Z > 0$

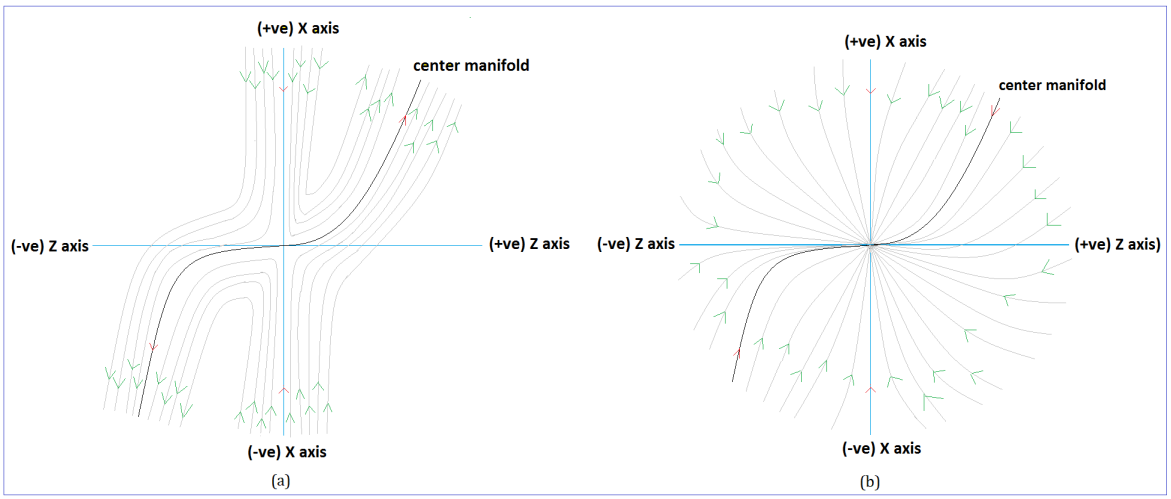

Figure 4.1: These figures show the vector field near the origin corresponding to the critical point A_1 in XZ-plane. The phase plot (a) is for $\mu > 0$ and (b) is for $\mu < 0$.

and $Z' < 0$ for $Z < 0$. Hence, we conclude that for $\mu > 0$ the origin is a saddle node and unstable in nature (FIG.4.1(a)). Again if $\mu < 0$ then $Z' < 0$ for $Z > 0$ and $Z' > 0$ for $Z < 0$. So we conclude that for $\mu < 0$ the origin is a stable node, *i.e.,* asymptotically stable in nature (FIG.4.1(b)).

2. *Critical Point* A_2

The Jacobian matrix at A_2 can be put as

$$J(A_2) = \begin{bmatrix} -3 & 0 & -\frac{\lambda}{2} \\ 0 & -3 & 0 \\ 0 & 0 & 0 \end{bmatrix}. \tag{4.34}$$

The eigenvalues of the above matrix are -3, -3 and 0. $[1,0,0]^T$ and $[0,1,0]^T$ are the eigenvectors corresponding to the eigenvalue -3 and $\left[-\frac{\lambda}{6},0,1\right]^T$ is the eigenvector corresponding to the eigenvalue 0. Since the critical point A_2 is non-hyperbolic in nature, so we use Center

Manifold Theory for analyzing the stability of this critical point. We first transform the coordinates into a new system $x = X,\ y = Y + 1,\ z = Z$, such that the critical point A_2 moves to the origin. By using the eigenvectors of the Jacobian matrix $J(A_2)$, we introduce another set of new coordinates $(u,\ v,\ w)$ in terms of $(X,\ Y,\ Z)$ as

$$\begin{bmatrix} u \\ v \\ w \end{bmatrix} = \begin{bmatrix} 1 & 0 & \frac{\lambda}{6} \\ 0 & 1 & 0 \\ 0 & 0 & 1 \end{bmatrix} \begin{bmatrix} X \\ Y \\ Z \end{bmatrix} \tag{4.35}$$

and in these new coordinates the equations $(4.22 - 4.24)$ are transformed into

$$\begin{bmatrix} u' \\ v' \\ w' \end{bmatrix} = \begin{bmatrix} -3 & 0 & 0 \\ 0 & -3 & 0 \\ 0 & 0 & 0 \end{bmatrix} \begin{bmatrix} u \\ v \\ w \end{bmatrix} + \begin{bmatrix} non \\ linear \\ terms \end{bmatrix}. \tag{4.36}$$

By center manifold theory there exists a continuously differentiable function $h : \mathbb{R} \to \mathbb{R}^2$ such that

$$h(w) = \begin{bmatrix} u \\ v \end{bmatrix} = \begin{bmatrix} a_1 w^2 + a_2 w^3 + \mathcal{O}(w^4) \\ b_1 w^2 + b_2 w^3 + \mathcal{O}(w^4) \end{bmatrix}. \tag{4.37}$$

Differentiating both sides with respect to N, we get

$$u' = (2a_1 w + 3a_2 w^2) w' + \mathcal{O}(w^3), \tag{4.38}$$
$$v' = (2b_1 w + 3b_2 w^2) w' + \mathcal{O}(w^3) \tag{4.39}$$

where $a_i, b_i \in \mathbb{R}$. We only concern about the nonzero coefficients of the lowest power terms in CMT as we analyze the stability in arbitrary small neighbourhood of the origin. Comparing coefficients corresponding to power of w both sides of (4.38) and (4.39), we get $a_1 = 0$, $a_2 = \frac{\lambda^2}{108}$ and $b_1 = \frac{\lambda^2}{72}$, $b_2 = 0$. So the center manifold can be written as

$$u = \frac{\lambda^2}{108} w^3 + \mathcal{O}(w^5), \tag{4.40}$$
$$v = \frac{\lambda^2}{72} w^2 + \mathcal{O}(w^4) \tag{4.41}$$

and the flow on the center manifold is determined by

$$w' = \frac{\lambda}{6} w^3 + \mathcal{O}(w^4). \tag{4.42}$$

Here we see that the center manifold and the flow on the center manifold is completely same as the center manifold and the flow which was determined in [609] and the stability of the vector field near the origin depends on the sign of λ. If $\lambda < 0$ then $w' < 0$ for $w > 0$ and $w' > 0$ for $w < 0$. So for $\lambda < 0$ the origin is a stable node, *i.e.,* asymptotically stable in nature. Further if $\lambda > 0$ then $w' > 0$ for $w > 0$ and $w' < 0$ for $w < 0$. So for $\lambda > 0$ the origin is a saddle node, *i.e.,* unstable in nature. The vector field near the origin for both of the cases is shown separately in (wu)-plane (FIG.4.2) and (wv)-plane (FIG.4.3). As the new coordinate system $(u,\ v,\ w)$ is topologically equivalent to the old one, hence the origin in the new coordinate system, *i.e.,* the critical point A_2 in the old coordinate system $(x,\ y,\ z)$ is a stable node for $\lambda < 0$ and a saddle node for $\lambda > 0$.

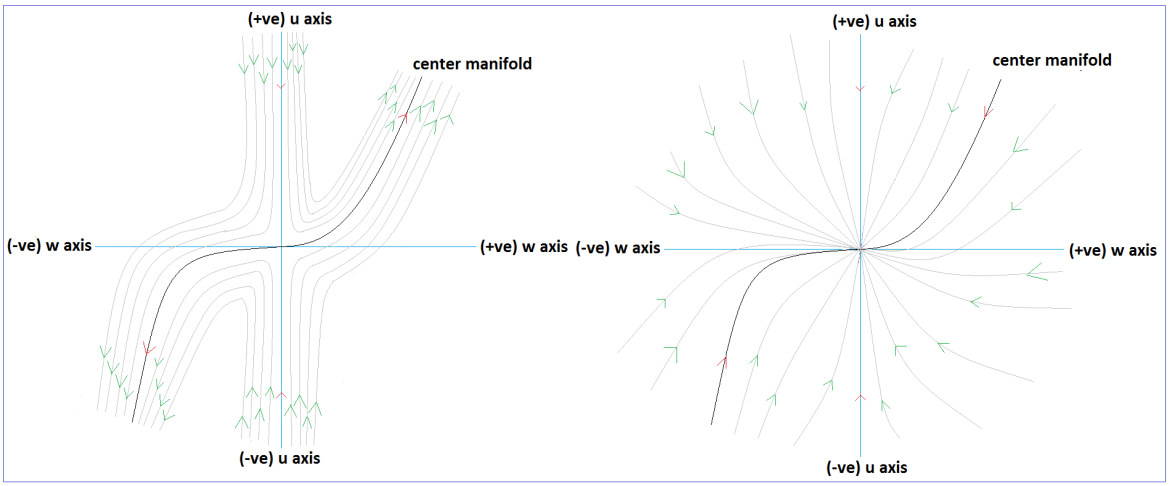

Figure 4.2: These figures show the vector field near the origin corresponding to A_2 in (uw)-plane. The phase plot (a) is for $\lambda > 0$ and (b) is for $\lambda < 0$.

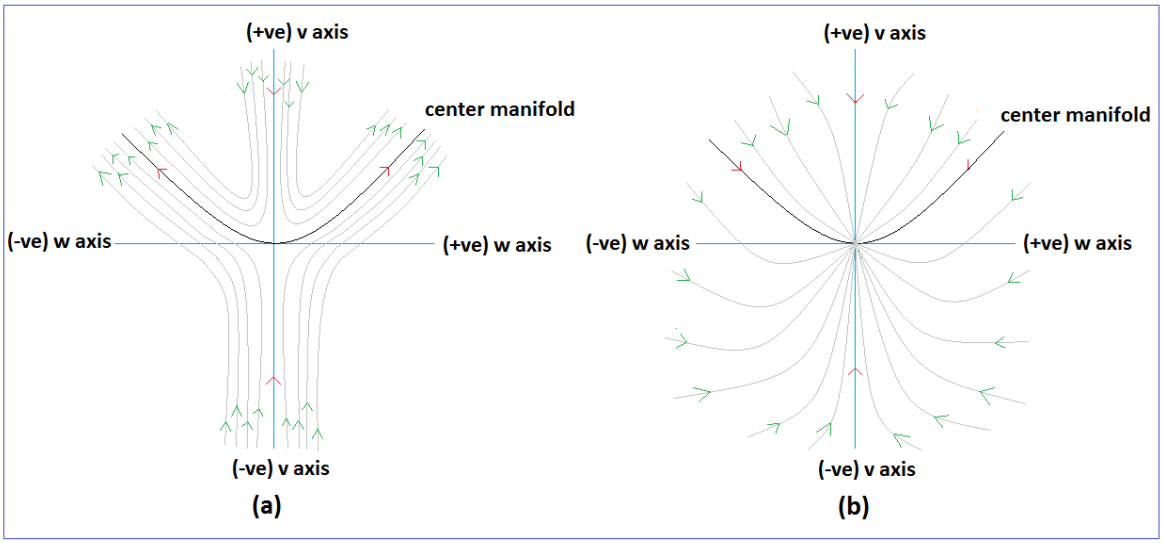

Figure 4.3: These figures show the vector field near the origin corresponding to A_2 in (vw)-plane. The phase plot (a) is for $\lambda > 0$ and (b) is for $\lambda < 0$.

3. *Critical Point* A_3

The Jacobian matrix at the critical point A_3 is same as (4.34). So the eigenvalues and corresponding eigenvectors are also same as above. Now we transform the coordinates into a new system $x = X,\ y = Y - 1,\ z = Z$, such that the critical point A_2 transforms to the origin. Then by using the matrix transformation (4.35) and after putting similar arguments as above, the expressions of the center manifold can be written as

$$u = -\frac{\lambda^2}{108}w^3 + \mathcal{O}(w^5), \tag{4.43}$$

$$v = -\frac{\lambda^2}{72}w^2 + \mathcal{O}(w^4) \tag{4.44}$$

and the flow on the center manifold is determined by

$$w' = \frac{\lambda}{6}w^3 + \mathcal{O}(w^4). \tag{4.45}$$

Here also the stability of the vector field near the origin depends on the sign of λ. Further as the expression of the flow on the center manifold is same as (4.42), so we can conclude as above that for $\lambda < 0$ the origin is a stable node, *i.e.,* asymptotically stable in nature and for $\lambda > 0$ the origin is unstable due to its saddle nature. The vector fields near the origin in uw-plane and vw-plane are shown as in FIG.4.4 and FIG.4.5 respectively. Hence, the critical point A_3 is a stable node for $\lambda < 0$ and a saddle node for $\lambda > 0$.

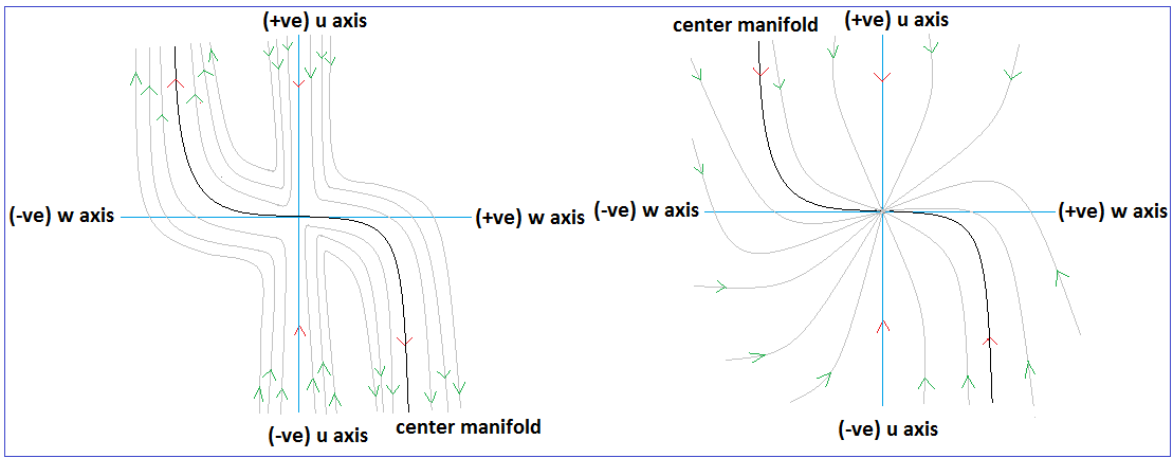

Figure 4.4: These figures show the vector field near the origin for the critical point A_3 in (uw)-plane. L.H.S. phase plot is for $\lambda > 0$ and R.H.S. phase plot is for $\lambda < 0$.

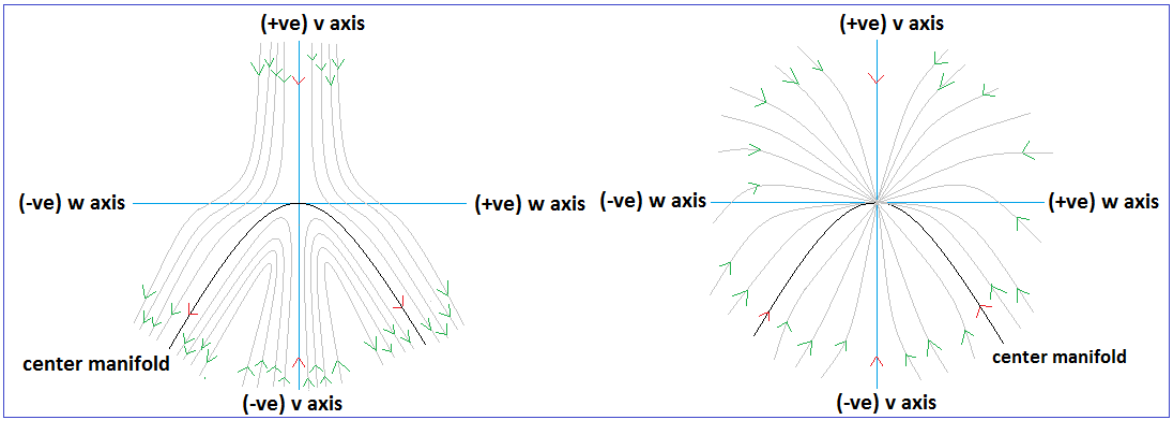

Figure 4.5: These figures show the vector field near the origin corresponding to the critical point A_3 in (vw)-plane. L.H.S. phase plot is for $\lambda > 0$ and R.H.S. phase diagram is for $\lambda < 0$.

Case-(ii) $\mu \neq 0$ and $\lambda = 0$

In this case the autonomous system $(4.22 - 4.24)$ changes into

$$x' = -3x + \frac{3}{2}x(1 - x^2 - y^2) - \frac{\mu}{2}z(1 + x^2 - y^2), \tag{4.46}$$

$$y' = \frac{3}{2}y(1 - x^2 - y^2), \tag{4.47}$$

$$z' = -xz^2. \tag{4.48}$$

We have also three critical points corresponding to the above autonomous system, in which two are space of critical points. The critical points corresponding to this autonomous system are $C_1(0, 0, 0)$, $C_2(0, 1, z_c)$ and $C_3(0, -1, z_c)$ where z_c is any real number. Note that the critical point C_3 is not physically meaningful. Corresponding to the critical points C_1, C_2 and C_3 the eigenvalues of the Jacobian matrix are same as the critical points A_1, A_2 and A_3 respectively and also the value of cosmological parameters at C_1 and C_2 are same as of A_1 and A_2 respectively.

1. *Critical Point* C_1

The Jacobian matrix $J(C_1)$ for the autonomous system $(4.46 - 4.48)$ at this critical point is same as (4.25). So, all the eigenvalues and the corresponding eigenvectors are the same as for $J(C_1)$. If we put forward argument like the stability analysis of the critical point A_1 then the center manifold can be expressed as $(4.31 - 4.32)$ and the flow on the center manifold is determined by (4.33). So the stability of the vector field near the origin is same as for the critical point A_1.

2. *Critical Point* C_2

The Jacobian matrix at the critical point C_2 can be put as

$$J(C_2) = \begin{bmatrix} -3 & \mu z_c & 0 \\ 0 & -3 & 0 \\ -z_c^2 & 0 & 0 \end{bmatrix}. \tag{4.49}$$

The eigenvalues of the above matrix are $-3,\ -3,\ 0$. $\left[1, 0, \frac{z_c^2}{3}\right]^T$ and $[0, 1, 0]^T$ are the eigenvectors corresponding to the eigenvalue -3 and $[0, 0, 1]^T$ is the eigenvector corresponding to the eigenvalue 0. To apply CMT for a fixed z_c, first we transform the coordinates into a new system $x = X,\ y = Y + 1,\ z = Z + z_c$, such that the critical point is at the origin and after that if we put forward argument as above to determine center manifold, then the center manifold can be written as

$$X = 0, \tag{4.50}$$
$$Y = 0 \tag{4.51}$$

and the flow on the center manifold is determined by

$$Z' = 0. \tag{4.52}$$

So, the center manifold is lying on the Z-axis and the flow on the center manifold can not be determined by (4.52). Now, if we project the vector field on the plane which is parallel to XY-plane, *i.e.,* the plane $Z = constant$ (say), the vector field is shown as in FIG.4.6. So every point on Z-axis is a stable star.

2. *Critical Point* C_3

If we put forward argument as above to obtain the center manifold and the flow on the center manifold, we will get the center manifold same as $(4.50 - 4.51)$ and the flow on the center manifold is determined by (4.52). In this case also we will get the same vector field as FIG.4.6.

From the above discussion, firstly we have seen that the space of critical points C_2 and C_3 are non-hyperbolic in nature but by using CMT we could not determine the vector field near those critical points and also the flow on the vector field. So, in this case the last eqn.(4.48) of the autonomous system $(4.46 - 4.48)$ did not provide any special behaviour. For this reason and as the expressions of Ω_ϕ, ω_ϕ and ω_{total} depends only on x and y coordinates, we want to take only the first two equations of the autonomous system $(4.46 - 4.48)$ and try to analyze the stability of the critical points which are lying on the plane, parallel to $xy-$plane, *i.e.,* the plane $z = constant = c$ (say). In $z = c$ plane the first two equations in $(4.46 - 4.48)$ can be written as

$$x' = -3x + \frac{3}{2}x(1 - x^2 - y^2) - \frac{\mu}{2}c(1 + x^2 - y^2), \tag{4.53}$$
$$y' = \frac{3}{2}y(1 - x^2 - y^2). \tag{4.54}$$

In this case we have five critical points E_1, E_2, E_3, E_4 and E_5 corresponding to the autonomous system $(4.53 - 4.54)$. The set of critical points, their existence and the value of cosmological parameters are shown in Table 4.3. The eigenvalues of the Jacobian matrix at each critical points and their nature are shown in Table 4.4. Note that for critical point E_3, $\Omega_\phi = -\frac{\mu^2 c^2}{3}$ and for critical point E_4, $\Omega_\phi = 1 - \frac{18}{\mu^2 c^2}$. As $0 \leq \Omega_\phi \leq 1$ [642] and so we can say that E_3 is physically relevant only for $c = 0$ and E_4 is physically relevant while $0 \leq 1 - \frac{18}{\mu^2 c^2} \leq 1 \implies \mu c \geq 3\sqrt{2}$ or $\mu c \leq -3\sqrt{2}$.

To avoid similar arguments which we have mentioned for analyzing the stability of the above critical points, we only state the stability and the reason behind the stability of these critical points in a tabular form, which is shown as in Table 4.5. Note that $|\mu c| \geq 3$ is

Table 4.3: Table shows the set of critical points, existence of critical points and the value of cosmological parameters corresponding to the autonomous system (4.53 − 4.54).

CPs	$Existence$	x	y	Ω_ϕ	ω_ϕ	ω_{tot}	q
E_1	$For\ all\ \mu\ and\ c$	0	1	1	-1	-1	-1
$E_2{}^a$	$For\ all\ \mu\ and\ c$	0	-1	1	-1	-1	-1
E_3	$For\ all\ \ \mu\ and\ c$	$-\frac{\mu c}{3}$	0	$-\frac{\mu^2c^2}{9}$	-1	$-\frac{\mu^2c^2}{9}$	$\frac{1}{2}\left(1-\frac{\mu^2c^2}{3}\right)$
E_4	$For\ c\neq 0\ and$ $for\ all\ \mu\in\left(-\infty,-\frac{3}{c}\right]\cup\left[\frac{3}{c},\infty\right)$	$-\frac{3}{\mu c}$	$\sqrt{1-\frac{9}{\mu^2c^2}}$	$\left(1-\frac{18}{\mu^2c^2}\right)$	$\frac{\mu^2c^2}{18-\mu^2c^2}$	-1	-1
$E_5{}^a$	$For\ c\neq 0\ and$ $for\ all\ \mu\in\left(-\infty,-\frac{3}{c}\right]\cup\left[\frac{3}{c},\infty\right)$	$-\frac{3}{\mu c}$	$-\sqrt{1-\frac{9}{\mu^2c^2}}$	$\left(1-\frac{18}{\mu^2c^2}\right)$	$\frac{\mu^2c^2}{18-\mu^2c^2}$	-1	-1

The critical points E_2 and E_5 are not physically relevant [672, 642].

Table 4.4: Table shows the eigenvalues (λ_1, λ_2) of the Jacobian matrix corresponding to the critical points and the nature of all critical points $(E_1 - E_5)$.

Critical Points	λ_1	λ_2	Nature of Critical points
E_1	-3	-3	Hyperbolic
E_2	-3	-3	Hyperbolic
E_3	$-\frac{3}{2}\left(1+\frac{\mu^2c^2}{9}\right)$	$\frac{3}{2}\left(1-\frac{\mu^2c^2}{9}\right)$	Non-hyperbolic for $\mu c = \pm 3$ and hyperbolic for $\mu c \neq \pm 3$
E_4	$\frac{-3+\sqrt{45-\frac{324}{\mu^2c^2}}}{2}$	$\frac{-3-\sqrt{45-\frac{324}{\mu^2c^2}}}{2}$	Non-hyperbolic for $\mu c = \pm 3$ and hyperbolic for $\mu c \neq \pm 3$
E_5	$\frac{-3+\sqrt{45-\frac{324}{\mu^2c^2}}}{2}$	$\frac{-3-\sqrt{45-\frac{324}{\mu^2c^2}}}{2}$	Non-hyperbolic for $\mu c = \pm 3$ and hyperbolic for $\mu c \neq \pm 3$

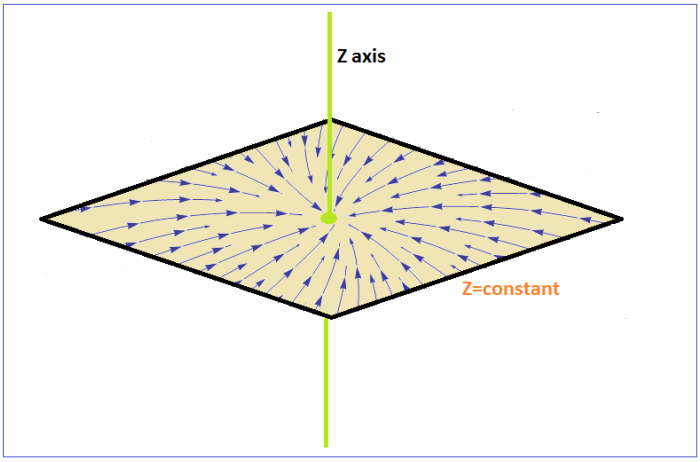

Figure 4.6: This figure shows the vector field near about every point on $Z-$axis corresponding to the critical points C_2 and C_3.

the domain of existence of the critical point E_4 and E_5 and due to this reason we did not determine the stability analysis of the critical points E_4 and E_5 while $\mu c \in (-3, 3)$. In FIG.4.8 by using Mathematica software, we have shown the vector field corresponding to the autonomous system [4.53 – 4.54] for $\mu c = -3$. From this phase plot, we can conclude that the stability of the critical points E_1, E_2 and E_3 is same as the statements about the stability which we have written in Table 4.5.

Case-(iii) $\mu = 0$ and $\lambda \neq 0$

In this case the autonomous system (4.22 – 4.24) changes into

$$x' = -3x + \frac{3}{2}x(1 - x^2 - y^2) - \frac{\lambda y^2 z}{2}, \tag{4.55}$$

$$y' = \frac{3}{2}y(1 - x^2 - y^2) - \frac{\lambda xyz}{2}, \tag{4.56}$$

$$z' = -xz^2. \tag{4.57}$$

Corresponding to the above autonomous system we have three space of critical points $P_1(0, 0, z_c)$, $P_2(0, 1, 0)$ and $P_3(0, -1, 0)$ where z_c is any real number. The value of cosmological parameters, eigenvalues of the Jacobian matrix at those critical points corresponding to the autonomous system (4.55 – 4.57) and the nature of critical points P_1, P_2 and P_3 are same as for the critical points A_1, A_2 and A_3 respectively, shown as in Table 4.1.

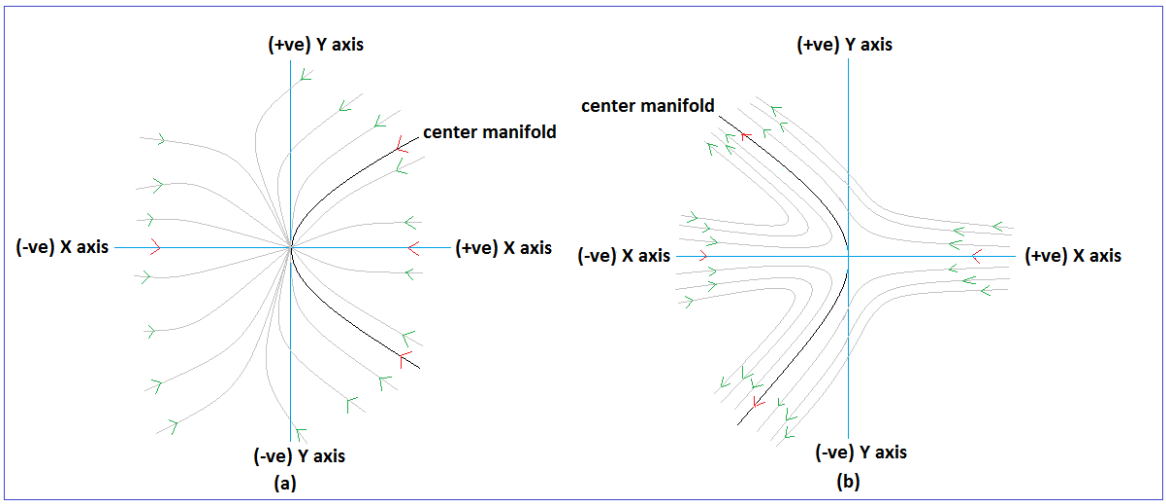

Figure 4.7: These figures show the vector field near the origin corresponding to the critical point E_3. The phase diagram (a) is for $\mu c = 3$ and (b) is for $\mu c = -3$.

1. *Critical Point* P_1

The Jacobian matrix at the critical point P_1 can be put as

$$J(P_1) = \begin{bmatrix} -\frac{3}{2} & 0 & 0 \\ 0 & \frac{3}{2} & 0 \\ -z_c^2 & 0 & 0 \end{bmatrix}. \tag{4.58}$$

The eigenvalues of the above matrix are $-\frac{3}{2}$, $\frac{3}{2}$ and 0, and $\left[1, 0, \frac{2}{3}z_c^2\right]^T$, $[0,1,0]^T$ and $[0,0,1]^T$ are the corresponding eigenvectors, respectively. For a fixed z_c, first we shift the critical point P_0 to the origin by the coordinate transformation $x = X$, $y = Y$ and $z = Z + z_c$, and then if we put forward argument as above for nonhyperbolic critical points, the center manifold can be written as $(4.50 - 4.51)$ and the flow on the center manifold is determined by (4.52). Similarly as above (the discussion of stability for the critical point C_2) we can conclude that the center manifold for the critical point P_1 is also lying on the $Z-$axis but the flow on the center manifold can not be determined. Now, if we project the vector field on the plane which is parallel to XY-plane, *i.e.,* the plane $Z = constant$ (say), then we get the vector field FIG.4.9. So every point on Z-axis is a saddle node. Further if we want to obtain the stability of the critical points in the plane which is parallel to xy-plane, *i.e.,* $z = constant = c$ (say), then we only take the first two equations (4.55) and (4.56) of the autonomous system $(4.55 - 4.57)$ and replace z by c. Then we can see that there exists three hyperbolic critical points $B_1(0,0)$, $B_2\left(-\frac{\lambda c}{6}, \sqrt{1+\frac{\lambda^2 c^2}{36}}\right)$ and $B_3\left(-\frac{\lambda c}{6}, -\sqrt{1+\frac{\lambda^2 c^2}{36}}\right)$. In which B_3 is not physically relevant. So by obtaining the eigenvalues of the Jacobian matrix corresponding to the autonomous system at those critical points and using the Hartman-Grobman theorem we only state the stability of all critical points and also write the value of cosmological parameters corresponding to these critical points in tabular form, which is shown as in Table 4.6.

Table 4.5: Table shows the stability and the reason behind the stability of the critical points ($E_1 - E_5$).

CPs	*Stability*	*Reason behind the stability*
E_1, E_2	Both are stable star	As both eigenvalues λ_1 and λ_2 are negative and equal. By Hartman-Grobman theorem we can conclude that the critical points E_1 and E_2 both are stable star.
E_3	Saddle node for $\mu c = \pm 3$, stable node for $\mu c > 3$ *or*, < -3, saddle node for $-3 < \mu c < 3$	For $\mu c = -3$: After shifting the this critical point into the origin by taking the transformation $x = X - \frac{\mu c}{3}$, $y = Y$ and by using CMT, the CM is given by $X = -Y^2 + \mathcal{O}(Y^4)$ and the flow on the CM is determined by $Y' = \frac{3}{2}Y^3 + \mathcal{O}(Y^5)$. $Y' < 0$ while $Y < 0$ and for $Y > 0$, $Y' > 0$. So, the critical point E_3 is a saddle node and unstable in nature. For $\mu c = 3$: The center manifold is given by $X = Y^2 + \mathcal{O}(Y^4)$ and the flow on the center manifold is determined by $Y' = \frac{3}{2}Y^3 + \mathcal{O}(Y^5)$. $Y' < 0$ while $Y < 0$ and for $Y > 0$, $Y' > 0$. So, the critical point E_3 is a saddle node for this case also. For $\mu c > 3$ *or*, $\mu c < -3$: Both of the eigenvalues λ_1 and λ_2 are negative and unequal. So by Hartman-Grobman theorem the critical point E_3 is a stable node. For $-3 < \mu c < 3$: λ_1 is negative and λ_2 is positive. So by Hartman-Grobman theorem the critical point E_3 is a saddle node.
E_4, E_5	Both are saddle node for $\mu c \in (-\infty, -3] \cup [3, \infty)$	For $\mu c = 3$ and $\mu c = -3$: The expression of the center manifold and the flow on the center manifold is same as the expressions for $\mu c = 3$ and $\mu c = -3$ cases respectively of E_3. For $\mu c > 3$, *or* < -3 : λ_1 is positive and λ_2 is negative. Hence, by Hartman-Grobman theorem we can conclude that the critical points E_4 and E_5 both are saddle node and unstable in nature.

For the critical points P_2 and P_3, we have the same Jacobian matrix (4.34) and if we will take the similar transformations (shifting and matrix) and using the similar arguments as A_2 and A_3 respectively, we conclude that the stability of P_2 and P_3 is same as A_2 and A_3, respectively.

Case-(iv) $\mu = 0$ and $\lambda = 0$

In this case the autonomous system (4.22 – 4.24) changes into

$$x' = -3x + \frac{3}{2}x(1 - x^2 - y^2), \tag{4.59}$$

$$y' = \frac{3}{2}y(1 - x^2 - y^2), \tag{4.60}$$

$$z' = -xz^2. \tag{4.61}$$

Table 4.6: Table shows the eigenvalues (λ_1, λ_2) of the Jacobian matrix, stability and value of cosmological parameters corresponding to every critical points $(B_1 - B_3)$.

CPs	λ_1	λ_2	*Stability*	Ω_ϕ	ω_ϕ	ω_{tot}	q
B_1	$-\frac{3}{2}$	$\frac{3}{2}$	Saddle node	0	Undetermined	0	$\frac{1}{2}$
B_2, B_3	$-3\left(1+\frac{\lambda^2c^2}{18}\right)$	$-3\left(1+\frac{\lambda^2c^2}{36}\right)$	Stable star for $\lambda c = 0$ and stable node for $\lambda c \neq 0$	1	$-\left(1+\frac{\lambda^2c^2}{18}\right)$	$-\left(1+\frac{\lambda^2c^2}{18}\right)$	$-\left(1+\frac{\lambda^2c^2}{12}\right)$

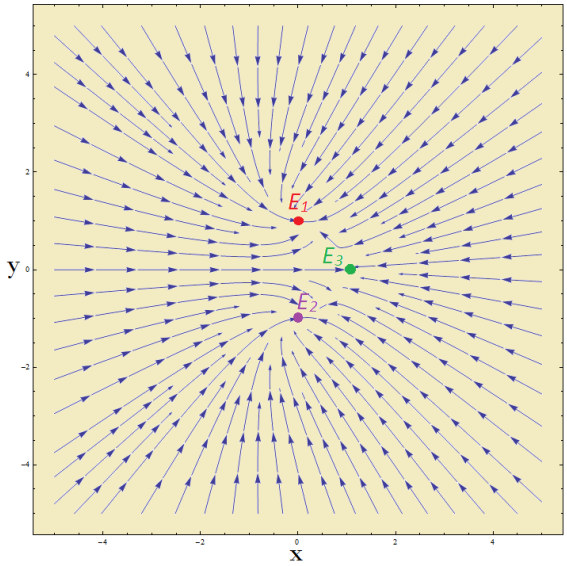

Figure 4.8: This figure shows the vector field corresponding to the autonomous system (4.53 − 4.54) for $\mu c = -3$.

Corresponding to the above autonomous system we have three space of critical points $S_1(0, 0, z_c)$, $S_2(0, 1, z_c)$ and $S_3(0, -1, z_c)$ where z_c is any real number. The critical points S_1, S_2 and S_3 are similar as C_1, C_2 and C_3 respectively. In this case also all critical points are non-hyperbolic in nature. By taking the possible shifting transformations (for S_1 $(x = X, y = Y, z = Z + z_c)$, for S_2 $(x = X, y = Y + 1, z = Z + z_c)$ and for S_3 $(x = X, y = Y - 1, z = Z + z_c)$) as above we can conclude that for all critical points the center manifold is given by (4.50 − 4.51) and the flow on the center manifold is determined by (4.52), *i.e.,* for all critical points, the center manifold is lying on the Z-axis. Further, if we take the projection of the vector field on $Z = constant$ plane, we can see that for the critical point S_1 every points on Z-axis behave as a saddle node (same as FIG.4.9) and for S_2 and S_3 every points on Z-axis are stable star (same as FIG.4.6) and asymptotically stable in nature.

4.3.2 Model 2: Power-law potential and exponentially-dependent dark-matter particle mass

In this consideration, evolution equations in Section 4.2 can be converted to the autonomous system as follows

$$x' = -3x + \frac{3}{2}x(1 - x^2 - y^2) - \frac{\lambda y^2 z}{2} - \sqrt{\frac{3}{2}}\mu(1 + x^2 - y^2), \tag{4.62}$$

$$y' = \frac{3}{2}y(1 - x^2 - y^2) - \frac{\lambda xyz}{2}, \tag{4.63}$$

$$z' = -xz^2. \tag{4.64}$$

We have five critical points L_1, L_2, L_3, L_4 and L_5 corresponding to the above autonomous system. The set of critical points, their existence, and the value of cosmological parameters at those critical points are shown as in Table 4.7 and the eigenvalues of the Jacobian matrix

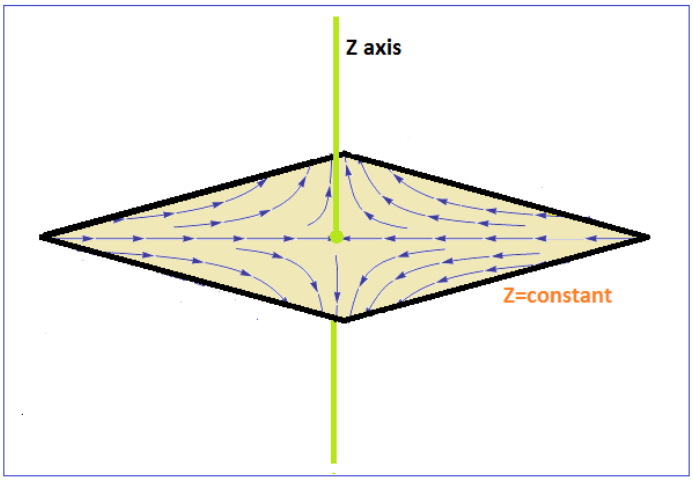

Figure 4.9: This phase diagram shows the vector field near about every point on $Z-$axis corresponding to the critical point P_1.

corresponding to the autonomous system $(4.62-4.64)$ at those critical points and the nature of the critical points are shown in Table 4.8.

Here we are only concerned about the stability of the critical points for $\mu \neq 0$ and $\lambda \neq 0$ because for another possible cases we will get the similar types of results that we have obtained for Model 1.

1. *Critical Point* L_1

The Jacobian matrix corresponding to the autonomous system $(4.62-4.64)$ at the critical point L_1 can be put as

$$J(L_1) = \begin{bmatrix} -3 & \sqrt{6}\mu & -\frac{\lambda}{2} \\ 0 & -3 & 0 \\ 0 & 0 & 0 \end{bmatrix}. \tag{4.65}$$

The eigenvalues of $J(L_1)$ are -3, -3, 0 and $[1,0,0]^T$, $\left[-\frac{\lambda}{6},0,1\right]^T$ are the eigenvectors corresponding to the eigenvalues -3 and 0, respectively. Since the algebraic multiplicity corresponding to the eigenvalue -3 is 2 but the dimension of the eigenspace corresponding to that eigenvalue is 1, *i.e.,* algebraic multiplicity and geometric multiplicity corresponding to the eigenvalue -3 are not equal. So, the Jacobian matrix $J(L_1)$ is not diagonalizable. To determine the center manifold for this critical point, a problem arises due to the presence of the nonzero element in the top position of the third column of the Jacobian matrix. First, we take the coordinate transformation $x = X, y = Y + 1, z = Z$ which shift the critical point L_1 to the origin. Now let's introduce another coordinate system that will remove the term in the top position of the third column. Since, there are only two linearly independent eigenvectors, so we have to obtain another linearly independent column vector that will help to construct the new coordinate system. Since, $[0,1,0]^T$ is the column vector, linearly independent to the eigenvectors of $J(L_1)$, thus a new coordinate system (u,v,w) can be written in terms of (X,Y,Z) as (4.35) and in this new coordinate system the equations $(4.62-4.64)$

Table 4.7: Table shows the set of critical points corresponding to the autonomous system (4.62 – 4.64) their existence and value of cosmological parameters.

Critical Points	*Existence*	x	y	z	Ω_ϕ	ω_ϕ	ω_{tot}	q
L_1	For all μ and λ	0	1	0	1	-1	-1	-1
L_2	For all μ and λ	0	-1	0	1	-1	-1	-1
L_3	For all $\mu \in \left(-\infty, -\sqrt{\frac{3}{2}}\right] \cup \left[\sqrt{\frac{3}{2}}, \infty\right)$ and all λ	$-\frac{1}{\mu}\sqrt{\frac{3}{2}}$	$\sqrt{1-\frac{3}{2\mu^2}}$	0	$1-\frac{3}{\mu^2}$	$\frac{\mu^2}{3-\mu^2}$	-1	-1
L_4[a]	For all $\mu \in \left(-\infty, -\sqrt{\frac{3}{2}}\right] \cup \left[\sqrt{\frac{3}{2}}, \infty\right)$ and all λ	$-\frac{1}{\mu}\sqrt{\frac{3}{2}}$	$-\sqrt{1-\frac{3}{2\mu^2}}$	0	$1-\frac{3}{\mu^2}$	$\frac{\mu^2}{3-\mu^2}$	-1	-1
L_5[a]	For all μ and λ	$-\sqrt{\frac{2}{3}}\mu$	0	0	$-\frac{2}{3}\mu^2$	1	$-\frac{2}{3}\mu^2$	$\frac{1}{2}\left(1-2\mu^2\right)$

[a]Note that the critical points L_4 and L_5 are not physically relevant because near the critical point L_4 the universe contracts and for L_5, $\Omega_\phi < 0$ for all $\mu \neq 0$ [672, 642].

Table 4.8: The eigenvalues $(\lambda_1, \lambda_2, \lambda_3)$ of the Jacobian matrix corresponding to the autonomous system (4.62 − 4.64) at each of the critical points $(L_1 - L_5)$ and the nature of the critical points.

CPs	λ_1	λ_2	λ_3	*Nature of critical Points*
L_1	-3	-3	0	Nonhyperbolic, behaves as stable node for $\lambda < 0$ and saddle node for $\lambda > 0$.
L_2	-3	-3	0	Nonhyperbolic, behaves as stable node for $\lambda < 0$ and saddle node for $\lambda > 0$.
L_3	$-\frac{3}{2}\left(1+\frac{1}{\mu}\sqrt{-6+5\mu^2}\right)$	$-\frac{3}{2}\left(1-\frac{1}{\mu}\sqrt{-6+5\mu^2}\right)$	0	Nonhyperbolic, behaves as saddle node for all possible values of μ.
L_4	$-\frac{3}{2}\left(1+\frac{1}{\mu}\sqrt{-6+5\mu^2}\right)$	$-\frac{3}{2}\left(1-\frac{1}{\mu}\sqrt{-6+5\mu^2}\right)$	0	Nonhyperbolic, behaves as saddle node for all possible values of μ.
L_5	$-\frac{3}{2}$	$\frac{3}{2}$	0	Nonhyperbolic, unstable in nature for all possible values of μ.

are transformed into

$$\begin{bmatrix} u' \\ v' \\ w' \end{bmatrix} = \begin{bmatrix} -3 & \sqrt{6}\mu & 0 \\ 0 & -3 & 0 \\ 0 & 0 & 0 \end{bmatrix} \begin{bmatrix} u \\ v \\ w \end{bmatrix} + \begin{bmatrix} non \\ linear \\ terms \end{bmatrix}. \tag{4.66}$$

By similar arguments which we have derived in the stability analysis of the critical point A_2, the center manifold can be written as (4.40-4.41) and the flow on the center manifold is determined by (4.42). As the expression of center manifold and the flow are same as for the critical point A_2, so the stability of the critical point L_1 is same as the stability of A_2.

2. *Critical Point* L_2

After shifting this critical point to the origin (by taking the shifting transformations ($x = X, y = Y - 1, z = Z$) and the matrix transformation (4.35) and by putting similar arguments which we have mentioned for the analysis of L_1, the center manifold can be expressed as ($4.43 - 4.44$) and the flow on the center manifold is determined by (4.45). So the stability of the critical point L_2 is same as the stability of A_3.

3. *Critical Point* L_3

The Jacobian matrix corresponding to the autonomous system ($4.62 - 4.64$) at the critical point L_3 can be put as

$$J(L_3) = \begin{bmatrix} -\frac{9}{2\mu^2} & \sqrt{1-\frac{3}{2\mu^2}}\left(\frac{3}{\mu}\sqrt{\frac{3}{2}}+\sqrt{6}\mu\right) & -\frac{\lambda}{2}\left(1-\frac{3}{2\mu^2}\right) \\ \frac{3}{\mu}\sqrt{\frac{3}{2}}\sqrt{1-\frac{3}{2\mu^2}} & -3\left(1-\frac{3}{2\mu^2}\right) & \frac{\lambda}{2\mu}\sqrt{\frac{3}{2}}\sqrt{1-\frac{3}{2\mu^2}} \\ 0 & 0 & 0 \end{bmatrix}. \tag{4.67}$$

The eigenvalues corresponding to the Jacobian matrix $J(L_3)$ are shown in Table.4.8. From the existence of the critical point L_3 we can conclude that the eigenvalues of $J(L_3)$ always real. Since the critical point L_3 exists for $\mu \leq -\sqrt{\frac{3}{2}}$ or $\mu \geq \sqrt{\frac{3}{2}}$, our aim is to define the stability in all possible regions of μ. Due to this reason we will define the stability at four possible choices of μ for simplicity. We first determine the stability of this critical point at $\mu = \pm\sqrt{\frac{3}{2}}$. Then for $\mu < -\sqrt{\frac{3}{2}}$, we shall determine the stability of L_3 at $\mu = -\sqrt{3}$ and for $\mu > \sqrt{\frac{3}{2}}$, we shall determine the stability of L_3 at $\mu = \sqrt{3}$.

For $\mu = \pm\sqrt{\frac{3}{2}}$, the Jacobian matrix $J(L_3)$ converts into

$$\begin{bmatrix} -3 & 0 & 0 \\ 0 & 0 & 0 \\ 0 & 0 & 0 \end{bmatrix}$$

and as the critical point L_3 converts into $(\mp 1, 0, 0)$, first we take the transformation $x = X \mp 1, y = Y, z = Z$ so that L_3 moves into the origin. As the critical point is nonhyperbolic in nature, we use CMT to determine the stability of this critical point. From center manifold theory, there exist a continuously differentiable function $h : \mathbb{R}^2 \to \mathbb{R}$ such that $X = h(Y, Z) = aY^2 + bYZ + cZ^2 +$ higher order terms, where $a,\ b,\ c \in \mathbb{R}$. By taking differentiation both sides with respect to N yields

$$\frac{dX}{dN} = \begin{bmatrix} 2aY + bZ & bY + 2cZ \end{bmatrix} \begin{bmatrix} \frac{dY}{dN} \\ \\ \frac{dZ}{dN} \end{bmatrix}. \tag{4.68}$$

Comparing L.H.S. and R.H.S. of (4.68) we get, $a = 1$, $b = 0$ and $c = 0$, *i.e.,* the center manifold can be written as

$$X = \pm Y^2 + \text{higher order terms} \tag{4.69}$$

and the flow on the center manifold is determined by

$$\frac{dY}{dN} = \pm\frac{\lambda}{2}YZ + \text{higher order terms}, \tag{4.70}$$

$$\frac{dZ}{dN} = \pm Z^2 + \text{higher order terms}. \tag{4.71}$$

We only concerned about the non-zero coefficients of the lowest power terms in CMT as we analyze an arbitrarily small neighborhood of the origin and here the lowest power term of the expression of center manifold depends only on Y. So, we draw the vector field near the origin only on XY-plane, *i.e.,* the nature of the vector field implicitly depends on Z not explicitly. Now we try to write the flow equations $(4.70 - 4.71)$ in terms of Y only. For this reason, we divide the corresponding sides of (4.70) by the corresponding sides of (4.71) and then we will get

$$\frac{dY}{dZ} = \frac{\lambda}{2}\frac{Y}{Z},$$

$$Z = \left(\frac{Y}{C}\right)^{2/\lambda}, \quad \text{where } C \text{ is a positive arbitrary constant.}$$

After substituting this any of (4.70) or (4.71), we get

$$\frac{dY}{dN} = \frac{\lambda}{2C^{2/\lambda}}Y^{1+2/\lambda}. \tag{4.72}$$

As the power of Y can not be negative or fraction, so we have only two choices of λ, $\lambda = 1$ or $\lambda = 2$. For $\lambda = 1$ or, $\lambda = 2$ both of the cases the origin is a saddle node, *i.e.,* unstable in nature (FIG.4.10 is for $\mu = \sqrt{3/2}$ and FIG.4.11 is for $\mu = -\sqrt{3/2}$). Hence, for $\mu = \pm\sqrt{\frac{3}{2}}$, in the old coordinate system the critical point L_3 is unstable due to its saddle nature.

For $\mu = \sqrt{3}$, the Jacobian matrix $J(L_3)$ converts into

$$\begin{bmatrix} -\frac{3}{2} & \frac{9}{2} & -\frac{\lambda}{4} \\ \\ \frac{3}{2} & -\frac{3}{2} & \frac{\lambda}{4} \\ \\ 0 & 0 & 0 \end{bmatrix}.$$

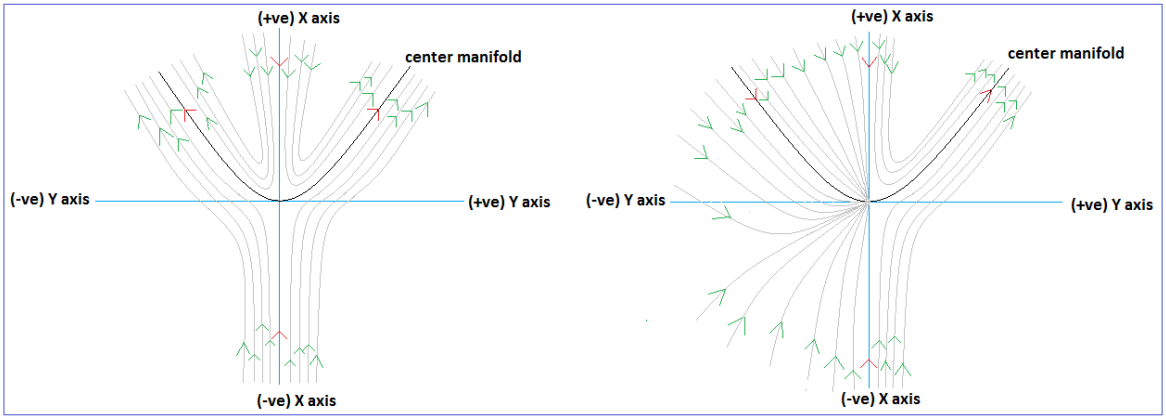

Figure 4.10: These figures show the vector field near the origin for $\mu = \sqrt{\frac{3}{2}}$ corresponding to the critical point L_3. L.H.S. phase plot is for $\lambda = 1$ and R.H.S. phase plot is for $\lambda = 2$.

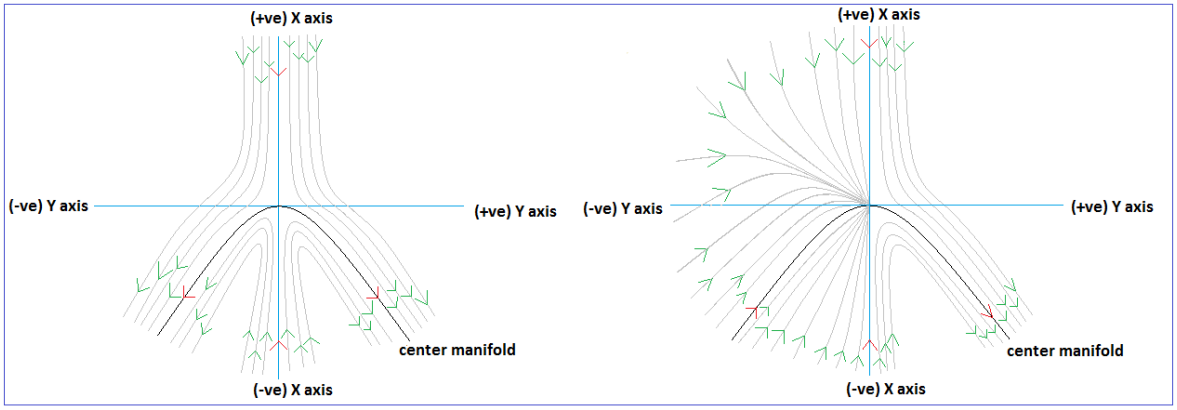

Figure 4.11: These figures show the vector field near the origin for $\mu = -\sqrt{\frac{3}{2}}$ corresponding to L_3. L.H.S. phase plot is for $\lambda = 1$ and R.H.S. phase plot is for $\lambda = 2$.

The eigenvalues of the above Jacobian matrix are $-\frac{3}{2}(1+\sqrt{3})$, $-\frac{3}{2}(1-\sqrt{3})$ and 0 and the corresponding eigenvectors are $[-\sqrt{3}, 1, 0]^T$, $[\sqrt{3}, 1, 0]^T$ and $\left[-\frac{\lambda}{6}, 0, 1\right]^T$, respectively. As for $\mu = \sqrt{3}$, the critical point L_3 converts into $\left(-\frac{1}{\sqrt{2}}, \frac{1}{\sqrt{2}}, 0\right)$; so first we take the transformations $x = X - \frac{1}{\sqrt{2}}$, $y = Y + \frac{1}{\sqrt{2}}$ and $z = Z$ which shift the critical point to the origin. By using the eigenvectors of the above Jacobian matrix, we introduce a new coordinate system (u, v, w) in terms of (X, Y, Z) as

$$\begin{bmatrix} u \\ v \\ w \end{bmatrix} = \begin{bmatrix} -\frac{1}{2\sqrt{3}} & \frac{1}{2} & -\frac{\lambda}{12\sqrt{3}} \\ \frac{1}{2\sqrt{3}} & \frac{1}{2} & \frac{\lambda}{12\sqrt{3}} \\ 0 & 0 & 1 \end{bmatrix} \begin{bmatrix} X \\ Y \\ Z \end{bmatrix} \tag{4.73}$$

and in this new coordinate system the equations $(4.62-4.64)$ are transformed into

$$\begin{bmatrix} -u'+v' \\ u'+v' \\ w' \end{bmatrix} = \begin{bmatrix} \frac{3}{2}(1+\sqrt{3}) & -\frac{3}{2}(1-\sqrt{3}) & 0 \\ -\frac{3}{2}(1+\sqrt{3}) & -\frac{3}{2}(1-\sqrt{3}) & 0 \\ 0 & 0 & 0 \end{bmatrix} \begin{bmatrix} u \\ v \\ w \end{bmatrix} + \begin{bmatrix} non \\ linear \\ terms \end{bmatrix}. \tag{4.74}$$

Now if we add 1st and 2nd equation of the above matrix equation and then divide both sides by 2, then we get v'. Further, if we subtract 1st equation from 2nd equation and divide both sides by 2, we get u'. Finally, in the new coordinate system, the autonomous system in matrix form can be written as

$$\begin{bmatrix} u' \\ v' \\ w' \end{bmatrix} = \begin{bmatrix} -\frac{3}{2}(1+\sqrt{3}) & 0 & 0 \\ 0 & -\frac{3}{2}(1-\sqrt{3}) & 0 \\ 0 & 0 & 0 \end{bmatrix} \begin{bmatrix} u \\ v \\ w \end{bmatrix} + \begin{bmatrix} non \\ linear \\ terms \end{bmatrix}. \tag{4.75}$$

If we put similar arguments which we have mentioned for the analysis of A_2, then the center manifold can be expressed as

$$u = \frac{2}{3(1+\sqrt{3})}\left\{\frac{(\sqrt{3}-1)\lambda^2-4\lambda}{48\sqrt{6}}\right\}w^2+\mathcal{O}(w^3), \tag{4.76}$$

$$v = -\frac{2}{3(\sqrt{3}-1)}\left\{\frac{(\sqrt{3}+1)\lambda^2+4\lambda}{48\sqrt{6}}\right\}w^2+\mathcal{O}(w^3) \tag{4.77}$$

and the flow on the center manifold is determined by

$$w' = \frac{1}{\sqrt{2}}w^2+\mathcal{O}(w^3). \tag{4.78}$$

From the flow equation, we can easily conclude that the origin is a saddle node and unstable in nature. The vector field near the origin in uw-plane is shown as in FIG.4.12 and the vector field near the origin in vw-plane is shown as in FIG.4.13. Hence, in the old coordinate system (x, y, z), for $\mu = \sqrt{3}$ the critical point L_3 is unstable due to its saddle nature.

Lastly, for $\mu = -\sqrt{3}$, we have the same eigenvalues $-\frac{3}{2}(1+\sqrt{3})$, $-\frac{3}{2}(1-\sqrt{3})$ and 0 and the corresponding eigenvectors are $[\sqrt{3}, 1, 0]^T$, $[-\sqrt{3}, 1, 0]^T$ and $\left[-\frac{\lambda}{6}, 0, 1\right]^T$ respectively of $J(L_3)$. After putting corresponding arguments which we have mentioned for $\mu = \sqrt{3}$ case, then we will get the same expressions $(4.76-4.77)$ for center manifold and (4.78) for the flow on the center manifold. So, for this case also we conclude that the critical point L_3 is a saddle-node and unstable in nature.

4. *Critical Point* L_4

The Jacobian matrix corresponding to the autonomous system $(4.62-4.64)$ at the critical

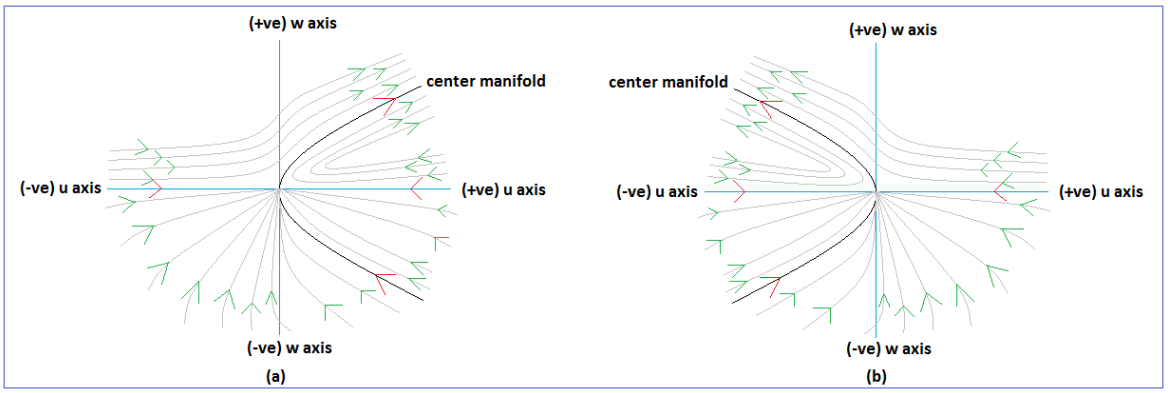

Figure 4.12: These figures show the vector field near the origin in uw-plane for $\mu = \sqrt{3}$ corresponding to the critical points L_3 and L_4. For the critical point L_3, the phase plot (a) is for $\lambda < 0$ or $\lambda > \frac{4}{\sqrt{3}-1}$ and the phase plot (b) is for $0 < \lambda < \frac{4}{\sqrt{3}-1}$. For the critical point L_4, the phase plot (a) is for $0 < \lambda < \frac{4}{\sqrt{3}-1}$ and the phase plot (b) is for $\lambda < 0$ or $\lambda > \frac{4}{\sqrt{3}-1}$.

point L_4 can be put as

$$J(L_4) = \begin{bmatrix} -\frac{9}{2\mu^2} & -\sqrt{1-\frac{3}{2\mu^2}}\left(\frac{3}{\mu}\sqrt{\frac{3}{2}}+\sqrt{6}\mu\right) & -\frac{\lambda}{2}\left(1-\frac{3}{2\mu^2}\right) \\ -\frac{3}{\mu}\sqrt{\frac{3}{2}}\sqrt{1-\frac{3}{2\mu^2}} & -3\left(1-\frac{3}{2\mu^2}\right) & -\frac{\lambda}{2\mu}\sqrt{\frac{3}{2}}\sqrt{1-\frac{3}{2\mu^2}} \\ 0 & 0 & 0 \end{bmatrix}. \tag{4.79}$$

For this critical point also we analyze the stability for the above four choices of μ, *i.e.*, $\mu = \pm\sqrt{\frac{3}{2}}$, $\mu = \sqrt{3}$ and $\mu = -\sqrt{3}$.

For $\mu = \pm\sqrt{\frac{3}{2}}$, we will get the same expressions of center manifold (4.69) and the flow on the center manifold (4.70 – 4.71). So, for this case the critical point L_4 is unstable due to its saddle nature.

For $\mu = \sqrt{3}$, after putting corresponding arguments as L_3, the center manifold can be written as

$$u = \frac{2}{3(1+\sqrt{3})}\left\{\frac{(1-\sqrt{3})\lambda^2+4\lambda}{48\sqrt{6}}\right\}w^2 + \mathcal{O}(w^3), \tag{4.80}$$

$$v = \frac{2}{3(\sqrt{3}-1)}\left\{\frac{(\sqrt{3}+1)\lambda^2+4\lambda}{48\sqrt{6}}\right\}w^2 + \mathcal{O}(w^3) \tag{4.81}$$

and the flow on the center manifold is determined by

$$w' = \frac{1}{\sqrt{2}}w^2 + \mathcal{O}(w^3). \tag{4.82}$$

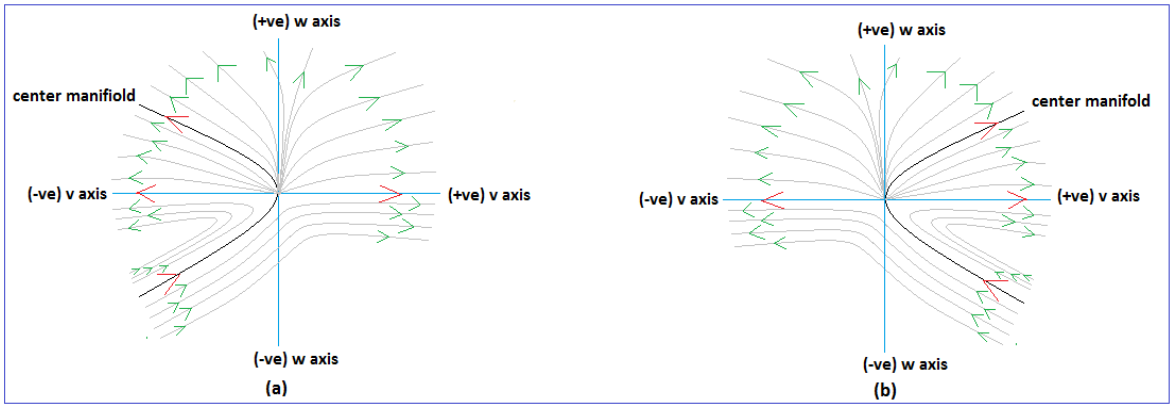

Figure 4.13: These figures show the vector field near the origin in vw-plane for $\mu = \sqrt{3}$ corresponding to the critical points L_3 and L_4. For the critical point L_3, the phase plot (a) is for $\lambda < -\frac{4}{\sqrt{3}+1}$ or $\lambda > 0$ and the phase plot (b) is for $-\frac{4}{\sqrt{3}+1} < \lambda < 0$. For the critical point L_4, the phase plot (a) is for $-\frac{4}{\sqrt{3}+1} < \lambda < 0$ and the phase plot (b) is for $\lambda < -\frac{4}{\sqrt{3}+1}$ or $\lambda > 0$.

From the flow equation we can conclude that the origin is a saddle node and hence in the old coordinate system L_4 is a saddle node, *i.e.,* unstable in nature. The vector field near the origin in uw-plane is shown as in FIG.4.12 and the vector field near the origin in vw-plane is shown as in FIG.4.13.

For $\mu = -\sqrt{3}$ we also get the same expression of center manifold and flow equation as for $\mu = \sqrt{3}$ case.

5. *Critical Point* L_5

First, we shift the critical point L_5 to the origin by the transformation $x = X - \sqrt{\frac{2}{3}}\mu$, $y = Y$ and $z = Z$. For avoiding similar arguments which we have mentioned for the above critical points, we only state the main results center manifold and the flow equation for this critical point. The center manifold for this critical point can be written as

$$X = 0, \tag{4.83}$$
$$Y = 0 \tag{4.84}$$

and the flow on the center manifold can be obtained as

$$\frac{dZ}{dN} = \sqrt{\frac{2}{3}}\mu Z^2 + \mathcal{O}(Z^3). \tag{4.85}$$

From the expressions of the center manifold we can conclude that the center manifold is lying on the Z-axis. From the flow on the center manifold FIG.4.14, we conclude that the origin is unstable for both of the cases $\mu > 0$ or $\mu < 0$.

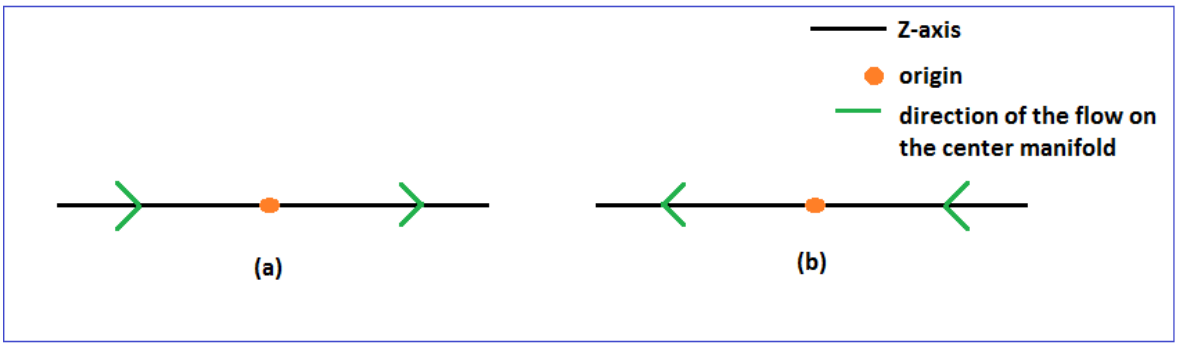

Figure 4.14: These figures show the flow on the center manifold near the origin corresponding to the critical point L_5. The phase plot (a) is for $\mu > 0$ and (b) is for $\mu < 0$.

4.3.3 Model 3: Exponential potential and power-law-dependent dark-matter particle mass

In this case evolution equations in Section 4.2 can be written to the autonomous system as follows

$$x' = -3x + \frac{3}{2}x(1 - x^2 - y^2) - \sqrt{\frac{3}{2}}\lambda y^2 - \frac{\mu}{2}z(1 + x^2 - y^2), \tag{4.86}$$

$$y' = \frac{3}{2}y(1 - x^2 - y^2) - \sqrt{\frac{3}{2}}\lambda xy, \tag{4.87}$$

$$z' = -xz^2. \tag{4.88}$$

We have three critical points R_1, R_2 and R_3 corresponding to the above autonomous system. The set of critical points, their existence and the value of cosmological parameters at those critical points corresponding to the autonomous system (4.86 – 4.88) shown in Table 4.9 and the eigenvalues of the Jacobian matrix corresponding to the autonomous system (4.86 – 4.88) at those critical points and the nature of the critical points are shown in Table 4.10.

Here we are also concerned about the stability of the critical points for $\mu \neq 0$ and $\lambda \neq 0$ because for other possible cases, we will get the similar results that we obtained for Model 1.

To avoid similar types of argument, we only state the stability of every critical point and the reason behind the stability in the tabular form, shown as in Table 4.11.

4.3.4 Model 4: Exponential potential and exponentially-dependent dark-matter particle mass

In this consideration evolution equations in Section 4.2 can be written to the autonomous system as follows

$$x' = -3x + \frac{3}{2}x(1 - x^2 - y^2) - \sqrt{\frac{3}{2}}\lambda y^2 - \sqrt{\frac{3}{2}}\mu(1 + x^2 - y^2), \tag{4.89}$$

$$y' = \frac{3}{2}y(1 - x^2 - y^2) - \sqrt{\frac{3}{2}}\lambda xy. \tag{4.90}$$

We ignore the equation corresponding to the auxiliary variable z in the above autonomous system because the R.H.S. expression of x' and y' does not depend on z.

Table 4.9: Table shows the set of critical points corresponding to the autonomous system (4.86 – 4.88) their existence and value of cosmological parameters.

CPs	$Existence$	x	y	z	Ω_ϕ	ω_ϕ	ω_{tot}	q
R_1	$\forall\mu$ and λ	0	0	0	0	Undetermined	0	$\frac{1}{2}$
R_2	$\forall\mu$ and λ	$-\frac{\lambda}{\sqrt{6}}$	$\sqrt{1+\frac{\lambda^2}{6}}$	0	1	$-1-\frac{\lambda^2}{3}$	$-1-\frac{\lambda^2}{3}$	$-1-\frac{\lambda^2}{2}$
$R_3{}^a$	$\forall\mu$ and λ	$-\frac{\lambda}{\sqrt{6}}$	$-\sqrt{1+\frac{\lambda^2}{6}}$	0	1	$-1-\frac{\lambda^2}{3}$	$-1-\frac{\lambda^2}{3}$	$-1-\frac{\lambda^2}{2}$

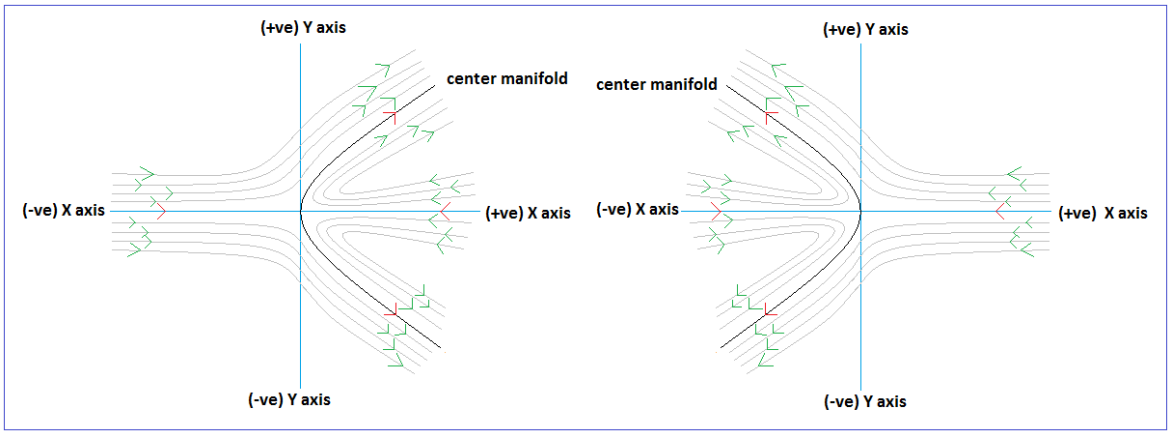

Figure 4.15: These figures show the vector field near the origin corresponding to the critical point M_1. L.H.S. phase plot is for $\mu > 3$ and R.H.S. phase plot is for $\mu < 0$.

Corresponding to the above autonomous system we have four critical points M_1, M_2, M_3 and M_4. The set of critical points, their existence and the value of cosmological parameters at those critical points corresponding to the autonomous system (4.89 – 4.90) shown in Table 4.12 and the eigenvalues of the Jacobian matrix corresponding to the autonomous system (4.89 – 4.90) at those critical points and the nature of the critical points are shown in Table 4.13.

Note that for the critical point M_4 we have written the eigenvalues in terms of a, b, c and d, where $a = -\frac{3}{2(\lambda-\mu)^2}(\lambda^2+3-\lambda\mu)$, $b = \mp\sqrt{\frac{3}{2}}\left(\frac{3}{(\lambda-\mu)^2}+2\right)\sqrt{-\frac{3}{2}-\mu(\lambda-\mu)}$, $c = \mp\sqrt{\frac{3}{2}}\left\{\frac{\lambda^2+3-\lambda\mu}{(\lambda-\mu)^2}\right\}\sqrt{-\frac{3}{2}-\mu(\lambda-\mu)}$, $d = -\frac{3}{(\lambda-\mu)^2}\left\{\left(\mu^2-\frac{3}{2}\right)-\lambda\mu\right\}$.

Here we only stated the stability of every critical point $(M_1 - M_4)$ and the reason behind the stability in the tabular form, which is shown in Table 4.14.

From the Table 4.14, we see that M_1, M_2 and M_3 are stable node (in some region of λ or μ) although the point M_1 and M_3 are not physically meaningful. Note that M_1, M_2 and M_3

Table 4.10: The eigenvalues $(\lambda_1, \lambda_2, \lambda_3)$ of the Jacobian matrix corresponding to the autonomous system $(4.86 - 4.88)$ at those critical points $(R_1 - R_3)$ and the nature of the critical points.

$Critical Points$	λ_1	λ_2	λ_3	$Nature\ of\ critical\ Points$
R_1	$-\frac{3}{2}$	$\frac{3}{2}$	0	Non-hyperbolic
R_2	$-(3+\lambda^2)$	$-\left(3+\frac{\lambda^2}{2}\right)$	0	Non-hyperbolic
R_3	$-(3+\lambda^2)$	$-\left(3+\frac{\lambda^2}{2}\right)$	0	Non-hyperbolic

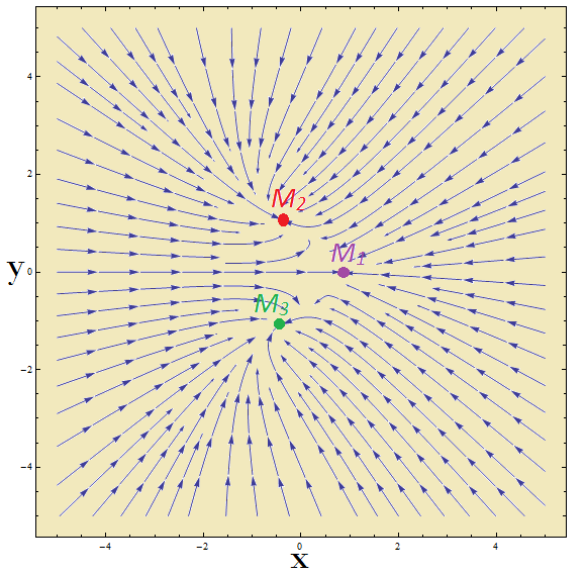

Figure 4.16: This figure shows the vector field corresponding to the autonomous system $(4.89 - 4.90)$ for $\lambda = 1$ and $\mu = -1$.

are stable for $\lambda = 1$, $\mu = -1$. Now let's check that for $\lambda = 1$ and $\mu = -1$ which of the critical points are attracting the system. To see that we plot the vector field corresponding to the autonomous system $(4.89-4.90)$ by using Mathematica software for $\lambda = 1$ and $\mu = -1$. From the phase plot (Fig.4.16) we can conclude that the ultimate fate of the system depends on the initial position of it. More precisely, we can say that if the initial position of the system is in the basin of attraction or on the stable manifold that asymptotically disembogues into the basin of attraction of the critical point M_i then the system is attracted by the critical point M_i for $i = 1, 2, 3$. Also note that for hyperbolic case of M_4, the components of the Jacobian matrix a, b, c and d are very complicated and after determining the eigenvalues, it

Table 4.11: Table shows the stability and the reason behind the stability of the critical points $(R_1 - R_3)$.

CPs	*Stability*	*Reason behind the stability*
R_1	For $\mu > 0$, R_1 is a saddle node and for $\mu < 0$, R_1 is a stable node	After introducing the coordinate transformation (4.26), we will get the same expression of center manifold (4.31 − 4.32) and the flow on the center manifold is determined by (4.33)(FIG.4.1).
R_2, R_3	For $\lambda > 0$ or $\lambda < 0$, R_2 and R_3 both are unstable	After shifting R_2 and R_3 to the origin by using coordinate transformation $\left(x = X - \frac{\lambda}{\sqrt{6}}, y = Y + \sqrt{1 + \frac{\lambda^2}{6}}, z = Z\right)$ and $\left(x = X - \frac{\lambda}{\sqrt{6}}, y = Y - \sqrt{1 + \frac{\lambda^2}{6}}, z = Z\right)$ respectively, we can conclude that the center manifold is lying on Z-axis and the flow on the center manifold is determined by $\frac{dZ}{dN} = \frac{\lambda}{\sqrt{6}}Z^2 + \mathcal{O}(Z^3)$. The origin is unstable for both of the cases $\lambda > 0$ (same as FIG.4.14(**a**)) and $\lambda < 0$ (same as FIG.4.14(**b**)).

Table 4.12: Table shows the set of all critical points corresponding to the autonomous system (4.89 – 4.90), their existence and value of cosmological parameters.

CPs	*Existence*	x	y	Ω_ϕ	ω_ϕ	ω_{tot}	q
$M_1{}^a$	For all μ and λ	$-\sqrt{\frac{2}{3}}\mu$	0	$-\frac{2}{3}\mu^2$	1	$-\frac{2}{3}\mu^2$	$\frac{1}{2}\left(1-2\mu^2\right)$
M_2	For all μ and λ	$-\frac{\lambda}{\sqrt{6}}$	$\sqrt{1+\frac{\lambda^2}{6}}$	1	$-1-\frac{\lambda^2}{3}$	$-1-\frac{\lambda^2}{3}$	$-\frac{1}{2}\left(2+\lambda^2\right)$
$M_3{}^a$	For all μ and λ	$-\frac{\lambda}{\sqrt{6}}$	$-\sqrt{1+\frac{\lambda^2}{6}}$	1	$-1-\frac{\lambda^2}{3}$	$-1-\frac{\lambda^2}{3}$	$-\frac{1}{2}\left(2+\lambda^2\right)$
M_4	For $\mu \neq \lambda$ and $\min\{\mu^2-\frac{3}{2}, \lambda^2+3\} \geq \lambda\mu$	$\frac{\sqrt{\frac{3}{2}}}{\lambda-\mu}$	$\frac{\sqrt{-\frac{3}{2}-\mu(\lambda-\mu)}}{\lvert\lambda-\mu\rvert}$	$\frac{\mu^2-\lambda\mu-3}{(\lambda-\mu)^2}$	$\frac{\mu(\lambda-\mu)}{\mu^2-\lambda\mu-3}$	$\frac{\mu}{\lambda-\mu}$	$\frac{1}{2}\left(\frac{\lambda+2\mu}{\lambda-\mu}\right)$

Note that the point M_1 and M_3 are not physically relevant because $\Omega_\phi < 0$ for $\mu \neq 0$ for M_1 and near the critical point M_3, the universe contracts [672, 642].

Table 4.13: The eigenvalues (λ_1, λ_2) of the Jacobian matrix corresponding to the autonomous system (4.89 − 4.90) at the critical points $(M_1 - M_4)$ and their nature.

CPs	λ_1	λ_2	*Nature of critical points*
M_1	$-\left(\frac{3}{2}+\mu^2\right)$	$-\left(\mu^2-\frac{3}{2}\right)+\lambda\mu$	Hyperbolic if $\left(\mu^2-\frac{3}{2}\right)\neq\lambda\mu$, non-hyperbolic if $\left(\mu^2-\frac{3}{2}\right)=\lambda\mu$
M_2	$-(3+\lambda^2)+\lambda\mu$	$-\left(3+\frac{\lambda^2}{2}\right)$	Hyperbolic if $(\lambda^2+3)\neq\lambda\mu$, non-hyperbolic if $(\lambda^2+3)=\lambda\mu$
M_3	$-(3+\lambda^2)+\lambda\mu$	$-\left(3+\frac{\lambda^2}{2}\right)$	Hyperbolic if $(\lambda^2+3)\neq\lambda\mu$, non-hyperbolic if $(\lambda^2+3)=\lambda\mu$
M_4	$\frac{a+d+\sqrt{(a-d)^2+4bc}}{2}$	$\frac{a+d-\sqrt{(a-d)^2+4bc}}{2}$	Hyperbolic when $\mu^2-\frac{3}{2}>\lambda\mu$ and $\lambda^2+3>\lambda\mu$, non-hyperbolic when $\mu^2-\frac{3}{2}=\lambda\mu$ or $\lambda^2+3=\lambda\mu$

is very difficult to provide any conclusion about the stability and for this reason we skip the stability analysis for this case.

Table 4.14: Table shows the stability and the reason behind the stability of the critical points $(M_1 - M_4)$.

CPs	*Stability*	*Reason behind the stability*
M_1	Stable node for $\left(\mu^2 - \frac{3}{2}\right) > \lambda\mu$ and saddle node for $\left(\mu^2 - \frac{3}{2}\right) \leq \lambda\mu$	For $\left(\mu^2 - \frac{3}{2}\right) > \lambda\mu$, as both eigenvalues of the Jacobian matrix at M_1 are negative, so by Hartman-Grobman theorem we can conclude that the critical point M_1 is a stable node. For $\left(\mu^2 - \frac{3}{2}\right) < \lambda\mu$, as one eigenvalue is positive and another is negative, so by Hartman-Grobman theorem we can conclude that the critical point M_1 is a saddle node. For $\left(\mu^2 - \frac{3}{2}\right) = \lambda\mu$, after shifting the critical point M_1 to the origin by the coordinate transformation $\left(x = X - \sqrt{\frac{2}{3}}\mu, y = Y\right)$, the center manifold can be written as $X = \frac{1}{\mu}\sqrt{\frac{3}{2}}Y^2 + \mathcal{O}(Y^3)$ and the flow on the center manifold can be determined as $\frac{dY}{dN} = \frac{9}{4\mu^2}Y^3 + \mathcal{O}(Y^4)$. Hence, for both of the cases $\mu > 0$ and $\mu < 0$ the origin is a saddle node and unstable in nature.
M_2, M_3	Stable node for $\left(\lambda^2 + 3\right) > \lambda\mu$ and saddle node for $\left(\lambda^2 + 3\right) \leq \lambda\mu$	For $\left(\lambda^2 + 3\right) > \lambda\mu$, as both eigenvalues of the Jacobian matrix at M_2 are negative, so by Hartman-Grobman theorem we can conclude that the critical point M_2 is a stable node. For $\left(\lambda^2 + 3\right) < \lambda\mu$, as one eigenvalue is positive and another is negative, so by Hartman-Grobman theorem we can conclude that the critical point M_2 is a saddle node. For $\left(\lambda^2 + 3\right) = \lambda\mu$, after shifting the critical point M_1 to the origin by the coordinate transformation $\left(x = X - \frac{\lambda}{\sqrt{6}}, y = Y \pm \sqrt{1 + \frac{\lambda^2}{6}}\right)$, the center manifold can be written as $Y = \mp\frac{1}{2\sqrt{1+\frac{\lambda^2}{6}}}X^2 + \mathcal{O}(X^3)$ and the flow on the center manifold can be determined as $\frac{dX}{dN} = \frac{\lambda}{2}\sqrt{\frac{3}{2}}\left\{1 - \frac{6}{\lambda^2} \pm \frac{12}{\lambda^2}\left(1 + \frac{\lambda^2}{6}\right)^{\frac{3}{2}}\right\}X^2 + \mathcal{O}(X^4)$. Hence, for all possible values λ due to the even power X in the R.H.S. of the flow equation, the origin is a saddle node and unstable in nature.
M_4	Saddle node for both of the cases, i.e., $\mu^2 - \frac{3}{2} = \lambda\mu$ or $\lambda^2 + 3 = \lambda\mu$	For $\mu^2 - \frac{3}{2} = \lambda\mu$, as M_4 converts into M_1, so we get the same stability like M_1. For $\lambda^2 + 3 = \lambda\mu$ as M_4 converts into M_2 and M_3, so we get the same stability like M_2 and M_3.

4.3.5 Model 5: Product of exponential and power-law potential and product of exponentially-dependent and power-law-dependent dark-matter particle mass

In this consideration evolution equations in Section 4.2 can be written to the autonomous system as follows

$$x' = -3x + \frac{3}{2}x(1-x^2-y^2) - \sqrt{\frac{3}{2}}\lambda y^2 - \frac{\lambda}{2}y^2 z - \sqrt{\frac{3}{2}}\mu(1+x^2-y^2) - \frac{\mu}{2}z(1+x^2-y^2), \tag{4.91}$$

$$y' = \frac{3}{2}y(1-x^2-y^2) - \sqrt{\frac{3}{2}}\lambda xy - \frac{\lambda}{2}xyz, \tag{4.92}$$

$$z' = -xz^2. \tag{4.93}$$

To determine the critical points corresponding to the above autonomous system, we first equate the R.H.S. of (4.93) with 0. Then we have either $x = 0$ or $z = 0$. For $z = 0$ then the above autonomous system converts in to the autonomous system of Model 4. So, then we will get the similar types of result as Model 4. When $x = 0$, we have three physically meaningful critical points corresponding to the above autonomous system for $\mu \neq 0$ and $\lambda \neq 0$. For another choices of μ and λ like Model 1, we will get similar types of results. The critical points are $N_1(0, 0, -\sqrt{6})$, $N_2(0, 1, -\sqrt{6})$ and $N_3(0, -1, -\sqrt{6})$ and all are hyperbolic in nature. Although the critical point N_3 is not physically relevant because near this critical point the universe contracts. Note that x and y coordinates of these critical points are same as A_1, A_2 and A_3 and the value of cosmological parameters are not depending on z coordinate, so we get the same result for the value of cosmological parameters as A_1, A_2 and A_3 respectively, which are presented in Table 4.1.

1. *Critical Point* N_1

The Jacobian matrix corresponding to the autonomous system (4.91-4.93) at the critical point N_1 has three eigenvalues $\frac{3}{2}$, $-\frac{1}{4}\left(3+\sqrt{9+48\mu}\right)$ and $-\frac{1}{4}\left(3-\sqrt{9+48\mu}\right)$ and the corresponding eigenvectors are $[0,1,0]^T$, $\left[\frac{1}{24}\left(3+\sqrt{9+48\mu}\right), 0, 1\right]^T$ and $\left[\frac{1}{24}\left(3-\sqrt{9+48\mu}\right), 0, 1\right]^T$, respectively. As the critical point is hyperbolic in nature, so we use Hartman-Grobman theorem for analyzing the stability of this critical point. From the determination of eigenvalues, we conclude that the stability of the critical point N_1 depends on μ. For $\mu < -\frac{9}{48}$, the last two eigenvalues are complex conjugate with negative real parts. For $\mu \geq -\frac{9}{48}$, all eigenvalues are real.

For $\mu < -\frac{9}{48}$, due to presence of negative real parts of last two eigenvalues, xz-plane is the stable subspace and as one eigenvalue is positive and this is corresponding to the y coordinate, y-axis is the unstable subspace. Hence, the critical point N_1 is saddle-focus, *i.e.,* unstable in nature. The phase portrait in xyz coordinate system is shown as in FIG.4.17.

For $\mu \geq -\frac{9}{48}$, always we have at least one positive eigenvalue and at least one negative eigenvalue and consequently the critical point N_1 is unstable due to its saddle node nature.

2. *Critical Point* N_2 & N_3

The Jacobian matrix corresponding to the autonomous system $(4.91 - 4.93)$ at the critical point N_2 and N_3 has three eigenvalues -3, $-\frac{1}{2}\left(3+\sqrt{9+12\lambda}\right)$ and $-\frac{1}{2}\left(3-\sqrt{9+12\lambda}\right)$ and the corresponding eigenvectors are $[0,1,0]^T$, $\left[\frac{1}{12}\left(3+\sqrt{9+12\lambda}\right), 0, 1\right]^T$ and

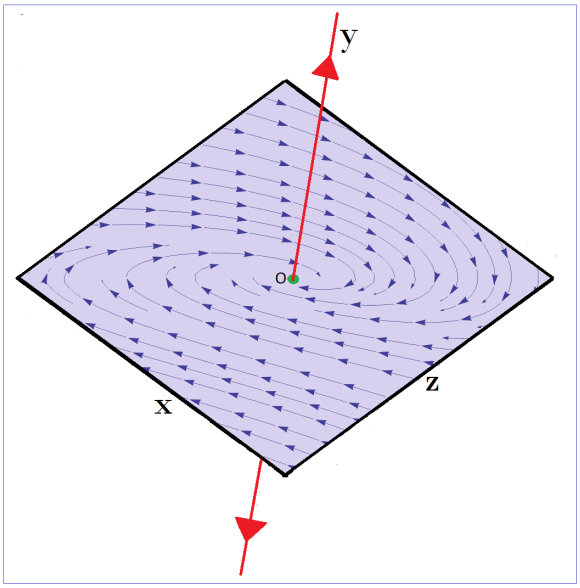

Figure 4.17: This figure shows the phase portrait near the origin for the critical point N_1 in xyz coordinate system when $\mu < -\frac{9}{48}$. To draw the projection of the vector field on xz-coordinate plane, we consider $\mu = -1$.

$\left[\frac{1}{12}\left(3-\sqrt{9+12\lambda}\right), 0, 1\right]^T$, respectively. From the determination of the eigenvalue, we conclude that the last two eigenvalues are complex conjugate while $\lambda < -\frac{3}{4}$ and the eigenvalues are real while $\lambda \geq -\frac{3}{4}$.

For $\lambda < -\frac{3}{4}$, we can see that the last two eigenvalues are complex conjugate to each other with negative real parts and the first eigenvalue is always negative. Hence, by Hartman-Grobman theorem we conclude that the critical points N_2 and N_3 both are stable focus-node in this case. The phase portrait in $xyz-$coordinate system corresponding to the critical point N_2 is shown as in FIG.4.18.

For $-\frac{3}{4} \leq \lambda < 0$, we can see that all eigenvalues are negative. So, by Hartman-Grobman theorem we conclude that the critical points N_2 and N_3 both are stable node in this case.

For $\lambda > 0$, we have two negative and one positive eigenvalues. Hence, by Hartman-Grobman theorem we conclude that the critical points N_2 and N_3 both are saddle node and unstable in nature.

4.4 Bifurcation Analysis by Poincaré index and Global Cosmological evolution

The flat potential plays a crucial role to obtain the bouncing solution. After the bounce, the flat potential naturally allows the universe to penetrate the slow-roll inflation regime, as a result of that making the bouncing universe compatible with observations. We can divide the evolution of the universe with respect to the critical points into two groups: representing

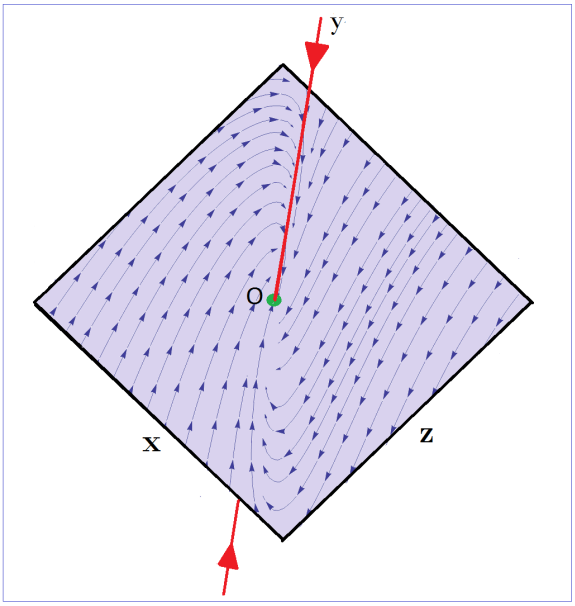

Figure 4.18: This figure shows the phase portrait near the origin corresponding to the critical point N_2 in xyz coordinate system when $\lambda < -\frac{3}{4}$. To draw the projection of the vector field on xz-coordinate plane we consider $\lambda = -1$.

generic and non-generic evolution. The generic evolution occurs,when there exists a family of solutions satisfying given initial conditions, while the non-generic evolution takes place if one particular solution exists for given initial conditions [544].
In Model 1 (4.3.1), for the inflationary scenario, we consider λ and μ very small positive number so that $V(\phi) \approx V_0$ and $M_{DM} \approx M_0$. The Eqn. (4.24) mainly regulate the flow along Z-axis. Due to Eqn. (4.24) the overall 3-dimensional phase space splits up into two compartments and the ZY-plane becomes the separatrix. In the right compartment, for $x > 0$, we have $z' < 0$ and $z' > 0$ in the left compartment. On the ZY plane we have $z' \approx 0$. For $\lambda \neq 0$ and $\mu \neq 0$, all critical points are located on the Y-axis. As all cosmological parameters can be expressed in terms of x and y, so we rigorously inspect the vector field on XY-plane. Due to Eqn. (4.15), the viable phase-space region (say S) satisfies $y^2 - x^2 \leqslant 1$ which is inside of a hyperbola centered at the origin (FIG.4.19). On the XY-plane $z' \approx 0$. So on the XY-plane, by Hartman-Grobman theorem we can conclude there are four hyperbolic sectors around A_1 (α-limit set) and one parabolic sector around each of A_2 and A_3 (ω-limit sets). So, by Bendixson theorem, it is to be noted that, the index of $A_1|_{XY}$ is 1 and the index of $A_2|_{XY}$ and $A_3|_{XY}$ is -1. If the initial position of the universe is in left compartment and near to the α-limit, then the universe remains in the left compartment and moves towards ω-limit set asymptotically at late time. Similar phenomenon happens in right compartment also.

• The universe experiences a fluid dominated non-generic decelerating evolution near A_1 for $\mu > 0$ and a generic evolution for $\mu < 0$. For the perturbation of sufficiently flat potential, near A_2 and A_3, a scalar field dominated de-Sitter non-generic and generic evolution occur for $\lambda > 0$ and $\lambda < 0$ respectively.

The Poincaé index theorem [474] helps us to determine Euler Poincaré characteristic which is $\chi(S) = n - f - s$, where n, f, s are the number of nodes, foci and saddle on S.

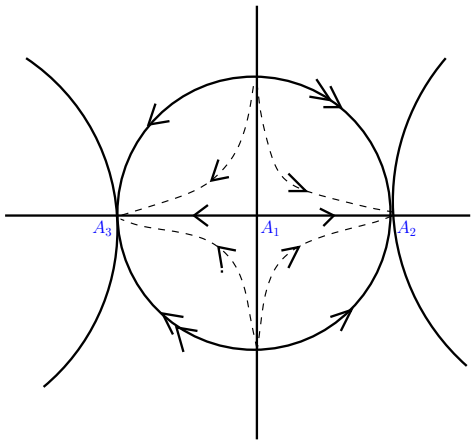

Figure 4.19: This figure shows the vector field on the projective plane by antipodal points identified of the disk.

Henceforward we consider 'index' as 'Poincaé index'. If we confine the vector field of case-(i) on XY-plane (S), then one may note that $\chi(S) = 1$. This flow is topologically equivalent to a vector field on the projective plane, *i.e.,* if we consider a closed disk on the XY-plane of radius one and centered at the origin embedded in 3-dimensional phase-space, then we have the same vector field on the projective plane by antipodal point identified (see FIG. 4.19). On the other hand, the vertical flow along Z-axis regulates the character of the vector field on $z = constant(\neq 0)$-plane, ergo the characterization of vector field changes from the previous instance.

Using Bendixson theorem [474] we can find the index of non-hyperbolic critical points by restricting the vector field on a suitable two-dimensional subspace.

• If we restrict ourselves on XZ-plane, A_1 is saddle in nature for $\mu > 0$. On the XZ plane the index of A_1 is -1 for $\mu > 0$ as four hyperbolic sectors are separated by two separatices around A_1. For $\mu < 0$, there is only one parabolic sector and the index is zero (FIG.4.1). On the YZ plane A_1 swap its index with the index on XZ plane depending on the sign of μ.

So on the XZ plane near A_1 the universe transits its phase from matter dominated decelerating phase to scalar field dominated de-Sitter phase when μ crosses zero from negative to positive, while on the YZ plane generic scalar field dominated de-Sitter late time solution is observed for $\mu > 0$ and $\lambda < 0$ owing to the effect of the flow on center manifold (4.33).

On uv-plane the index A_2 or A_3 is 1 and does not depend on λ. On the uw and vw-plane around A_2 or A_3 the number of hyperbolic sectors is four and there is no elliptic sector. So each of the index of A_2 and A_3 $(origin)|_{uw\ plane/vw\ plane}$ is -1 for $\lambda > 0$ and for $\lambda < 0$ each of the index is 1 as there is no hyperbolic or elliptic orbit.

A set of non-isolated equilibrium points is said to be normally hyperbolic if the only eigenvalues with zero real parts are those whose corresponding eigenvectors are tangent to the set. For the case (ii) to case (iv), we come by normally hyperbolic critical points as the eigenvector $[0\ 0\ 1]^T$ (in new (u, v, w) coordinate system), corresponding to only zero eigenvalue, is tangent to the line of critical points. The stability of a set which is normally hyperbolic can be completely classified by considering the signs of the eigenvalues in the remaining directions. So the character of the flow of the phase space for each $z = constant$ plane is identical to the XY-plane in the previous case. Thus the system (4.22-4.24) is structurally unstable [474] at $\lambda = 0$ or $\mu = 0$ or both. On the other hand, the potential

changes its character from runaway to non-runaway as λ crosses zero from positive to negative. Thus $\lambda = 0$ and $\mu = 0$ are the bifurcation values[611]. However we do not detect any phase transition of the universe near the bifurcation points A_2 and A_3. The universe is scalar field dominated and has late time de-Sitter phase solution near these critical points.

Model 2 (4.3.2) contains five critical points $L_1 - L_5$. Near L_1 the flow is unstable for $\lambda > 0$ and for $\lambda < 0$, the flow on the center manifold is stable. Around L_2, the character of the vector field similar to L_1. For $\mu = \pm\sqrt{\frac{3}{2}}$, the flow on the center manifold at L_3 or L_4 depends on the sign of λ (FIG.4.10 & FIG.4.11). For $\mu > 0$, the flow on the center manifold at L_5 moves increasing direction of Z. On the other hand, for $\mu < 0$, the flow on the center manifold aims at decreasing direction of Z. The index of L_1 is indistinguishable from A_2. For $\mu = \pm\sqrt{\frac{3}{2}}$ and $\lambda = 1$, the index of $L_2|_{XY plane}$ is -1 as there are only four hyperbolic sectors. But for $\lambda = 2$, there are two hyperbolic and one parabolic sectors, ergo the index is zero. The index of L_3 is indistinguishable from L_2. The index of L_4 on ZX or XY plane is zero as there are two hyperbolic and one parabolic sector for each $\mu > 0$ and $\mu < 0$. So it is to be noted that, for $\lambda = 0, \pm\sqrt{\frac{3}{2}}$ and $\mu = 0$ the system is structurally unstable.

• Cosmological phase transition occurs at $\mu = \pm\sqrt{3}$ near L_3 or L_4. Near these points the universe is in matter dominated era at $\mu = \pm\sqrt{3}$ but changes its phase to scaling solution as $\mu \in (-\infty, -\sqrt{3})$ or $\mu \in (\sqrt{3}, \infty)$.

The universe experiences a scalar field dominated non-generic evolution near L_1 and L_2 for $\lambda > 0$ and a scalar field dominated generic evolution for $\lambda < 0$. Near L_3 and L_4, a scalar field dominated non-generic evolution of the universe transpires at $\mu \approx \pm\sqrt{\frac{3}{2}}$. At $\mu \approx 0$ a scaling non-generic evolution takes place near L_5.

Model 3 (4.3.3) contains three critical points $R_1 - R_3$. R_1 is saddle in nature for all values of μ. On the xy -plane the index of R_1 is same as A_1. On the projection of the xy-plane R_2 and R_3 are stable nodes for all values of λ. On the center manifold at R_2 or R_3, the vector field goes towards positive direction of Z-axis for $\lambda > 0$ and goes towards negative direction of Z-axis for $\lambda < 0$. On the XZ or YZ-plane, the index of R_2 or R_3 is zero due to there are two hyperbolic and one parabolic sectors around each of them. Thus we note that, for $\mu = 0$ and $\lambda = 0$, the stability of the system bifurcate.

• We observe that no scaling solutions or a tracking solutions exist in this specific model like in the quintessence theory. However, the critical points which describe the de-Sitter solution, do not exist in the case of quintessence for the exponential potential. The universe experiences a fluid dominated non-generic evolution near critical point R_1 and a scalar field dominated generic evolution ($\mu > 0$) near critical point R_2 and R_3 due to the flow on the center manifold (see Table 4.11). For sufficiently flat potential, early or present phantom/non-phantom universe is attracted towards ΛCDM cosmological model. However, for the generic cases near R_1 the universe transits its phase from matter dominated decelerating late time solution to non-generic scalar field dominated de-Sitter solution when μ crosses zero from negative to positive. Near R_2 or R_3 the universe asymptotic to phantom boundary due to unstable nature of the flow on center manifold.

Model 4 (4.3.4) contains four critical points $M_1 - M_4$. M_1 is stable-node for $(\mu^2 - \frac{3}{2}) > \lambda\mu$. On the other hand, $M_2 - M_4$ are stable node (index 1) for $\left(\lambda^2 + 3\right) > \lambda\mu$ and $(\mu^2 - \frac{3}{2}) > \lambda\mu$. For other parameter values the stability of these points turn out to be saddle in nature.

• It is to be noted that the evolution of the universe is generic in nature for $\left(\lambda^2+3\right) > \lambda\mu$ and $(\mu^2-\frac{3}{2}) > \lambda\mu$ and non-generic otherwise. For generic case, we find the kinetic dominated late time solution near M_1 and scalar field dominated late time solutions near M_2 and M_3. Near M_1 we observe a scaling solution but as the parameters cross the bifurcation region and enter into the saddle condition the non-generic evolution of the universe turns out to be either scaling or scalar field dominated solution. On the other hand, the universe immerses in the phantom phase from phantom boundary for perturbation of λ at zero. So the phase changes at the bifurcation line $\lambda = 0$ (constant potential) and $\mu^2 > \frac{3}{2}$. At the bifurcation line we acquire late time accelerating solution of the evolution of the universe near M_2 and M_3.

Model 5 (4.3.5) contains three critical points N_1, N_2, N_3. For $\mu < -\frac{3}{16}$, the Shilnikov's saddle index [651] of N_1 is $\nu_{N_1} = \frac{\rho_{N_1}}{\gamma_{N_1}} = 0.5$ and saddle value is $\sigma_{N_1} = -\rho_{N_1} + \gamma_{N_1} = 0.75$. So Shilnikov condition [651] is satisfied as $\nu_{N_1} < 1$ and $\sigma_{N_1} > 0$. The second Shilnikov's saddle value is $\sigma^{(2)}_{N_1} = -2\rho_{N_1} + \gamma_{N_1} = 0$. Accordingly, by L. Shilnikov's theorem (Shilnikov, 1965) [651], there are countably many saddle periodic orbits in a neighborhood of the homoclinic loop of the saddle-focus N_1. As ν_{N_1} is invariant for any choice of μ, ergo Shilnikov's bifurcation does not appear.

However, for $-\frac{3}{16} < \mu < 0$, the vector field near N_1 is saddle-node in nature. On the other hand, N_1 is saddle for $\mu > 0$. Thus, $\mu = 0$ and $-\frac{3}{16}$ are bifurcation values for the bifurcation point N_1. Similarly, N_2 and N_3 change its stability from stable-focus to stable-node as λ crosses $-\frac{3}{4}$ to $-\frac{3}{4} < \lambda < 0$ and stable-node to saddle-node as λ crosses zero from negative to positive. So, $\lambda = 0, -\frac{3}{4}$ turn out to be bifurcation values for the bifurcation points N_2 and N_3.

• It is to be noted that, for $\lambda < 0$ we have scalar field dominated de-Sitter late time generic solution of the universe near N_2 or N_3. But as λ crosses zero to positive, the attractor depends on the initial conditions of the universe and immerses in non-generic evolution. So the evolution of the universe bifurcates from constant scalar field potential.

4.5 Brief discussion and concluding remarks

The present work deals with a detailed dynamical system analysis of the interacting DM and DE cosmological model in the background of FLRW geometry. The DE is chose as a phantom scalar field with self-interacting potential while varying mass (a function of the scalar field) DM is chosen as dust. The potential of the scalar field and the varying mass of DM are chosen as exponential or power-law form (or a product of them) and five possible combination of them are studied.

Model 1: $V(\phi) = V_0\phi^{-\lambda}, M_{_{DM}}(\phi) = M_0\phi^{-\mu}$

For case (i), *i.e.,* $\mu \neq 0, \lambda \neq 0$; there are three non-hyperbolic critical points A_1, A_2, A_3 of which A_1 corresponds to DM dominated decelerating phase (dust era) while A_2 and A_3 purely DE dominated and they represent the ΛCDM model (*i.e.,* de-Sitter phase) of the universe.

For case (ii), *i.e.,* $\mu \neq 0, \lambda = 0$; there is one critical point and two space of critical points. The cosmological consequence of these critical points are similar to case (i).

For case (iii), *i.e.,* $\mu = 0, \lambda \neq 0$; there is one space of critical points and two distinct critical points. But as before the cosmological analysis is identical to case (i).

For the fourth case, *i.e.,* $\mu = 0, \lambda = 0$; there are three space of critical points (S_1, S_2, S_3) which are all non-hyperbolic in nature and are identical to the critical points in case (ii). Further, considering the vector fields in $Z = constant$ plane, it is found that for the critical point S_1, every point on $Z-$ axis is a saddle node while for critical points S_2 and S_3 every point on $Z-$axis is a stable star.

Model 2: $V(\phi) = V_0\phi^{-\lambda}, M_{_{DM}}(\phi) = M_1 e^{-\kappa\mu\phi}$

The autonomous system for this model has five non-hyperbolic critical points L_i, $i = 1, \ldots, 5$. For L_1 and L_2, the cosmological model is completely DE dominated and the model describes cosmic evolution at the phantom barrier. The critical points L_3 and L_4 are DE dominated cosmological solution ($\mu^2 > 3$) representing the ΛCDM model. The critical point L_5 corresponds to ghost (phantom) scalar field and it describes the cosmic evolution in phantom domain ($2\mu^2 > 3$).

Model 3: $V(\phi) = V_1 e^{-\kappa\lambda\phi}, M_{_{DM}}(\phi) = M_0\phi^{-\mu}$

There are three non-hyperbolic critical points in this case. The first one (*i.e.,* R_1) is purely DM dominated cosmic evolution describing the dust era while the other two critical points (*i.e.,* R_2, R_3) are fully dominated by DE and both describe the cosmic evolution in the phantom era.

Model 4: $V(\phi) = V_1 e^{-\kappa\lambda\phi}, M_{_{DM}}(\phi) = M_1 e^{-\kappa\mu\phi}$

The autonomous system so formed in this case has four critical points M_i, $i = 1, \ldots, 4$ which may be hyperbolic/non-hyperbolic depending on the parameters involved. The critical point M_1 represents DE as ghost scalar field and it describes the cosmic evolution in the phantom domain. For the critical points M_2 and M_3, the cosmic evolution is fully DE dominated and is also in the phantom era. The cosmic era corresponding to the critical point M_4 describes scaling solution where both DM and DE contribute to the cosmic evolution.

Model 5: $V(\phi) = V_2\phi^{-\lambda}e^{-\kappa\lambda\phi}, M_{_{DM}}(\phi) = M_2\phi^{-\mu}e^{-\kappa\mu\phi}$

This model is very similar to either model 4 or model 1, depending on the choices of the dimensionless variables x and z. For $z = 0$, the model reduces to model 4 while for $x = 0$ the model is very similar to model 1 and hence the cosmological analysis is very similar to that.

Finally, using Poincaré index theorem, Euler Poincaré characteristic is determined for bifurcation analysis of the above cases from the point of view of the cosmic evolution described by the equilibrium points. Lastly, inflationary era of cosmic evolution is studied by using bifurcation analysis.

CHAPTER 5

A DYNAMICAL SYSTEM ANALYSIS OF BOUNCING COSMOLOGY WITH SPATIAL CURVATURE

5.1 Prelude

The ΛCDM model is the simplest and very well-known cosmological model that describes the evolution of the universe from the early inflationary paradigm to the present era of expansion. Despite being successful, according to the largest part of the cosmology community, in describing the formation and evolution of the large scale structure in the universe, ΛCDM model has a large family of challenges that have not been resolved. Also, it is not consistent with many observations e.g. H0-tension [745], missing satellites [746], cosmological constant problems [747], the initial condition of the universe before the inflationary era [723, 721, 724, 724, 718] etc.

As the present observations are consistent with the expanding universe so it is reasonable to choose a model of the universe which keeps expanding from the very beginning till the present era [731]. However, from theoretical point of view, the universe may have an era of contraction in the very early epoch before inflation or the universe may experience a contracting phase at far future [740, 732, 741]. Friedmann equations tell us that for negative spatial curvature, the universe is an ever-expanding model, for flat model the expansion continues until the total energy of the universe is positive, for positive spatial curvature the expansion will halt at a finite time and there will be a phase of contraction [700]. Further, for a scalar field cosmology, there will have a contraction followed by an expanding era for a range of values of the scalar field. Usually, in the contracting phase, the kinetic energy of the scalar field increases, and it stands to dominate the evolution. Then there will be no mechanism to halt this collapse leading to a singularity [730].

However, it will be interesting if by some mechanism the contraction can be halted and again there is expansion - the bouncing model universe. If the bouncing phase occurs before the plank energy scale, then Einstein's gravity may be chosen as an effective field theory. Further, the existence of the bouncing solution depends on the spatial curvature of the space-

time. For flat or open universe, bouncing phase is characterized by the null energy condition while for closed model of the universe, the bouncing era occurs when the curvature term balances the total energy of the universe. Thus there are two essential ingredients for the bouncing scenario namely the positive spatial curvature and the scalar potential that gradually becomes flatter as the scalar field goes away from the minimum. It is to be noted that the transition from expansion to contraction is possible due to positive spatial curvature. Due to the suppression of the kinetic energy as the potential becomes sufficiently flat, the scalar field slow-rolls over a flat part of the potential and as a result, there is an accelerated contraction of the universe. Thus for the occurrence of the bouncing scenario, the positive curvature term should balance the scalar field energy [738, 737, 736, 735, 734].

The present work deals with scalar field cosmology in the background of FLRW space-time with positive spatial curvature. The potential of the scalar field is chosen to be flatter as the scalar field goes away from the minimum. One can induce a transition from expansion to contraction either by the spatial curvature. The scalar field continues to climb up the potential after passing through the minimum potential and by converting most of the kinetic energy to the potential energy. More specifically, for sufficiently flat potential (by suppressing kinetic energy) the scalar field experiences a slow roll on a flat plateau of the potential, and as a result, there will be an accelerated contracting phase of the universe. Further, if the positive spatial curvature term is equivalent to the scalar field energy during this epoch then a bouncing scenario will occur. Thus the accelerated contracting phase due to the flat potential is very much relevant for the bouncing universe [700, 702].

From an observational point of view the bouncing model is not a universally accepted model because positive curvature can at most be weakly supported by the latest CMB observation [721, 718] but in addition, when lensing and baryon acoustic oscillation constraints are incorporated then the flat model is the best choice. However, if future observations favor positive curvature then one may interpret it as the remnant of a contracting phase at the very early universe, firstly, it is to be mentioned that there are few works in the literature [716, 717] related to the cyclic universe where a negative cosmological constant and positive spatial curvature were considered. Instead of the scalar field, they have used domain walls for the requirement of the bouncing era.

The entirety of our work is swotted as follows: section 5.2 deals with the basic equations of the present cosmological model. Also, the corresponding Einstein field equations, matter conservation equations, and the condition for the bouncing scenarios are also presented in this section. With a suitable choice of the variables the evolution, equations are converted to an autonomous system in section 5.3. The non-hyperbolic critical points are analyzed using center manifold theory and stability analysis has been discussed in the same section 5.3. We expound compactification and dynamics around the points at infinity in section 5.4. We present cosmological implications in a section 5.5. Finally, the brief discussion and concluding remarks of the present work are proposed in section 5.6.

5.2 Basic Equations

In the background of Friedmann-Lemaître-Robertson-Walker (FLRW) space-time with line element

$$ds^2 = -dt^2 + a^2(t)\left[\frac{dr^2}{1-\mathcal{K}r^2} + r^2(d\theta^2 + \sin^2 d\Phi^2)\right], \tag{5.1}$$

in co-moving coordinates (t, r, θ, ϕ), where $a(t)$ is the scale factor and $\mathcal{K}$ is the spatial curvature with $\mathcal{K} = 0, 1, -1$ corresponding to a flat, closed, or open universe, respectively. We consider the Einstein-Hilbert action with a real scalar field ϕ [700],

$$S = \int d^4x\sqrt{-g}\left(\frac{1}{2}R - \frac{1}{2}g^{\mu\nu}\partial_\mu\phi\partial_\nu\phi - V(\phi)\right), \tag{5.2}$$

where R is the Ricci scalar and $V(\phi)$ is the scalar potential. Now the Friedmann equations are given by

$$3\left(H^2 + \frac{\mathcal{K}}{a^2}\right) = \rho_\phi, \tag{5.3}$$

$$2\left(\dot{H} - \frac{\mathcal{K}}{a^2}\right) = -(\rho_\phi + p_\phi), \tag{5.4}$$

where the 'dot' denotes the derivative with respect to time, and $H = \frac{\dot{a}}{a}$ is the Hubble parameter. Here ρ_ϕ and p_ϕ are energy density and pressure of the scalar field having expression

$$\rho_\phi = \frac{1}{2}\dot{\phi}^2 + V(\phi), \tag{5.5}$$

$$p_\phi = \frac{1}{2}\dot{\phi}^2 - V(\phi). \tag{5.6}$$

Differentiate both sides of (5.3) with respect to 't' we get

$$6H\dot{H} - 6\mathcal{K}\frac{H}{a^2} = \dot{\rho_\phi}.$$

and substituting the expression of $\dot{H}$ from second Friedmann equation (*i.e.,* eqn. (5.4) in our manuscript), we get the continuity equation of scalar field as follows

$$\dot{\rho_\phi} = -3H(\rho_\phi + p_\phi). \tag{i}$$

Now differentiate both sides of (5.5) with respect to 't' we get

$$\dot{\rho_\phi} = \dot{\phi}\ddot{\phi} + V'(\phi)\dot{\phi}. \tag{ii}$$

Now adding the corresponding sides of (5.5) and (5.6) and substituting the value $\rho_\phi + p_\phi$ in the right hand side of (i), we get

$$\dot{\rho_\phi} = -3\dot{\phi}^2 H.$$

Putting this expression of $\dot{\rho_\phi}$ in (ii), we get the evolution equation of the scalar field ϕ as

$$\ddot{\phi} + 3H\dot{\phi} + V'(\phi) = 0, \tag{5.7}$$

where $V'(\phi)$ denotes differentiation of the scalar potential $V(\phi)$ with respect to ϕ. Now the above field equations (5.3 – 5.4) can be rewritten as

$$3H^2 = \rho_\phi + \rho_\mathcal{K}, \tag{5.8}$$

$$2\dot{H} = -(\rho_\phi + p_\phi) - (\rho_\mathcal{K} + p_{\mathcal{K})} \tag{5.9}$$

where

$$\rho_{\mathcal{K}} = -\frac{3\mathcal{K}}{a^2}, \quad \text{and} \quad p_{\mathcal{K}} = \frac{\mathcal{K}}{a^2} \tag{5.10}$$

are energy density and pressure of the hypothetical curvature fluid having equation of state parameter $\omega_{\mathcal{K}} = -\frac{1}{3}$. Thus the density parameter associated with the curvature fluid in the above first Friedmann equations is given by [700]

$$\Omega_{\mathcal{K}} = \frac{\rho_{curv}}{\rho_{critical}} = -\frac{\mathcal{K}}{a^2H^2}.$$

One may note from the first Friedmann equation (*i.e.,* Eq.(5.3)) that for a given scalar field energy density if the positive curvature term is significant then it gradually tries to reduce the expansion of the universe. The expansion can even be stopped if the curvature term balances the scalar field energy density. However, from the second Friedmann equation (*i.e.,* Eq.(5.4)), it is easy to see that at the very early era when 'a' is very small then positive curvature term dominates over the kinetic energy of the scalar field and consequently $\dot{H}$ is positive (*i.e.,* H is increasing) and the universe is going through an expanding era. But with the expansion, the scale factor gradually increases and at one stage the curvature term balances the kinetic energy term of the scalar field and $\dot{H}$ vanishes at that instant. Subsequently, due to dominance of the kinetic energy of the scalar field $\dot{H}$ becomes negative. So H gradually decreases and then there are two possibilities (i) H reaches a minimum (where $H > 0$) and then again H starts increasing indicating a bouncing era at minimum H, or (ii) H gradually decreases, passing through zero and then becomes negative, indicating a contracting phase [700]. This may be considered as an example how Einstein gravity may also describe a contracting phase for which so far there are no observational predictions.

On the other hand, during the contracting phase the scalar field experiences a negative friction contribution (anti-friction) and if $|H|$ is assumed to be small compared to the mass or characteristic curvature of the scalar potential. Then the friction (*i.e.,* second term in equation (6.18)) will be negligible compare to the acceleration term and the force term. So, the evolution equation of the scalar field approximately becomes

$$\ddot{\phi} + \frac{\partial V}{\partial \phi} \approx 0.$$

In particular, if $V = \frac{1}{2}m^2\phi^2$ then the scalar field oscillates like a simple harmonic oscillator. Subsequently, when $|H|$ becomes comparable to (or larger than) the characteristic mass scale, then the kinetic term gradually grows rapidly and the universe enters the big crunch. However, to avoid this ever-contracting evolution, one may note that during the simple harmonic motion of the scalar field, the kinetic term temporarily vanishes at the two endpoints. If the potential has a flat nature at the endpoints with $V(\phi) > 0$, then the evolution will be dominated by the potential energy for a longer time. But as the kinetic term grows much faster so at some epoch it balances the potential term and also the positive curvature term and the Hubble parameter vanishes again. This phase is known as the bouncing era. After this bounce, the universe again starts expanding. The well-known bouncing solution in cosmology is the de-Sitter bounce solution given by

$$a(t) = \sqrt{\frac{3\mathcal{K}}{\Lambda}} \cosh\left(\sqrt{\frac{\Lambda}{3}}t\right),$$

where $\mathcal{K} > 0$ is the spatial curvature and Λ is the positive cosmological constant [700].

5.3 Formation of the autonomous system: critical point and stability analysis

We try to obtain a qualitative picture of this cosmological model, that's why we adopt a dynamical system approach and for that choose the following dynamical variables

$$x := \frac{\dot{\phi}}{\sqrt{6}H}, \tag{5.11}$$

$$y := \frac{\sqrt{V}}{\sqrt{3}H}, \tag{5.12}$$

$$z := \frac{\sqrt{6}}{\phi}, \tag{5.13}$$

$$u := \frac{1}{\sqrt{3}\dot{a}}. \tag{5.14}$$

By using these dynamical variables the cosmic evolution equation (in the last section) can be written in an autonomous system as

$$\frac{dx}{dN} = -3x - \sqrt{\frac{3}{2}}\left(\frac{V'}{V}\right)y^2 + 3x(x^2 - \mathcal{K}u^2), \tag{5.15}$$

$$\frac{dy}{dN} = 3y(x^2 - \mathcal{K}u^2) + \sqrt{\frac{3}{2}}\left(\frac{V'}{V}\right)xy, \tag{5.16}$$

$$\frac{dz}{dN} = -xz^2, \tag{5.17}$$

$$\frac{du}{dN} = u(2x^2 - y^2) \tag{5.18}$$

together with $N = \ln a$. Using dynamical variables, the first Friedmann equation (5.8) can be rewritten as

$$\Omega_{\mathcal{K}} + x^2 + y^2 = 1, \tag{5.19}$$

where the density parameter due to the curvature term can be expressed as

$$\Omega_{\mathcal{K}} = \frac{\rho_{\mathcal{K}}}{3H^2} = -3\mathcal{K}u^2. \tag{5.20}$$

It is to be noted that the dynamical variable u is proportional to the comoving Hubble horizon. The amplitude of the scalar field ϕ is inversely related to the variable z. From Eq.(5.19) we can clearly conclude about the meaning of the dynamical variables (5.11) and (5.12): x^2 stands for the relative kinetic energy density of the scalar field while y^2 stands for its relative potential energy density of ϕ and the total relative energy density parameter due to the scalar field can be written as [739]

$$\Omega_{\phi} = \frac{\rho_{\phi}}{3H^2} = x^2 + y^2. \tag{5.21}$$

The equation of state parameter (ω_{ϕ}) can be expressed as

$$\omega_{\phi} = \frac{x^2 - y^2}{x^2 + y^2} \tag{5.22}$$

and the equation of state parameter corresponding to the combined matter field is given by

$$\omega_{total} = x^2 - y^2. \tag{5.23}$$

From (5.19), (5.20) and (5.21), we can conclude that the variables x, y, and u are not independent, they are dependent by the constraint equation

$$x^2 + y^2 - 3\mathcal{K}u^2 = 1. \tag{5.24}$$

This equation is nothing but the conservation of energy with proper scaling. In Proposition (3), we have shown that (5.15), (5.16) and (5.18) are not independent, in other words Eq.(5.18) can be obtained by using Eqs.(5.15), (5.16) and the constraint equation (5.24). Thus we omit equation (5.18) from the autonomous system and by substituting (from 5.24)

$$\mathcal{K}u^2 = \frac{1}{3}(x^2 + y^2 - 1)$$

into the right hand side of (5.15) and (5.16), we get the following modified autonomous system

$$\frac{dx}{dN} = -2x - \sqrt{\frac{3}{2}}\left(\frac{V'}{V}\right) y^2 - xy^2 + 2x^3, \tag{5.25}$$

$$\frac{dy}{dN} = y + \sqrt{\frac{3}{2}}\left(\frac{V'}{V}\right) xy + 2x^2 y - y^3, \tag{5.26}$$

$$\frac{dz}{dN} = -xz^2. \tag{5.27}$$

Note that the scalar field model corresponds to stiff matter if potential energy (P.E.) is negligible compared to kinetic energy (K.E.), while it corresponds to ΛCDM if kinetic energy is negligible compared to potential energy. In between these two extreme cases radiation will occur if K.E.=2 times the P.E. In that case the dimensionless variables x and y are not independent and the system becomes a 2D system. Also as we are interested in late time cosmology so radiation is not taken into account.

To determine a suitable form of the autonomous system, we consider several choices of the scalar field potential [742, 711, 712, 713, 714, 715, 743, 705, 706, 707, 709]. But only for power-law [706, 707] $V(\phi) = V_0\phi^{-\mu}$ and the exponential dependence [704, 705, 706, 707] as $V(\phi) = V_1 e^{-\nu\phi}$ where $V_0, V_1 > 0$ and μ, ν are constant parameters, we get the suitable form of the autonomous system. These two potentials are interesting because we find that scalar-field potential is "nonlinear" (*i.e.,* the scalar-field equation of motion is nonlinear); usually it tends to be made from exponential of the scalar field. We have not succeeded in determining the general solution of the scalar-field equation of motion (6.18), but a special solution (cosmologically relevant) can be found (in which the scalar-field energy density redshifts in a requisite manner). Somehow particularly, we find that this solution dominates at large time and a study of phase space shows that it is an attractive, time-dependent, equilibrium point [708].

5.3.1 Model 1: Power-law potential

At first we shall analyze the above dynamical system for power-law potential. The above system of first order differential equations (5.25 – 5.27) reduces to an autonomous system. The justification for such a power law form is that it satisfies the sufficiently steep condition

namely $\Gamma = \frac{V''V}{(V')^2} \geq 1$. As a result the scalar field rolls down such a potential and favours a common evolutionary path for a wide range of initial conditions [748, 742]. The form of power law can be expressed as

$$V(\phi) = V_0\phi^{-\mu}.$$

Substituting this into the right hand side of Equation (5.25) and Equation (5.26) and then the system (5.25 – 5.27) modifies to

$$\frac{dx}{dN} = -2x + \frac{\mu}{2}y^2z - xy^2 + 2x^3, \tag{5.28}$$

$$\frac{dy}{dN} = y - \frac{\mu}{2}xyz + 2x^2y - y^3, \tag{5.29}$$

$$\frac{dz}{dN} = -xz^2. \tag{5.30}$$

We have a total of five critical points corresponding to the autonomous system (5.28–5.30) out of which four are isolated critical points and another point is a line of the critical point. The set of critical points and the value of cosmological parameters corresponding to the above autonomous system are shown in Table 5.1.

Table 5.1: Table shows the set of critical points, the existence of critical points, and the value of cosmological parameters corresponding to the autonomous system (5.28–5.30):

CPs	Existence	x	y	z	$\Omega_\mathcal{K}$	Ω_ϕ	ω_ϕ	ω_{total}	q
C_1	For all $\mu \neq 0$	0	1	0	0	1	-1	-1	-1
C_2	For all $\mu \neq 0$	0	-1	0	0	1	-1	-1	-1
C_3	For all μ	1	0	0	0	1	1	1	2
C_4	For all μ	-1	0	0	0	1	1	1	2
C_5	For all μ	0	0	z_c	1	0	Not applicable	0	$\frac{1}{2}$

Stability analysis

• The critical points C_1 and C_2 exist for all $\mu \neq 0$. Near these points the curvature is negligible. These solutions are completely dominated by scalar field ($\Omega_\phi = 1$) which behaves as cosmological constant ($\omega_{total} = -1$). The cosmic evolution near the points characterizes

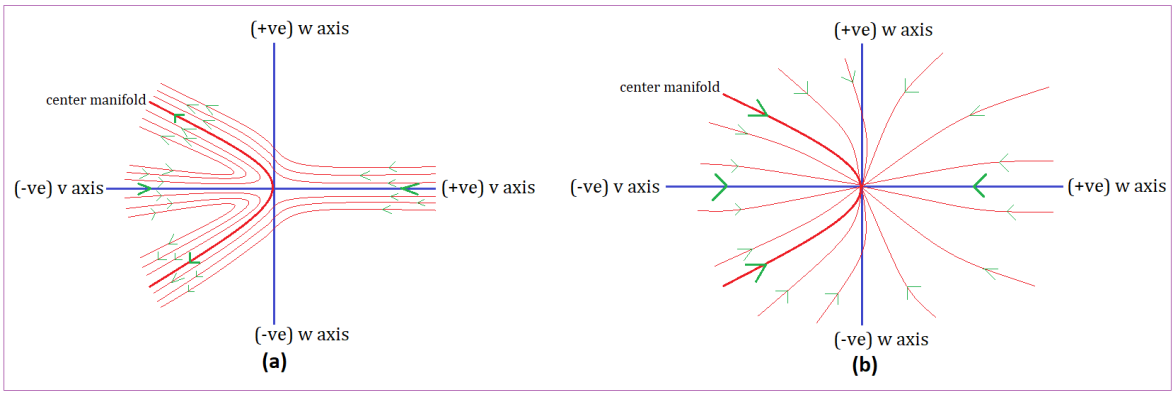

Figure 5.1: This figure shows the vector field near the origin corresponding to the critical point C_1 for positive and negative values of the parameter μ. **(a)** is for $\mu < 0$ and **(b)** is for $\mu > 0$. This figure indicates that for $\mu < 0$ the critical point C_1 behaves as a saddle node and for $\mu > 0$ the critical point C_1 behaves as a stable node.

the de-Sitter expansion ($q = -1$) of the universe. On the other hand, we note that $|\Omega_{\mathcal{K}}| \approx 0$. Then from equation (5.9) we have $\dot{H} \approx 0$, *i.e.,* the expansion rate H becomes constant.

The eigenvalues of the Jacobian matrix $J(C_1)\,(J(C_2))$ are $\lambda_1 = -3$, $\lambda_2 = -2$, and $\lambda_3 = 0$ corresponding to the eigenvectors $\mathbf{v}^{(1)} = [1, 0, 0]^T$, $\mathbf{v}^{(2)} = [0, 1, 0]^T$, and $\mathbf{v}^{(3)} = \left[\frac{\mu}{6}, 0, 1\right]^T$ respectively. Since the Jacobian matrix has one zero eigenvalue so we use center manifold theory to discuss the stability of the critical point. To apply center manifold theory, first, we use the shifting transformation $x = X$, $y = Y \pm 1$, $z = Z$ to transform the critical point $C_1(C_2)$ into the origin. Next, we use a coordinate transformation $\mathbf{u} = P\mathbf{v}$ where $\mathbf{u} = [X\ Y\ Z]^T$, $\mathbf{v} = [u\ v\ w]^T$, $P = \left[\mathbf{v}^{(1)}\ \mathbf{v}^{(2)}\ \mathbf{v}^{(3)}\right]$. From the calculation (see Proposition (4) in the Appendix), the expressions of center manifold are given by $u = 0$ and $v = \mp\frac{\mu^2}{72}w^2 + \mathcal{O}(w^4)$ and the flow on the center manifold is determined by $\frac{dw}{dN} = -\frac{\mu}{6}w^3 + \mathcal{O}(w^4)$. Notice that the flow on the center manifold depends on the sign of μ. If $\mu < 0$ then $\frac{dw}{dN} > 0$ for $w > 0$ and $\frac{dw}{dN} < 0$ for $w < 0$. So, for $\mu < 0$ the origin is a saddle point, *i.e.,* unstable in nature. Further if $\mu > 0$ then $\frac{dw}{dN} < 0$ for $w > 0$ and $\frac{dw}{dN} > 0$ for $w < 0$. Thus for $\mu > 0$ the origin is a stable node. The vector field near the origin for both of the cases are shown in figures (5.1) and (5.2). It is to be noted that the new coordinate system (u, v, w) is topologically equivalent to the old one, hence the origin in the new coordinate system, *i.e.,* the critical point $C_1(C_2)$ in the old coordinate system (x, y, z) is a saddle point for $\mu < 0$ and a stable node for $\mu > 0$.

if we take the projection of the vector field in $z = 0$ plane, that is, on the xy-plane, we can see that the system converges to the critical point $C_1(C_2)$. Note that the eigenvalues of the Jacobian matrix at the point $C_1(C_2)$ are real and negative, it follows that the critical points C_1 and C_2 are stable node and asymptotically stable in nature (see figure (5.3)).

Near C_1 and C_2 the evolution equation (6.18) takes the form $\ddot{\phi} + V'(\phi) \approx 0$. So the scalar field potential behaves as a simple harmonic oscillator and for $\mu > 0$ the oscillation amplitude decreases gradually due to the stability of the critical points.

• The critical points C_3 and C_4 exist for $\mu \in \mathbb{R}$. The critical points correspond to solutions where the constraint equation (5.9) is dominated by the kinetic energy of the scalar field with a stiff equation of state $\omega_d = 1$. There exists a decelerating phase of the universe and we also have $|\Omega_{\mathcal{K}}| \approx 0$ near these critical points. Then from equation (5.9) we have $\dot{H}$ is negative,

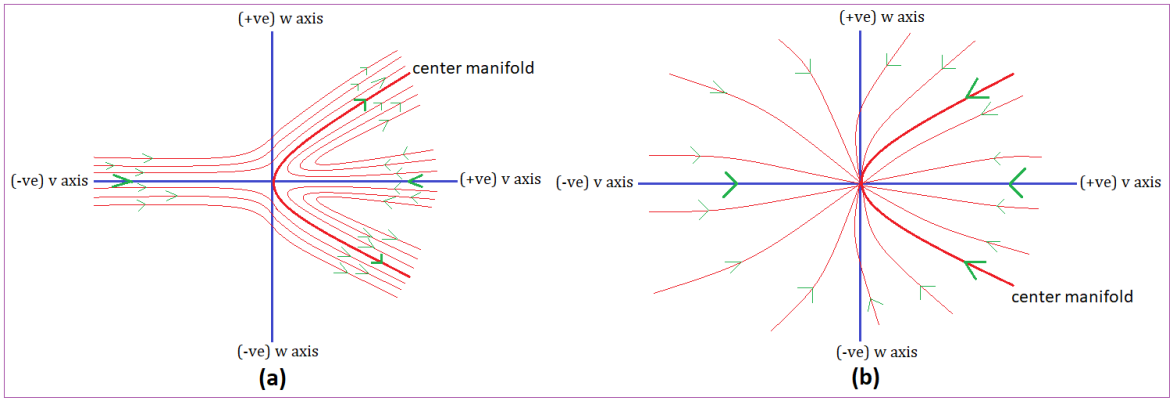

Figure 5.2: This figure shows the vector field near the origin corresponding to the critical point C_2 for positive and negative values of the parameter μ. **(a)** is for $\mu < 0$ and **(b)** is for $\mu > 0$. This figure indicates that for $\mu < 0$ the critical point C_2 behaves as a saddle node and for $\mu > 0$ the critical point C_2 behaves as a stable node.

i.e., the expansion rate H decreases.

The eigenvalues of the Jacobian matrix $J(C_3)\,(J(C_4))$ are 4, 3, and 0 corresponding to the eigenvectors $[1,0,0]^T$, $[0,1,0]^T$ and $[0,0,1]^T$ respectively. After applying shifting transformation $x = X + 1$, $y = Y$ and $z = Z$ to the autonomous system $(5.28 - 5.30)$ and then by using the center manifold theory, the equation of center manifold can be expressed as $X = 0$, $Y = 0$. This implies that the center manifold completely lying on the Z axis and the flow on the center manifold is determined by $\frac{dZ}{dN} = \mp Z^2$. Notice that $\frac{dZ}{dN} < 0$ for both of the cases $Z > 0$ or $Z < 0$ for the critical point C_3, and $\frac{dZ}{dN} > 0$ for both of the cases $Z > 0$ or $Z < 0$ for the critical point C_4. From which one concludes that the critical point $C_3(C_4)$ is a saddle node, that is, along the Z direction the orbits approach critical point C_3 for positive(negative) Z and move away from it for negative(positive) Z. The flow on the center manifold is shown as in figure (5.4) which implies that the critical points C_3 and C_4 are unstable due to its saddle-node nature.

Now if we take the projection of the vector field in $z = 0$ plane, that is, on the xy-plane, the system diverges from the critical point $C_3(C_4)$. Note that the eigenvalues are real and positive which implies that the critical point $C_3(C_4)$ is unstable in nature due to the unstable node type instability (see figure (5.3)).

If the kinetic energy grows much faster than the radiation, matter, or curvature to prevent the kinetic energy from dominating the universe, the universe continues to contract until its size becomes zero. So the Big Crunch may happen if the flow of the vector field goes towards C_3 or C_4 asymptotically. As the critical points are saddle in nature, so to avoid the Big Crunch we need to fine-tune the initial condition.

• The set of critical points C_5 exist for all $\mu \in \mathbb{R}$. This set of critical points is normally hyperbolic where the stability is confirmed by the signature of the remaining non-vanishing eigenvalues. The constraint equation (5.9) is dominated by spatial curvature near this set of points. In this case, the kinetic term is subdominant compared to the curvature contribution in eq. (5.9). Then, for $\mathcal{K} > 0$, $\dot{H}$ is positive, and the expansion rate H increases. On the other hand, for $\mathcal{K} < 0$, $\dot{H}$ is negative, and the expansion rate H decreases. Note that the line of critical point C_5 arises on the z axis so to determine the vector field near C_5

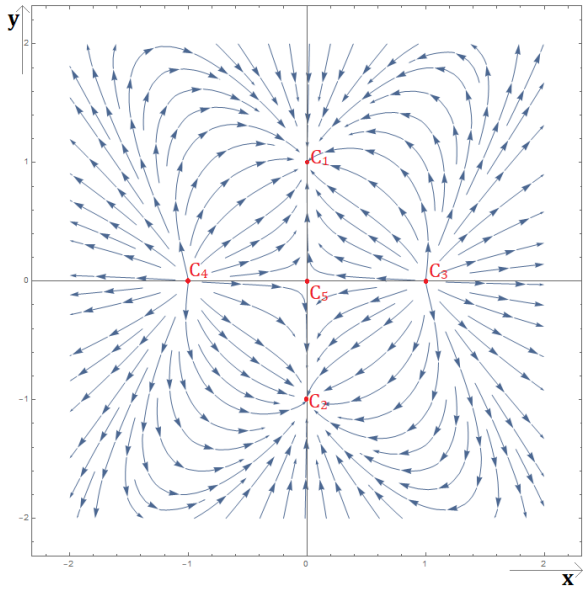

Figure 5.3: Profile of the global analysis in finite phase space for several values of μ. This figure shows the projection of the vector field on the xy plane corresponding to the autonomous system (5.28 − 5.30). The horizontal axis represents variable x and the vertical axis represents variable y. This phase plot indicates that in xy plane the critical points C_1 and C_2 behave as a stable node, C_3 and C_4 behave as an unstable node, and the critical point C_5 behaves as a saddle node for all μ.

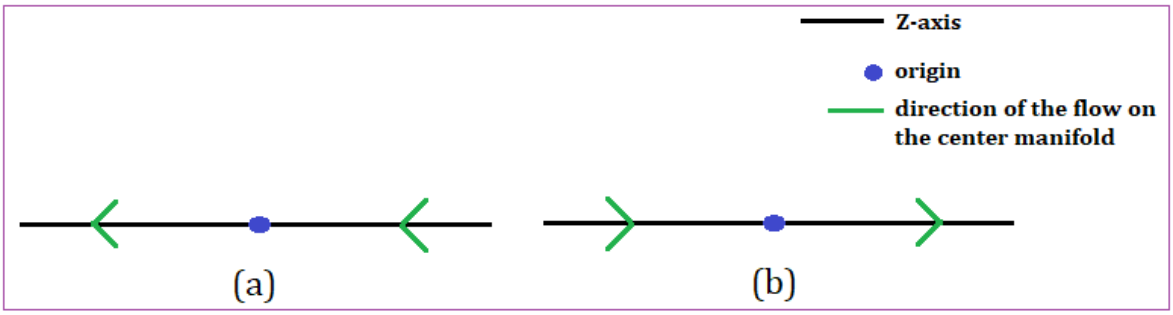

Figure 5.4: This figure shows flow direction on the center manifold corresponding to the critical point C_3 and C_4. **(a)** is for the critical point C_3 and **(b)** is for the critical point C_4. The direction of the flow on the center manifold indicates that both of the critical points are saddle-node in nature.

we consider only the first two equations of the autonomous system (5.28 – 5.30) and taking $z = const.$ Due to presence of one positive and one negative eigenvalue corresponding to first two equations of the autonomous system, by Hartman-Grobman theorem, we conclude that the line of critical point C_5 is a saddle point and unstable in nature (figure (5.5)) for all μ. So depending on the initial condition there exists late time (along stable eigen direction) decelerating dust-dominated universe.

The eigenvalues of the Jacobian matrix at all critical points corresponding to the autonomous system (5.28 – 5.30) and the nature of critical points are shown in Table 5.2.

Table 5.2: Table shows the eigenvalues ($\lambda_1,\ \lambda_2,\ \lambda_3$) of the Jacobian matrix corresponding to the autonomous system (5.28 – 5.30) at each critical points and the nature of all critical points :

CPs	λ_1	λ_2	λ_3	Nature of Critical points
C_1	-3	-2	0	Saddle node for $\mu < 0$ and stable node for $\mu > 0$.
C_2	-3	-2	0	Saddle node for $\mu < 0$ and stable node for $\mu > 0$.
C_3	4	3	0	Saddle node for all μ (unstable node in xy-plane).
C_4	4	3	0	Saddle node for all μ (unstable node in xy-plane).
C_5	-2	1	0	Saddle node for all μ.

5.3.2 Model 2: Exponential potential

As before this choice of the potential simplifies the system of equations (5.25 – 5.27) into an autonomous system. The choice of exponential potential corresponds to an extreme example of quintessence [748, 742]. Exponential potential will remain subdominant if it was so initially. Further, nucleosynthesis constraints the energy density of the quintessence field to be smaller than the associated background energy density at the early era. The form of exponential dependence can be expressed as

$$V(\phi) = V_0 e^{-\nu\phi}.$$

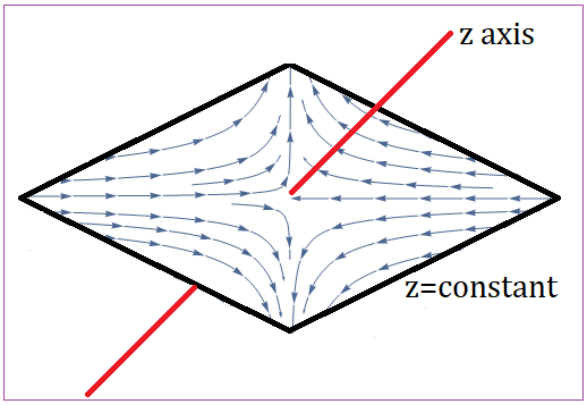

Figure 5.5: This figure shows the projection of the vector field near C_5 on $z = const.$ plane. This phase plot indicates that the line of critical points C_5 behaves as a saddle node for all μ.

Substituting this into the right hand side of Eq.(5.25) and Eq.(5.26) and then the system $(5.25 - 5.27)$ modifies to

$$\frac{dx}{dN} = -2x + \sqrt{\frac{3}{2}}\nu y^2 - xy^2 + 2x^3, \tag{5.31}$$

$$\frac{dy}{dN} = y - \sqrt{\frac{3}{2}}\nu xy + 2x^2 y - y^3, \tag{5.32}$$

$$\frac{dz}{dN} = -xz^2. \tag{5.33}$$

We can see that the first two equations of the autonomous system $(5.31 - 5.33)$ are independent of the variable z. So when we are going to determine the critical points, we can see that most of the physical meaningful critical points are lying on the xy-plane. Thus the last equation of the autonomous system, that is, equation (5.33) is not interesting to provide the stability criteria of the critical points corresponding to the autonomous system $(5.31 - 5.33)$. Further, note that the variable z can not impact physically on this model as all the expressions of the cosmological parameters are independent of z. That's why it is more interesting if we consider $z = 0$ and analyze the stability of the critical points in xy-plane. We have a total of seven physically meaningful isolated critical points corresponding to the autonomous system $(5.31 - 5.32)$. The set of critical points corresponding to this autonomous system and the value of cosmological parameters are shown in Table 5.3.

Stability analysis

• The critical point P_0 exists for all ν. For this solution, the kinetic term is subdominant compared to the curvature contribution in eq. (5.9). Then, for $\mathcal{K} > 0$, $\dot{H}$ is positive, and the expansion rate H increases. On the other hand, for $\mathcal{K} < 0$, $\dot{H}$ is negative, and the expansion rate H decreases.

The eigenvalues of the Jacobian matrix $J(P_0)$ are $\lambda_1 = -2$, and $\lambda_2 = 1$. Since $J(P_0)$ has no eigenvalue whose absolute value is equal to 0, the fixed point P_0 is hyperbolic. Since $\lambda_1 < 0$ and $\lambda_2 > 0$, thus by using the Hartman-Grobman theorem, we conclude that the critical point P_0 is a saddle-node and unstable in nature (see figure (5.6)). depending on

Table 5.3: Table shows the set of critical points, the existence of critical points, and the value of cosmological parameters corresponding to the autonomous system (5.31 − 5.32) :

CPs	Existence	x	y	$\Omega_{\mathcal{K}}$	Ω_ϕ	ω_ϕ	ω_{total}	q
P_0	For all ν	0	0	1	0	NA	0	$\frac{1}{2}$
P_1	For all ν	1	0	0	1	1	1	2
P_2	For all ν	-1	0	0	1	1	1	2
P_3	For $0 \leq \nu^2 \leq 6$	$\frac{\nu}{\sqrt{6}}$	$\sqrt{1-\frac{\nu^2}{6}}$	0	1	$\frac{\nu^2}{3}-1$	$\frac{\nu^2}{3}-1$	$\frac{1}{2}(\nu^2-2)$
P_4	For $0 \leq \nu^2 \leq 6$	$\frac{\nu}{\sqrt{6}}$	$-\sqrt{1-\frac{\nu^2}{6}}$	0	1	$\frac{\nu^2}{3}-1$	$\frac{\nu^2}{3}-1$	$\frac{1}{2}(\nu^2-2)$
P_5	For all $\nu \neq 0$	$\frac{1}{\nu}\sqrt{\frac{2}{3}}$	$\frac{2}{\sqrt{3}\nu}$	$1-\frac{2}{\nu^2}$	$\frac{2}{\nu^2}$	$-\frac{1}{3}$	$-\frac{2}{3\nu^2}$	$\frac{1}{2}\left(1-\frac{2}{\nu^2}\right)$
P_6	For all $\nu \neq 0$	$\frac{1}{\nu}\sqrt{\frac{2}{3}}$	$-\frac{2}{\sqrt{3}\nu}$	$1-\frac{2}{\nu^2}$	$\frac{2}{\nu^2}$	$-\frac{1}{3}$	$-\frac{2}{3\nu^2}$	$\frac{1}{2}\left(1-\frac{2}{\nu^2}\right)$

the initial condition there exists a late time (along stable eigen direction) decelerating dust-dominated universe.

• Similar to the case of C_3 and C_4, the critical point P_1 and P_2 exist for all ν and correspond to the solutions where the constraint equation (5.9) is dominated by the kinetic energy of the scalar field with a stiff equation of state $\omega_d = 1$. There exists a decelerating phase of the universe and we also have $|\Omega_{\mathcal{K}}| \approx 0$ near these critical points. Then from equation (5.9) we have $\dot{H}$ is negative, *i.e.,* the expansion rate H decreases.

The eigenvalues of the Jacobian matrix $J(P_1)$ are $\lambda_1 = 4$, and $\lambda_2 = 3 - \sqrt{\frac{3}{2}}\nu$. Notice that the eigenvalue λ_1 is always positive which implies that the critical point P_1 is always unstable in nature but the type of instability is determined by the nature of the eigenvalue λ_2. The critical point P_1 is hyperbolic for $\nu \neq \sqrt{6}$ and nonhyperbolic for $\nu = \sqrt{6}$. For $\nu < \sqrt{6}$, the eigenvalue λ_2 is positive which implies that the critical point P_1 is an unstable node. For $\nu > \sqrt{6}$, we have $\lambda_2 < 0$ and consequently the critical point P_1 is a saddle node. To determine the stability of P_1 for $\nu = \sqrt{6}$, we use center manifold theory which we have already applied to discuss the stability of the critical point C_1. To apply this theory, first,

we use a shifting transformation ($x = X + 1, y = Y$) to transform the fixed point P_1 into the origin. Then using the similar arguments that we have used to determine the stability analysis of C_1, we obtained that the expression of the center manifold is $X = -\frac{1}{2}Y^2 + \mathcal{O}(Y^3)$ and the flow on the center manifold is determined by the equation $\frac{dY}{dN} = -\frac{3}{2}Y^3 + \mathcal{O}(Y^4)$. Note that $\frac{dY}{dN} < 0$ while $Y > 0$ and $\frac{dY}{dN} > 0$ for $Y < 0$. This implies that the flow on the center manifold is stable but the origin is a saddle node. As the transformed system (X, Y) is topologically equivalent to the old one, the critical point P_1 also exhibits saddle-node type instability for $\nu = \sqrt{6}$. Hence, the critical point P_1 is a saddle-node for $\nu \geq \sqrt{6}$ and unstable node for $\nu < \sqrt{6}$ (see figure (5.6)).

The eigenvalues of the Jacobian matrix $J(P_2)$ are $\lambda_1 = 4$, and $\lambda_2 = 3 + \sqrt{\frac{3}{2}}\nu$. Notice that the eigenvalue λ_1 is always positive which implies that the critical point P_2 is always unstable in nature but the type of instability is determined by the nature of the eigenvalue λ_2. The critical point P_2 is hyperbolic for $\nu \neq -\sqrt{6}$ and nonhyperbolic for $\nu = -\sqrt{6}$. For $\nu > -\sqrt{6}$, the eigenvalue λ_2 is positive which implies that the critical point P_2 is an unstable node. For $\nu < -\sqrt{6}$, we have $\lambda_2 < 0$ and consequently the critical point P_2 is a saddle node. To determine the stability of P_2 for $\nu = \sqrt{6}$, we use center manifold theory and to apply this theory, first, we use a shifting transformation ($x = X - 1, y = Y$) to transform the fixed point P_2 into the origin. Then the expression of the center manifold is given by $X = \frac{1}{2}Y^2 + \mathcal{O}(Y^3)$ and the flow on the center manifold is determined by the equation $\frac{dY}{dN} = -\frac{3}{2}Y^3 + \mathcal{O}(Y^4)$. Note that $\frac{dY}{dN} < 0$ while $Y > 0$ and $\frac{dY}{dN} > 0$ for $Y < 0$. This implies that the flow on the center manifold is stable but the origin is a saddle node. Hence, the critical point P_2 is a saddle-node for $\nu \leq -\sqrt{6}$ and unstable node for $\nu > -\sqrt{6}$ (see figure (5.6)).

So the Big Crunch can be avoided for $-\sqrt{6} < \nu < \sqrt{6}$ due to the instability of the critical points. One may note that depending on the initial condition there exists a late time (along stable eigen direction) kinetic dominated decelerating universe.

• The fixed point P_3 and P_4 exist for $\nu^2 \leq 6$. Varying ν we get a non-isolated set of critical points which are completely dominated by kinetic energy ($\Omega_\phi = 1$ and $\dot{\phi} \neq 0$). The DE can represent either quintessence or any other exotic type fluid depending on the parameter ν. Specially, the depletion $\nu^2 < 2$ ($\nu \neq 0$) implies that the scalar field behaves as quintessence like fluid and there exists an accelerated universe (since for this case, $-1 < \omega_{total} < -\frac{1}{3}, q < 0$) near these critical points whereas the scalar field DE behaves as dust for $\nu^2 = 3$ ($\omega_\phi = 0$) and in this case the solutions insinuate dust-dominated decelerating phase ($\omega_{total} = 0,\ q = \frac{1}{2},\ \Omega_\mathcal{K} = 0,\ \Omega_\phi = 1$) of the cosmic evolution.

The eigenvalues of the Jacobian matrix $J(P_3)$ are $\lambda_1 = -2 + \nu^2$, and $\lambda_2 = \frac{1}{2}(\nu^2 - 6)$. The critical point P_3 is hyperbolic for $\nu \neq \pm\sqrt{2}, \pm\sqrt{6}$ because $\lambda_1 = 0$ for $\nu = \pm\sqrt{2}$ and $\lambda_2 = 0$ for $\nu = \pm\sqrt{6}$. Consequently, the critical point P_3 is nonhyperbolic if $\nu = \pm\sqrt{2}$ or $\nu = \pm\sqrt{6}$.

Hyperbolic case $\left(\nu \neq \pm\sqrt{2}, \pm\sqrt{6}\right)$: As the region of existence of the critical point is $-\sqrt{6} \leq \nu \leq \sqrt{6}$, to determine the stability of this critical point in this case, we consider three intervals (i) $-\sqrt{6} < \nu < -\sqrt{2}$, (ii) $-\sqrt{2} < \nu < \sqrt{2}$, and (iii) $\sqrt{2} < \nu < \sqrt{6}$. For $\nu \in (-\sqrt{6}, -\sqrt{2})$, we have $\lambda_1 > 0$ and $\lambda_2 < 0$, it follows that the critical point P_3 is a saddle node and unstable in nature. For $\nu \in (-\sqrt{2}, \sqrt{2})$, we can see that $\lambda_1, \lambda_2 < 0$ and this implies that P_3 is a stable node and asymptotically stable in nature. Lastly, for $\nu \in (\sqrt{2}, \sqrt{6})$, we have $\lambda_1 > 0$ and $\lambda_2 < 0$, thus in this interval of ν the critical point P_3 is a saddle-node and unstable in nature (see figure (5.6)).

Nonhyperbolic case $\left(\nu = \sqrt{2}$ or $\nu = -\sqrt{2}$ or $\nu = \sqrt{6}$ or $\nu = -\sqrt{6}\right)$:

We use the center manifold theory to determine the stability of P_3 for this case. To

apply this theory, first, we use a shifting transformation $\left(x = X + \frac{\nu}{\sqrt{6}}, y = Y + \sqrt{1 - \frac{\nu^2}{6}}\right)$ to transform the critical point P_3 into the origin. Next, we use a coordinate transformation $\mathbf{u} = P\mathbf{v}$ where $\mathbf{u} = [X\ Y]^T$, $\mathbf{v} = [U\ V]^T$, $P = [\mathbf{v_1}\ \mathbf{v_2}]$ and $\mathbf{v_1}$, and $\mathbf{v_2}$ are the eigenvectors corresponding to the eigenvalues λ_1, and λ_2 respectively. For $\nu = \sqrt{2}$, the equations of center manifold is given by $U = \sqrt{\frac{3}{2}}V^2 + \mathcal{O}(V^3)$, and the flow on the center manifold is determined by $\frac{dV}{dN} = 4\sqrt{6}V^2 + \mathcal{O}(V^3)$. Note that $\frac{dV}{dN} > 0$ for $V > 0$ or $V < 0$ which implies that the origin is a saddle-node and unstable in nature (see figure (5.6)). For $\nu = -\sqrt{2}$, the expression of the center manifold and the flow on the center manifold are the same as of $\nu = \sqrt{2}$ case and consequently, the origin exhibits a similar type of stability in this case also. For $\nu = \sqrt{6}$ the critical point P_3 converts into P_1 and for $\nu = -\sqrt{6}$, P_3 converts into P_2 and the stability analysis of these critical points already discussed.

The eigenvalues of the Jacobian matrix $J(P_4)$ are $\lambda_1 = -2 + \nu^2$, and $\lambda_2 = \frac{1}{2}(\nu^2 - 6)$. The critical point P_4 is hyperbolic for $\nu \neq \pm\sqrt{2}, \pm\sqrt{6}$ because $\lambda_1 = 0$ for $\nu = \pm\sqrt{2}$ and $\lambda_2 = 0$ for $\nu = \pm\sqrt{6}$. Consequently, the critical point P_4 is nonhyperbolic if $\nu = \pm\sqrt{2}$ or $\nu = \pm\sqrt{6}$.

Hyperbolic case $\left(\nu \neq \pm\sqrt{2}, \pm\sqrt{6}\right)$: As the region of existence of the critical point is $-\sqrt{6} \leq \nu \leq \sqrt{6}$, to determine the stability of this critical point in this case, we consider three intervals (i) $-\sqrt{6} < \nu < -\sqrt{2}$, (ii) $-\sqrt{2} < \nu < \sqrt{2}$, and (iii) $\sqrt{2} < \nu < \sqrt{6}$. For $\nu \in (-\sqrt{6}, -\sqrt{2})$, we have $\lambda_1 > 0$ and $\lambda_2 < 0$ which implies that the critical point P_4 is a saddle node and unstable in nature. Now while $\nu \in (-\sqrt{2}, \sqrt{2})$, we can see that $\lambda_1, \lambda_2 < 0$ and this implies that P_4 is a stable node and asymptotically stablein nature. Lastly, for $\nu \in (\sqrt{2}, \sqrt{6})$, we have $\lambda_1 > 0$ and $\lambda_2 < 0$ which implies that the critical point P_4 is a saddle-node and unstable in nature (see figure (5.6)).

Nonhyperbolic case $\left(\nu = \sqrt{2}$ or $\nu = -\sqrt{2}$ or $\nu = \sqrt{6}$ or $\nu = -\sqrt{6}\right)$:

We use the center manifold theory to determine the stability of P_4 for this case. To apply this theory, first, we use a shifting transformation $\left(x = X + \frac{\nu}{\sqrt{6}}, y = Y - \sqrt{1 - \frac{\nu^2}{6}}\right)$ to transform the critical point P_4 into the origin. Next, we use a coordinate transformation $\mathbf{u} = P\mathbf{v}$ where $\mathbf{u} = [X\ Y]^T$, $\mathbf{v} = [U\ V]^T$, $P = [\mathbf{v_1}\ \mathbf{v_2}]$ and $\mathbf{v_1}$, and $\mathbf{v_2}$ are the eigenvectors corresponding to the eigenvalues λ_1, and λ_2 respectively. For $\nu = \sqrt{2}$, the equations of center manifold is given by $U = -\sqrt{\frac{3}{2}}V^2 + \mathcal{O}(V^3)$, and the flow on the center manifold is determined by $V' = -4\sqrt{6}V^2 + \mathcal{O}(V^3)$. Note that $V' < 0$ for $V > 0$ or $V < 0$ which implies that the origin is a saddle-node and unstable in nature (see figure (5.6)). For $\nu = -\sqrt{2}$, the expression of the center manifold and the flow on the center manifold are the same as of $\nu = \sqrt{2}$ case and consequently the origin exhibits the similar type of stability in this case also. For $\nu = \sqrt{6}$ the critical point P_4 converts into P_1 and for $\nu = -\sqrt{6}$, P_4 converts into P_2 and the stability analysis of these critical points already discussed.

Therefore, one can conclude that the points P_3 and P_4 correspond to kinetic dominated solutions which behaves as quintessence like fluid ($\nu^2 < 2$) and there exists an accelerated universe at late times, although cosmological coincidence problem can not be alleviated by these points. On the other hand, late time decelerated solution ($2 \leq \nu^2 \leq 6$) depending on the initial condition of the autonomous system of model 2.

• Scaling solutions represented by the critical points P_5 and P_6 exist for all $\nu \neq 0$. Varying ν we get a non-isolated set of critical points where the nature (hyperbolic or normally-hyperbolic) of points depending on the values of ν. Near these critical points scalar field DE behaves as quintessence boundary ($\omega_\phi = -\frac{1}{3}$). As $0 \leq \Omega_\phi \leq 1$ when $\mathcal{K} < 0$ (from

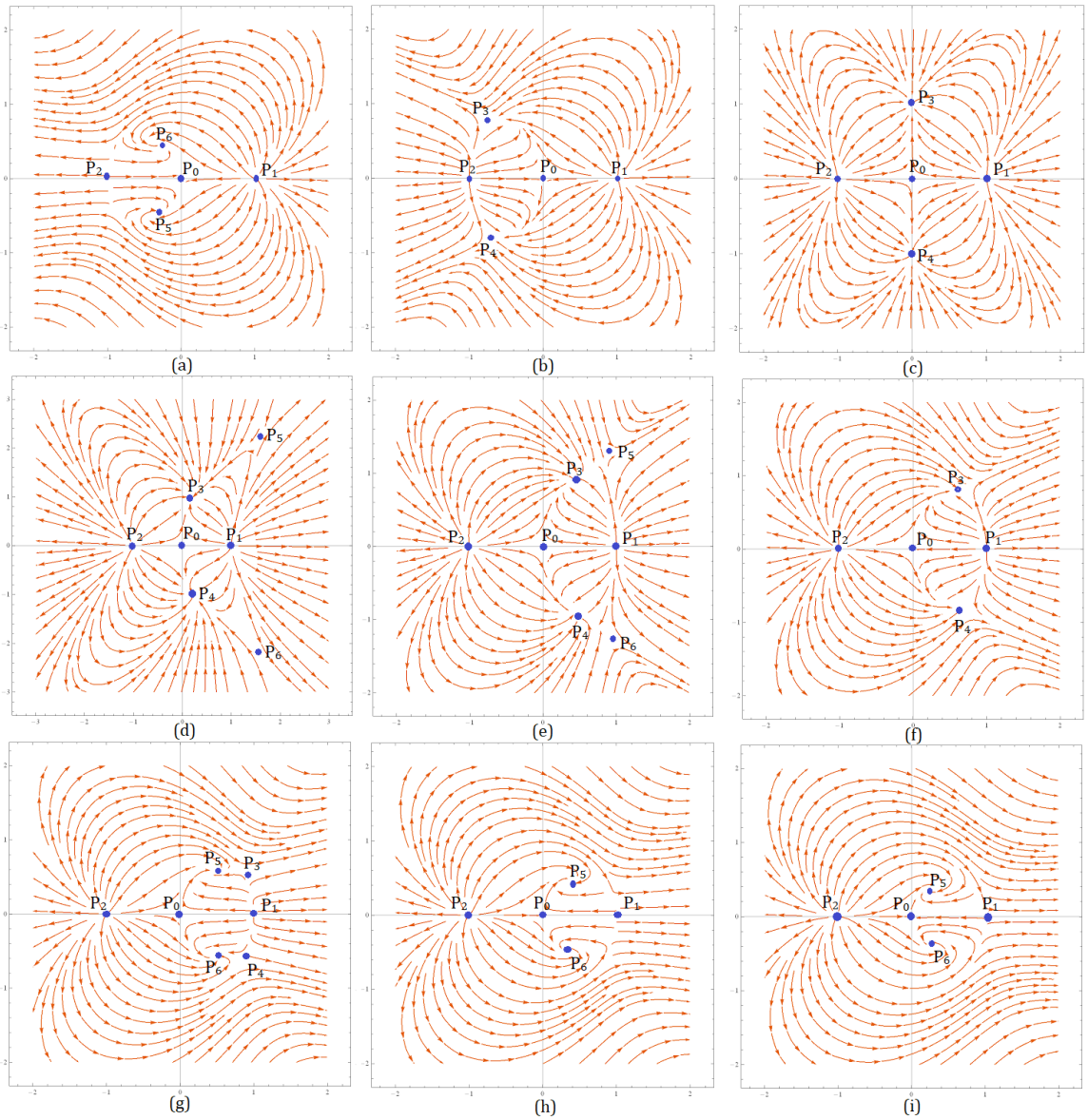

Figure 5.6: Profile of the global analysis in finite phase space for several values of ν. The horizontal axis represents variable 'x' and vertical axis represents variable 'y'. (a) corresponds to $\nu = -\sqrt{6}$: P_0 and P_2 are saddle node, P_1 is an unstable node, and P_5 and P_6 are spiral sink, (b) corresponds to $\nu = -\sqrt{2}$: P_0, P_3 and P_4 are saddle node, P_1 and P_2 are unstable node, (c) corresponds to $\nu = 0$: P_0 is a saddle node, P_1 and P_2 are unstable node, and P_3 and P_4 are stable node, (d) corresponds to $\nu = \frac{1}{2}$: where P_0 is a saddle node, P_1 and P_2 are unstable node, P_3 and P_4 are stable node, and P_5 and P_6 are saddle node, (e) corresponds to $\nu = 1$: P_0 is a saddle node, P_1 and P_2 are unstable node, P_3 and P_4 are stable node, and P_5 and P_6 are saddle node, (f) corresponds to $\nu = \sqrt{2}$: P_0, P_3 and P_4 are saddle node, P_1 and P_2 are unstable node, (g) corresponds to $\nu = 2$: P_0, P_3 and P_4 are saddle node, P_1 and P_2 are unstable node, and P_5 and P_6 are spiral sink, (h) corresponds to $\nu = \sqrt{6}$: P_0 and P_1 are saddle node, P_2 is an unstable node, and P_5 and P_6 are spiral sink, and (i) corresponds to $\nu = 3$: P_0 and P_1 are saddle node, P_2 is an unstable node, and P_5 and P_6 are spiral sink.

eq.(5.24)), so for cosmological viability the parameter ν must satisfy $\nu^2 \geq 2$. In this case, there exists always a decelerating universe. On the other hand, for $\mathcal{K} > 0$ there exists an accelerating universe when $\nu^2 < 2$. Cosmic coincidence problem can be alleviated by these points depending on the values of ν.

The eigenvalues of the Jacobian matrices $J(P_5)$ and $J(P_6)$ are same and those are $\lambda_1 = \frac{-\nu^2+\sqrt{(8-3\nu^2)\nu^2}}{\nu^2}$, and $\lambda_2 = \frac{-\nu^2-\sqrt{(8-3\nu^2)\nu^2}}{\nu^2}$. Thus the critical points P_5 and P_6 are hyperbolic for $\nu \neq \pm\sqrt{2}$ and nonhyperbolic for $\nu = \pm\sqrt{2}$. For $\nu^2 < 2$, we can observe that $\lambda_1 > 0$ and $\lambda_2 < 0$ which concludes that P_5 and P_6 saddle point and unstable in nature. For $2 < \nu^2 < \frac{8}{3}$, we can see that $\lambda_1, \lambda_2 < 0$ which implies that the critical points P_5 and P_6 are asymptotically stable in nature due to the stable node type stability. For $\nu^2 > \frac{8}{3}$, the eigenvalues are complex conjugate to each other with negative real part which implies that the critical points P_5 and P_6 are spiral sink and asymptotically stable in nature (see figure (5.6)). For $\nu = \pm\sqrt{2}$, the coordinate of $P_5(P_6)$ is the same as of $P_3(P_4)$ for $\nu = \pm\sqrt{2}$ and the stability analysis corresponding to these two cases already discussed. From the discussion, we conclude that P_5 and P_6 both are saddle-node and unstable in nature for $\nu = \pm\sqrt{2}$. The eigenvalues of the Jacobian matrix at all critical points corresponding to the autonomous system (5.31 – 5.32) and the nature of critical points are shown in Table 5.4.

Therefore, the kinetic dominated solution at $\nu^2 = 2$ is saddle-node in nature. For sufficiently flat potential $\nu^2 \leq 2$ one may get accelerating universe at late time depending on the initial condition of the model 2. Depending on some parameter restrictions, the decelerating universe is the late-time attractor describing by these points.

If we consider our analysis in the three-dimensional coordinate system, that is, in (x, y, z) coordinate system, then we can observe that for all possible cases, the critical points are nonhyperbolic in nature. To determine the stability of the critical points by applying the center manifold theory, we conclude that for all critical points, the center manifolds are lying on the z-axis and the flows on the center manifold are unstable in nature.

5.4 Compactification and the dynamics around the critical points at infinity

The idea to compactify the space $\mathbb{R}^n$ by the addition of points at infinity and to map them into finite points is frequently used in the setting of two-dimensional differential equations [725, 726, 727]. An early study of analyzing the global behavior of a planar dynamical system via compactification was carried out by Bendixson using the stereographic projection of the sphere (often called Bendixson sphere) onto the plane. However, this stereographic projection has the drawback of obliterating the "different directions at infinity" [728]. French mathematician Henri Poincaré overcame this difficulty by projecting $\mathbb{R}^2$ onto the Poincaré hemisphere through its center.

In this compactification scheme, we draw straight lines starting from the center of the unit sphere $S^2 = \{(X, Y, Z) \in \mathbb{R}^3 \mid X^2 + Y^2 + Z^2 = 1\}$ to xy-plane which is tangent to S^2 at either the north or south pole. It is to be noted that each straight line meets the unit sphere once and the xy plane once. Let a straight line intersects the sphere at (X_1, Y_1, Z_1) and the xy-plane at (x_1, y_1), then our projective transformation is realized by the transformation

$$x_1 = \frac{X_1}{Z_1}, \; y_1 = \frac{Y_1}{Z_1}. \tag{5.34}$$

Table 5.4: Table shows the eigenvalues ($\lambda_1,\ \lambda_2$) of the Jacobian matrix corresponding to the autonomous system (5.31 − 5.32) at each critical points and the nature of all critical points :

CPs	λ_1	λ_2	Nature of Critical points
P_0	-2	1	Saddle node for all ν.
P_1	4	$3-\sqrt{\frac{3}{2}}\nu$	Saddle node for $\nu \geq \sqrt{6}$ and unstable node for $\nu < \sqrt{6}$.
P_2	4	$3+\sqrt{\frac{3}{2}}\nu$	Saddle node for $\nu \leq -\sqrt{6}$ and unstable node for $\nu > -\sqrt{6}$.
P_3	$-2+\nu^2$	$\frac{1}{2}(\nu^2-6)$	Stable node for $\nu^2 < 2$ and saddle-node for $2 \leq \nu^2 \leq 6$.
P_4	$-2+\nu^2$	$\frac{1}{2}(\nu^2-6)$	Stable node for $\nu^2 < 2$ and saddle-node for $2 \leq \nu^2 \leq 6$.
P_5	$\frac{-\nu^2+\sqrt{(8-3\nu^2)\nu^2}}{\nu^2}$	$\frac{-\nu^2-\sqrt{(8-3\nu^2)\nu^2}}{\nu^2}$	Saddle node for $\nu^2 \leq 2$, stable node for $2 < \nu^2 \leq \frac{8}{3}$, and stable focus if $\nu^2 > \frac{8}{3}$.
P_6	$\frac{-\nu^2+\sqrt{(8-3\nu^2)\nu^2}}{\nu^2}$	$\frac{-\nu^2-\sqrt{(8-3\nu^2)\nu^2}}{\nu^2}$	Saddle node for $\nu^2 \leq 2$, stable node for $2 < \nu^2 \leq \frac{8}{3}$, and stable focus if $\nu^2 > \frac{8}{3}$.

So an arbitrary point (x, y) on the xy-plane can be expressed uniquely by a point (X, Y, Z) on the upper/lower half of the sphere as (5.34) [728]. This scheme has the advantage that the critical points of different directions at infinity are spread out along the equator of the sphere.

Given an autonomous system of differential equations on $\mathbb{R}^2$

$$x' = P(x, y), \tag{5.35}$$
$$y' = Q(x, y) \tag{5.36}$$

where P and Q are polynomial functions of x and y. We can write (5.35) and (5.36) in the form of a single differential equation

$$\frac{dy}{dx} = \frac{Q(x, y)}{P(x, y)}$$

which yields

$$Q(x, y)dx - P(x, y)dy = 0. \tag{5.37}$$

Now for any point (x, y), using (5.34), we obtain

$$dx = \frac{ZdX - XdZ}{Z^2}, \; dy = \frac{ZdY - YdZ}{Z^2}. \tag{5.38}$$

Hence, the differential equation (5.37) can be represented as

$$Q(ZdX - XdZ) - P(ZdY - YdZ) = 0 \tag{5.39}$$

where

$$P = P(x, y) = P\left(X/Z, Y/Z\right)$$

and

$$Q = Q(x, y) = Q\left(X/Z, Y/Z\right).$$

Let m be the maximum degree of the terms in P and Q. We multiply both side of the equation (5.39) by Z^m to eliminate Z from the denominator and obtain

$$ZQ^*dX - ZP^*dY + (YP^* - XQ^*)dZ = 0 \tag{5.40}$$

where

$$P^*(X, Y, Z) = Z^m P(X/Z, Y/Z)$$

and

$$Q^*(X, Y, Z) = Z^m Q(X/Z, Y/Z)$$

are polynomials in (X, Y, Z).

The equator of S^2 can be expressed by $\{(X, Y, 0)|X^2 + Y^2 = 1\}$. So, the critical points of (5.40) on the equator of S^2 where $Z = 0$ are given by the equation

$$XQ^* - YP^* = 0. \tag{5.41}$$

On the equator of the Poincaré sphere we can derive

$$\begin{aligned} XQ^* - YP^* &= XQ_m(X, Y) - YP_m(X, Y) \\ &= \mathcal{S} \;\; \text{(say)}, \end{aligned} \tag{5.42}$$

where P_m and Q_m are homogeneous m^{th} degree polynomials in x and y of the system (5.35)$-$(5.36). So the critical points at infinity are the set $\{(X, Y, 0) \mid X^2+Y^2 = 1 \text{ and } \mathcal{S} = 0\}$. Here we do not consider the Eq.(5.30) of the autonomous system (5.28 – 5.30) and Eq.(5.33) of the autonomous system (5.31 – 5.33). It is to be noted that we get vanishing center manifold equation and vanishing flow near the point at infinity for both of the models for the two equations (5.30) and (5.33). So it is convenient to study the characteristics of the vector field on xy plane for the autonomous systems (5.28 – 5.30) and (5.31 – 5.33). Then both of the above autonomous systems can be converted to the following two-dimensional system

$$\frac{dx}{dN} = -2x - xy^2 + 2x^3, \tag{5.43}$$

$$\frac{dy}{dN} = y + 2x^2y - y^3. \tag{5.44}$$

For the autonomous system (5.43 – 5.44), we obtain the equation (5.41) as

$$XQ_3(X, Y) - YP_3(X, Y) = X(2X^2Y - Y^3) - Y(-XY^2 + 2X^3) = 0. \tag{5.45}$$

Hence, the critical points on the Poincaré sphere are $(X_c, Y_c, 0)$ with $X_c^2 + Y_c^2 = 1$.

It is to be noted that the critical points are non-isolated in nature and the flow in a neighborhood of any critical point $(X_c, Y_c, 0)$ on the equator of the Poincaré sphere S^2, except the points $(0, \pm 1, 0)$, is topologically equivalent to the flow defined by the following system

$$\begin{aligned} \pm\frac{dv}{dN} &= vw^m P\left(\frac{1}{w}, \frac{v}{w}\right) - w^m Q\left(\frac{1}{w}, \frac{v}{w}\right) \\ \pm\frac{dw}{dN} &= w^{m+1} P\left(\frac{1}{w}, \frac{v}{w}\right) \end{aligned} \tag{5.46}$$

where

$$\begin{aligned} P\left(\frac{1}{w}, \frac{v}{w}\right) &= -\frac{2}{w} - \frac{v^2}{w^3} + \frac{2}{w^3}, \\ Q\left(\frac{1}{w}, \frac{v}{w}\right) &= \frac{v}{w} + 2\frac{v}{w^3} - \frac{v^3}{w^3}. \end{aligned}$$

or equivalently,

$$\frac{dv}{dN} = 3vw^2, \tag{5.47}$$

$$\frac{dw}{dN} = -2w + 2w^3 + v^2w. \tag{5.48}$$

by considering negative signs. Note that $(v_c, 0)$ is non-isolated critical points for the above system (5.47). The eigenvalues of the Jacobian matrix at $(v_c, 0)$ are 0 and $-2+v_c^2$. For $|v_c| \leq 1$, we get so $-2+v_c^2 < 0$ which follows that the vector field near the critical point $(v_c, 0)$ is stable along w axis. On the other hand, for $w \neq 0$ and $v > 0$, we have form equation (5.47) that $\frac{dv}{dN} > 0$ and for $v < 0$, we have $\frac{dv}{dN} < 0$. One may note that the flow comes towards

the line of critical points rapidly compare to it goes away from the critical line. So we can conclude that except the points $(0, \pm 1, 0)$, the other non-isolated points on the equator of the Poincaré sphere are saddle node (see figure (5.7(a))) in nature and cosmological bounce may happen near the points at infinity (see section 5.5.3).

Similarly, the flow in a neighborhood of any critical point $(X_c, Y_c, 0)$ on the equator of the Poincaré sphere S^2, except the points $(\pm 1, 0, 0)$, is topologically equivalent to the flow defined by the following system

$$\begin{aligned} \pm\frac{du}{dN} &= uw^m Q\left(\frac{u}{w}, \frac{1}{w}\right) - w^m P\left(\frac{u}{w}, \frac{1}{w}\right) \\ \pm\frac{dw}{dN} &= w^{m+1} Q\left(\frac{u}{w}, \frac{1}{w}\right) \end{aligned} \tag{5.49}$$

where

$$\begin{aligned} P\left(\frac{u}{w}, \frac{1}{w}\right) &= -2\frac{u}{w} - \frac{u}{w^3} + 2\frac{u^3}{w^3}, \\ Q\left(\frac{u}{w}, \frac{1}{w}\right) &= \frac{1}{w} + 2\frac{u^2}{w^3} - \frac{1}{w^3}. \end{aligned}$$

or equivalently,

$$\frac{du}{dN} = 3uw^2, \tag{5.50}$$

$$\frac{dw}{dN} = -w + 2u^2 w + w^3. \tag{5.51}$$

by considering positive signs. Notice that $(u_c, 0)$ is non-isolated critical points for the above system (5.50). The eigenvalues of the Jacobian matrix at $(u_c, 0)$ are 0 and $-1 + 2u_c^2$. Since $|u_c| \leq 1$ so $-1 \leq -1 + 2u_c^2 \leq 1$ which follows that the vector field near the critical point $(u_c, 0)$ is repelling along w axis if $\frac{1}{\sqrt{2}} < u_c \leq 1$ or $-1 \leq u_c < -\frac{1}{\sqrt{2}}$ and attracting along w axis if $-\frac{1}{\sqrt{2}} < u_c < \frac{1}{\sqrt{2}}$. On the other hand, for $w \neq 0$ and $u > 0$, we have form equation (5.50) that $\frac{du}{dN} > 0$ and for $u < 0$, we have $\frac{du}{dN} < 0$. One may note that the flow comes towards the line of critical points rapidly compare to it goes away from the critical line (see figure (5.7(b))). So the vector field near the $\left(\pm\frac{1}{\sqrt{2}}, 0\right)$ are also saddle in nature. Cosmological bounce may take place near the points at infinity when the non-isolated critical points on the equator of the Poincaré sphere are saddle in nature (see section 5.5.3).

5.5 Cosmological Implication

5.5.1 Cosmological Implication for Model 1

For the critical points C_1 and C_2, as along the eigen-direction of x, x decreases to 0 so $\dot{\phi} \to 0$. This implies $\phi = const.$ and it indicates that the scalar field behaves as a cosmological constant. Further due to the presence of negative eigenvalue corresponding to y coordinate, along the eigen-direction of y, $y \to \pm 1$ which follows that $V(\phi) \to 3H^2 = Constant$. So we

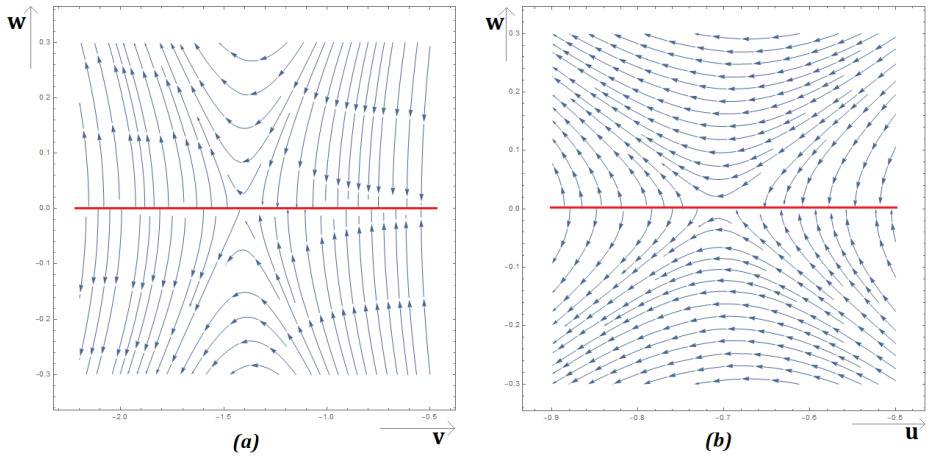

Figure 5.7: Vector fields near non-isolated critical points except $(0, \pm 1, 0)$ are shown in figure (a), and vector fields near non-isolated critical points except $(\pm 1, 0, 0)$ are shown in figure (b) on the equator of the Poincaré sphere.

have the Hubble parameter to be constant. Thus the scale factor grows exponentially. Hence, the critical points described the quasi-deSitter expansion in the early inflationary era.

Now from the stability analysis of C_1 and C_2, we have that $z \to 0$ for $\mu > 0$, $z \to \infty$ for $\mu < 0$ along the eigen-direction of z which implies that $\phi \to \infty$ for $\mu > 0$ and $\phi \to 0$ for $\mu < 0$. Thus for $\mu < 0$ the scalar field behaves as a cosmological constant and for $\mu > 0$ the observation is not cosmologically significant.

For the critical points C_3 and C_4, as along the eigen-direction $x \to \infty$ so $\dot{\phi} \to \infty$ and this is not interesting from a cosmological point of view. Further due to the presence of positive eigenvalue corresponding to y coordinate along the eigen-direction of y, $y \to \infty$ which follows that $V(\phi) \to \infty$ and this is not interesting from a cosmological point of view. Now from the stability analysis of C_3 and C_4, we have $z \to \infty$ along the eigen-direction of z which implies that $\phi \to 0$ and so the scalar field behaves as the cosmological constant.

5.5.2 Cosmological Implication for Model 2

For the critical point P_0 : along the eigen-direction of x as $t \to \infty$, $x \to 0$ which follows that $\dot{\phi} \to 0$. This implies $\phi = const.$ and it indicates that the scalar field behaves as a cosmological constant. Further along the eigen-direction of y as $t \to \infty$, $y \to \infty$ which follows that $V(\phi \to \infty$. For the critical point P_1 : along the eigen-direction of x as $t \to \infty$, $x \to \infty$ which follows that $\dot{\phi} \to \infty$. Further along the eigen-direction of y as $t \to \infty$, $y \to 0$ for $\nu > \sqrt{6}$ and $y \to \infty$ for $\nu < \sqrt{6}$. It follows that $V \to 0$ for $\nu > \sqrt{6}$ and $V \to \infty$ for $\nu < \sqrt{6}$. For the critical point P_2 : along the eigen-direction of x as $t \to \infty$, $x \to \infty$ which follows that $\dot{\phi} \to \infty$. Further along the eigen-direction of y as $t \to \infty$, $y \to 0$ for $\nu > -\sqrt{6}$ and $y \to \infty$ for $\nu < -\sqrt{6}$. It follows that $V \to 0$ for $\nu > -\sqrt{6}$ and $V \to \infty$ for $\nu < -\sqrt{6}$. These results are not interesting in cosmological point of view.

For the critical points P_3 and P_4 : along the eigen-direction of x as $t \to \infty$, $x \to \frac{\nu}{\sqrt{6}}$ if $|\nu| < \sqrt{2}$ and $x \to \infty$ if $\nu > \sqrt{2}$ or $\nu < -\sqrt{2}$. It follows that as $t \to \infty$, $\dot{\phi} \to \nu H \implies \phi \to \nu \lim_{t\to\infty} \ln a(t) \implies \phi \to \infty$ for $|\nu| < \sqrt{2}$ and also $\dot{\phi} \to \infty$ if $\nu > \sqrt{2}$ or $\nu < -\sqrt{2}$. As the critical points P_3 and P_4 both exist for $0 < \nu^2 < 6$, so as $t \to \infty$, $y \to \pm\sqrt{1 - \frac{\nu^2}{6}}$

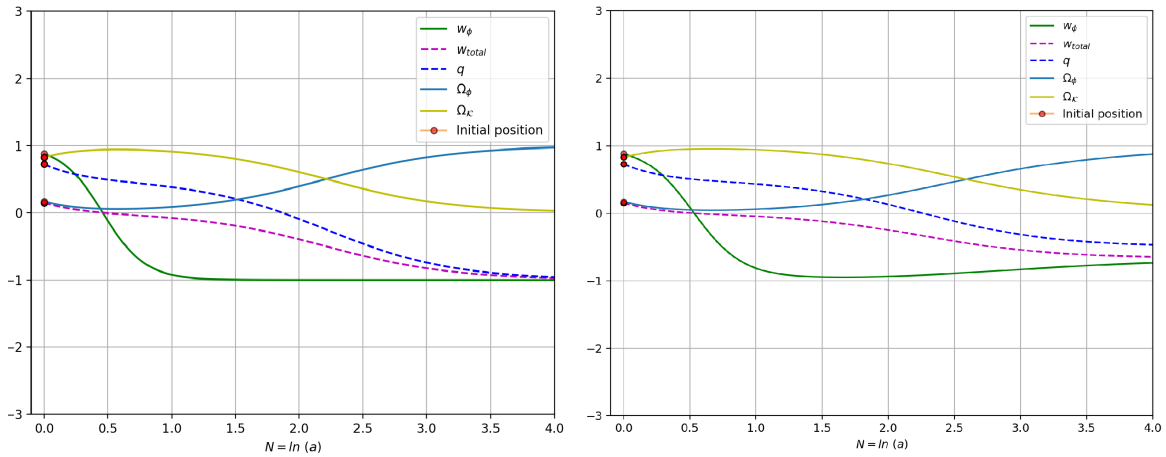

Figure 5.8: The figures shows the time evolution of cosmological parameters of our cosmological model. In panel (a), Power potential: Late time solutions of cosmological parameters. For $\mu = 1$, the kinetic energy dominated late time accelerated solutions are attracted towards phantom boundary. In panel (b), Exponential potential: Late time solutions of cosmological parameters. For $\nu^2 < 2$, the kinetic energy dominated late time accelerated solutions are attracted towards quintessence era which agrees the present observed accelerated universe $(-0.56 < q < -0.49)$.

which follows that $V \to 3H^2\left(1 - \frac{\nu^2}{6}\right)$ so for $\nu = 0$ it leads to an accelerated era of evolution. Further for the critical points P_5 and P_6 : along the eigen-directions of x and y as $t \to \infty$, $x \to \frac{1}{\nu}\sqrt{\frac{2}{3}}$ and $y \to \frac{2}{\sqrt{3}\nu}$ respectively while $|\nu| > \frac{2\sqrt{2}}{\sqrt{3}}$ which follows that as $t \to \infty$, $\dot{\phi} \to \frac{2}{\nu}$ and $V \to \frac{4H^2}{\nu^2}$ while $|\nu| > \frac{2\sqrt{2}}{\sqrt{3}}$. Further for $\nu \in \left(-\sqrt{2}, 0\right) \cup \left(0, \sqrt{2}\right)$ as $t \to \infty$, $x \to \infty$ and $y \to \frac{2}{\sqrt{3}\nu}$ which follows that as $t \to \infty$, $\dot{\phi} \to \infty$ and $V \to \frac{4H^2}{\nu^2}$ while $\nu \in \left(-\sqrt{2}, 0\right) \cup \left(0, \sqrt{2}\right)$. It leads to an accelerated phase of the universe for $\nu = \pm\frac{2}{\sqrt{3}}$.

5.5.3 Cosmological Bouncing Scenarios

Generally speaking, the cosmological bounce takes place for $\dot{a} \approx 0$ and $\ddot{a} > 0$ or $\ddot{a} < 0$. On the other hand, one can derive that $\ddot{a} > 0$ or $\ddot{a} < 0$ iff $\rho_\phi + 3p_\phi < 0$ or $\rho_\phi + 3p_\phi > 0$ respectively (see Proposition (1) in Appendix). For $\ddot{a} > 0$ the universe experiences accelerating phase and for $\ddot{a} < 0$ the universe experiences decelerating phase of evolution. Now for $\dot{a} \approx 0$ we have $\dot{H} \approx \frac{\ddot{a}}{a}$. So, in terms of Hubble parameter H we can say that the bounce takes place when $H \approx 0$ and $\dot{H} > \ or \ < 0$. We also note that $\ddot{a} > \ or \ < 0$ iff $y^2 > 2x^2$ or $y^2 < 2x^2$ respectively (see Proposition (2) in the Appendix and Table (5.5)).

• For model 1, as mentioned previously, near the critical points $C_1 - C_4$ the solutions are completely dominated by scalar field and $\dot{H} \approx 0$ due to the condition $|\Omega_\mathcal{K}| \approx 0$. So bounce does not take place if the initial conditions are given near these points. Nevertheless, near C_3 and C_4 (unstable in nature) the spatial curvature is negligible and $\dot{H}$ is negative. As expected, we also note that $y^2 < 2x^2$ near these critical points and $\ddot{a} < 0$ (see Table (5.5))

for all values of μ. So, if the Hubble parameter takes positive sign (expanding universe) near these critical points, the expansion rate begins to decrease (as $\ddot{a} < 0$) and the trajectory goes towards the critical points at infinity (Minkowski limit with $H \to 0$) in the compactified phase space (see section (5.4)). The trajectory soon commences to go away from those critical points (at infinity) which are saddle/saddle node in nature and H becomes soon negative, *i.e.,* the universe begins to contract.

On the other hand, near the critical point C_5, $\dot{H}$ is positive for positive spatial curvature. So, if the Hubble parameter takes negative sign (contracting universe) near these critical points, the expansion rate begins to increase and the trajectory goes towards the critical points at infinity (Minkowski limit with $H \to 0$) in the compactified phase space (see section (5.4)). The trajectory soon commences to go away from those critical points (at infinity) which are saddle/saddle node in nature and contrary to the previous instance, H becomes soon positive, *i.e.,* the universe begins to expand. The cosmological bounce takes place for $\mu > 0$ when the Hubble parameter H changes its sign and the trajectory asymptotically goes towards C_1 or C_2 (see table 5.5).

So on the proviso that the bounce takes place, there may appear homoclinic and hetroclinic orbits due to the existence of saddle points. So, there are several prospects to acquire various late time solutions which depends on the initial condition; for instances, we acquire scalar field dominated late time de-Sitter solution to the evolution of the universe if the trajectory asymptotically goes towards C_1 or C_2 (see figure (5.3)) on the XY plane, late time decelerating dust-dominated universe if the trajectory asymptotically goes towards C_5 along stable eigen direction.

• For model 2, we have discussed earlier that near P_0 (saddle for all ν) the kinetic term is subdominant compared to the curvature contribution. If initially the universe is in the contracting phase then near P_0 the expansion rate H increases for positive spatial curvature. Depending on initial condition if the flow goes away from P_0 towards infinity (as $H \to 0$) where the Hubble parameter changes its sign (when critical points at infinity are saddle/saddle node in nature) then the universe begins to expand. The expansion rate decreases soon when the spatial curvature contribution becomes negligible.

On the other hand, near P_1 and P_2 (saddle node / unstable node) the solutions are dominated by the kinetic energy of the scalar field and $\dot{H}$ is negative. As expected, it is also to be noted that $y^2 < 2x^2$ near these critical points and $\ddot{a} < 0$ (see Table (5.5)) for all values of ν. Similar to the case of C_3 and C_4 in Model 1, the cosmological bounce takes place when the Hubble parameter changes its sign at Minkowski limit with $H \to 0$, *i.e.,* at critical points (at infinity) which are saddle/saddle node in nature.

The non-isolated critical points P_3 and P_4 are completely dominated by kinetic energy and saddle-node in nature for $2 \leq \nu^2 \leq 6$ and $\dot{H}$ is negative near these points. Unsurprisingly, $y^2 < 2x^2$ near these critical points and $\ddot{a} < 0$ (see Table (5.5)) for $2 < \nu^2 \leq 6$. So depending on initial condition, the cosmological bounce may take place if the flow starts near these critical points. The non-isolated critical points P_5 and P_6 are saddle in nature for $\nu^2 \leq 2$. If $\nu \to 0$, then the critical points are dominated by spatial curvature and the sign of $\dot{H}$ depends on the sign of $\mathcal{K}$. If $\nu^2 \approx 2$, then the critical points are completely dominated by kinetic energy and $\dot{H} < 0$. Similar to the previous case, the initial condition plays an important role to initiate the cosmological bounce.

Similar to the model 1 when it comes to the case of cosmological bounce, there may appear homoclinic and hetroclinic orbits due to the existence of saddle points. So, there are several prospects to acquire various late time solutions which depends on the initial condition; for instances, we come by late time decelerating dust-dominated universe if trajectory

Table 5.5: Table shows the sign of '$\ddot{a}$' near the critical points of Model 1 and 2 in terms of dynamical variables (for details, see Proposition 2 in Appendix)

Model	Critical points	$y^2 > 2x^2$ *i.e.*, $\ddot{a} > 0$	$y^2 < 2x^2$ *i.e.*, $\ddot{a} < 0$
Model 1	C_1	Satisfied for all $\mu \neq 0$	Not applicable
	C_2	Satisfied for all $\mu \neq 0$	Not applicable
	C_3	Not applicable	Satisfied for all μ
	C_4	Not applicable	Satisfied for all μ
	C_5	Not applicable	Not applicable
Model 2	P_0	Not applicable	Not applicable
	P_1	Not applicable	Satisfied for all ν
	P_2	Not applicable	Satisfied for all ν
	P_3	Satisfied for $0 \leq \nu^2 < 2$	Satisfied for $2 < \nu^2 \leq 6$
	P_4	Satisfied for $0 \leq \nu^2 < 2$	Satisfied for $2 < \nu^2 \leq 6$
	P_5, P_6	Not applicable	Not applicable

asymptotically approaches towards P_0, late time kinetic energy dominated solutions with a stiff equation of state if trajectory asymptotically approaches towards P_1 or P_2, late time kinetic energy dominated accelerated solution as trajectory asymptotically approaches towards P_3 or P_4, late time scaling solutions where DE behaves as quintessence boundary if trajectory asymptotically approaches towards P_5 or P_6.

5.6 Brief discussion and concluding remarks

We have studied the cosmological model with spatial curvature in the background of FLRW metric where the scalar field is minimally coupled and plays a role of dark matter content. Two models have been discussed here. In the first model, potential $V(\phi)$ of scalar field is taken as power-law function of scalar field ϕ. Whereas in the second interaction model, the potential term is taken as the exponential function of scalar field ϕ. Since the cosmological

evolution equations are non-linear and complicated in nature, we have performed dynamical system analysis to accomplish the qualitative behavior of the cosmological model. We have explained all possible scenarios of the bouncing universe and the corresponding late-time solutions.

We have obtained five non-hyperbolic type critical points from model 1 and from model 2 we have obtained seven critical points which are characterized (hyperbolic and non-hyperbolic) by the parameter ν. To study the nature of hyperbolic critical points we apply linear stability theory (Hartman-Grobman theorem). On the other hand, to analyze non-hyperbolic points center manifold theory is employed to obtain the exact dynamical nature of the points on the sets. Since at the bouncing scenarios, some variables become singular, we have performed the dynamical analysis around the critical points at infinity in section IV. At infinity, the critical points are normally hyperbolic and saddle/saddle-node in nature (see figure (5.7)). Model 1 can not alleviate the cosmic coincidence problem whereas model 2 can take the edge off the cosmic coincidence problem depending on the parameter ν.

In Model 1, there are five non-hyperbolic equilibrium points. The first two equilibrium points C_1 and C_2 describe the flat model of the universe with a cosmological constant and they describe the phantom barrier of accelerated expansion. The point C_1 represents an expanding model while C_2 corresponds to a contracting model of the universe. The other three equilibrium points C_3, C_4, C_5 represent a decelerating phase of expansion. From a cosmological point of view only equilibrium point C_5 is interesting, it describes a dust era of evolution. Further, the critical points C_1 and C_2 are purely DE dominant ($\Omega_\phi = 1$) and they are analogous to the observationally favored ΛCDM model. The critical points C_3 and C_4 are not of much interest. Here the result matter behaves as stiff fluid which is effective at the very early era when quantum effects are important. The last critical point C_5 has no effect of DE ($\Omega_\phi = 0,\ \Omega_\mathcal{K} = 1$) and the resulting fluid behaves as dust.

In Model 2, there are seven equilibrium points all of which are non-hyperbolic in nature. The dust era of decelerated expansion is characterized by the equilibrium point P_0. The equilibrium points P_1 and P_2 are not interesting from a cosmological point of view. The other four equilibrium points P_3, P_4, P_5, and P_6 represent scaling cosmological solutions. The equilibrium points P_3 and P_4 describe a flat FLRW model with an accelerating phase of expansion for $\nu^2 < 2$ and the scalar field describes a dark energy model. The equilibrium points P_5 and P_6 also describe the decelerating era of expansion for $\nu^2 > 2$ and here curvature contribution of the matter is non-zero and the scalar field behaves as perfect fluid at the quintessence barrier. Further, if $\nu > 2$ then curvature matter contribution will dominate over the scalar field while if $\sqrt{2} < \nu < 2$ then the scalar field is the dominant matter component. Moreover, from cosmological view point the critical point P_0 describes a dust era of evolution having no effect of DE ($\Omega_\phi = 0$). Due to unacceptable cosmological parameters the critical points P_1 and P_2 may be discarded. The critical points P_3 and P_4 are completely dominated by DE ($\Omega_\phi = 1$). For $0 \leq \nu^2 \leq 2$ the present model describes the late time accelerated phase (as predicted by observational data) and $\nu = 0$ describes the observationally supported ΛCDM model (as expected $V(\phi)$ becomes V_0, a constant), while for $2 < \nu^2 \leq 3$ the model goes back to the decelerated era of evolution with $\nu^2 = 3$ represents the dust epoch. Lastly the critical points P_5 and P_6 have similar behaviour as P_3 and P_4 and they describe the ΛCDM model with the choice $\nu^2 = 2/3$. Thus it is possible to have an analogy of the present models with the well-known ΛCDM cosmology. Moreover, if $\nu^2 < 2/3$ then the critical points P_5 and P_6 may go beyond ΛCDM and they may be related to other tensions in cosmology. Though both the potential models are cosmologically viable yet model 2 has an edge over model 1. In model 2, there are scaling solutions (corresponding to critical points $P_3 - P_6$)

indicating the possibility of decelerating era of expansion to the present accelerated expansion phase. However, such type of expansion is not possible for power law of potential.

Thus, in summary, the present cosmological model based on the spatial curvature with power law and exponential potential may describe different evolutionary phases of the universe for which bounce takes place. To study the bouncing universe we need to analyze the behavior of the vector field at the Minkowski limit with $H \to 0$, *i.e.,* at critical points (at infinity) which are saddle/saddle-node in nature. Depending on the initial condition, either the transition comes to pass from expansion to contraction and vice versa, from contraction to expansion of the universe. It is a well-known fact that so far no observational evidences show the bouncing nature of the Universe nor there is any evidence of contracting phase of evolution. But due to rapid improvement in the observational data specially after detection of gravitational wave, no one can firmly say that such phases of evolution will not reveal through the observations in future as theoretically it is consistent with Einstein gravity.

The present model describes a change in the universe's expansion rate (*i.e.,* from expansion to contraction) so it may be possible to have an explanation or it may alleviate the standard H_0-tension. The uncoupled scalar field models do not really increase the H_0 value [718, 430]. Though a coupled scalar field model can reduce the H_0 tension, a proper choice of the coupling function between the scalar field and dark matter [431], it is possible to increase the H_0 value compared to the ΛCDM based Plank's estimation [718]. As a result, the obtained value of H_0 could be closer to the SH0ES value [432]. One may note that the inclusion of curvature in the cosmological models does not offer any solution to the Hubble constant tension, rather the tension on H_0 increases. Therefore, even if the consideration of the curvature of the Universe gives a complete picture of the underlying cosmological model, however, the increasing tension in H_0 needs special attention with the growing sensitivity in the upcoming astronomical probes. In addition, two other additional tensions related to H_0-tension in cosmology, namely the σ_8 tension and the galaxy rotation curves problem may have some issues which we shall study in a future work.

5.7 Some important propositions of this chapter

Proposition 1 *If ρ_ϕ is the energy density and p_ϕ is the pressure of the scalar field (given by equations (5.5) and (5.6)) then the second order derivative of the scale factor $a(t)$ with respect to the cosmic time t, that is, $\ddot{a} > 0$ or $\ddot{a} < 0$ iff $\rho_\phi + 3p_\phi < 0$ or $\rho_\phi + 3p_\phi > 0$ respectively.*

Proof: The expression of Hubble parameter $H(t)$ in terms of scale factor $a(t)$ is defined by

$$H = \frac{\dot{a}}{a}.$$

Taking differentiation on both sides of the above with respect to t yields

$$\dot{H} = \frac{\ddot{a}}{a} - \frac{\dot{a}^2}{a^2}.$$

Substituting $H = \frac{\dot{a}}{a}$ in left hand side of Eq.(5.8) yields

$$\begin{aligned} 3\frac{\dot{a}^2}{a^2} &= \frac{1}{2}\dot{\phi}^2 + V(\phi) - 3\frac{\mathcal{K}}{a^2}, \\ \frac{\dot{a}^2}{a^2} &= \frac{1}{3}\left(\frac{1}{2}\dot{\phi}^2 + V(\phi) - 3\frac{\mathcal{K}}{a^2}\right). \end{aligned} \tag{5.52}$$

Plugging the values of $\dot{H}$ in left hand side of Eq.(5.9) and using (5.52) yields

$$\begin{aligned} 2\left(\frac{\ddot{a}}{a} - \frac{\dot{a}^2}{a^2}\right) &= -\dot{\phi}^2 + 2\frac{\mathcal{K}}{a^2}, \\ 2\frac{\ddot{a}}{a} &= 2\frac{\dot{a}^2}{a^2} - \dot{\phi}^2 + 2\frac{\mathcal{K}}{a^2}, \\ 2\frac{\ddot{a}}{a} &= \frac{2}{3}\left(\frac{1}{2}\dot{\phi}^2 + V(\phi) - 3\frac{\mathcal{K}}{a^2}\right) - \dot{\phi}^2 + 2\frac{\mathcal{K}}{a^2}, \\ 2\frac{\ddot{a}}{a} &= \frac{1}{3}\dot{\phi}^2 + \frac{2}{3}V(\phi) - \dot{\phi}^2, \\ \frac{\ddot{a}}{a} &= -\frac{1}{3}(\dot{\phi}^2 - V(\phi)). \end{aligned} \tag{5.53}$$

From equations (5.5) and (5.6), we have

$$\begin{aligned} \rho_\phi &= \frac{1}{2}\dot{\phi}^2 + V(\phi), \\ p_\phi &= \frac{1}{2}\dot{\phi}^2 - V(\phi). \end{aligned}$$

Note that

$$\rho_\phi + 3p_\phi = \frac{1}{2}\dot{\phi}^2 + V(\phi) + \frac{3}{2}\dot{\phi}^2 - 3V(\phi) = 2(\dot{\phi}^2 - V(\phi))$$

which implies

$$\dot{\phi}^2 - V(\phi) = \frac{1}{2}(\rho_\phi + 3p_\phi).$$

Using the above result on the right-hand side of (5.53) yields

$$\frac{\ddot{a}}{a} = -\frac{1}{6}(\rho_\phi + 3p_\phi). \tag{5.54}$$

Now one may note from the equation (5.54) that $\ddot{a} > 0$ iff

$$\begin{aligned} -\frac{1}{6}(\rho_\phi + 3p_\phi) &> 0, \\ \rho_\phi + 3p_\phi &< 0. \end{aligned}$$

and $\ddot{a} < 0$, iff

$$\rho_\phi + 3p_\phi > 0.$$

This completes the proof.

Proposition 2 *The second order derivative of the scale factor $a(t)$ with respect to the cosmic time t, that is, $\ddot{a} > 0$ or $\ddot{a} < 0$ iff $y^2 > 2x^2$ or $y^2 < 2x^2$ respectively where x and y are the dynamical variables given by the equations (5.11) and (5.12).*

PROOF: In the previous proposition, we have shown that at the point of bouncing condition

$$\rho_\phi + 3p_\phi < 0 \text{ or } \rho_\phi + 3p_\phi > 0.$$

From the equations (5.5) and (5.6), we have

$$\rho_\phi = \frac{1}{2}\dot{\phi}^2 + V(\phi),$$
$$p_\phi = \frac{1}{2}\dot{\phi}^2 - V(\phi).$$

Plugging the expressions of ρ_ϕ and p_ϕ into the first bouncing condition (*i.e.,* $\rho_\phi + 3p_\phi < 0$) yields

$$\begin{aligned} \frac{1}{2}\dot{\phi}^2 + V(\phi) + 3\left(\frac{1}{2}\dot{\phi}^2 - V(\phi)\right) &< 0, \\ 2\dot{\phi}^2 - 2V(\phi) &< 0, \\ \dot{\phi}^2 &< V(\phi). \end{aligned} \tag{5.55}$$

In terms of dynamical variables, from equations (5.11) and (5.12), we have

$$\dot{\phi} = \sqrt{6}Hx,$$
$$V(\phi) = 3H^2y^2.$$

Substituting these into (5.55) yields

$$\begin{aligned} (\sqrt{6}Hx)^2 &< 3H^2y^2, \\ 6H^2x^2 &< 3H^2y^2, \\ y^2 &> 2x^2. \end{aligned}$$

Similarly, by substituting the values of p_ϕ and ρ_ϕ from the equations (5.5) and (5.6) into the second bouncing condition (*i.e.,* $\rho_\phi + 3p_\phi > 0$), we can show that $y^2 < 2x^2$. This completes the proof.

Proposition 3 *Equation (5.18) can be obtained by using equations (5.15), (5.16) and the constraint equation (5.24).*

PROOF: By taking differentiation both sides of (5.24) with respect to N yields

$$2x\frac{dx}{dN} + 2y\frac{dy}{dN} - 6\mathcal{K}u\frac{du}{dN} = 0,$$
$$\frac{du}{dN} = \frac{1}{3\mathcal{K}u}\left\{x\frac{dx}{dN} + y\frac{dy}{dN}\right\}.$$

Now by substituting the equations (5.15) and (5.16) in the right hand side of above yields

$$\begin{aligned} \frac{du}{dN} &= \frac{1}{3\mathcal{K}u}\left\{-3x^2 - \sqrt{\frac{3}{2}}\left(\frac{V'}{V}\right)xy^2 + 3x^4 - 3\mathcal{K}u^2x^2 + 3y^2x^2 - 3\mathcal{K}u^2y^2 + \sqrt{\frac{3}{2}}\left(\frac{V'}{V}\right)xy^2\right\} \\ &= \frac{1}{3\mathcal{K}u}\{-3\mathcal{K}u^2(x^2+y^2) + 3x^2(y^2+x^2-1)\}. \end{aligned}$$

From the equation (5.24), we have

$$x^2 + y^2 - 1 = 3\mathcal{K}u^2.$$

Plugging this into the second term of the right-hand side of the last expression yields

$$\begin{aligned}\frac{du}{dN} &= \frac{1}{3\mathcal{K}u}\{9\mathcal{K}u^2x^2 - 3\mathcal{K}u^2(x^2+y^2)\}\\ &= \frac{1}{3\mathcal{K}u}\{3\mathcal{K}u^2(3x^2 - x^2 - y^2)\}\\ &= u(2x^2 - y^2).\end{aligned}$$

This completes the proof.

Proposition 4 *The expressions of the center manifold corresponding to the critical point C_1 are given by $u = 0$ and $v = -\frac{\mu^2}{72}w^2 + \mathcal{O}(w^4)$, and the flow on the center manifold is determined by $w' = -\frac{\mu}{6}w^3 + \mathcal{O}(w^4)$.*

Proof: The Jacobian matrix at the critical point C_1 can be put as

$$J(C_1) = \begin{bmatrix} -3 & 0 & \frac{\mu}{2} \\ 0 & -2 & 0 \\ 0 & 0 & 0 \end{bmatrix}. \tag{5.56}$$

The eigenvalues of the above matrix are -3, -2 and 0 with $[1,0,0]^T$, $[0,1,0]^T$ and $\left[\frac{\mu}{6},0,1\right]^T$ are the corresponding eigenvectors respectively. To apply center manifold theory, first, we transform the coordinates into a new system $x = X,\ y = Y+1,\ z = Z$, such that the critical point C_1 moves to the origin. By using the eigenvectors of the Jacobian matrix $J(C_1)$, we introduce another set of new coordinates $(u,\ v,\ w)$ in terms of $(X,\ Y,\ Z)$ as

$$\begin{bmatrix} u \\ v \\ w \end{bmatrix} = \begin{bmatrix} 1 & 0 & -\frac{\mu}{6} \\ 0 & 1 & 0 \\ 0 & 0 & 1 \end{bmatrix} \begin{bmatrix} X \\ Y \\ Z \end{bmatrix} \tag{5.57}$$

and in these new coordinate system, the equations $(5.28 - 5.30)$ are transformed into

$$\begin{bmatrix} u' \\ v' \\ w' \end{bmatrix} = \begin{bmatrix} -3 & 0 & 0 \\ 0 & -2 & 0 \\ 0 & 0 & 0 \end{bmatrix} \begin{bmatrix} u \\ v \\ w \end{bmatrix} + \begin{bmatrix} non \\ linear \\ terms \end{bmatrix}. \tag{5.58}$$

By center manifold theory there exists a continuously differentiable function $h : \mathbb{R} \to \mathbb{R}^2$ such that

$$h(w) = \begin{bmatrix} u \\ v \end{bmatrix} = \begin{bmatrix} a_1w^2 + a_2w^3 + \mathcal{O}(w^4) \\ b_1w^2 + b_2w^3 + \mathcal{O}(w^4) \end{bmatrix}. \tag{5.59}$$

Differentiating both sides with respect to N, we get

$$u' = (2a_1 w + 3a_2 w^2)w' + \mathcal{O}(w^3) \tag{5.60}$$
$$v' = (2b_1 w + 3b_2 w^2)w' + \mathcal{O}(w^3) \tag{5.61}$$

where $a_i,\ b_i \in \mathbb{R}$. We only concern about the non-zero coefficients of the lowest power terms in CMT as we analyze the stability in an arbitrarily small neighborhood of the origin. Comparing coefficients corresponding to power of w both sides of (5.60) and (5.61), we get $a_i = 0$ and $b_1 = \frac{\mu^2}{72}$, $b_2 = 0$. So, the center manifold can be written as

$$u = 0, \tag{5.62}$$
$$v = -\frac{\mu^2}{72}w^2 + \mathcal{O}(w^4) \tag{5.63}$$

and the flow on the center manifold is determined by

$$w' = -\frac{\mu}{6}w^3 + \mathcal{O}(w^4). \tag{5.64}$$

CHAPTER 6

DYNAMICAL SYSTEM ANALYSIS OF QUINTESSENCE DARK ENERGY MODEL

6.1 Prelude

In cosmology, till the early 90's the challenging issue was to find the analytic solution of the evolution equations which are highly non-linear and coupled in nature. As a result, it was very hard to find any cosmological inferences from the cosmological models. But the situation changes since late 90's [749] when the dynamical system approach has been applied in the field of cosmology. Dynamical system analysis is a very powerful mathematical tool that provides information from the evolution equations without any reference to initial conditions or any specific behavior at any intermediate instant [750]. There may be infinite possible evolution for a general cosmological scenario but its asymptotic behavior particularly at late times are limited to a few different classes. These few classes can be identified as stable critical points if the cosmic evolution equations can be converted into an autonomous form. Thus by analyzing such critical points, one may infer about the late time evolution of the universe without going for any analytic solution or ambiguity to the initial conditions not arise. So far most of the dynamical analysis at cosmological scenarios is restricted to the background level, *i.e.,* formation of autonomous system, determination of critical points, and estimation of the relevant cosmological parameters namely density parameter, the equation of state parameter and so on.

This chapter deals with a standard cosmological model in the context of the present accelerating phase namely the quintessence dark energy scalar field model having exponential potential. Using suitable choice of the variables the evolution equations are converted into a discrete type autonomous system and the critical points are analyzed using center manifold theory and stability analysis has been presented with Schwarzian derivative. The manuscript is organized as follows: In Section 6.2 we discuss the background of Quintessence scenarios under flat FLRW space-time. In Section 6.3 we construct the autonomous system corresponding to the basic equations of the cosmological model and critical points are determined

in this section. Stability analysis of all critical points for various choices of the involving parameters is shown in Section 6.4 from the perspective of discrete dynamical system analysis. We present global dynamical analysis and cosmological implications in Section 6.5. Finally, a brief discussion and important concluding remarks of this work are proposed in Sec. 6.6.

6.2 Background of Quintessence Scenarios

In the perspective of phase space analysis of the basic dynamical dark energy scenario, namely the quintessence one with an exponential potential, which is the archetype quintessence scenario due to the well-posed theoretical justification of exponential potentials [751, 752, 753, 754, 755]. In the background of flat FLRW space-time, the Friedman equations for the general cosmological model are (choosing $8\pi G = 1 = c$)

$$3H^2 = \rho_m + \rho_d \tag{6.1}$$

and

$$2\dot{H} = -\{(\rho_m + p_m) + (\rho_d + p_d)\} \tag{6.2}$$

with (ρ_m, p_m) and (ρ_d, p_d) the energy density and thermodynamic pressure for the matter component and the dark energy component respectively. The 'dot' denotes the derivative with respect to time, $H = \frac{\dot{a}}{a}$ is the Hubble parameter. The energy-momentum conservation relations for these matter components are (assuming non-interacting)

$$\dot{\rho_m} + 3H(\rho_m + p_m) = 0, \tag{6.3}$$
$$\dot{\rho_d} + 3H(\rho_d + p_d) = 0 \tag{6.4}$$

with $\omega_m = p_m/\rho_m$ and $\omega_d = p_d/\rho_d$, the equation of state parameters for the two components.

As a particular choice, if we assume $p_d = -\rho_d = -\Lambda$, the cosmological constant, ω_m (*i.e.,* p_m) $= 0$, then the above cosmological model is termed as ΛCDM model. On the other hand, if the dark energy is introduced as a scalar field ϕ with self-interacting potential $V(\phi)$, we have the basic quintessence model, *i.e.,*

$$\rho_d = \rho_\phi = \frac{1}{2}\dot{\phi}^2 + V(\phi), \tag{6.5}$$

and

$$p_d = p_\phi = \frac{1}{2}\dot{\phi}^2 - V(\phi) \tag{6.6}$$

then the conservation equation (6.4) becomes the Klein-Gordon equation

$$\ddot{\phi} + 3H\dot{\phi} + \frac{\partial V}{\partial \phi} = 0 \tag{6.7}$$

where $V'(\phi) \equiv \partial V/\partial\phi$. This is usually known as the quintessence dark energy model.

On the other hand, the equation (6.2) can be written as the following

$$2\dot{H} = -\dot{\phi}^2 - (1 + \omega_m)\rho_m \tag{6.8}$$

As the above evolution equations are coupled and nonlinear in nature so it is hard to solve them analytically. However, even without any solution, it is possible to get information about cosmological evaluation by using a dynamical system approach [756, 757, 639, 636, 758]. This powerful method does not depend on the initial conditions or the evolution pattern at any intermediate instant [750]. Using suitable dimensionless variables the evolution equation can be converted into an autonomous set whose stable critical points correspond to different cosmological epochs. Since late 90's, this approach has been widely used in various cosmological models to get inferences from critical points. These studies are mainly confined to the background level and the critical points mostly correspond to behavior at early cosmological eras [749, 759, 760, 761]. The dynamical analysis can be enriched further with using bifurcation theory methods [421]. In this method, we inspect the phase transition of the evolution of the Universe. We also characterize the generic and non-generic evolution of the Universe based on the initial and late time states of the evolution of the Universe [762, 763, 764, 708].

6.3 Formation of the autonomous system and critical points determination

The essence of the dynamical system approach is to transform the equations into an autonomous system using $\tau \equiv \ln a$ as the dynamical variable. In the case of the quintessence scenario, the potential as of the form $V = V_0 e^{-\lambda\phi}$ (exponential potential) [627, 754, 765, 707] is imposed on the scalar field. We introduce the auxiliary variables

$$x \equiv \frac{\dot{\phi}}{\sqrt{6}H}, \quad y \equiv \frac{\sqrt{V}}{\sqrt{3}H}, \tag{6.9}$$

where x^2 stands for the relative kinetic energy density of the scalar field and y^2 stands for its relative potential energy density of ϕ.

The equations (6.7) and (6.8) can be expressed as the following autonomous system using the above auxiliary variables

$$x' = \frac{3}{2}x\left[2x^2 + \gamma_m(1 - x^2 - y^2)\right] - 3x + \sqrt{\frac{3}{2}}\lambda y^2, \tag{6.10}$$

$$y' = \frac{3}{2}y\left[2x^2 + \gamma_m(1 - x^2 - y^2)\right] - \sqrt{\frac{3}{2}}\lambda xy, \tag{6.11}$$

with $\gamma_m \equiv \omega_m + 1$, in terms of which the various density parameters are expressed as $\Omega_d = x^2 + y^2$, $\Omega_m = 1 - \Omega_d$, while $\omega_d = \frac{x^2 - y^2}{x^2 + y^2}$ and the expressions of total equation of state parameter ω_{total} and deceleration parameter q are given by

$$\omega_{total} = 2x^2 - 1 + \gamma_m(1 - x^2 - y^2),$$
$$q = \frac{3}{2}\gamma_m(1 - x^2 - y^2) + 3x^2 - 1.$$

In this paper, we study the discrete time dynamical systems associated with the system (6.10 – 6.11). To study discrete time dynamical system analysis, first, we write the following proposition:

Proposition 5 *Let us consider the two dimensional nonlinear system of equations*

$$\frac{dx}{dt} = f(x, y), \tag{6.12}$$
$$\frac{dy}{dt} = g(x, y). \tag{6.13}$$

The discrete dynamical system corresponding to the above system is given by

$$x_{n+1} = x_n + hf(x_n, y_n),$$
$$y_{n+1} = y_n + hg(x_n, y_n).$$

Proof: We start with a discrete set of points $t_0,\ t_1, \ldots,\ t_n, \ldots$, with $h = t_{n+1} - t_n$ as step size. Then, for $t_n \leq t < t_{n+1}$, we approximate $x(t)$ by $x(t_n)$ and $\frac{dx}{dt} = f(x(t), y(t))$ by $\frac{x(t_{n+1})-x(t_n)}{h}$ where $x(t)$ and $y(t)$ respectively denotes $\frac{\dot{\phi}(t)}{\sqrt{6}H(t)}$ and $\frac{\sqrt{V(t)}}{\sqrt{3}H(t)}$. Equation (6.12) can be approximated as

$$x(t_{n+1}) = x(t_n) + hf(x(t_n), y(t_n))$$

Proceeding in similar way, from (6.13), we get

$$y(t_{n+1}) = y(t_n) + hg(x(t_n), y(t_n))$$

Consideing $x(t_n) = x_n$, $x(t_{n+1}) = x_{n+1}$, we can write the above two equations in the simpler form

$$x_{n+1} = x_n + hf(x_n, y_n),$$
$$y_{n+1} = y_n + hg(x_n, y_n).$$

The discrete time dynamical systems associated with the system (6.10 – 6.11) can be expressed as

$$x_{n+1} = h\left(\frac{3}{2}x_n\left[2x_n^2 + \gamma_m(1 - x_n^2 - y_n^2)\right] - 3x_n + \sqrt{\frac{3}{2}}\lambda y_n^2\right) + x_n, \tag{6.14}$$
$$y_{n+1} = h\left(\frac{3}{2}y_n\left[2x_n^2 + \gamma_m(1 - x_n^2 - y_n^2)\right] - \sqrt{\frac{3}{2}}\lambda x_n y_n\right) + y_n. \tag{6.15}$$

Let us define the operator $W : \mathbb{R}^2 \to \mathbb{R}^2$ by $W(x, y) = (\overline{x}, \overline{y})$, where (considering the step size $h = 1$ [421])

$$\overline{x} = \frac{3}{2}x\left[2x^2 + \gamma_m(1 - x^2 - y^2)\right] - 3x + \sqrt{\frac{3}{2}}\lambda y^2 + x, \tag{6.16}$$
$$\overline{y} = \frac{3}{2}y\left[2x^2 + \gamma_m(1 - x^2 - y^2)\right] - \sqrt{\frac{3}{2}}\lambda xy + y. \tag{6.17}$$

Here, we considered $x_{n+1} = \overline{x}, y_{n+1} = \overline{y}$ and $x_n = x, y_n = y$ for simplicity of calculation.

Definition 6.3.1 (Fixed points.) *A point $z \in \mathbb{R}^2$ is called a fixed point [421] of W if $W(z) = z$.*

By using the definition of fixed points, we can obtain the fixed points corresponding to the system $(6.16 - 6.17)$ which are shown in Table 6.1. The existence of the fixed points is also shown in this table.

Table 6.1: Table shows the set of critical points and their existence corresponding to the autonomous system $(6.16 - 6.17)$:

CPs	Existence	x	y	Ω_d	ω_d	ω_{total}	q
A	For all λ	0	0	0	NA	$\gamma_m - 1$	$\frac{3}{2}\gamma_m - 1$
B	For all λ	1	0	1	1	1	2
C	For all λ	-1	0	1	1	1	2
D	$-\sqrt{6} \leq \lambda \leq \sqrt{6}$	$\frac{\lambda}{\sqrt{6}}$	$\sqrt{1 - \frac{\lambda^2}{6}}$	1	$\frac{\lambda^2}{3} - 1$	$\frac{\lambda^2}{3} - 1$	$\frac{\lambda^2}{2} - 1$
E	$\lambda^2 > 3\gamma_m$	$\sqrt{\frac{3}{2}}\frac{\gamma_m}{\lambda}$	$\sqrt{\frac{3(2-\gamma_m)\gamma_m}{2\lambda^2}}$	$\frac{3\gamma_m}{\lambda^2}$	$\gamma_m - 1$	$\gamma_m - 1$	$\frac{3}{2}\gamma_m - 1$

6.4 STABILITY ANALYSIS

In this section, we will establish some simple but powerful criteria for the local stability of fixed points [422, 766, 767]. Fixed (equilibrium) points may be divided into two types: hyperbolic and nonhyperbolic. A fixed point x^* of a map f is said to be hyperbolic if $|f'(x^*)| \neq 1$. Otherwise, it is nonhyperbolic. To find the type of a fixed point of the system $(6.16 - 6.17)$ we write the Jacobian matrix at (x, y):

$$J(x,y) = \begin{pmatrix} \left(-2 + \frac{3}{2}\gamma_m\right) + x^2\left(9 - \frac{9\gamma_m}{2}\right) - \frac{3}{2}\gamma_m y^2 & -3\gamma_m xy + \sqrt{6}\lambda y \\ 6xy - 3\gamma_m xy - \sqrt{\frac{3}{2}}\lambda y & \left(\frac{3}{2}\gamma_m + 1\right) - \sqrt{\frac{3}{2}}\lambda x + \left(3 - \frac{3}{2}\gamma_m\right)x^2 - \frac{9}{2}\gamma_m y^2 \end{pmatrix}$$

Now we discuss the stability of all fixed points corresponding to the system $(6.16 - 6.17)$.

• The fixed point A exists for all λ. For this solution, the kinetic term is subdominant compared to the matter contribution in equation (6.8). The DE can represent either quitessence or any other exotic type fluid depending on the parameter γ_m. Specially, for $0 < \gamma_m < \frac{2}{3}$, the scalar field behaves as quintessence like fluid and there exists an accelerated universe (since for this case, $-1 < \omega_{total} < -\frac{1}{3}$, $q < 0$) near the critical point whereas the scalar field DE behaves as cosmological constant for $\gamma_m = 0$ and in this case the cosmic evolution near the point characterizes the ΛCDM model ($\omega_{total} = 0$, $q = -1$, $\Omega_d = 0$) of evolution.

The eigenvalues of the Jacobian matrix $J(A)$ are $\lambda_1 = -2 + \frac{3}{2}\gamma_m$ and $\lambda_2 = \frac{3}{2}\gamma_m + 1$. The fixed point A is hyperbolic if $\gamma_m \neq 0, \frac{2}{3}$ because for these values of γ_m (that is, for $\gamma_m = 0, \frac{2}{3}$), the absolute value of one of the eigenvalues of $J(A)$ is 1 and the fixed point is nonhyperbolic if $\gamma_m = 0$ or $\frac{2}{3}$. Now we analyze the stability of the critical point A for both of the cases (hyperbolic and nonhyperbolic).

Hyperbolic case $\left(\gamma_m \neq 0, \frac{2}{3}\right)$:

For the physically meaningful case: $0 \leq \gamma_m < 2$. So for the hyperbolic case we consider the value of γ_m only when $\gamma_m \in \left(0, \frac{2}{3}\right) \cup \left(\frac{2}{3}, 2\right)$. We can easily see that $0 < \lambda_1 < 1$ for $\gamma_m \in \left(\frac{4}{3}, 2\right)$, $-1 < \lambda_1 < 0$ for $\gamma_m \in \left(\frac{2}{3}, \frac{4}{3}\right)$, $\lambda_1 < -1$ if $\gamma_m \in \left(0, \frac{2}{3}\right)$ and $\lambda_2 > 1$ for $\gamma_m \in (0, 2)$. That means, for $\gamma_m \in \left(\frac{4}{3}, 2\right)$ we have $0 < \lambda_1 < 1 < \lambda_2$ which implies that the critical point A is a *saddle point*, for $\gamma_m \in \left(\frac{2}{3}, \frac{4}{3}\right)$ we have $-1 < \lambda_1 < 0, \lambda_2 > 1$ which suggests that the critical point A is also a *saddle point*, and for $\gamma_m \in \left(0, \frac{2}{3}\right)$ we have $\lambda_1 < -1, \lambda_2 > 1$ which concludes that the critical point A is a *source*.

Nonhyperbolic case $\left(\gamma_m = 0 \text{ or } \frac{2}{3}\right)$:

To analyze the fixed point A for this case, we use the center manifold theory. For $\gamma_m = 0$, the system (6.16 – 6.17) modifies to

$$\overline{x} = -2x + 3x^3 + \sqrt{\frac{3}{2}}\lambda y^2,$$
$$\overline{y} = y + 3x^2 y - \sqrt{\frac{3}{2}}\lambda xy.$$

Consider the map $F = \begin{pmatrix} f \\ g \end{pmatrix}$ defined by

$$\begin{pmatrix} x \\ y \end{pmatrix} \longmapsto \begin{pmatrix} -2 & 0 \\ 0 & 1 \end{pmatrix} \begin{pmatrix} x \\ y \end{pmatrix} + \begin{pmatrix} 3x^3 + \sqrt{\frac{3}{2}}\lambda y^2 \\ 3x^2 y - \sqrt{\frac{3}{2}}\lambda xy \end{pmatrix}.$$

Then,

$$M_c = \left\{(x, y) \in \mathbb{R}^2 : x = h(y), h(0) = h'(0) = 0\right\}.$$

The function h must satisfy Equation (1.180)

$$h\left(By + g(h(y), y)\right) - Ah(y) - f(h(y), y) = 0$$

or

$$h\left(y + 3yh^2(y) - \sqrt{\frac{3}{2}}\lambda y h(y)\right) + 2h(y) - \left(3h^3(y) + \sqrt{\frac{3}{2}}\lambda y^2\right) = 0. \tag{6.18}$$

Let us assume that $h(y)$ takes the form

$$h(y) = c_1 y^2 + c_2 y^3 + \mathcal{O}(y^4). \tag{6.19}$$

Then, substituting Equation (6.19) in Equation (6.18) and writing the terms upto degree 3 yields

$$c_1 y^2 + c_2 y^3 + 2(c_1 y^2 + c_2 y^3) - \sqrt{\frac{3}{2}}\lambda y^2 + \cdots = 0.$$

As we analyze the arbitrary neighborhood of the origin so by comparing both sides the coefficient of y^2 and y^3 yields

$$c_1 + 2c_1 - \sqrt{\frac{3}{2}}\lambda = 0 \implies c_1 = \frac{\lambda}{\sqrt{6}};$$
$$c_2 + 2c_2 = 0 \implies c_2 = 0.$$

Consequently, $h(y) = \frac{\lambda}{\sqrt{6}} y^2 + \mathcal{O}(y^4)$ and the map g on the center manifold is given by

$$y \longmapsto y - \frac{\lambda^2}{2} y^3 + \mathcal{O}(y^4).$$

Notice that $y^* = 0$ is a fixed point of g at which $g'(0) = 1$, $g''(0) = 0$, and $g'''(0) = -3\lambda^2 < 0$. This implies by Theorem 4 that the critical point A is *asymptotically stable* (see figure 6.1) under the map $F = \begin{pmatrix} f \\ g \end{pmatrix}$. To verify our conclusion, we also draw the phase portrait of the original system numerically (see figure 6.2). From that plot, we can conclude that our theoretical result is exactly the same as the result which is obtained by plotting the system numerically.

For $\gamma_m = \frac{2}{3}$, the calculation of the center manifold is shown in Appendix 2. From the calculation and the second equation corresponding to the autonomous system, we can conclude that the critical point A is unstable in nature for this case.

• The critical point B corresponds to solution where the constraint equation (6.8) is dominated by the kinetic energy of the scalar field with a stiff equation of state $\omega_d = 1$ and there exist a decelerating phase of the universe.

The eigenvalues of the Jacobian matrix $J(B)$ are $\lambda_1 = 7 - 3\gamma_m$ and $\lambda_2 = 4 - \sqrt{\frac{3}{2}}\lambda$. The fixed point B is hyperbolic if $\lambda \neq \sqrt{6}, \frac{5\sqrt{2}}{\sqrt{3}}$ because for these values of λ (that is, for $\lambda = \sqrt{6}, \frac{5\sqrt{2}}{\sqrt{3}}$), the absolute value of one of the eigenvalues of $J(B)$ is 1 and the fixed point is nonhyperbolic if $\lambda = \sqrt{6}$ or $\lambda = \frac{5\sqrt{2}}{\sqrt{3}}$. Now we analyze the stability of the critical point B for both of the cases (hyperbolic and nonhyperbolic).

Hyperbolic case $\left(\lambda \neq \sqrt{6}, \frac{5\sqrt{2}}{\sqrt{3}}\right)$:

For the physically meaningful case: $0 \leq \gamma_m < 2$. We can easily see that $\lambda_1 > 1$ for all $\gamma_m \in [0, 2)$. Further, we can see that $\lambda_2 > 1$ when $\lambda < \sqrt{6}$, $0 < \lambda_2 < 1$ when $\sqrt{6} < \lambda < \frac{4\sqrt{2}}{\sqrt{3}}$, $-1 < \lambda_2 < 0$ when $\frac{4\sqrt{2}}{\sqrt{3}} < \lambda < \frac{5\sqrt{2}}{\sqrt{3}}$, and $\lambda_2 < -1$ when $\lambda > \frac{5\sqrt{2}}{\sqrt{3}}$. It follows that the fixed point B is a *source* for $\lambda < \sqrt{6}$ or $\lambda > \frac{5\sqrt{2}}{\sqrt{3}}$, and *saddle point* for $\lambda \in \left(\sqrt{6}, \frac{4\sqrt{2}}{\sqrt{3}}\right) \cup \left(\frac{4\sqrt{2}}{\sqrt{3}}, \frac{5\sqrt{2}}{\sqrt{3}}\right)$.

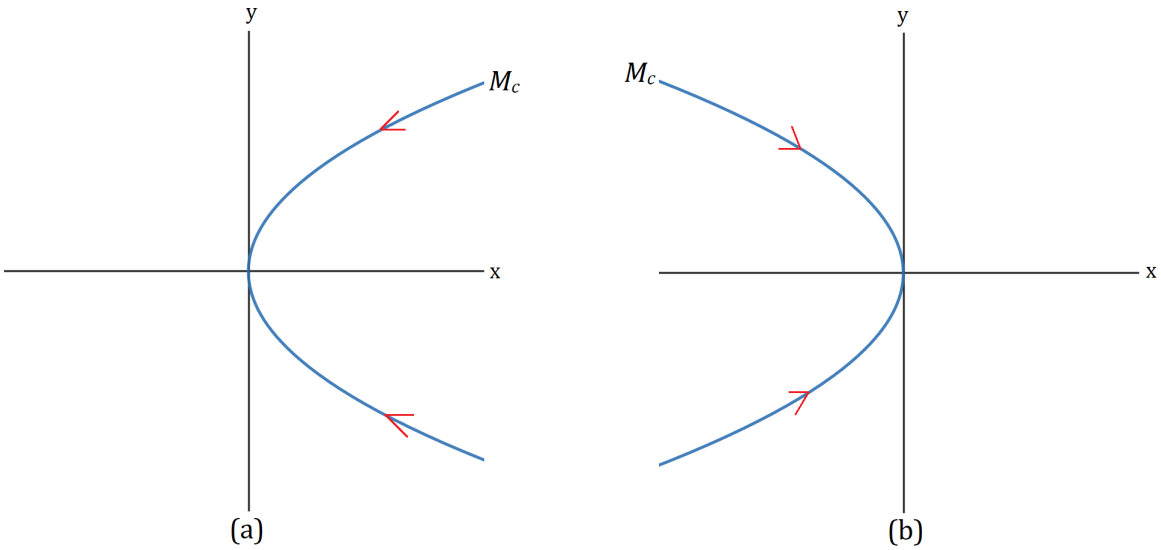

Figure 6.1: The curve $h(y) = \frac{\lambda}{\sqrt{6}}y^2 + \mathcal{O}(y^4)$ is the graph of the center manifold M_c. The orbits on the x-axis oscillate but converge to the origin. (a) is for $\lambda > 0$ and (b) is for $\lambda < 0$.

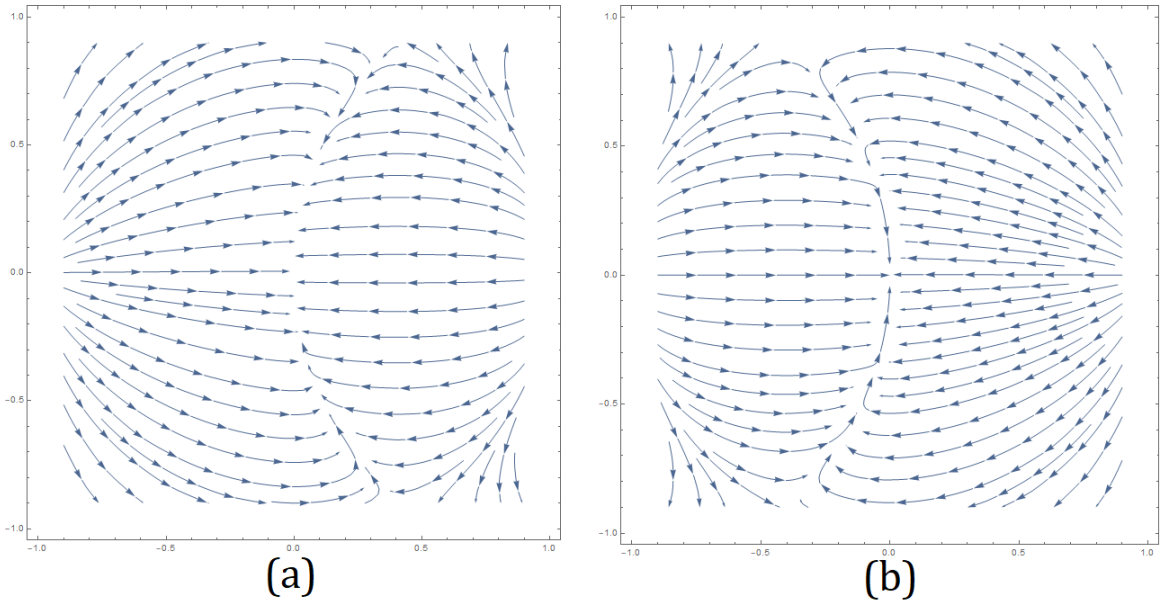

Figure 6.2: The panel of the figures show the phase portrait of autonomous system (6.10 – 6.11) corresponding to the fixed point A. (a) is for $\lambda > 0$ and (b) is for $\lambda < 0$. From these plots, we can easily observe that there exists a curve along which the system converges to the origin and that curve is nothing but the center manifold which we have obtained theoretically.

Nonhyperbolic case $\left(\lambda = \sqrt{6} \text{ or } \lambda = \frac{5\sqrt{2}}{\sqrt{3}}\right)$:

To apply center manifold theory, first, we have to transform the critical point B to the origin. To do that, we consider the shifting transformation $x = X + 1$, $y = Y$ and after applying the shifting transformation and putting $\lambda = \sqrt{6}$, we can determine that the equations of center manifold [422] is given by $h(Y) = -\frac{1}{2}Y^2 + \mathcal{O}(Y^4)$ and the map g on the center manifold is

$$Y \longmapsto Y - \frac{3}{2}Y^3 + \mathcal{O}(Y^5).$$

Notice that $Y^* = 0$ is a fixed point of g at which $g'(0) = 1$, $g''(0) = 0$, and $g'''(0) = -9 < 0$. This implies by Theorem 4 that the flow is stable along the center manifold but the critical point is *unstable (semistable)* as $\lambda_1 > 1$ for all γ_m.

After applying the shifting transformation and putting $\lambda = \frac{5\sqrt{2}}{\sqrt{3}}$, the equation of the center manifold is given by $h(Y) = \frac{10-3\gamma_m}{2(3\gamma_m-6)}Y^2 + \mathcal{O}(Y^4)$ and the map g on the center manifold is given by

$$Y \longmapsto -Y + \frac{5}{6}\left(\frac{2-3\gamma_m}{\gamma_m-2}\right)Y^3 + \mathcal{O}(Y^5).$$

Notice that $Y^* = 0$ is a fixed point of g at which $g'(0) = -1$. Now we determine the Schwarzian derivative, Sg, of the function g.

$$Sg(0) = -g'''(0) - \frac{3}{2}\left[g''(0)\right]^2 = \frac{5(3\gamma_m - 2)}{\gamma_m - 2}.$$

We can easily check that $Sg(0) > 0$ while $\gamma_m < \frac{2}{3}$ and $Sg(0) < 0$ while $\frac{2}{3} < \gamma_m < 2$. Thus by using Theorem 5, we can conclude that $Y^* = 0$ is stable along the center manifold when $\frac{2}{3} < \gamma_m < 2$ but as $\lambda_1 > 1$ for all γ_m, this implies that $Y^* = 0$ is semi stable for $\frac{2}{3} < \gamma_m < 2$ and unstable under the map g when $\gamma_m < \frac{2}{3}$. This implies by Theorem 8 that for $\lambda = \frac{5\sqrt{2}}{\sqrt{3}}$ the fixed point B is *semi stable* under the map F for $\frac{2}{3} < \gamma_m < 2$ and *unstable* under the map F for $\gamma_m < \frac{2}{3}$.

• Similar to the critical point B, the critical point C also corresponds to solution where the constraint equation (6.8) is dominated by the kinetic energy of the scalar field with a stiff equation of state $\omega_d = 1$ and there exist a decelerating phase of the universe.

The eigenvalues of the Jacobian matrix $J(C)$ are $\lambda_1 = 7 - 3\gamma_m$ and $\lambda_2 = 4 + \sqrt{\frac{3}{2}}\lambda$. The fixed point C is hyperbolic if $\lambda \neq -\sqrt{6}$, $-\frac{5\sqrt{2}}{\sqrt{3}}$ because for these two values of λ, the absolute value of one of the eigenvalues of $J(C)$ is 1 and the fixed point is nonhyperbolic if $\lambda = -\sqrt{6}$ or $\lambda = -\frac{5\sqrt{2}}{\sqrt{3}}$. Now we analyze the stability of the critical point C for both of the cases (hyperbolic and nonhyperbolic).

Hyperbolic case $\left(\lambda \neq -\sqrt{6}, -\frac{5\sqrt{2}}{\sqrt{3}}\right)$:

For the physically meaningful case: $0 \leq \gamma_m < 2$. We can easily see that $\lambda_1 > 1$ for all $\gamma_m \in [0, 2)$. Further, we can see that $\lambda_2 > 1$ when $\lambda > -\sqrt{6}$, $0 < \lambda_2 < 1$ when $-\frac{4\sqrt{2}}{\sqrt{3}} < \lambda < -\sqrt{6}$, $-1 < \lambda_2 < 0$ when $-\frac{5\sqrt{2}}{\sqrt{3}} < \lambda < -\frac{4\sqrt{2}}{\sqrt{3}}$, and $\lambda_2 < -1$ when $\lambda < -\frac{5\sqrt{2}}{\sqrt{3}}$. It follows that the fixed point C is a *source* for $\lambda \in (-\infty, -\frac{5\sqrt{2}}{\sqrt{3}}) \cup (-\sqrt{6}, \infty)$, and *saddle point*

for $\lambda \in \left(-\frac{4\sqrt{2}}{\sqrt{3}}, -\sqrt{6}\right) \cup \left(-\frac{5\sqrt{2}}{\sqrt{3}}, -\frac{4\sqrt{2}}{\sqrt{3}}\right)$.

Nonhyperbolic case $\left(\lambda = -\sqrt{6} \text{ or } \lambda = -\frac{5\sqrt{2}}{\sqrt{3}}\right)$:

To apply center manifold theory, first, we have to transform the critical point B to the origin. To do that, we consider the shifting transformation $x = X - 1$, $y = Y$ and after applying the shifting transformation and putting $\lambda = -\sqrt{6}$, the equation of the center manifold can be written as $h(Y) = \frac{1}{2}Y^2 + \mathcal{O}(Y^4)$ and the map g on the center manifold is given by

$$Y \longmapsto Y - \frac{3}{2}Y^3 + \mathcal{O}(Y^5).$$

Notice that $Y^* = 0$ is a fixed point of g at which $g'(0) = 1$, $g''(0) = 0$, and $g'''(0) = -9 < 0$. This implies by Theorem 4 that the critical point C is stable along the center manifold but as $\lambda_1 > 1$ for all γ_m so the critical point is *semi stable* in nature.

After applying the shifting transformation and putting $\lambda = -\frac{5\sqrt{2}}{\sqrt{3}}$, the equation of the center manifold can be written as $h(Y) = \frac{3\gamma_m - 10}{2(3\gamma_m - 6)}Y^2 + \mathcal{O}(Y^4)$ and the map g on the center manifold is given by

$$Y \longmapsto -Y + \frac{5}{6}\left(\frac{2 - 3\gamma_m}{\gamma_m - 2}\right)Y^3 + \mathcal{O}(Y^5).$$

Notice that $Y^* = 0$ is a fixed point of g at which $g'(0) = -1$. Now we determine the Schwarzian derivative, Sg, of the function g.

$$Sg(0) = -g'''(0) - \frac{3}{2}\left[g''(0)\right]^2 = \frac{5(3\gamma_m - 2)}{\gamma_m - 2}.$$

We can easily check that $Sg(0) > 0$ while $\gamma_m < \frac{2}{3}$ and $Sg(0) < 0$ while $\frac{2}{3} < \gamma_m < 2$. Thus by using Theorem 5, we conclude that $Y^* = 0$ is asymptotically stable for $\frac{2}{3} < \gamma_m < 2$ and unstable under the map g when $\gamma_m < \frac{2}{3}$. This implies by Theorem 8 that for $\lambda = -\frac{5\sqrt{2}}{\sqrt{3}}$, the fixed point C is *asymptotically stable* under the map F for $\frac{2}{3} < \gamma_m < 2$ and *unstable* under the map F for $\gamma_m < \frac{2}{3}$.

• The critical point D exists for $-\sqrt{6} \leq \lambda \leq \sqrt{6}$. Varying λ we get a non-isolated set of critical points which are completely dominated by kinetic energy ($\Omega_d = 1$ and $\dot{\phi} \neq 0$). It is to be noted that the DE can represent either quintessence or any other exotic type fluid depending on the parameter λ. The restriction $0 < \lambda^2 < 2$ implies that the scalar field behaves as quintessence like fluid and there exists an accelerated universe (since for this case, $-1 < \omega_{total} < -1/3$, $q < 0$) near these critical points whereas the scalar field DE behaves as dust for $\lambda^2 = 3$ ($\omega_\phi = 0$) and in this case, the solutions insinuate decelerating phase of the cosmic evolution.

The eigenvalues of the Jacobian matrix $J(D)$ are $\lambda_1 = \frac{1}{2}(\lambda^2 - 4)$ and $\lambda_2 = 1 + \lambda^2 - 3\gamma_m$. The fixed point D is hyperbolic if $\gamma_m \neq \frac{\lambda^2}{3}, \frac{\lambda^2+2}{3}$; $\lambda \neq \pm\sqrt{6}, \pm\sqrt{2}$ because for these values of γ_m and λ, the absolute value of one of the eigenvalues of $J(D)$ is 1 and the fixed point is nonhyperbolic if $\gamma_m = \frac{\lambda^2}{3}$ or $\gamma_m = \frac{\lambda^2+2}{3}$ or $\lambda = \pm\sqrt{6}$ or $\lambda = \pm\sqrt{2}$. Now we analyze the stability of the critical point D for both of the cases (hyperbolic and nonhyperbolic).

Hyperbolic case $\left(\gamma_m \neq \frac{\lambda^2}{3}, \frac{\lambda^2+2}{3}; \lambda \neq \pm\sqrt{6}, \pm\sqrt{2}\right)$:

For $\gamma_m \in [0,2)$, we can see that $\lambda_1, \lambda_2 < 1$ while $\lambda^2 < 3\gamma_m$; $\lambda_1 < 1, \lambda_2 > 1$ while $3\gamma_m < \lambda^2 < 6$; $\lambda_1, \lambda_2 > 1$ while $\lambda^2 > 6$. It follows that for $\gamma_m \in [0,2)$, the fixed point D is a *stable node (sink)* while $\lambda^2 < 3\gamma_m$, saddle point while $3\gamma_m < \lambda^2 < 6$ and *unstable node (source)* while $\lambda^2 > 6$.

Nonhyperbolic case $\left(\gamma_m = \frac{\lambda^2}{3}$ or $\gamma_m = \frac{\lambda^2+2}{3}$ or $\lambda = \pm\sqrt{6}$, or $\lambda = \pm\sqrt{2}\right)$:

First of all, note that for $\lambda = \sqrt{6}$ the coordinate of critical point D is equivalent to the coordinate of critical point B and the stability of the critical point B for $\lambda = \sqrt{6}$ already discussed. Further note that for $\lambda = -\sqrt{6}$ the coordinate of critical point D is equivalent to the coordinate of critical point C and the stability of the critical point C for $\lambda = -\sqrt{6}$ already discussed. So here we will not discuss the stability of the fixed point D for $\lambda = \pm\sqrt{6}$. Now we discuss the stability of the fixed point D for $\lambda = \sqrt{2}$.

To analyze the fixed point D for $\lambda = \sqrt{2}$, we use center manifold theory. To apply center manifold theory, first, we have to transform the critical point D to the origin. To do that, we consider the shifting transformation $x = X + \frac{\lambda}{\sqrt{6}}$, $y = Y + \sqrt{1 - \frac{\lambda^2}{6}}$ and after applying the shifting transformation and putting $\lambda = \sqrt{2}$, the discrete dynamical system associated with the system (6.10 – 6.11)can be written as

$$\begin{aligned}
\overline{X} &= X - \frac{3}{2}X^3\gamma_m - \frac{3\sqrt{3}}{2}X^2\gamma_m - X\gamma_m - \frac{3}{2}XY^2\gamma_m - \sqrt{6}XY\gamma_m - \frac{\sqrt{3}}{2}Y^2\gamma_m - \sqrt{2}Y\gamma_m \\
&\quad + 3X^3 + 3\sqrt{3}X^2 + \sqrt{3}Y^2 + 2\sqrt{2}Y, \\
\overline{Y} &= Y - \sqrt{\frac{3}{2}}X^2\gamma_m - \frac{3}{2}X^2Y\gamma_m - \sqrt{2}X\gamma_m - \sqrt{3}XY\gamma_m - \frac{3}{2}Y^3\gamma_m - 3\sqrt{\frac{3}{2}}Y^2\gamma_m - 2Y\gamma_m \\
&\quad + 3X^2Y + \sqrt{6}X^2 + \sqrt{3}XY + \sqrt{2}X.
\end{aligned}$$

Next, we use a coordinate transformation $\mathbf{u} = P\mathbf{v}$ where $\mathbf{u} = (X\ Y)^T$, $\mathbf{v} = (u\ v)^T$, $P = (\mathbf{v_1}\ \mathbf{v_2})$, and $\mathbf{v_1}$, $\mathbf{v_2}$ are the eigenvectors corresponding to the eigenvalues λ_1, λ_2 respectively. The equation of center manifold can be written as $h(u) = \frac{9\sqrt{3}(\gamma_m-2)}{2(2-3\gamma_m)(4-3\gamma_m)}u^2 + \mathcal{O}(u^3)$ and the map f on the center manifold is given by

$$u \longmapsto -u + \frac{1}{4-3\gamma_m}\left(-5\sqrt{6} + 9\sqrt{\frac{3}{2}}\gamma_m\right)u^2 + \frac{3\left(27\gamma_m^3 - 54\gamma_m^2 - 12\gamma_m + 56\right)}{2\left(4-3\gamma_m\right)^2\left(3\gamma_m - 2\right)}u^3 + \mathcal{O}(u^4).$$

Notice that $u^* = 0$ is a fixed point of f at which $f'(0) = -1$. Now we determine the Schwarzian derivative, Sf, of the function f.

$$Sf(0) = -f'''(0) - \frac{3}{2}\left[f''(0)\right]^2 = -\frac{162\left(15\gamma_m^3 - 42\gamma_m^2 + 36\gamma_m - 8\right)}{(4-3\gamma_m)^2(3\gamma_m - 2)}.$$

We can check that $Sf(0) < 0$ when $\gamma_m < 0.342$ or $\gamma_m > \frac{2}{3}$ and while $0.342 < \gamma_m < \frac{2}{3}$ then $Sf(0) > 0$. Thus by using Theorem 5, we can conclude that $u^* = 0$ is *asymptotically stable* under the map f when $\gamma_m < 0.342$ or $\gamma_m > \frac{2}{3}$ and *unstable* under the map f while $0.342 < \gamma_m < \frac{2}{3}$. This implies by Theorem 8 that for $\lambda = \sqrt{2}$ the fixed point D is *asymptotically stable* under the map F when $\gamma_m < 0.342$ or $\gamma_m > \frac{2}{3}$ and *unstable* under the map F

when $0.342 < \gamma_m < \frac{2}{3}$.

For $\lambda = -\sqrt{2}$, after considering the shifting transformation $x = X + \frac{\lambda}{\sqrt{6}}$, $y = Y + \sqrt{1 - \frac{\lambda^2}{6}}$ and putting $\lambda = -\sqrt{2}$, the system $(6.16 - 6.17)$ modifies to

$$\begin{aligned}\overline{X} &= X - \frac{1}{2}3X^3\gamma_m + \frac{3}{2}\sqrt{3}X^2\gamma_m - X\gamma_m - \frac{3}{2}XY^2\gamma_m - \sqrt{6}XY\gamma_m + \frac{1}{2}\sqrt{3}Y^2\gamma_m + \sqrt{2}Y\gamma_m \\ &\quad + 3X^3 - 3\sqrt{3}X^2 - \sqrt{3}Y^2 - 2\sqrt{2}Y, \\ \overline{Y} &= Y - \sqrt{\frac{3}{2}}X^2\gamma_m - \frac{3}{2}X^2Y\gamma_m + \sqrt{2}X\gamma_m + \sqrt{3}XY\gamma_m - \frac{1}{2}3Y^3\gamma_m - 3\sqrt{\frac{3}{2}}Y^2\gamma_m - 2Y\gamma_m \\ &\quad + 3X^2Y + \sqrt{6}X^2 - \sqrt{3}XY - \sqrt{2}X.\end{aligned}$$

Next, we use a coordinate transformation $\mathbf{u} = P\mathbf{v}$ where $\mathbf{u} = (X\ Y)^T$, $\mathbf{v} = (u\ v)^T$, $P = (\mathbf{v_1}\ \mathbf{v_2})$, and $\mathbf{v_1}$, $\mathbf{v_2}$ are the eigenvectors corresponding to the eigenvalues λ_1, λ_2 respectively. The equation of center manifold can be written as $h(u) = \frac{9\sqrt{3}(2-\gamma_m)}{2(2-3\gamma_m)(4-3\gamma_m)}u^2 + \mathcal{O}(u^3)$ and the map f on the center manifold is given by

$$u \longmapsto -u + \frac{1}{4-3\gamma_m}\left(-5\sqrt{6} + 9\sqrt{\frac{3}{2}}\gamma_m\right)u^2 + \frac{3\left(27\gamma_m^3 - 54\gamma_m^2 - 12\gamma_m + 56\right)}{2\left(9\gamma_m^2 - 18\gamma_m + 8\right)}u^3 + \mathcal{O}(u^4).$$

Notice that $u^* = 0$ is a fixed point of f at which $f'(0) = -1$. Now we determine the Schwarzian derivative, Sf, of the function f.

$$Sf(0) = -f'''(0) - \frac{3}{2}\left[f''(0)\right]^2 = -\frac{9\left(81\gamma_m^4 - 27\gamma_m^3 - 522\gamma_m^2 + 876\gamma_m - 424\right)}{(4-3\gamma_m)^2(3\gamma_m - 2)}.$$

We can check that $Sf(0) < 0$ while $\gamma_m > 1.245$ or $\gamma_m < \frac{2}{3}$ and $Sf(0) > 0$ while $\frac{2}{3} < \gamma_m < 1.245$. Thus by using Theorem 5, we can conclude that $u^* = 0$ is asymptotically stable under the map f when $\gamma_m > 1.245$ or $\gamma_m < \frac{2}{3}$ and unstable under the map g when $\frac{2}{3} < \gamma_m < 1.245$. This implies by Theorem 8 that for $\lambda = -\sqrt{2}$ the fixed point D is *asymptotically stable* under the map F when $\gamma_m > 1.245$ or $\gamma_m < \frac{2}{3}$ and *unstable* under the map F when $\frac{2}{3} < \gamma_m < 1.245$.

To analyze the fixed point D for $\gamma_m = \frac{\lambda^2}{3}$, we use center manifold theory. To apply center manifold theory, first, we have to transform the critical point D to the origin. To do that, we consider the shifting transformation $x = X + \frac{\lambda}{\sqrt{6}}$, $y = Y + \sqrt{1 - \frac{\lambda^2}{6}}$ and after applying the shifting transformation and putting $\gamma_m = \frac{\lambda^2}{3}$, the system $(6.16 - 6.17)$ modifies to

$$\begin{pmatrix} X \\ \\ Y \end{pmatrix} \longmapsto \begin{pmatrix} -2 + \frac{3}{2}\lambda^2 - \frac{\lambda^4}{6} & \sqrt{6}\left(1 - \frac{\lambda^2}{6}\right)^{3/2} \\ \\ \sqrt{\frac{3}{2}}\lambda\sqrt{1 - \frac{\lambda^2}{6}}\left(1 - \frac{\lambda^2}{3}\right) & 1 - \lambda^2 + \frac{\lambda^4}{6} \end{pmatrix}\begin{pmatrix} X \\ \\ Y \end{pmatrix} + \begin{pmatrix} non \\ linear \\ terms. \end{pmatrix}.$$

Next, we use a coordinate transformation $\mathbf{u} = P\mathbf{v}$ where $\mathbf{u} = (X\ Y)^T$, $\mathbf{v} = (u\ v)^T$, $P = (\mathbf{v_1}\ \mathbf{v_2})$, and $\mathbf{v_1}$, $\mathbf{v_2}$ are the eigenvectors corresponding to the eigenvalues λ_1, λ_2 respectively. The equation of center manifold can be represented as $h(u) = -\sqrt{\frac{3}{2}}\frac{\lambda^2(2\lambda^2-3)}{\sqrt{6-\lambda^2}(\lambda^2-3)^2}u^2 + \mathcal{O}(u^3)$ and the map f on the center manifold is given by

$$u \longmapsto u + \frac{\sqrt{6}\lambda^2(6-\lambda^2)}{(\lambda^2-3)^2}u^2 + \frac{\lambda^2\sqrt{6-\lambda^2}(9-12\lambda^2)}{(\lambda^2-3)^3}u^3 + \mathcal{O}(u^4).$$

Notice that $u^* = 0$ is a fixed point of f at which

$$f'(0) = 1,$$
$$f''(0) = \frac{2\sqrt{6}\lambda^2(6-\lambda^2)}{(\lambda^2-3)^2},$$
$$f'''(0) = \frac{18\lambda^2(3-4\lambda^2)\sqrt{6-\lambda^2}}{(\lambda^2-3)^3}.$$

This implies by Theorem 4 that the critical point D is *unstable (semistable)* when $\lambda \neq 0, \pm\sqrt{6}$. For $\lambda = 0$ or $\lambda = \pm\sqrt{6}$ no conclusion can be determined. Also note that for $\lambda = \pm\sqrt{6}$, the corresponding value of γ_m is $\gamma_m = 2$ which is not also physically meaningful case.

To analyze the fixed point D for $\gamma_m = \frac{\lambda^2+2}{3}$, we use center manifold theory. To apply center manifold theory, first, we have to transform the critical point D to the origin. To do that, we consider the shifting transformation $x = X + \frac{\lambda}{\sqrt{6}}$, $y = Y + \sqrt{1-\frac{\lambda^2}{6}}$ and after applying the shifting transformation and putting $\gamma_m = \frac{\lambda^2+2}{3}$, the system (6.16−6.17) modifies to

$$\begin{pmatrix} X \\ Y \end{pmatrix} \longmapsto \begin{pmatrix} -\frac{\lambda^4}{6} + \frac{7\lambda^2}{6} - 2 & \frac{2}{3}\lambda\sqrt{6-\lambda^2} - \frac{1}{6}\lambda^3\sqrt{6-\lambda^2} \\ \frac{1}{6}\lambda\sqrt{6-\lambda^2} - \frac{1}{6}\lambda^3\sqrt{6-\lambda^2} & \frac{\lambda^4}{6} - \frac{2\lambda^2}{3} - 1 \end{pmatrix} \begin{pmatrix} X \\ Y \end{pmatrix} + \begin{pmatrix} non \\ linear \\ terms. \end{pmatrix}.$$

Next, we use a coordinate transformation $\mathbf{u} = P\mathbf{v}$ where $\mathbf{u} = (X\ Y)^T$, $\mathbf{v} = (u\ v)^T$, $P = (\mathbf{v_1}\ \mathbf{v_2})$, and $\mathbf{v_1}$, $\mathbf{v_2}$ are the eigenvectors corresponding to the eigenvalues λ_1, λ_2 respectively. The equation of centermanifold can be represented as $h(u) = \sqrt{\frac{3}{2}}\frac{\lambda}{\sqrt{6-\lambda^2}}\left(\frac{2\lambda^6-15\lambda^4+30\lambda^2-8}{2-\lambda^2}\right)u^2 + \mathcal{O}(u^3)$ and the map f on the center manifold is given by

$$u \longmapsto -u + \frac{-6\sqrt{6}\left(\lambda^2-6\right)\left(\lambda^8-12\lambda^6+41\lambda^4-48\lambda^2+12\right)}{2(\lambda^2-2)}u^2$$
$$+ \frac{9\sqrt{6-\lambda^2}\left(2\lambda^{12}-47\lambda^{10}+357\lambda^8-1168\lambda^6+1692\lambda^4-896\lambda^2+96\right)}{2(\lambda^2-2)}u^3 + \mathcal{O}(u^4).$$

Notice that $u^* = 0$ is a fixed point of f at which $f'(0) = -1$. Now we determine the Schwarzian derivative, Sf, of the function f.

$$Sf(0) = -f'''(0) - \frac{3}{2}\left[f''(0)\right]^2$$
$$= -6\left(\frac{6\sqrt{6}\left(\lambda^2-6\right)\left(\lambda^8-12\lambda^6+41\lambda^4-48\lambda^2+12\right)}{2\left(\lambda^2-2\right)}\right)^2$$
$$- \frac{6\left(9\sqrt{6-\lambda^2}\left(2\lambda^{12}-47\lambda^{10}+357\lambda^8-1168\lambda^6+1692\lambda^4-896\lambda^2+96\right)\right)}{2\left(\lambda^2-2\right)}.$$

By considering various values of λ, we can check that $Sf(0) < 0$. As $-\sqrt{6} < \lambda < \sqrt{6}$, to determine the value of $Sf(0)$, we have taken $\lambda = 0, \pm 1, \pm 2$ and see that for these values of λ, $Sf(0) < 0$. Thus by using Theorem 5, we can conclude that $u^* = 0$ is asymptotically stable under the map f. This implies by Theorem 8 that for $\gamma_m = \frac{\lambda^2+2}{3}$ the fixed point D is

asymptotically stable under the map F for all values of $\lambda \in (-\sqrt{6}, \sqrt{6})$.

• The critical point E exists for $\lambda^2 > 3\gamma_m$. Scaling solutions are represented by these critical points. These non-isolated set of critical points are hyperbolic or normally-hyperbolic in nature depending on the values of λ and γ_m. At $\gamma_m = \frac{2}{3}$, the scalar field DE behaves as a quintessence boundary. The cosmic coincidence problem can be alleviated by these points depending on the values of λ and γ_m.

The critical point E has more complicated stability conditions. The stability status of E is depicted in Figure 6.3. In those figures, we have shown the phase portrait near the critical point E numerically for several physically meaningful values of λ and γ_m. From these plots, we can conclude that the critical point E is a *spiral sink* and *asymptotically stable* in nature for $(\lambda = \pm 2, \gamma_m = 1)$, $\left(\lambda = \pm\sqrt{6}, \gamma_m = \frac{4}{3}\right)$.

6.5 Cosmological Implications

It is to be noted that the constraint equation $\Omega_\phi = x^2 + y^2$ yields $0 \leq x^2 + y^2 \leq 1$, for a non-negative fluid density $\rho_d \geq 0$. So the evolution of this system is completely confined to a unit disc. The lower half-disc, *i.e.,* $y < 0$ transpires $H < 0$ which corresponds to contracting universes. Without loss of generality, we restrict our discussion to the upper-half disc ($y \geq 0$) due to the symmetry of the system under reflection and time reversal.

The fixed point $(x = 0, y = 0)$ corresponds to the dark matter dominated solution where $\Omega_d = 0$ is saddle for $\gamma_m \in \left(\frac{2}{3}, \frac{4}{3}\right) \cup \left(\frac{4}{3}, 2\right)$, source for $\gamma_m \in (0, \frac{2}{3})$ and unstable in nature at $\gamma_m = \frac{2}{3}$. The matter-dominated solution is stable for $\omega_m = -1$. Two of the fixed points $(x = \pm 1, y = 0)$ correspond to scalar field-dominated solutions where $\omega_d = 1$ is unstable in nature. For $\lambda = -\frac{5\sqrt{2}}{\sqrt{3}}$, the fixed point C is asymptotically stable for $\frac{2}{3} < \gamma_m < 2$. On the other hand, the fixed point D is corresponds to scalar field dominated solution ($\Omega_d = 1$) which exists for $-\sqrt{6} \leq \lambda \leq \sqrt{6}$. $\omega_d = \frac{\lambda^2}{3} - 1$ gives rise to a power law inflationary expansion ($q < 0$) for $\lambda^2 < 2$. We have shown that D is a stable node while $\lambda^2 < 3\gamma_m$ and hyperbolic fixed point. For non-hyperbolic case: for $\lambda = \sqrt{2}$, D is asymptotically stable when $\gamma_m < 0.342$ or $\gamma_m > \frac{2}{3}$. For $\lambda = -\sqrt{2}$, D is asymptotically stable when $\gamma_m > 1.245$ or $\gamma_m < \frac{2}{3}$. For $\lambda \in (-\sqrt{6}, \sqrt{6})$ the point D is asymptotically stable when $\gamma_m = \frac{\lambda^2+2}{3}$.

Barotropic fluid dominated solution $(x = 0, y = 0)$ is hyperbolic where $\Omega_d = 0$ is saddle in nature $\frac{2}{3} < \gamma_m < 2$ source for $0 < \gamma_m < \frac{2}{3}$. For $\gamma_m = \frac{2}{3}$ and 0, this solution is unstable and asymptotically stable accordingly and non-hyperbolic in nature.

Two of the fixed points $(x = \pm 1, y = 0)$ correspond to solutions where the constraint equation (6.8) is dominated by the kinetic energy of the scalar field with a stiff equation of state, $\Omega_d = 1$. The fixed point B is hyperbolic in nature and source for $\lambda < \sqrt{6}$ or $\lambda > \frac{5\sqrt{2}}{\sqrt{3}}$, and saddle for $\lambda \in \left(\sqrt{6}, \frac{4\sqrt{2}}{\sqrt{3}}\right) \cup \left(\frac{4\sqrt{2}}{\sqrt{3}}, \frac{5\sqrt{2}}{\sqrt{3}}\right)$. B is non-hyperbolic and semistable for $\lambda = \sqrt{6}, \frac{5\sqrt{2}}{\sqrt{3}}$ and $\frac{2}{3} < \gamma_m < 2$ and unstable for $\lambda = \frac{5\sqrt{2}}{\sqrt{3}}$ and $\gamma_m < \frac{2}{3}$.

The fixed point C is hyperbolic in nature and source for $\lambda \in (-\infty, -\frac{5\sqrt{2}}{\sqrt{3}}) \cup (-\sqrt{6}, \infty)$, and saddle point for $\lambda \in \left(-\frac{4\sqrt{2}}{\sqrt{3}}, -\sqrt{6}\right) \cup \left(-\frac{5\sqrt{2}}{\sqrt{3}}, -\frac{4\sqrt{2}}{\sqrt{3}}\right)$. C is non-hyperbolic and semistable

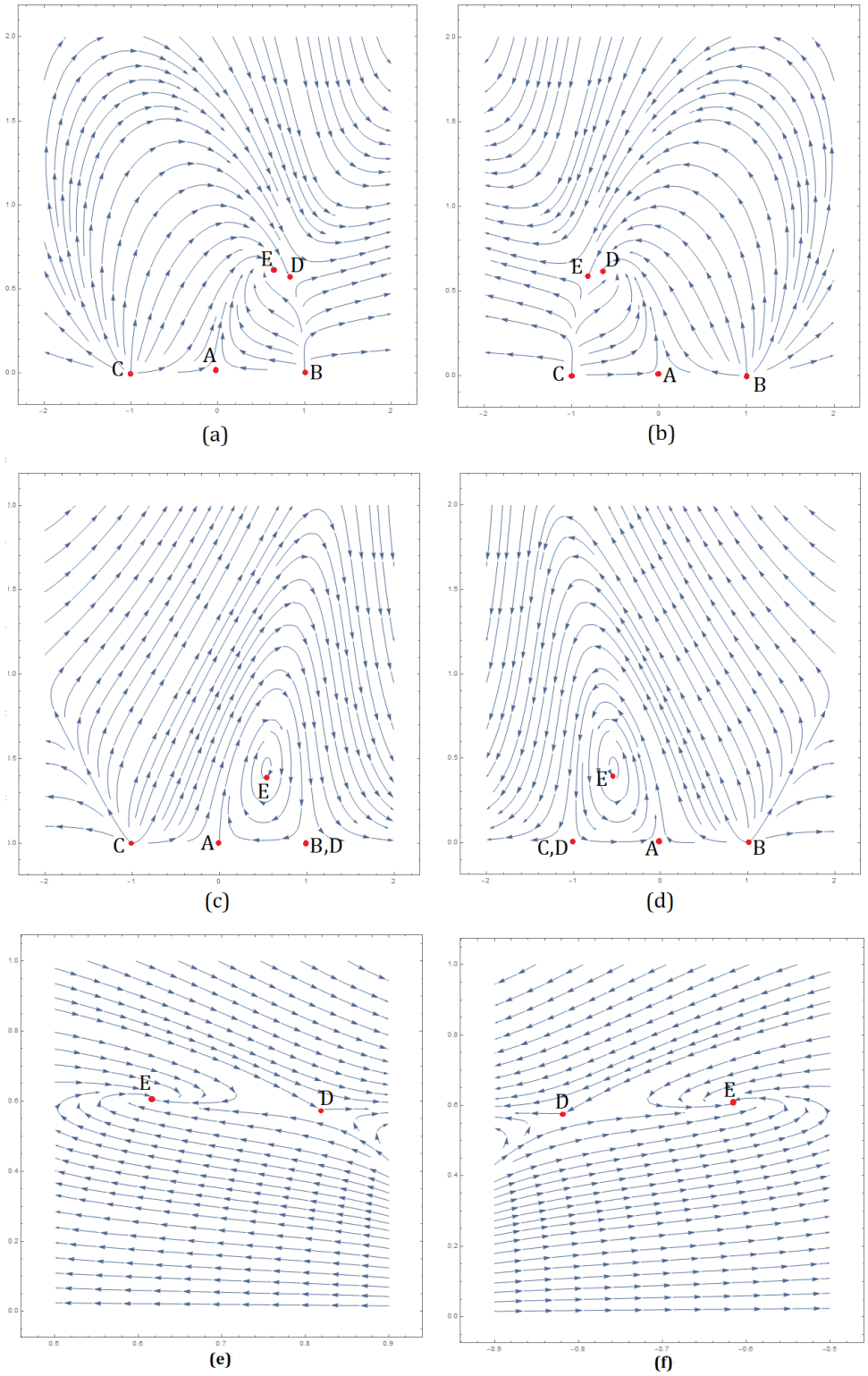

Figure 6.3: These figures show the behavior of the trajectories near each of the critical points. Especially in this case, we want to focus on the phase portrait near the critical point E. (a) is for $\lambda = 2, \gamma_m = 1$, (b) is for $\lambda = -2, \gamma_m = 1$, (c) is for $\lambda = \sqrt{6}, \gamma_m = \frac{4}{3}$, and (d) is for $\lambda = -\sqrt{6}, \gamma_m = \frac{4}{3}$. Figures (e) and (f) show the phase portraits in a very small neighborhood of the critical points D and E to distinguish the behavior of stability of the critical points for $\lambda = \pm 2$, $\gamma_m = 1$.

Table 6.2: Table shows the stability of each critical point for both hyperbolic and nonhyperbolic cases corresponding to every fixed point:

CPs	Stability for hyperbolic case	Stability for nonhyperbolic case
A	Saddle point for $\frac{2}{3} < \gamma_m < 2$, source for $0 < \gamma_m < \frac{2}{3}$	Asymptotically stable for $\gamma_m = 0$, unstable for $\gamma_m = \frac{2}{3}$
B	Source for $\lambda < \sqrt{6}$ or $\lambda > \frac{5\sqrt{2}}{\sqrt{3}}$, saddle point for $\lambda \in \left(\sqrt{6}, \frac{5\sqrt{2}}{\sqrt{3}}\right)$	Semistable for $\lambda = \sqrt{6}$ and all γ_m, semistable for $\lambda = \frac{5\sqrt{2}}{\sqrt{3}}$ and $\frac{2}{3} < \gamma_m < 2$, unstable for $\lambda = \frac{5\sqrt{2}}{\sqrt{3}}$ and $\gamma_m < \frac{2}{3}$
C	Source for $\lambda > -\sqrt{6}$ or $\lambda < -\frac{5\sqrt{2}}{\sqrt{3}}$, saddle point for $\lambda \in \left(-\frac{5\sqrt{2}}{\sqrt{3}}, -\sqrt{6}\right)$	Semistable for $\lambda = -\sqrt{6}$ and all γ_m, asymptotically stable for $\lambda = -\frac{5\sqrt{2}}{\sqrt{3}}$ and $\frac{2}{3} < \gamma_m < 2$, unstable for $\lambda = -\frac{5\sqrt{2}}{\sqrt{3}}$ and $\gamma_m < \frac{2}{3}$
D	Stable node for $\lambda^2 < 3\gamma_m$, saddle point for $3\gamma_m < \lambda^2 < 6$, unstable node for $\lambda^2 > 6$	Asymptotically stable for $\lambda = \sqrt{2}$ and $\gamma_m < 0.342$ or $\gamma_m > \frac{2}{3}$, unstable for $\lambda = \sqrt{2}$ and $0.342 < \gamma_m < \frac{2}{3}$, asymptotically stable for $\lambda = -\sqrt{2}$ and $\gamma_m > 1.245$ or $\gamma_m < \frac{2}{3}$, unstable for $\lambda = -\sqrt{2}$ and $\frac{2}{3} < \gamma_m < 1.245$, asymptotically stable for $\gamma_m = \frac{\lambda^2+2}{3}$ where $\lambda \in (-\sqrt{6}, \sqrt{6})$
E	Spiral sink for $\lambda = \pm 2, \gamma_m = 1$ and $\lambda = \pm\sqrt{6}, \gamma_m = \frac{4}{3}$.	Very complicated to analyze.

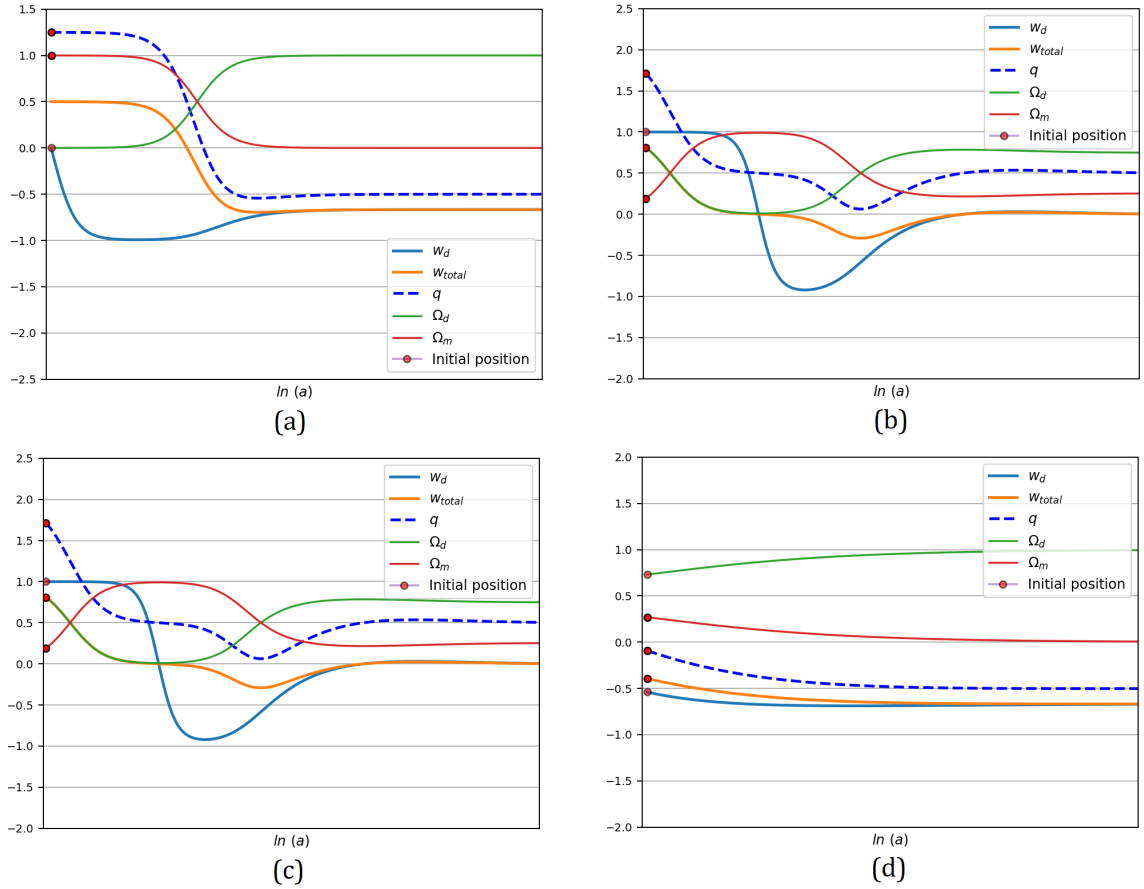

Figure 6.4: The figure shows the time evolution of cosmological parameters of our cosmological model. In panel (a), initial position near the critical point A, for $\lambda = 1$ and $\gamma_m = 1.5$ the kinetic energy dominated late time accelerated solutions attracted towards quintessence era. In panel (b) and (c), initial position near the critical points B and C respectively, for $\lambda = 2$ and $\gamma_m = 1$ we get the kinetic energy and dust dominated late-time decelerated solutions. In panel (d), the behavior of the late solution near the critical point D is similar to panel (a).

for $\lambda = -\sqrt{6}$, asymptotically stable for $\lambda = \frac{-5\sqrt{2}}{\sqrt{3}}$. C is non-hyperbolic and semistable for $\lambda = \frac{-5\sqrt{2}}{\sqrt{3}}$ and $\frac{2}{3} < \gamma_m < 2$, unstable for $\lambda = \frac{-5\sqrt{2}}{\sqrt{3}}$ and $\gamma_m = \frac{2}{3}$.

The critical point D corresponds to a scalar field-dominated solution is hyperbolic in nature and late-time attractor for $\lambda^2 < 3\gamma_m$, saddle for $3\gamma_m < \lambda^2 < 6$, and unstable node for $\lambda^2 > 6$. On the other hand, D is non-hyperbolic in nature and corresponds to late time attractor for $\lambda = \sqrt{2}$ and $0.342 < \gamma_m < \frac{2}{3}$, late time attracting solution for $\lambda = -\sqrt{2}$ and $\gamma_m > 1.245$ or $\gamma_m = \frac{2}{3}$, unstable for $\lambda = -\sqrt{2}$ and $\frac{2}{3} < \gamma_m < 1.245$, late time attracting solution for $\gamma_m = \frac{\lambda^2+2}{3}$, where $\lambda \in (-\sqrt{6}, \sqrt{6})$. E corresponds to scaling solution. E is hyperbolic in nature and spiral sink for $\lambda = \pm 2$, $\gamma = 1$ and $\lambda = \pm\sqrt{6}, \gamma_m = \frac{4}{3}$. We can divide the evolutionary character of the Universe into two groups: (a) generic evolution (b) non-generic evolution. For $\gamma_m = 0$, generic evolution occurs near the point A as the family

of orbits emerges from a stable equilibrium in the past and then finishes towards A which represents the ΛCDM era. And for $0 < \gamma_m < \frac{2}{3}$, a generic evolution occurs near A which represents the quintessence state as the orbit emerges from an unstable equilibrium point A in the past and finishes at D.

6.6 Brief Discussion and Concluding Remarks

The present work is an example of a discrete dynamical system analysis in cosmology. In a particular cosmological study of the scalar field, cosmology has been analyzed using a dynamical system at the background level. For simplicity of the formation of the dynamical system, the scalar field potential is chosen in the exponential form. At the background level, there are five critical points for which the resulting equation of state parameter of the resulting total fluid has been given in the last but one column of Table 6.1. The value of ω_{total} for the fixed points B and C indicates that the resulting fluid is a stiff fluid which is very important at the very early era of evolution, particularly when the quantum effects are important. The fixed points A and E will corresponds to dark energy model if $\gamma_m < \frac{2}{3}$, while the resulting fluid will be a normal fluid if $\gamma_m > \frac{2}{3}$. Similarly, the fixed point D corresponds to a dark energy fluid if $\lambda^2 < 2$. Thus the critical points A, D, and E may have dark energy fluid as the resulting fluid with proper choice of the parameter involved. Finally, we have the following observations from the perspective of stability. For the critical points A and E, there will be matter dominated era when $\gamma_m \in \left(\frac{2}{3}, 2\right)$ and it is a stable configuration for $\gamma_m = 0$ and unstable when $\gamma_m \neq 0$. The critical point B is unstable for all possible choices of λ whereas the fixed point C will be stable if $\frac{2}{3} < \gamma_m < 2$, $\lambda = -\frac{5\sqrt{2}}{\sqrt{3}}$ and it will be unstable for other possible values of λ and γ_m. Lastly, the critical point D is stable for $\lambda^2 < 3\gamma_m$ and unstable for other possible cases where $\gamma_m \in [0, 2)$. Further, when $\lambda = \sqrt{2}$, the critical point is stable when $\gamma_m < 0.342$ or $\gamma_m > \frac{2}{3}$ and similarly when $\lambda = -\sqrt{2}$, the fixed point will be stable for $\gamma_m > 1.245$ or $\gamma_m < \frac{2}{3}$. However, the model will be stable if $\gamma_m = \frac{\lambda^2+2}{3}$ and $\lambda \in (-\sqrt{6}, \sqrt{6})$. Finally, the satbility analysis shows the matter dominated phase or the present accelerated expansion of the universe depending on the choices of the appropriate parameters and they may corresponds to stable or unstable configuration depending on the restrictions on the parameter.

CHAPTER 7

BRIEF SUMMARY AND FUTURE PROSPECT

In this thesis, there has been an attempt to validate some of the expansionary cosmological models depicting the late time acceleration. Dynamical variables have been constructed from the cosmological parameters. The fundamental equations have been turned into dynamical systems. Non-hyperbolic stability analysis by employing center manifold methods has been carried out. To be precise,

Chapter 2 dealt with Cosmological model of a three-form field, minimally coupled to gravity and interacting with cold dark matter in the background of flat FLRW space-time. By suitable choice of the dimensionless variables, the evolution equations are converted to an autonomous system and cosmological study is done by dynamical system analysis. The critical points are determined and the stability of the (non-hyperbolic) equilibrium points are examined by center manifold Theory. Possible bifurcation scenarios have been examined by the Poincaré index theory to identify possible cosmological phase transition. Also stabilities of the critical points have been analyzed globally using geometric features.

A cosmological model having matter field as (non) interacting dark energy (DE) and baryonic matter and minimally coupled to gravity has been considered in Chapter 3 with flat FLRW space time. The DE is chosen in the form of a three-form field while radiation and dust (*i.e.,* cold dark matter) are the baryonic part. The cosmic evolution is studied through dynamical system analysis of the autonomous system so formed from the evolution equations by suitable choice of the dimensionless variables. The stability of the non-hyperbolic critical points are examined by Center manifold theory and possible bifurcation scenarios have been examined.

Chapter 4 is an example of the application of the dynamical system analysis in the context of cosmology. Here cosmic evolution is considered in the background of homogeneous and isotropic flat FLRW space-time with interacting dark energy and varying mass dark matter as the matter content. The DE is chosen as phantom scalar field with self-interacting potential while the DM is in the form of dust. The potential of the scalar field and the mass function

of dark matter are chosen as exponential or power-law form or in their product form. Using suitable dimensionless variables the Einstein field equations and the conservation equations constitute an autonomous system. The stability of the non-hyperbolic critical points are analyzed by using center manifold theory. Finally, cosmological phase transitions have been detected through bifurcation analysis which has been done by Poincaré index theory.

Chapter 5 analyzed a FLRW cosmological model with spatial curvature and minimally coupled scalar field as the matter content. The curvature term behaves as a perfect fluid with the equation of state parameter $\omega_{\mathcal{K}} = -\frac{1}{3}$. Using suitable transformation of variables, the evolution equations are reduced to an autonomous system for both power law and exponential form of the scalar potential. The critical points are analyzed with center manifold theory and stability has been discussed. Also, critical points at infinity have been studied using the notion of Poincaré sphere. Finally, the cosmological implications of the critical points and cosmological bouncing scenarios are discussed. It is found that the cosmological bounce takes place near the points at infinity when the non-isolated critical points on the equator of the Poincaré sphere are saddle or saddle-node in nature.

Chapter 6 dealt with the dynamical system analysis of quintessence dark energy scalar field model with exponential potential. A dynamical system analysis has been applied at the background level. Using suitable transformation of variables, the evolution equations are reduced to an autonomous system for exponential form of the scalar potential. The critical points are analyzed with center manifold theory and stability has been discussed by using Schwarzian derivative. Finally, cosmological implications of the critical points are discussed and it is found that the stability of the late-time attractor changes for quintessence dark energy model.

Scope of future work:

This thesis has investigated some of the well known theories on accelerated expansion in the light of non-hyperbolic stability analysis. In particular, center manifold methods have been applied in all the models that have been considered here. Another ingredient from the higher order stability theory is the Liyapunov method. In this method, one attempts to construct the Liyapunov function which guarantees the stability or the instability of a system. So one of the future projects may be to attempt to construct Liyapunov functions for the cosmological models. An even better project may be to find some necessary or sufficient conditions for the existence of the Lyapunov function.

Another approach is to employ some advanced semi-analytical techniques such as the homotopy perturbation method or homotopy analysis method to investigate the cosmological systems. The homotopy analysis method is a topological method to generate a convergent series solution of the non-linear systems. Such techniques from the theory of differential equations may be valuable to study cosmological models in future.

The qualitative structure of the solutions of an autonomous system may change when the system parameters passes through certain values called the bifurcation values. Bifurcation theory is a rich area of mathematics which may shed light to the structure of solutions of the cosmological systems. In fact, there is a branch of bifurcation theory called chaos. Chaotic systems are ubiquitous in Nature. An application of the chaos theory to the cosmological

models could be both novel and exciting.

Therefore the possibilities are endless and it will be very satisfying to work in the juncture of cosmology and mathematical analysis as long as the beauty of geometry and physics continues to intrigue...

BIBLIOGRAPHY

[1] J. Wainwright and G. F. R. Ellis, "Dynamical Systems in Cosmology", *Cambridge University Press*, Cambridge, UK, (1997).

[2] P. Coles and F. Lucchin, "The Origin and Evolution of Cosmic Structer", *John Wiely, Ltd.* **2002**.

[3] P. J. E. Peebles, "Principles of Physical Cosmology", *Princeton University Press.* **1993**.

[4] W. Hu and S. Dodelson, "Cosmic Microwave Background Anisotropies", *Ann. Rev. Astron. Astrophys.* **40**, 171 (2002) (arXiv:astro-ph/0110414).

[5] G. F. R. Ellis and W. Stoeger, "The 'fitting problem' in cosmology", *Class. Quantum Grav.* **4**, 1697 (1987).

[6] T. Buchert, "On average properties of inhomogeneous fluids in general relativity I: Dust cosmologies", *Gen. Relativ. Gravit.* **32**, 105 (2000) (arXiv: gr-qc/9906015).

[7] E. W. Kolb, S. Matarrese, A. Notari, and A. Riotto, "The effect of inhomogeneities on the expansion rate of the Universe", *Phys. Rev., D* **71**, 023524 (2005) (arXiv: hep-ph/0409038).

[8] A. Paranjape, and T. P. Singh, "The Possibility of cosmic acceleration via spatial averaging in Lemaître–Tolman–Bondi Models", *Class. Quantum Grav.* **23**, 6955 (2006) (arXiv: astro-ph/0605195).

[9] C. -H. Chuang, J. -A. Gu, and W. -Y. P. Hwang, "Inhomogeneity–induced cosmic acceleration in a dust Universe", *Class. Quantum Grav.* **25**, 175001 (2008) (arXiv: astro-ph/0512651).

[10] A. Einstein, Cosmological considerations in the General Theory of Relativity, Sitzungsber. Preuss. Akad. Wiss. Phys.-math. Klasse VI (1917) 142.

[11] S. Dodelson, "Modern Cosmology", Academic Press, Elsevier Science, (2003).

[12] A. Friedmann, "On the curvature of space", *Z. Phys* **10**, 377 (1922).

[13] G. Lemaître, "Expansion of the Universe: A homogeneous Universe of constant mass and increasing radius accounting for the radial velocity of extra-galactic nebulae", *Mon. Not. R. Astron. Soc.* **91**, 483 (1931).

[14] H. P. Robertson, "Kinematics and world-structure", *Astrophys. J.* **82**, 284 (1935).

[15] A. G. Walker, "On milne's theory of world-structure", *Proc. London. Math. Soc.* **s2-42** 90 (1937).

[16] E. Komatsu *et al.,* (WMAP Collaboration), "Seven-year Wilkinson microwave anisotropy probe (WMAP) observations: Cosmological interpretation" *Astrophys. J. Suppl.* **192**, 18 (2011) (arXiv: 1001.4538 [astro-ph.CO]).

[17] A. G. Riess *et al.,* (High-redshift Supernovae Search Team Collaboration), "Observational evidence from supernovae for an accelerating Universe and a cosmological constant", *Astron. J.* **116**, 1009 (1998) (arXiv: astro-ph/9805201).

[18] S. Perlmutter *et al.,* (Supernovae Cosmology Project Collaboration), "Measurements of Omega and Lambda from 42 high redshift supernovae", *Astrophys. J.* **517**, 565 (1999) (arXiv: astro-ph/9812133).

[19] P. de Bernardis *et al.,* (Boomerang Collaboration), "A flat Universe from high-resolution maps of the cosmic microwave background radiation", *Nature* **404**, 955 (2000) (arXiv: astro-ph/0004404).

[20] D. N. Spergel *et al.,* (WMAP Collaboration), "First year Wilkinson microwave anisotropy probe (WMAP) observations: Determination of cosmological parameters", *Astrophys. J. Suppl.* **148**, 175 (2003) (arXiv: astro-ph/0302209).

[21] J. H. Goldstein *et al.,* (ACBAR Collaboration), "Estimates of cosmological parameters using the CMB angular power spectrum of ACBAR", *Astrophys. J.* **599**, 773 (2003) (arXiv: astro-ph/0212517).

[22] A. C. S. Readhead *et al.,* "Extended mosaic observations with the cosmic background imager", *Astrophys. J.* **609**, 498 (2004) (arXiv: astro-ph/0402359).

[23] D. N. Spergel *et al.,* (WMAP Collaboration), "Wilkinson microwave anisotropy probe (WMAP) three year results: implications for cosmology", *Astrophys. J. Suppl.* **170**, 377 (2007) (arXiv: astro-ph/0603449).

[24] E. Komatsu *et al.,* (WMAP Collaboration), "Five-year Wilkinson microwave anisotropy probe (WMAP) observations: Cosmological interpretation" , *Astrophys. J. Suppl.* **180**,

330 (2009) (arXiv:0803.0547 [astro-ph]).

[25] W. J. Percival *et al.,* (2dFGRS Collaboration), "The 2dF galaxy redshift survey: The power spectrum and the matter content of the Universe", *Mon. Not. R. Astron. Soc.* **327**, 1297 (2001) (arXiv: astro-ph/0105252).

[26] M. Tegmark *et al.,* (SDSS Collaboration), "Cosmological parameters from SDSS and WMAP", *Phys. Rev. D* **69**, 103501 (2004) (arXiv: astro-ph/0310723).

[27] U. Seljak *et al.,* (SDSS Collaboration), "Cosmological parameter analysis including SDSS Ly-alpha forest and galaxy bias: Constraints on the primordial spectrum of fluctuations, neutrino mass, and dark energy", *Phys. Rev. D* **71**, 103515 (2005) (arXiv: astro-ph/0407372).

[28] D. J. Eisenstein *et al.,* (SDSS Collaboration), "Detection of the baryon acoustic peak in the large-scale correlation function of SDSS luminous red galaxies", *Astrophys. J.* **633**, 560 (2005) (arXiv: astro-ph/0501171).

[29] A. G. Sanchez *et al.,* "The clustering of galaxies in the SDSS-III baryon oscillation spectroscopic survey: cosmological implications of the large-scale two-point correlation function", *Mon. Not. R. Astron. Soc.* **425**, 415 (2012) (arXiv: 1203.6616 [astro-ph.CO]).

[30] B. Jain and A. Taylor, "Cross-correlation tomography: measuring dark energy evolution with weak lensing", *Phys. Rev. Lett.* **91**, 141302 (2003) (arXiv: astro-ph/0306046).

[31] A. G. Riess *et al.*, "New Hubble Space Telescope Discoveries of Type Ia Supernovae at $z >= 1$: Narrowing Constraints on the Early Behavior of Dark Energy", *Astrophys. J.* **659**, 98 (2007) (arXiv: astro-ph/0611572).

[32] T. M. Davis *et al.*, "Scrutinizing Exotic Cosmological Models Using ESSENCE Supernova Data Combined with Other Cosmological Probes", *Astrophys. J.* **666**, 716 (2007) (arXiv: astro-ph/0701510).

[33] W. M. Wood-Vasey *et al.*, "Observational Constraints on the Nature of the Dark Energy: First Cosmological Results from the ESSENCE Supernova Survey", *Astrophys. J.* **666**, 694 (2007) (arXiv: astro-ph/0701041).

[34] N. Jarosik *et al.*, "Seven-Year Wilkinson Microwave Anisotropy Probe (WMAP) Observations: Sky Maps, Systematic Errors, and Basic Results", *Astrophys. J. Suppl.* **192**, 14 (2011) (arXiv:1001.4744 [astro-ph.CO]).

[35] D. Larson *et al.*, "Seven-Year Wilkinson Microwave Anisotropy Probe (WMAP) Observations: Power Spectra and WMAP-Derived Parameters", *Astrophys. J. Suppl.* **192**, 16 (2011) (arXiv: 1001.4635 [astro-ph.CO]).

[36] S. Cole *et al.*, "The 2dF Galaxy Redshift Survey: Power-spectrum analysis of the final dataset and cosmological implications", *Mon. Not. R. Astron. Soc.* **362**, 505 (2005) (arXiv:astro-ph/0501174).

[37] M. Kowalski *et al.*, "Improved Cosmological Constraints from New, Old and Combined Supernova Datasets", *Astrophys. J.* **686**, 749 (2008) (arXiv:0804.4142 [astro-ph]).

[38] T. P. Sotiriou and V. Faraoni, "$f(R)$ theories of gravity", *Rev. Mod. Phys.* **82**, 451 (2010) (arXiv: 0805.1726 [gr-qc]).

[39] S. Nojiri and S. D. Odintsov, "Unified cosmic history in modified gravity: from F(R) theory to Lorentz non-invariant models", *Phys. Rept.* **505**, 59 (2011) (arXiv:1011.0544 [gr-qc]).

[40] Y.-B. Wu *et al.*, "Thermodynamic laws for generalized f(R) gravity with curvature-matter coupling", *Phys. Lett. B* **717**, 323 (2012).

[41] S. Capozziello, "Curvature quintessence", *Int. J. Mod. Phys. D*, **11**, 483 (2002) (arXiv: gr-qc/0201033).

[42] E. Hubble, "A relation between distance and radial velocity among extra-galactic nebulae", *Proc. Nat. Acad. Sci.* **15**, 168 (1929).

[43] P. J. E. Peebles and B. Ratra, "The cosmological constant and dark energy", *Rev. Mod. Phys* **75**, 559 (2003) (arXiv: astro-ph/0207347).

[44] T. Padmanabhan, "Cosmological constant — the weight of the vacuum", *Phys. Rept.* **380**, 235 (2003) (arXiv: hep-th/0212290).

[45] S. Weinberg, "The cosmological constant problem", *Rev. Mod. Phys.* **61**, 1 (1989).

[46] S. M. Carroll, "The cosmological Constant", *Liv. Rev. Relt.* **4**, 1 (2001) (arXiv: astro-ph/0004075).

[47] E. J. Copeland, M. Sami, and S. Tsujikawa, "Dynamics of dark energy", *Int. J. Mod. Phys. D* **15**, 1753 (2006) (arXiv: hep-th/0603057).

[48] I. Zlatev, L. Wang, and P. J. Steinhardt, "Quintessence, Cosmic Coincidence, and the Cosmological Constant", *Phys. Rev. Lett.* **82**, 896 (1999) (arXiv: astro-ph/9807002).

[49] P. A. R. Ade *et al.* (Planck Collaboration), "Planck 2015 results. XIII. Cosmological parameters", *Astron. Astrophys.* **594**, A13 (2016) (arXiv:1502.01589 [astro-ph.CO]).

[50] L. Amendola and S. Tsujikawa, "DARK ENERGY: Theory and Observations", *Cambridge University Press*, 2010.

[51] P. Salucci, C. F. Martins, and A. Lapi, "DMAW 2010 LEGACY the Presentation Review: Dark Matter in Galaxies with its Explanatory Notes", arXiv:1102.1184 (2011).

[52] G. Bertone, D. Hooper, and J. Silk, "Particle dark matter: Evidence, candidates and constraints," *Phys. Rept.* **405**, 279 (2005) (arXiv:hep-ph/0404175).

[53] F. Zwicky, "Die Rotverschiebung von extragalaktischen Nebeln," *Helvetica Physica Acta* **6**, 110 (1933).

[54] F. Zwicky, "On the Masses of Nebulae and of Clusters of Nebulae," *Astrophys. J.* **86**, 217 (1937).

[55] J. Binney and S. Tremaine, "Galactic dynamics", Princeton University Press, Princeton (1987).

[56] M. Persic, P. Salucci, and F. Stel, "The universal rotation curve of spiral galaxies; 1, the dark matter connection", *Mon. Not. R. Astron. Soc.* **281**, 27 (1996).

[57] A. Boriello and P. Salucci, "The Dark Matter Distribution in Disk Galaxies", *Mon. Not. R. Astron. Soc.* **323**, 285 (2001) (arXiv: astro-ph/0001082).

[58] T. Harko and F. S. N. Lobo, "Irreversible thermodynamic description of interacting dark energy - dark matter cosmological models", *Phys. Rev. D* **87**, 044018 (2013) (arXiv: 1210.3617 [gr-qc]).

[59] R. D. Peccei and H. R. Quinn, "CP conservation in the presence of instantons", *Phys. Rev. Lett.* **38**, 1440 (1977).

[60] J. M. Overduin and P. S. Wesson, "Dark Matter and Background Light", *Phys. Rept.* **402**, 267 (2004).

[61] G. Jungman, M. Kamionkowski, and K. Griest, "Supersymmetric dark matter," *Phys. Rept.* **267**, 195 (1996) (arXiv:hep-ph/9506380 [hep-ph]).

[62] G. B. Gelmini, "Search for dark matter", *Int. J. Mod. Phys. A* **23**, 4273(2008).

[63] N. Fornengo, "Status and perspectives of indirect and direct dark matter searches", *Adv. Space Res.* **41**, 2010 (2008).

[64] G. Bertone, "Dark matter: A multidisciplinary approach", arXiv:astro-ph/0710.5603 (2007).

[65] M. Baldi, "Interactions between Dark Energy and Dark Matter", *PhD thesis*, Munich, (2009).

[66] Y. Fujii, "Origin of the gravitational constant and particle masses in scale invariant scalar-tensor theory", *Phys. Rev. D* **26**, 2580 (1982).

[67] R. D. Peccei, J. Sola, and C. Wetterich, "Adjusting the cosmological constant dynamically: cosmons and a new force weaker than gravity", *Phys. Lett. B* **195**, 183 (1987).

[68] L. H. Ford, "Cosmological constant damping by unstable scalar fields", *Phys. Rev. D* **35**, 2339 (1987).

[69] C. Wetterich, "Cosmology and the fate of dilatation symmetry", *Nucl. Phys. B* **302**, 668 (1988).

[70] B. Ratra and P. J. E. Peebles, "Cosmological consequences of a rolling homogeneous scalar field", *Phys. Rev D* **37**, 3406 (1988).

[71] Y. Fujii and T. Nishioka, "Model of a decaying cosmological constant", *Phys. Rev. D* **42**, 361 (1990).

[72] T. Chiba, N. Sugiyama, and T. Nakamura, "Cosmology with x-matter", *Mon. Not. R. Astron. Soc.* **289**, L5 (1997).

[73] P. G. Ferreira and M. Joyce, "Structure formation with a self-tuning scalar field", *Phys. Rev. Lett.* **79**, 4740 (1997).

[74] P. G. Ferreira and M. Joyce, "Cosmology with a primordial scaling field", *Phys. Rev. D* **58**, 023503 (1998).

[75] R. R. Caldwell, R. Dave, and P. J. Steinhardt, "Cosmological imprint of an energy component with general equation of state", *Phys. Rev. Lett.* **80**, 1582 (1998) (arXiv: astro-ph/9708069).

[76] S. M. Carroll, "Quintessence and the rest of the world: Suppressing long-range interactions", *Phys. Rev. Lett.* **81**, 3067 (1998) (arXiv: astro-ph/9806099).

[77] A. Hebecker and C. Wetterich, "Quintessential adjustment of the cosmological constant", *Phys. Rev. Lett.* **85**, 3339 (2000).

[78] A. Hebecker and C. Wetterich, "Natural quintessence?", *Phys. Lett. B* **497**, 281 (2001).

[79] C. A. -Picon, T. Damour, and V. Mukhanov, "k-Inflation", *Phys. Lett. B* **458**, 209 (1999) (arXiv: hep-th/9904075).

[80] C. A. -Picon, V. Mukhanov, and P. J. Steinhardt, "Dynamical solution to the problem of a small cosmological constant and late-time cosmic acceleration", *Phys. Rev. Lett.* **85**, 4438 (2000) (arXiv: astro-ph/0004134).

[81] T. Chiba, T. Okabe, and M. Yamaguchi, "Kinetically driven quintessence", *Phys. Rev. D* **62**, 023511 (2000) (arXiv: astro-ph/9912463).

[82] C. A. -Picon, V. Mukhanov and P. J. Steinhardt, "Essentials of k-essence", *Phys. Rev. D* **63**, 103510 (2001) (arXiv: astro-ph/0006373).

[83] R. de Putter and E. V. Linder, "Kinetic k-essence and quintessence", *Astropart. Phys.* **28**, 263 (2007) (arXiv: 0705.0400 [astro-ph]).

[84] L. R. Abramo and N. Pinto-Neto, "On the stability of phantom k-essence theories", *Phys. Rev. D* **73**, 063522 (2006) (arXiv: astro-ph/0511562).

[85] T. Padmanabhan, "Accelerated expansion of the Universe driven by tachyonic matter", *Phys. Rev. D* **66**, 021301 (2002) (arXiv: hep-th/0204150).

[86] T. Padmanabhan and T. R. Choudhury, "Can the clustered dark matter and the smooth dark energy arise from the same scalar field?", *Phys. Rev. D* **66**, 081301 (2002) (arXiv: hep-th/0205055).

[87] A. Sen, "Supersymmetric world-volume action for non-BPS D-branes", *J. High. Energy. Phys.* **9910**, 008 (1999) (arXiv: hep-th/9909062).

[88] A. Sen, "Rolling Tachyon", *J. High. Energy. Phys.* **0204**, 048 (2002) (arXiv: hep-th/0203211).

[89] A. Sen, "Tachyon Matter", *J. High. Energy. Phys.* **0207**, 065 (2002) (arXiv: hep-th/0203265).

[90] M. R. Garousi, "Tachyon couplings on non-BPS D-branes and Dirac-Born-Infeld action", *Nucl. Phys. B* **584**, 284 (2000) (arXiv: hep-th/0003122).

[91] M. R. Garousi, "On-shell S-matrix and tachyonic effective actions", *Nucl. Phys. B* **647**, 117 (2002) (arXiv: hep-th/0209068).

[92] R. R. Caldwell, "A phantom menace? Cosmological consequences of a dark energy component with super-negative equation of state", *Phys. Lett. B* **545**, 23 (2002) (arXiv: astro-ph/9908168).

[93] A. Y. Kamenshchik, U. Moschella, and V. Pasquier, "An alternative to quintessence", *Phys. Lett. B* **511**, 265 (2001) (arXiv: gr-qc/0103004).

[94] N. Bilic, G. B. Tupper, and R. D. Viollier, "Unification of dark matter and dark energy: The inhomogeneous Chaplygin gas", *Phys. Lett. B* **535**, 17 (2002) (arXiv: astro-ph/0111325).

[95] M. C. Bento, O. Bertolami, and A. A. Sen, "Generalized Chaplygin gas, accelerated expansion and dark energy matter unification", *Phys. Rev. D* **66**, 043507 (2002) (arXiv: gr-qc/0202064).

[96] W. L. Freedman *et al.,* (HST Collaboration), "Final results from the Hubble space telescope key project to measure the Hubble constant", *Astrophys. J.* **553**, 47 (2001) (arXiv: astro-ph/0012376).

[97] A. R. Liddle and D. H. Lyth, "Cosmological inflation and large-scale structure", *Cambridge University Press*, (2000).

[98] G. A. Caldera-Cabral, "Interacting dark energy models of the late-time acceleration of the Universe", *PhD thesis*, (2009).

[99] W. Chakraborty, "ACCELERATING EXPANSION OF THE UNIVERSE", *PhD Thesis*, (2009), arXiv:1105.1087 [gr-qc].

[100] P. Brax and J. Martin, "Quintessence and supergravity", *Phys. Lett. B* **468**, 40 (1999) (arXiv: astro-ph/9905040).

[101] P. Brax and J. Martin, "The Robustness of quintessence", *Phys. Rev. D* **61**, 103502 (2000) (arXiv: astro-ph/9912046).

[102] V. Sahni and L. Wang, "New cosmological model of quintessence and dark matter", *Phys. Rev. D* **62**, 103517 (2000) (arXiv: astro-ph/9910097).

[103] V. Sahni and A. A. Starobinsky, "The Case for a Positive Cosmological Lambda-term", *Int. J. Mod. Phys. D* **9**, 373 (2000) (arxiv: astroph/9904398).

[104] L. A. U. -Lopez and T. Matos, "New cosmological tracker solution for quintessence", *Phys. Rev. D* **62**, 081302(R) (2000).

[105] T. Barreiro, E. J. Copeland, and N. J. Nunes, "Quintessence arising from exponential potentials", *Phys. Rev. D* **61**, 127301 (2000).

[106] N. Roy, "Dynamical Systems Analysis of Various Dark Energy Models", *PhD Thesis*, arXiv:1511.07978 [gr-qc].

[107] G. W. Gibbons, "Cosmological evolution of the rolling tachyon", *Phys. Lett. B* **537**, 1 (2002) (arXiv: hep-th/0204008).

[108] M. Sami, P. Chingangbam, and T. Qureshi, "Aspects of tachyonic inflation with an exponential potential", *Phys. Rev. D* **66**, 043530 (2002) (arXiv: hep-th/0205179).

[109] M. Sami, "Implementing power law inflation with rolling tachyon on the brane", *Mod. Phys. Lett. A* **18**, 691 (2003) (arXiv: hep-th/0205146).

[110] A. Mazumdar, S. Panda, and A. P. -Lorenzana, "Assisted inflation via tachyon condensation", *Nucl. Phys. B* **614**, 101 (2001) (arXiv: hep-ph/0107058).

[111] J. S. Bagla, H. K. Jassal, and T. Padmanabhan, "Cosmology with tachyon field as dark energy", *Phys. Rev. D* **67**, 063504 (2003) (arXiv: astro-ph/0212198).

[112] L. R. W. Abramo and F. Finelli, "Cosmological dynamics of the tachyon with an inverse power-law potential", *Phys. Lett. B* **575**, 165 (2003) (arXiv: astro-ph/0307208).

[113] J. M. Aguirregabiria and R. Lazkoz, "Tracking solutions in tachyon cosmology", *Phys. Rev. D* **69**, 123502 (2004) (arXiv: hep-th/0402190).

[114] Z. -K. Guo and Y. -Z. Zhang, "Cosmological scaling solutions of the tachyon with multiple inverse square potentials", *J. Cosmol. Astropart. Phys* **0408**, 010 (2004) (arXiv: hep-th/0403151).

[115] E. J. Copeland, M. R. Garousi, M. Sami, and S. Tsujikawa, "What is needed of a tachyon if it is to be the dark energy?", *Phys. Rev. D* **71**, 043003 (2005) (arxiv: hep-th/0411192).

[116] R. R. Caldwell, M. Kamionkowski, and N. N. Weinberg, "Phantom energy and cosmic doomsday", *Phys. Rev. Lett.* **91**, 071301 (2003) (arXiv: astro-ph/0302506).

[117] N. Suzuki *et al.,* "The Hubble space telescope cluster supernova survey: V. Improving the dark energy constraints above $z > 1$ and building an early-type-hosted supernova sample", *Astrophys. J.* **746**, 85 (2012) (arXiv: 1105.3470 [astro-ph.CO]).

[118] U. Debnath, A. Banerjee, and S. Chakraborty, "Role of modified Chaplygin gas in accelerated Universe", *Class. Quantum Grav.* **21**, 5609 (2004) (arXiv: gr-qc/0411015).

[119] H. B. Benaoum, "Accelerated Universe from modified Chaplygin gas and tachyonic fluid", arXiv: hep-th/0205140.

[120] L. Amendola, F. Finelli, C. Burigana, and D. Carturan, "WMAP and the generalized Chaplygin gas", *J. Cosmol. Astropart. Phys.* **0307**, 005 (2003) (arXiv: astro-ph/0304325).

[121] V. Salvatelli, N. Said, M. Bruni, A. Melchiorri, and D. Wands, "Indications of a Late-Time Interaction in the Dark Sector", *Phys. Rev. Lett.* **113**, 181301 (2014).

[122] R. C. Nunes, S. Pan, and E. N. Saridakis, "New constraints on interacting dark energy from cosmic chronometers," *Phys. Rev. D* **94** no.2, 023508 (2016), (arXiv:1605.01712 [astro-ph.CO]).

[123] S. Kumar and R. C. Nunes, "Probing the interaction between dark matter and dark energy in the presence of massive neutrinos," *Phys. Rev. D* **94** no.12, 123511 (2016) (arXiv:1608.02454 [astro-ph.CO]).

[124] N. Tamanini, "On phenomenological models of dark energy interacting with dark matter", *Phys. Rev. D* **92**, 043524 (2015) (arXiv: 1504.07397 [gr-qc]).

[125] C. G. Boehmer, G. Caldera-Cabral, R. Lazkoz, and R. Maartens, "Dynamics of dark energy with a coupling to dark matter", *Phys. Rev. D* **78**, 023505 (2008) (arXiv: 0801.1565 [gr-qc]).

[126] X. -ming Chen, Y. -gui Gong, and E. N. Saridakis, "Phase-space analysis of interacting phantom cosmology", *J. Cosmol. Astropart. Phys.* **0904**, 001 (2009) (arXiv: 0812.1117).

[127] Y. L. Bolotin, A. Kostenko, O. A. Lemets, and D. A. Yerokhin, "Cosmological Evolution With Interaction Between Dark Energy And Dark Matter", *Int. J. Mod. Phys. D* **24**, 1530007 (2015) (arXiv:1310.0085 [astro-ph.CO]).

[128] A. A. Costa, X. D. Xu, B. Wang, E. G. M. Ferreira, and E. Abdalla, "Testing the Interaction between Dark Energy and Dark Matter with Planck Data", *Phys. Rev. D* **89**, 103531 (2014) (arXiv: 1311.7380 [astro-ph.CO]).

[129] M. Khurshudyan, and R. Myrzakulov, "Phase space analysis of some interacting Chaplygin gas models", arXiv:1509.02263 [gr-qc].

[130] S. Kr. Biswas and S. Chakraborty, "Dynamical systems analysis of an interacting dark energy model in the brane scenario", *Gen. Relativ. Gravit.* **47**, 22 (2015).

[131] S. Kr. Biswas and S. Chakraborty, "Interacting Dark Energy in f(T) cosmology : A Dynamical System analysis", *Int. J. Mod. Phys. D* **24**, no.7, 1550046 (2015) (arXiv:1504.02431 [gr-qc]).

[132] L. P. Chimento, "Linear and nonlinear interactions in the dark sector", *Phys. Rev. D* **81**, 043525 (2010) (arXiv: 0911.5687 [astro-ph.CO]).

[133] L. P. Chimento, "Exactly solved models of interacting dark matter and dark energy", *AIP. Conf. Proc.* **1471**, 30 (2012) (arXiv: 1204.5797 [gr-qc]).

[134] J. S. Wang and F. Y. Wang, "Cosmological model of the interaction between dark matter and dark energy", *Astron. Astrophys.* **564**, A137 (2014) (arXiv:1403.4318 [astro-ph.CO]).

[135] S. Pan, S. Bhattacharya, and S. Chakraborty, "An analytic model for interacting dark energy and its observational constraints", *Mon. Not. R. Astron. Soc.* **452**, 3038 (2015) (arXiv:1210.0396[gr-qc]).

[136] M. Jamil and M. A. Rashid, "Constraining the coupling constant between dark energy and dark matter", *Eur. Phys. J. C* **60**, 141 (2009).

[137] M. Jamil and M. A. Rashid, "Interacting modified variable Chaplygin gas in a non-flat universe", *Eur. Phys. J. C* **58**, 111 (2008).

[138] M. Jamil and M. A. Rashid, "Interacting dark energy with inhomogeneous equation of state", *Eur. Phys. J. C* **56**, 429 (2008).

[139] M. Jamil and F. Rahaman, "On the resolution of cosmic coincidence problem and phantom crossing with triple interacting fluids", *Eur. Phys. J. C* **64**, 97 (2009).

[140] M. Jamil, "A Single model of interacting dark energy: Generalized phantom energy or generalized Chaplygin gas", *Int. J. Theor. Phys.* **49**, 144 (2010) (arXiv:0912.4468 [hep-th]).

[141] M. Jamil, M. Raja, and U. Debnath, "Statefinder Parameter for Varying G in Three Fluid System", *Astrophys. Space Sci.* **337**, 799 (2012).

[142] H. M. Sadjadi and M. Alimohammadi, "Cosmological coincidence problem in interacting dark energy models", *Phys. Rev. D* **74**, 103007 (2006) (arXiv: gr-qc/ 0610080).

[143] T. Clifton and J. D. Barrow, "Decaying gravity", *Phys. Rev. D* **73**, 104022 (2006).

[144] G. M. Kremer, "Cosmological models described by a mixture of van der Waals fluid and dark energy", *Phys. Rev. D* **68**, 123507 (2003).

[145] M. R. Setare, "Holographic Chaplygin gas model", *Phys. Lett. B* **648**, 329 (2007).

[146] M. R. Setare, "HOLOGRAPHIC CHAPLYGIN DGP COSMOLOGIES", *Int. J. Mod. Phys. D* **18**, 419 (2009).

[147] L. P. Chimento, A. S. Jakubi, D. Pavon, and W. Zimdahl, "Interacting quintessence solution to the coincidence problem", *Phys. Rev. D* **67**, 083513 (2003) (arXiv: astro-ph/0303145).

[148] C. Wetterich, "The cosmon model for an asymptotically vanishing time-dependent cosmological constant", *Astron. Astrophys.* **301**, 321 (1995) (arXiv: hep-th/9408025).

[149] L. Amendola, "Coupled quintessence", *Phys. Rev. D* **62**, 043511 (2000) (arXiv: astro-ph/9908023).

[150] L. Amendola, "Perturbations in a coupled scalar field cosmology", *Mon. Not. R. Astron. Soc.* **312**, 521 (2000) (arXiv: astro-ph/9906073).

[151] A. P. Billyard and A. A. Coley, "Interactions in scalar field cosmology", *Phys. Rev. D* **61**, 083503 (2000) (arXiv: astro-ph/9908224).

[152] W. Zimdahl, D. Pavon, and L. P. Chimento, "Interacting quintessence", *Phys. Lett. B* **521**, 133 (2001) (arXiv: astro-ph/0105479).

[153] R. Herrera, D. Pavon, and W. Zimdahl, "Exact solutions for the interacting tachyonic-dark matter system", *Gen. Relativ. Gravit.* **36**, 2161 (2004) (arXiv: astro-ph/0404086).

[154] L. Amendola and C. Quercellini, "Tracking and coupled dark energy as seen by WMAP", *Phys. Rev. D* **68**, 023514 (2003) (arXiv: astro-ph/0303228).

[155] M. Hoffman, "Cosmological constraints on a dark matter–dark energy interaction", arXiv: astro-ph/0307350.

[156] L. Amendola, "Linear and non-linear perturbations in dark energy models", *Phys. Rev. D* **69**, 103524 (2004) (arXiv: astro-ph/0311175).

[157] S. del Campo, R. Herrera, and D. Pavon, "Soft coincidence in late acceleration", *Phys. Rev. D* **71**, 123529 (2005) (arXiv: astro-ph/0506482)

[158] Z. -K. Guo, R. -G. Cai and Y. -Z. Zhang, "Cosmological evolution of interacting phantom energy with dark matter", *J. Cosmol. Astropart. Phys* **0505**, 002 (2005) (arXiv: astro-ph/0412624).

[159] W. Zimdahl, "Interacting dark energy and cosmological equations of state", *Int. J. Mod. Phys. D* **14**, 2319 (2005) (arXiv: gr-qc/0505056).

[160] J. F. Jesus, R. C. Santos, J. S. Alcaniz, and J. A. S. Lima, "New coupled quintessence cosmology", *Phys. Rev. D* **78**, 063514 (2008) (arXiv: astro-ph/0806.1366).

[161] D. Pavon and W. Zimdahl, "Holographic dark energy and cosmic coincidence", *Phys. Lett. B* **628**, 206 (2005) (arXiv: gr-qc/0505020).

[162] L. Amendola, S. Tsujikawa, and M. Sami, "Phantom damping of matter perturbations", *Phys. Lett. B* **632**, 155 (2006) (arXiv: astro-ph/0506222).

[163] J. -H. He and B. Wang, "Effects of the interaction between dark energy and dark matter on cosmological parameters", *J. Cosmol. Astropart. Phys* **0806**, 010 (2008) (arXiv: 0801.4233 [astro-ph]).

[164] S. Pan and S. Chakraborty, "A cosmographic analysis of holographic dark energy models", *Int. J. Mod. Phys. D* **23**, 1450092 (2014) (arXiv: 1410.8281 [gr-qc]).

[165] N. Dalal, *et al.,* "Testing the cosmic coincidence problem and the nature of dark energy", *Phys. Rev. Lett.* **87**, 141302 (2001) (arXiv: astro-ph/0105317).

[166] P. Wang and X. -H. Meng, "Can vacuum decay in our Universe?" *Class. Quant. Grav.* **22**, 283 (2005) (arXiv: astro-ph/0408495).

[167] F. E. M. Costa and J. S. Alcaniz, "Cosmological consequences of a possible Λ-dark matter interaction", *Phys. Rev. D* **81**, 043506 (2010) (arXiv: 0908.4251 [astro-ph.CO]).

[168] H. Wei, "Revisiting the cosmological constraints on the interacting dark energy models", *Phys. Lett. B* **691**, 173 (2010) (arXiv: 1004.0492 [gr-qc]).

[169] H. Wei and S. N. Zhang, "Observational $H(z)$ data and cosmological models", *Phys. Lett. B* **644**, 7 (2007) (arXiv: astro-ph/0609597).

[170] H. Wei and S. N. Zhang, "Interacting energy components and observational $H(z)$ data", *Phys. Lett. B* **654**, 139 (2007) (arXiv: 0704.3330 [astro-ph]).

[171] G. Mangano, G. Miele, and V. Pettorino, "Coupled quintessence and the coincidence problem", *Mod. Phys. Lett. A* **18**, 831 (2003) (arXiv: astro-ph/0212518).

[172] A. Albrecht *et al.,* "Reheating an inflationary Universe" *Phys. Rev. Lett.* **48**, 1437 (1982).

[173] H. P. d. Oliveira and R. O. Ramos, "Dynamical system analysis for inflation with dissipation", *Phys. Rev. D* **57**, 741 (1998) (arXiv: gr-qc/9710093).

[174] A. A. d. Costa, "Observational Constraints on Models with an Interaction between Dark energy and Dark Matter", *PhD Thesis*, (2014).

[175] B. Wang, E. Abdalla, F. Atrio-Barandela, and D. Pavon, "Dark matter and dark energy interactions: theoretical challenges, cosmological implications and observational signatures", *Reports on Progress in Physics*, **79** no.9, 096901 (2016) (arXiv:1603.08299 [astro-ph.CO]).

[176] R. C. G. Landim, "Dynamical analysis for a vector-like dark energy", *Eur. Phys. J. C* **76**, 480 (2016) (arXiv:1605.03550 [hep-th]).

[177] R. C. G. Landim, "Coupled dark energy: a dynamical analysis with complex scalar field," *Eur. Phys. J. C* **76**, 31 (2016) (arXiv:1507.00902 [gr-qc]).

[178] S. Das, P. S. Corasaniti, and J. Khoury, "Superacceleration as the signature of a dark sector interaction", *Phys. Rev. D* **73**, 083509 (2006).

[179] J. Grande, J. Sola, and H. Stefancic, "LXCDM: a cosmon model solution to the cosmological coincidence problem?", *J. Cosmol. Astropart. Phys.* **0608**, 011 (2006)

(arXiv:gr-qc/0604057).

[180] J. Grande, A. Pelinson, and J. Sola, "Dark energy perturbations and cosmic coincidence", *Phys. Rev. D* **79**, 043006 (2009) (arXiv:0809.3462 [astro-ph]).

[181] S. Basilakos and J. Sola, "Effective equation of state for running vacuum: "mirage" quintessence and phantom dark energy", *Mon. Not. R. Astron. Soc.* **437**, 3331 (2014) (arXiv:1307.4748 [astro-ph.CO]).

[182] J. Sola and H. Stefancic, "Effective equation of state for dark energy: mimicking quintessence and phantom energy through a variable Lambda", *Phys. Lett. B* **624**, 147 (2005) (arXiv:astro-ph/0505133).

[183] J. Sola and H. Stefancic, "Dynamical dark energy or variable cosmological parameters?", *Mod. Phys. Lett. A* **21**, 479 (2006) (arXiv:astro-ph/0507110).

[184] Z. K. Guo, N. Ohta, and S. Tsujikawa, "Probing the coupling between dark components of the Universe", *Phys. Rev. D* **76**, 023508 (2007) (arXiv: astro-ph/ 0702015).

[185] L. Amendola, G. C. Campos, and R. Rosenfeld, "Consequences of dark matter-dark energy interaction on cosmological parameters derived from SNIa data", *Phys. Rev. D* **75**, 083506 (2007), (arXiv: astro-ph/0610806).

[186] S. H. Pereira and J. F. Jesus, "Can dark matter decay in dark energy?", *Phys. Rev. D* **79**, 043517 (2009) (arXiv: 0811.0099 [astro-ph]).

[187] D. Pavon and B. Wang, "Le Chatelier-Braun principle in cosmological physics", *Gen. Relativ. Gravit.* **41**, 1 (2009) (arXiv: 0712.0565 [gr-qc]).

[188] J. -H. He, B. Wang, and E. Abdalla, "Stability of the curvature perturbation in dark sectors' mutual interacting models", *Phys. Lett. B* **671**, 139 (2009) (arXiv: 0807.3471 [gr-qc]).

[189] M. Quartin *et al.,* "Dark interactions and cosmological fine-uuning", *J. Cosmol. Astropart. Phys.* **0805**, 007 (2008) (arXiv: 0802.0546 [astro-ph]).

[190] B. M. Jackson, A. Taylor, and A. Berera, "On the large-scale instability in interacting dark energy and dark matter fluids", *Phys. Rev. D* **79**, 043526 (2009) (arXiv: 0901.3272 [astro-ph.CO]).

[191] L. Amendola, "Scaling solutions in general nonminimal coupling theories", *Phys. Rev. D* **60**, 043501 (1999).

[192] S. Nojiri and S. D. Odintsov, "Introduction to modified gravity and gravitational alternative for dark energy" *Int. J. Geom. Meth. Mod. Phys.* **4**, 115 (2007) (arXiv:

hep-th/0601213).

[193] S. Nojiri and S. D. Odintsov, "Modified gravity and its reconstruction from the Universe expansion history", *J. Phys. Conf. Ser* **66**, 012005 (2007) (arXiv: hep-th/0611071).

[194] S. Nojiri and S. D. Odintsov, "Modified gravity as an alternative for ΛCDM cosmology", *J. Phys. A* **40**, 6725 (2007) (arXiv: hep-th/0610164).

[195] F. S. N. Lobo, "The dark side of gravity: Modified theories of gravity", Dark Energy-Current Advances and Ideas, 173-204 (2009), Research Signpost. (arXiv:0807.1640v1 [gr-qc]).

[196] L. Randall and R. Sundrum, "A large mass hierarchy from a small extra dimension", *Phys. Rev. Lett.* **83**, 3370 (1999) (arXiv: hep-ph/9905221).

[197] L. Randall and R. Sundrum, "An alternative to compactification", *Phys. Rev. Lett.* **83**, 4690 (1999) (arXiv: hep-th/9906064).

[198] S. Nojiri and S. D. Odintsov, "Modified f(R) gravity consistent with realistic cosmology: From matter dominated epoch to dark energy Universe", *Phy. Rev. D* **74**, 086005 (2006) (arXiv: hep-th/0608008).

[199] A. A. Starobinsky, "A new type of isotropic cosmological models without singularity", *Phys. Lett. B* **91**, 99 (1980).

[200] R. Kerner, "Cosmology without singularity and nonlinear gravitational Lagrangians", *Gen. Relativ. Gravit.* **14**, 453 (1982).

[201] J. D. Barrow and A. C. Ottewill, "The stability of general relativistic cosmological theory", *J. Phys. A: Math. Gen.* **16**, 2757 (1983).

[202] V. Faraoni, "Matter instability in modified gravity", *Phys. Rev. D* **74**, 104017 (2006).

[203] H. J. Schmidth, "Fourth order gravity: Equations, history, and applications to cosmology", Int. J. Geom. Meth. Mod. Phys. **4**, 209 (2007), (arXiv: gr-qc/0602017).

[204] S. Nojiri and S. D. Odintsov, "Modified gravity with ln R terms and cosmic acceleration", *Gen. Relativ. Gravit.* **36**, 1765 (2004) (arXiv: hep-th/0308176).

[205] S. Nojiri and S. D. Odintsov, "The Minimal curvature of the universe in modified gravity and conformal anomaly resolution of the instabilities", *Mod. Phys. Lett. A* **19**, 627 (2004) (arXiv: hep-th/0310045).

[206] M. C. B. Abdalla, S. Nojiri, and S. D. Odintsov, "Consistent modified gravity: Dark energy, acceleration and the absence of cosmic doomsday", *Class. Quantum Grav.* **22**,

L35 (2005) (arXiv: hep-th/0409177).

[207] S. Nojiri and S. D. Odintsov, "Where new gravitational physics comes from: M Theory?", *Phys. Lett. B* **576**, 5 (2003) (arXiv: hep-th/0307071).

[208] S. M. Carroll, V. Duvvuri, M. Trodden, and M. S. Turner, "Is cosmic speed-up due to new gravitational physics?", *Phys. Rev. D* **70**, 043528 (2004) (arXiv: astro-ph/0306438).

[209] S. Capozziello, S. Nojiri, and S. D. Odintsov, "Dark energy: The Equation of state description versus scalar-tensor or modified gravity", *Phys. Lett. B* **634**, 93 (2006) (arXiv: hep-th/0512118).

[210] S. Nojiri, S. D. Odintsov, and D. S. -Gomes, "Cosmological reconstruction of realistic modified F(R) gravities", *Phys. Lett. B* **681**, 74 (2009) (arXiv:0908.1269 [hep-th]).

[211] G. R. Bengochea and R. Ferraro, "Dark torsion as the cosmic speed-up", *Phys. Rev. D* **79**, 124019 (2009) (arXiv:0812.1205 [astro-ph]).

[212] S. Capozziello, V. F. Cardone, S. Carloni, and A. Troisi, "Curvature quintessence matched with observational data", *Int. J. Mod. Phys. D* **12**, 1969 (2003) (arXiv: astro-ph/0307018).

[213] S. Capozziello, V. F. Cardone, and M. Francaviglia, "$f(R)$ theories of gravity in the Palatini approach matched with observations", *Gen. Relativ. Gravit.* **38**, 711 (2006) (arXiv: astro-ph/0410135).

[214] A. D. Felice and S. Tsujikawa, "$f(R)$ theories", *Living Rev. Rel.* **13**, 3 (2010) (arXiv: 1002.4928 [gr-qc]).

[215] P. G. Bergmann, "Comments on the scalar-tensor theory", *Int. J. Theor. Phys.* **1**, 25 (1968).

[216] B. N. Breizman, V. T. Gurovich, and V. P. Sokolov, "On the Possibility of Setting up Regular Cosmological Solutions", *Zh. Eksp. Teor. Fiz.* **59**, 288 (1971). *Soviet Journal of Experimental and Theoretical Physics* **32**, 155 (1971).

[217] H. A. Buchdahl, "Non-linear Lagrangians and cosmological theory", *Mon. Not. R. Astron. Soc.* **150**, 1 (1970).

[218] T. V. Ruzmaikina and A. A. Ruzmaikin, "Quadratic Corrections to the Lagrangian Density of the Gravitational Field and the Singularity", *Zh. Eksp. Teor. Fiz.* **57**, 680 (1970). *Soviet Journal of Experimental and Theoretical Physics* **30**, 372 (1969).

[219] J. P. Duruisseau, R. Kerner, and P. Eysseric, "Non-Einsteinian gravitational Lagrangians assuring cosmological solutions without collapse," *Gen. Relativ. Gravit.* **15**, 797

(1983).

[220] A. Palatini, "Deduzione invariantiva delle equazioni gravitazionali dal principio di Hamilton", Rend. Circ. Mat. Palermo, 43, 203, (1919).

[221] S. Capozziello, S. Carloni, and A. Troisi, "Quintessence without scalar fields", in Recent Research Developments in Astronomy and Astrophysics 1, p. 625, (Research Signpost, Trivandrum, India, 2003).

[222] S. Nojiri and S. D. Odintsov, "Modified gravity with negative and positive powers of the curvature: Unification of the inflation and of the cosmic acceleration", *Phys. Rev. D* **68**, 123512 (2003).

[223] K. Koyama, "The cosmological constant and dark energy in braneworlds", *Gen. Relativ. Gravit.* **40**, 421 (2008), (arXiv:0706.1557 [astro-ph]).

[224] R. Maartens, "Brane-world gravity", *Living Rev. Rel.* **7**, 7 (2004) (arXiv:gr-qc/0312059).

[225] R. Maartens, "Brane-world cosmological perturbations", p123-142 in Frontier in Astroparticle Physics & Cosmology, eds K Sato & S Nagataki (Universal Academy Press, 2004), (arXiv:astro-ph/0402485).

[226] R. Maartens, "Geometry and dynamics of the brane world", Reference Frames and Gravitomagnetism, ed. J Pascual-Sanchez et al. (World Sci., 2001), p93-119, (arXiv: gr-qc/0101059).

[227] K. Maeda, "The Einstein equations on a brane world", *Prog. Theo. Phys. Suppl.* **148**, 59 (2003).

[228] S. Chakraborty, A. Banerjee, and T. Bandyopadhyay, "Matter in the bulk and its consequences on the brane: A possible source of dark energy", arXiv: 0707.0199 [gr-qc].

[229] P. Brax and C. v. d. Bruck, "Cosmology and Brane Worlds: A Review", *Class. Quantum Grav.* **20**, R201 (2003) (arXiv:hep-th/0303095).

[230] P. Brax , C. v. d. Bruck, and A. -C. Davis, "Brane World Cosmology", *Rept. Prog. Phys.* **67**, 2183 (2004), (arXiv:hep-th/0404011).

[231] D. Langlois, "Cosmology of Brane-worlds", arXiv:astro-ph/0403579.

[232] D. Wands, "Brane-world Cosmology", arXiv:gr-qc/0601078.

[233] P. Horava and E. Witten, "Heterotic and Type I string dynamics from eleven-dimensions", *Nucl. Phys. B* **460**, 506 (1996) (arXiv: hep-th/9510209).

[234] P. Binetruy, C. Deffayet, and D. Langlois, "Non-conventional cosmology from a brane-Universe", *Nucl. Phys. B* **565**, 269 (2000) (arXiv: hep-th/9905012).

[235] C. Csaki, M. Graesser, C. Kolda, and J. Terning, "Cosmology of one extra dimension with localized gravity", *Phys. Lett. B* **462**, 34 (1999) (arXiv: hep-ph/9906513).

[236] J. M. Cline, C. Grojean, and G. Servant, "Cosmological expansion in the presence of an extra dimension", *Phys. Rev. Lett.* **83**, 4245 (1999) (arXiv: hep-ph/9906523).

[237] P. Binetruy, C. Deffayet, U. Ellwanger, and D. Langlois, "Brane cosmological evolution in a bulk with cosmological constant", *Phys. Lett. B* **477**, 285 (2000) (arXiv: hep-th/9910219).

[238] T. Shiromizu, K. Maeda and M. Sasaki, "The Einstein equation on the 3-brane world", *Phys. Rev. D* **62**, 024012 (2000) (arXiv: gr-qc/9910076).

[239] R. Maartens, D. Wands, B. A. Bassett, and I. P. C. Heard, "Chaotic inflation on the brane", *Phys. Rev. D* **62**, 041301 (2000) (arXiv: hep-ph/9912464).

[240] E. J. Copeland, A. R. Liddle, and J. E. Lidsey, "Steep inflation: ending braneworld inflation by gravitational particle production", *Phys. Rev. D* **64** 023509 (2001) (arXiv: astro-ph/0006421).

[241] R. Maartens, V. Sahni, and T. D. Saini, "Anisotropy dissipation in brane-world inflation", *Phys. Rev. D* **63**, 063509 (2001) (arXiv: gr-qc/0011105).

[242] V. Sahni, M. Sami, and T. Souradeep, "Relic gravity waves from braneworld inflation", *Phys. Rev. D* **65**, 023518 (2002) (arXiv: gr-qc/0105121).

[243] A. A. Coley, "The Dynamics of Brane-World Cosmological Models", arXiv:astro-ph/0504226.

[244] R. Maartens and K. Koyama, "Brane-world gravity", *Living Rev. Rel.* **13**, 5 (2010) (arXiv: 1004.3962 [hep-th]).

[245] V. Sahni and Y. Shtanov, "Brane world models of dark energy", *J. Cosmol. Astropart. Phys.* **0311**, 014 (2003) (arXiv: astro-ph/0202346).

[246] G. Dvali, G. Gabadadze, and M. Porrati, "4D gravity on a brane in 5D Minkowski space", *Phys. Lett. B* **485**, 208 (2000) (arXiv: hep-th/0005016).

[247] C. Deffayet, "Cosmology on a brane in Minkowski bulk", *Phys. Lett. B* **502**, 199 (2001) (arXiv: hep-th/0010186).

[248] C. Deffayet, G. Dvali, and G. Gabadadze, "Accelerated Universe from Gravity Leaking to Extra Dimensions", *Phys. Rev. D* **65** 044023 (2002) (arXiv:astro-ph/0105068).

[249] R. Weitzenböck, "Invarianten Theorie", Nordhoff, Groningen (1923).

[250] R. Aldrovandi and J. G. Pereira, "Teleparallel Gravity: An Introduction", Springer, Dordrecht (2013).

[251] K. Hayashi and T. Shirafuji, "New general relativity", *Phys. Rev. D* **19**, 3524 (1979) [Addendum-*ibid. D* **24**, 3312 (1982)].

[252] J. W. Maluf, "The teleparallel equivalent of general relativity", *Annalen der Phys.* **525**, 339 (2013) (arXiv:1303.3897).

[253] E. V. Linder, "Einstein's Other Gravity and the Acceleration of the Universe", *Phys. Rev. D* **81**, 127301 (2010) (arXiv: 1005.3039 [astro-ph.CO]).

[254] R. C. Nunes, S. Pan, and E. N. Saridakis, "New observational constraints on f(T) gravity from cosmic chronometers", *J. Cosmol. Astropart. Phys.* **1608** 011 (2016) no.08, (arXiv:1606.04359 [gr-qc]).

[255] S. -H. Chen, J. B. Dent, S. Dutta, and E. N. Saridakis, "Cosmological perturbations in f(T) gravity", *Phys. Rev. D* **83**, 023508 (2011) (arXiv: 1008.1250[astro-ph.CO]).

[256] Y. -F. Cai, S. Capozziello, M. D. Laurentis, and E. N. Saridakis, "f(T) Teleparallel Gravity and Cosmology", *Rept. Prog. Phys.* **79**, 106901 (2016) no.4, (arXiv:1511.07586).

[257] S. D. Odintsov, V. K. Oikonomou, and E. N. Saridakis, "Superbounce and Loop Quantum Ekpyrotic Cosmologies from Modified Gravity: F(R), F(G) and F(T) Theories", arXiv:1501.06591 [gr-qc].

[258] V. K. Oikonomou and E. N. Saridakis, "f(T) gravitational baryogenesis", *Phys. Rev. D* **94**, 124005 (2016) (arXiv:1607.08561v1 [gr-qc]).

[259] R. C. Nunes, A. Bonilla, S. Pan, and E. N. Saridakis, "Observational Constraints on f(T) gravity from varying fundamental constants", arXiv: 1608.01960 [gr-qc].

[260] T. Harko, F. S. N. Lobo, S. Nojiri, and S. D. Odintsov, "$f(R,T)$ gravity theory", *Phys. Rev. D* **84**, 024020 (2011) (arXiv: 1104.2669 [gr-qc]).

[261] R. Myrzakulov, "$F(T)$ gravity and k-essence", *Gen. Relativ. Gravit.* **44**, 3059 (2012) (arXiv: 1008.4486 [physics.gen-ph]).

[262] R. Myrzakulov, "Dark energy in $F(R,T)$ gravity", arXiv: 1205.5266 [physics.gen-ph].

[263] R. Myrzakulov, "Cosmology of $F(T)$ gravity and k-essence", *Entropy* **14**, 1627 (2012) (arXiv: 1212.2155 [gr-qc]).

[264] L. D. Landau and E. M. Lifshitz, "The Classical Theory of Fields", Butterworth-Heinemann, Oxford (1998).

[265] R. Myrzakulov, "FRW cosmology in $F(R,T)$ Gravity", *Eur. Phys. J. C* **72**, 2203 (2012) (arXiv: 1207.1039 [gr-qc]).

[266] S. Chakraborty, "An alternative $f(R,T)$ gravity theory and the dark energy problem", *Gen. Relativ. Gravit.* **45**, 2039 (2013) (arXiv: 1212.3050 [physics.gen-ph]).

[267] R. Maartens, "Causal thermodynamics in relativity", arXiv: astro-ph/9609119.

[268] C. Eckart, "The Thermodynamics of Irreversible Processes. III. Relativistic Theory of the Simple Fluid", *Phys. Rev.* **58**, 919 (1940).

[269] W. Zimdahl, "Cosmological particle production, causal thermodynamics, and inflationary expansion", *Phys.Rev. D* **61**, 083511 (2000) (arXiv:astro-ph/9910483).

[270] R. O. Ramos, M. V. d. Santos, and I. Waga, "Matter creation and cosmic acceleration", *Phys. Rev. D* **89**, 083524 (2014) (arXiv:1404.2604[astro-ph.CO]).

[271] J. A. S. Lima, S. Basilakos, and F. E. M. Costa, "New Cosmic Accelerating Scenario without Dark Energy", *Phys. Rev. D* **86**, 103534 (2012) (arXiv:1205.0868[astro-ph.CO]).

[272] N. Tamanini, "Dynamical Systems in Dark Energy Models", *PhD Thesis*, (2014).

[273] D. K. Arrowsmith and C. M. Place, "An introduction to dynamical systems", *Cambridge University Press*, (1990).

[274] M. W. Hirsch and S. Smale, "Differential equations, dynamical systems, and linear algebra", *Academic Press*, (1974).

[275] S. Lefschetz, "Differential equations: geometric theory", John Wiley and Sons, (1957).

[276] L. Perko, "Differential equations and dynamical systems", *Springer- Verlag*, (2001).

[277] S. H. Strogatz, "Nonlinear Dynamics and Chaos", *Perseus Books Publishing*, (1994).

[278] D. W. Jordan and P. Smith, "Nonlinear Ordinary Differential Equations", *Oxford University Press*, (2009).

[279] S. Wiggins, "Introduction to applied nonlinear dynamical systems and chaos", *Springer-Verlag*, (1990).

[280] N. Chan, "DYNAMICAL SYSTEMS IN COSMOLOGY", *PhD Thesis*, (2012).

[281] A. A. Coley, "Dynamical Systems in Cosmology", arXiv: gr-qc/9910074.

[282] J. Miritzis, "Introduction to Cosmological Dynamical Systems", Book Part- Part II, p-111, Springer Berlin Heidelberg, (2002).

[283] E. J. Copeland, A. R. Liddle, and D. Wands, "Exponential potentials and cosmological scaling solutions", *Phys. Rev. D* **57**, 4686 (1998) (arXiv: gr-qc/9711068).

[284] T. Matos, J. -R. Luevano, I. Quiros, L. A. U. -Lopez, and J. A. Vazquez, "Dynamics of Scalar Field Dark Matter With a Cosh-like Potential", *Phys. Rev. D* **80**, 123521 (2009) (arXiv:0906.0396 [astro-ph.CO]).

[285] C. G. Boehmer, N. Chan, and R. Lazkoz, "Dynamics of dark energy models and centre manifolds", *Phys. Lett. B* **714**, 11 (2012) (arXiv:1111.6247 [gr-qc]).

[286] C. G. Boehmer and N. Chan, "Dynamical systems in cosmology", arXiv:1409.5585[gr-qc].

[287] R. G-Salcedo, T. Gonzalez, F. A. Horta-Rangel, I. Quiros, and D. Sanchez-Guzman, "Introduction to the application of the dynamical systems theory in the study of the dynamics of cosmological models of dark energy", *Eur. J. Phys.* **36**, 025008 (2015) (arXiv:1501.04851v1 [gr-qc]).

[288] K. Akama, "An Early Proposal of 'Brane World'", *Lect. Notes Phys.* **176**, 267 (1982) (arXiv: hep-th/0001113).

[289] V. A. Rubakov, and M. E. Shaposhnikov, "Extra Space-Time Dimensions: Towards a Solution to the Cosmological Constant Problem", *Phys. Lett. B* **125**, 139 (1983).

[290] G. W. Gibbons and D. L. Wiltshire, "Space-Time as a Membrane in Higher Dimensions", *Nucl. Phys. B* **287**, 717 (1987) (arXiv: hep-th/0109093).

[291] P. Horava and E. Witten, "Eleven-dimensional supergravity on a manifold with boundary", *Nucl. Phys. B* **475**, 94 (1996) (arXiv: hep-th/9603142).

[292] N. Arkani-Hamed, S. Dimopoulos, and G. R. Dvali, "The Hierarchy problem and new dimensions at a millimeter", *Phys. Lett. B* **429**, 263 (1998) (arXiv: hep-ph/9803315).

[293] I. Antoniadis, N. A.-Hamed, S. Dimopoulos, and G. R. Dvali, "New dimensions at a millimeter to a Fermi and superstrings at a TeV", *Phys. Lett. B* **436**, 257 (1998) (arXiv: hep-ph/9804398).

[294] N. Kaloper, "Bent domain walls as brane worlds", *Phys. Rev. D* **60**, 123506 (1999) (arXiv: hep-th/9905210).

[295] T. Kaluza, "On the Problem of Unity in Physics", *Sitzungsber. Preuss. Akad. Wiss. Berlin (Math.Phys.)* **k1**, 966 (1921).

[296] O. Klein, "Quantum Theory and Five-Dimensional Theory of Relativity", *Z. Phys.* **37**, 895 (1926).

[297] R. M. Hawkins and J. E. Lidsey, "Inflation on a single brane: Exact solutions", *Phys. Rev. D* **63**, 041301 (2001) (arXiv: gr-qc/0011060).

[298] D. Langlois, "Brane cosmology: An Introduction", *Prog. Theor. Phys. Suppl.* ***148***, 181 (2003) (arXiv: hep-th/0209261).

[299] J. Garriga and T. Tanaka, "Gravity in the brane world", *Phys. Rev. Lett.* **84**, 2778 (2000) (arXiv: hep-th/9911055).

[300] S. B. Giddings, E. Katz, and L. Randall, "Linearized gravity in brane backgrounds", *J. High Energy, Phys.* **0003**, 023 (2000) (arXiv: hep-th/0002091).

[301] K. -ichi Maeda, "Brane quintessence", *Phys. Rev. D* **64**, 123525 (2001) (arXiv: astro-ph/0012313).

[302] P. F. G. -Diaz, "Quintessence in brane cosmology", *Phys. Lett. B* **481**, 353 (2000) (arXiv: hep-th/0002033).

[303] A. S. Majumdar, "From brane assisted inflation to quintessence through a single scalar field", *Phys. Rev. D* **64**, 083503 (2001) (arXiv: astro-ph/0105518).

[304] N. J. Nunes and E. J. Copeland, "Tracking quintessential inflation from brane worlds", *Phys. Rev. D* **66** , 043524 (2002) (arXiv: astro-ph/0204115).

[305] M. Sami and N. Dadhich, "Unifying brane world inflation with quintessence", TSPU Vestnik, **44** N7 : 25-36, (2004), (arXiv: hep-th/0405016).

[306] T. Gonzalez, T. Matos, I. Quiros, and A. V.-Gonzalez, "Self-interacting Scalar Field Trapped in a Randall-Sundrum Braneworld: The Dynamical Systems Perspective", *Phys. Lett. B* **676**, 161 (2009) (arXiv:0812.1734 [gr-qc]).

[307] Y. Leyva, D. Gonzalez, T. Gonzalez, T. Matos, and I. Quiros, "Dynamics of a self-interacting scalar field trapped in the braneworld for a wide variety of self-interaction potentials", *Phys. Rev. D* **80**, 044026 (2009) (arXiv:0909.0281 [gr-qc]).

[308] R. Lazkoz, G. Leon, and I. Quiros, "Quintom cosmologies with arbitrary potentials", *Phys. Lett. B* **649**, 103 (2007) (arXiv: astro-ph/0701353).

[309] W. Fang, Y. Li, K. Zhang, and H.-Qing Lu, "Exact Analysis of Scaling and Dominant Attractors Beyond the Exponential Potential", *Class. Quantum Grav.* **26**, 155005 (2009) (arXiv:0810.4193 [hep-th]).

[310] G. Leon, "On the Past Asymptotic Dynamics of Non-minimally Coupled Dark Energy", *Class. Quantum Grav.* **26**, 035008 (2009) (arXiv: 0812.1013 [gr-qc]).

[311] G. Leon, P. Silveira, and C. R. Fadragas, "Phase-space of flat Friedmann-Robertson-Walker models with both a scalar field coupled to matter and radiation", arXiv: 1009.0689 [gr-qc].

[312] G. Leon and C. R. Fadragas, "Cosmological Dynamical Systems", LAP Lambert Academic Publishing, Germany, (2011).

[313] G. Oliveras, F. A. - Barandela, and D. Pavon, "Observational constraints on interacting quintessence models", *Phys. Rev. D* **71**, 063523 (2005) (arXiv: astro-ph/0503242).

[314] G. Oliveras, F. A. - Barandela, and D. Pavon, "Matter density perturbations in interacting quintessence models", *Phys. Rev. D* **74**, 043521 (2006) (arXiv: astro-ph/0607604).

[315] L. Amendola, M. Gasperini, and F. Piazza, "SNLS data are consistent with acceleration at z=3", *Phys. Rev. D* **74**, 127302 (2006) (arXiv: astro-ph/0610574).

[316] A. Campos and C. F. Sopuerta, "Evolution of cosmological models in the brane world scenario", *Phys. Rev. D* **63**, 104012 (2001) (arXiv: hep-th/0101060).

[317] A. Campos and C. F. Sopuerta, "Bulk effects in the cosmological dynamics of brane world scenarios", *Phys. Rev. D* **64**, 104011 (2001) (arXiv: hep-th/0105100).

[318] A. A. Coley, "Dynamics of brane world cosmological models", *Phys. Rev. D* **66**, 023512 (2002) (arXiv: hep-th/0110049).

[319] P. Bowcock, C. Charmousis, and R. Gregory, "General brane cosmologies and their global space-time structure", *Class. Quantum Grav.* **17**, 4745 (2000) (arXiv: hep-th/0007177).

[320] N. Goheer and P. K. S. Dunsby, "Exponential potentials on the brane", *Phys. Rev. D* **67**, 103513 (2003) (arXiv: gr-qc/0211020).

[321] N. Goheer and P. K. S. Dunsby, "Braneworld dynamics of inflationary cosmologies with exponential potentials", *Phys. Rev. D* **66**, 043527 (2002) (arXiv: gr-qc/0204059).

[322] D. Escobar, C. R. Fadragas, G. Leon, and Y. Leyva, "Phase space analysis of quintessence fields trapped in a Randall-Sundrum braneworld: a refined study", *Class. Quantum Grav.* **29**, 175005 (2012) (arXiv: 1110.1736v3 [gr-qc]).

[323] F. Piazza and S. Tsujikawa, "Dilatonic ghost condensate as dark energy", *J. Cosmol. Astropart. Phys.* **0407**, 004 (2004) (arXiv: hep-th/0405054).

[324] N. Mahata and S. Chakraborty, "Dynamical System Analysis for a phantom model", *Gen. Relativ. Gravit.* **46**, 1721 (2014) (arXiv:1312.7644 [gr-qc]).

[325] S.- Y. Zhou, "A New Approach to Quintessence and a Solution of Multiple Attractors", *Phys. Lett. B* **660**, 7 (2008) (arXiv:0705.1577 [astro-ph]).

[326] A. Einstein, *Sitzungsber. Preuss. Akad. Wiss. Phys. Math. KI.* **217** (1928); *ibid.*, **401**, (1930).

[327] A. Einstein, "Auf die Riemann-Metrik und den Fern-Parallelismus gegrndete einheitliche Feldtheorie ", *Math. Annal.* **102**, 685 (1930).

[328] K. Hayashi and T. Shirafuji, "New general relativity", *Phys. Rev. D* **19**, 3524 (1979) [Addendum - *ibid.*, **24**, 3312 (1982)].

[329] H. I. Arcos and J. G. Pereira, "TORSION GRAVITY: A REAPPRAISAL", *Int. J. Mod. Phys. D* **13**, 2193 (2004).

[330] R. Ferraro and F. Fiorini, "Modified teleparallel gravity: Inflation without an inflaton", *Phys. Rev. D* **75**, 084031 (2007).

[331] R. Ferraro and F. Fiorini, "Born-Infeld gravity in Weitzenbck spacetime", *Phys. Rev. D* **78**, 124019 (2008).

[332] F. Fiorini and R. Ferraro, "A TYPE OF BORN-INFELD REGULAR GRAVITY AND ITS COSMOLOGICAL CONSEQUENCES", *Int. J. Mod. Phys. A* **24**, 1686 (2009).

[333] B. Li, T. P. Sotiriou, and J. D. Barrow, "f(T) gravity and local Lorentz invariance", *Phys. Rev. D* **83**, 064035 (2011).

[334] N. Mahata and S. Chakraborty, "Dynamical system analysis for DBI dark energy interacting with dark matter", *Mod. Phys. Lett. A* **30**, 1550009 (2015) (arXiv: 1501.04441).

[335] F. W. Hehl, P. Von Der Heyde, G. D. Kerlick, and J. M. Nester, "General relativity with spin and torsion: Foundations and prospects", *Rev. Mod. Phys.* **48**, 393 (1976).

[336] E. E. Flanagan and E. Rosenthal, "Can Gravity Probe B usefully constrain torsion gravity theories?", *Phys. Rev. D* **75**, 124016 (2007).

[337] J. Garecki, "Teleparallel equivalent of general relativity: a critical review", arXiv:1010.2654 [gr-qc].

[338] D. Liu, P. Wu, and H. Yu, "Gdel-type universes in f(T) gravity", *Int. J. Mod. Phys. D* **21**, 09 (2012) 1250074, (arXiv: **1203. 2016**[gr-qc]).

[339] P. Wu and H. Yu, "Observational constraints on f (T) theory", *Phys. Lett. B* **693**, 415 (2010).

[340] P. Wu and H. Yu, "f(T) models with phantom divide line crossing", *Eur. Phys. J. C* **71**, 1552 (2011).

[341] M. R. Setare and M. J. S. Houndjo, "Finite-time future singularities models in f(T) gravity and the effects of viscosity ", *Can. J. Phys.* **91**, 260 (2013) (arXiv: 1203. 1315 [gr-qc]).

[342] M. H. Daouda, M. E. Rodrigues, and M. J. S. Houndjo, "Reconstruction of f(T) gravity according to holographic dark energy", *Eur. Phys. J. C.* **72**, 1893 (2012).

[343] V. F. Cardone, N. Radicella, and S. Camera, "Accelerating f(T) gravity models constrained by recent cosmological data", *Phys. Rev. D* **85**, 124007 (2012).

[344] S. Camera, V. F. Cardone, and N. Radicella, "Detectability of torsion gravity via galaxy clustering and cosmic shear measurements", *Phys. Rev. D* **89**, 083520 (2014).

[345] K. Bamba, M. Jamil, D. Momeni, and R. Myrzakulov, "Generalized Second Law of Thermodynamics in f(T) Cosmology with Power-Law and Logarithmic Corrected Entropies", arXiv: 1202. 6114 [physics.gen-ph].

[346] P. A. R. Ade *et al.*, (Planck Collaboration. XVI), "Planck 2013 results. XVI. Cosmological parameters", *Astron. Astrophys.* **571**, A16 (2014) (arXiv:1303.5076 [astro-ph.CO]).

[347] A. Rest *et al.*, "Cosmological Constraints from Measurements of Type Ia Supernovae discovered during the first 1.5 years of the Pan-STARRS1 Survey", *Astrophys. J.* **795**, 44 (2014), (arXiv:1310.3828[astro-ph.CO]).

[348] J.-Q. Xia, H. Li, and X. Zhang, "Dark energy constraints after the new Planck data", *Phys. Rev. D* **88**, 063501 (2013).

[349] C. Cheng and Q.-G Huang, "Dark side of the Universe after Planck data", *Phys. Rev. D* **89**, 043003 (2014).

[350] D. L. Shafer and D. Huterer, "Chasing the phantom: A closer look at type Ia supernovae and the dark energy equation of state", *Phys. Rev. D* **89**, 063510 (2014).

[351] S. M. Carroll, M. Hoffman, and M. Trodden, "Can the dark energy equation-of-state parameter w be less than -1 ?", *Phys. Rev. D* **68**, 023509 (2003).

[352] J. M. Cline, S. Jeon, and G. D. Moore, "The phantom menaced: Constraints on low-energy effective ghosts", *Phys. Rev. D* **70**, 043543 (2004).

[353] S. D. H. Hsu, A. Jenkins, and M. B. Wise, "Gradient instability for w ¡ -1", *Phys. Lett. B* **597**, 270 (2004) (arXiv:astro-ph/0406043).

[354] F. Sbisa, "Classical and quantum ghosts", *Eur. J. Phys.* **36**, 015009 (2015), (arXiv:1406.4550 [hep-th]).

[355] M. Dabrowski, "Puzzles of the dark energy in the universe - phantom", *Eur. J. Phys.* **36**, 065017 (2015) (arXiv:1411.2827 [gr-qc]).

[356] G. Steigman, R. C. Santos, and J. A. S. Lima, "An Accelerating Cosmology Without Dark Energy", *J. Cosmol. Astropart. Phys.* **0906**, 033 (2009) (arXiv:0812.3912).

[357] J. A. S. Lima, J. F. Jesus, and F. A. Oliveira, "CDM accelerating cosmology as an alternative to ΛCDM model", *J. Cosmol. Astropart. Phys.* **2010**, no.11, 027 (2010).

[358] J. A. S. Lima, L. L. Graef, D. Pavon, and S. Basilakos, "Cosmic acceleration without dark energy: background tests and thermodynamic analysis", *J. Cosmol. Astropart. Phys.* **2014**, no.10, 042 (2014).

[359] J. C. Fabris, J. A. de F. Pacheco, and O. F. Piattella, "Is the continuous matter creation cosmology an alternative to ΛCDM?", *J. Cosmol. Astropart. Phys.* **2014**, no.06, 038 (2014).

[360] S. Chakraborty, S. Pan, and S. Saha, "A unified cosmic evolution: Inflation to late time acceleration", arXiv:1503.05552 [gr-qc].

[361] E. Schrödinger, "The proper vibrations of the expanding universe", *Physica* (Amsterdam) **6**, 899 (1939).

[362] L. Parker, "Particle Creation in Expanding Universes", *Phys. Rev. Lett.* **21**, 562 (1968);

[363] L. Parker, "Quantized Fields and Particle Creation in Expanding Universes. I", *Phys. Rev.* **183**, 1057 (1969);

[364] L. Parker, "Quantized Fields and Particle Creation in Expanding Universes. II", *Phys. Rev. D* **3**, 346 (1971);

[365] L. H. Ford and L. Parker, "Infrared divergences in a class of Robertson-Walker universes", *Phys. Rev. D* **16**, 245 (1977).

[366] N. D. Birrell and C. P. W. Davies, "Quantum Fields in Curved Space", Cambridge University Press, Cambridge, U.K. (1984).

[367] N. D. Birrell and C. P. W. Davies. "Massive particle production in anisotropic space-times", *J. Phys. A: Mathematical and General* **13**, 2109 (1980).

[368] A. A. Grib, B. A. Levitskii, and V. M. Mostepanenko, "Particle creation from vacuum by a nonstationary gravitational field in the canonical formalism", *Theor. Math. Phys.* **19**, 349 (1974).

[369] A. A. Grib, S. G. Mamayev, and V. M. Mostepanenko, "Vacuum Quantum Effects in Strong Fields", Friedman Laboratory Publishing 1994.

[370] A. A. Grib, S. G. Mamayev, and V. M. Mostepanenko, "Particle creation from vacuum in homogeneous isotropic models of the Universe", *Gen. Relativ. Gravit.* **7**, 535 (1976).

[371] Ya. B. Zeldovich and A. A. Starobinsky, "Particle production and vacuum polarization in an anisotropic gravitational field", *Sov. Phys. JETP* **34**, 1159 (1972).

[372] Ya B. Zeldovich and A. A. Starobinsky, "Rate of particle production in gravitational fields", *JETP Lett.* **26**, 252 (1977).

[373] I. Prigogine, J. Geheniau, E. Gunzig, and P. Nardone, "Thermodynamics and cosmology", *Gen. Relativ. Gravit.* **21**, 767 (1989).

[374] S. Weinberg, "Entropy Generation and the Survival of Protogalaxies in an Expanding Universe", *Astrophys. J.* **168**, 175 (1971).

[375] N. Straumann, Helv. Phys. Acta **49**, 269 (1976).

[376] M. A. Schweizer, "Transient and transport coefficients for radiative fluids", *Astrophys. J.* **258**, 798 (1982).

[377] N. Udey and W. Israel, "General relativistic radiative transfer: the 14-moment approximation", *Mon. Not. R. Astron. Soc.* **199**, 1137 (1982).

[378] W. Zimdahl, "'Understanding' cosmological bulk viscosity", *Mon. Not. R. Astron. Soc.* **280**, 1239 (1996) (arXiv:astro-ph/9602128).

[379] Ya B. Zeldovich, Particle production in cosmology (in Russian), *Zh. Eksp. Teor. Fiz. Pisma Red* **12**, 443 (1970) (English translation: JETP Lett. **12**, 307 (1970)).

[380] G. L. Murphy, "Big-Bang Model Without Singularities", *Phys. Rev. D* **8**, 4231 (1973).

[381] B. L. Hu, "Vacuum viscosity description of quantum processes in the early universe", *Phys. Lett. A* **90**, 375 (1982).

[382] M. O. Calvao, J. A. S. Lima, and I. Waga, "On the thermodynamics of matter creation in cosmology", *Phys. Lett. A* **162**, 223 (1992).

[383] S. Pan and S.Chakraborty, "Will there be future deceleration? A study of particle creation mechanism in non-equilibrium thermodynamics", *Advances in High Energy Phys.* **2015**, 654025 (2015) (arXiv: 1404.3273[gr-qc]).

[384] S. Chakraborty, S. Pan, and S. Saha, "A third alternative to explain recent observations: Future deceleration", *Phys. Lett. B* **738**, 424 (2014) (arXiv:1411.0941 [gr-qc]).

[385] S. Chakraborty, "Is emergent universe a consequence of particle creation process?", *Phys. Lett. B* **732**, 81 (2014).

[386] S. Chakraborty and S. Saha, "Complete cosmic scenario from inflation to late time acceleration: Nonequilibrium thermodynamics in the context of particle creation", *Phys. Rev. D* **90**, 123505 (2014).

[387] J. de. Haro and S.Pan, "Gravitationally induced adiabatic particle production: From Big Bang to de Sitter", *Class. Quantum Grav.* **33**, 165007 (2016) , (arXiv:1512.03100 [gr-qc]).

[388] S. Pan, J. de. Haro, A. Paliathanasis, and R. J. Slagter, " Evolution and Dynamics of a Matter creation model", *Mon. Not. R. Astron. Soc.* **460** (2), 1445 (2016) (arXiv:1601.03955 [gr-qc]).

[389] R. C. Nunes and D. Pavon, "Phantom behavior via cosmological creation of particles", *Phys. Rev. D* **91**, 063526 (2015) (arXiv:1503.04113 [gr-qc]).

[390] R. C. Nunes and S. Pan, "Cosmological consequences of an adiabatic matter creation process", *Mon. Not. R. Astron. Soc.* **459**, 673 (2016) (arXiv:1603.02573 [gr-qc]).

[391] W. Zimdahl, "Bulk viscous cosmology", *Phys. Rev. D* **53**, 5483 (1996).

[392] J. D. Barrow, Formation and Evolution of Cosmic Strings, edited by G. Gibbons, S. W. Hawking, and T. Vachaspati (Cambridge Univ. Press, Cambridge, England, 1990, pp. 449).

[393] J. A. S. Lima, F. E. Silva, and R. C. Santos, "Accelerating Cold Dark Matter Cosmology ($\Omega_\Lambda \equiv 0$)", *Class. Quantum Grav.* **25**, 205006 (2008) (arXiv: 0807.3379 [astro-ph]).

[394] J. P. Mimoso, and D. Pavon, "Entropy evolution of universes with initial and final de Sitter eras", *Phys. Rev. D* **87**, 047302 (2013) (arXiv:1302.1972).

[395] I. L. Shapiro, J. Sola, C. E. Bonet, and P. R. Lapuente, "Variable Cosmological Constant as a Planck Scale Effect", *Phys. Lett. B* **574**, 149 (2003) (arXiv:astro-ph/0303306).

[396] C. E. Bonet, P. R. Lapuente, I. L. Shapiro, and J. Sola, "Testing the running of the cosmological constant with Type Ia Supernovae at high z", *J. Cosmol. Astropart. Phys.* **0402**, 006 (2004) (arXiv:hep-ph/0311171).

[397] S. Basilakos, M. Plionis, and J. Sola, "Hubble expansion & Structure Formation in Time Varying Vacuum Models", Phys. Rev. D **80**, 083511 (2009) (arXiv:0907.4555 [astro-ph.CO]).

[398] A. G. Valent, J. Sola, and S. Basilakos, "Dynamical vacuum energy in the expanding Universe confronted with observations: a dedicated study", *J. Cosmol. Astropart. Phys.* **01**, 004 (2015) (arXiv:1409.7048 [astro-ph.CO]).

[399] J. Sola, A. G. Valent, and J. de Cruz Perez, "Hints of dynamical vacuum energy in the expanding Universe", *Astrophys. J.* **811**, L14 (2015) (arXiv:1506.05793 [gr-qc]).

[400] J. Sola, A. G. Valent, and J. de Cruz Perez, "First evidence of running cosmic vacuum: challenging the concordance model", arXiv:1602.02103 [astro-ph.CO].

[401] J. Sola, "Cosmological constant and vacuum energy: old and new ideas", *J. Phys. Conf. Ser.* **453**, 012015 (2013) (arXiv:1306.1527 [gr-qc]).

[402] R. Garcia-Salcedo, T. Gonzalez, and I. Quiros, "Phase Space Dynamics of Non-Gravitational Interactions between Dark Matter and Dark Energy: The Case of Ghost Dark Energy", arXiv: 1211.2738 [gr-qc].

[403] J. Sola, J. de Cruz Perez, A. G. Valent, and R. C. Nunes, "Dynamical Vacuum against a rigid Cosmological Constant", arXiv: 1606.00450.

[404] R. Cen, "Decaying Cold Dark Matter Model and Small-Scale Power", *Astrophys. J.* **546**, L77 (2001) (arXiv:astro-ph/0005206).

[405] M. Oguri, K. Takahashi, H. Ohno, and K. Kotake, "Decaying Cold Dark Matter and the Evolution of the Cluster Abundance", *Astrophys. J.* **597**, 645 (2003) (arXiv:astro-ph/0306020).

[406] K. A. Malik, D. Wands, and C. Ungarelli, "Large-scale curvature and entropy perturbations for multiple interacting fluids", *Phys. Rev. D* **67**, 063516 (2003).

[407] H. Ziaeepour,"Quintessence from the decay of superheavy dark matter", *Phys. Rev. D* **69**, 063512 (2004).

[408] A. A. Coley, "Dynamical systems and cosmology". (Kluwer Academic Publishers, Dordrecht Boston London, 2003).

[409] J. Dutta, and H. Zonunmawia, "Complete cosmic scenario in the Randall-Sundrum braneworld from the dynamical systems perspective", *The Eur. Phys. J. Plus* **130**, 221 (2015) (arXiv:1601.00283 [gr-qc]).

[410] C. Kaeonikhom, D. Singleton, S. V. Sushkov, and N. Yongram, "Dynamics of Dirac-Born-Infeld dark energy interacting with dark matter", *Phys. Rev. D* **86**, 124049 (2012) (arXiv:1209.5219 [gr-qc]).

[411] S. A. Pavluchenko, "Generality of inflation in closed cosmological models with some quintessence potentials", *Phys. Rev. D* **67**, 103518 (2003).

[412] A. G. Riess *et al.* [Supernova Search Team], "Observational evidence from supernovae for an accelerating universe and a cosmological constant," Astron. J. **116** (1998), 1009-1038 doi:10.1086/300499 [arXiv:astro-ph/9805201 [astro-ph]].

[413] S. Perlmutter *et al.* [Supernova Cosmology Project], "Measurements of Ω and Λ from 42 high redshift supernovae," Astrophys. J. **517** (1999), 565-586 doi:10.1086/307221 [arXiv:astro-ph/9812133 [astro-ph]].

[414] J. L. Feng, "Dark Matter Candidates from Particle Physics and Methods of Detection," Ann. Rev. Astron. Astrophys. **48** (2010), 495-545 doi:10.1146/annurev-astro-082708-101659 [arXiv:1003.0904 [astro-ph.CO]].

[415] M. Kowalski *et al.* [Supernova Cosmology Project], "Improved Cosmological Constraints from New, Old and Combined Supernova Datasets," Astrophys. J. **686** (2008), 749-778 doi:10.1086/589937 [arXiv:0804.4142 [astro-ph]].

[416] E. J. Copeland, A. R. Liddle and D. Wands, "Exponential potentials and cosmological scaling solutions," Phys. Rev. D **57** (1998), 4686-4690 doi:10.1103/PhysRevD.57.4686 [arXiv:gr-qc/9711068 [gr-qc]].

[417] L. Amendola, "Scaling solutions in general nonminimal coupling theories," Phys. Rev. D **60** (1999), 043501 doi:10.1103/PhysRevD.60.043501 [arXiv:astro-ph/9904120 [astro-ph]].

[418] C. Wetterich, "The Cosmon model for an asymptotically vanishing time dependent cosmological 'constant'," Astron. Astrophys. **301** (1995), 321-328 [arXiv:hep-th/9408025 [hep-th]].

[419] C. Wetterich, "The Cosmon model for an asymptotically vanishing time dependent cosmological 'constant'," Astron. Astrophys. **301** (1995), 321-328 [arXiv:hep-th/9408025 [hep-th]].

[420] C. G. Boehmer, G. Caldera-Cabral, R. Lazkoz and R. Maartens, "Dynamics of dark energy with a coupling to dark matter," Phys. Rev. D **78** (2008), 023505 doi:10.1103/PhysRevD.78.023505 [arXiv:0801.1565 [gr-qc]].

[421] Boxonov, Z. S, "A discrete-time dynamical system of mosquito population," Mathematics - Dynamical Systems, doi:10.48550/arXiv.2202.06648 [arXiv:2202.06648].

[422] Elaydi, Saber N, "Discrete Chaos, Second Edition : With Applications in Science and Engineering," CRC Press **2nd ed** (2007), isbn:978-1-4200-1104-3,1420011049.

[423] V. V. Kiselev, "Vector field as a quintessence partner," Class. Quant. Grav. **21** (2004), 3323-3336 doi:10.1088/0264-9381/21/13/014 [arXiv:gr-qc/0402095 [gr-qc]].

[424] C. Armendariz-Picon, "Could dark energy be vector-like?," JCAP **07** (2004), 007 doi:10.1088/1475-7516/2004/07/007 [arXiv:astro-ph/0405267 [astro-ph]].

[425] C. G. Boehmer and T. Harko, "Dark energy as a massive vector field," Eur. Phys. J. C **50** (2007), 423-429 doi:10.1140/epjc/s10052-007-0210-1 [arXiv:gr-qc/0701029 [gr-qc]].

[426] B. Himmetoglu, C. R. Contaldi and M. Peloso, "Instability of the ACW model, and problems with massive vectors during inflation," Phys. Rev. D **79** (2009), 063517 doi:10.1103/PhysRevD.79.063517 [arXiv:0812.1231 [astro-ph]].

[427] T. S. Koivisto, D. F. Mota and C. Pitrou, "Inflation from N-Forms and its stability," JHEP **09** (2009), 092 doi:10.1088/1126-6708/2009/09/092 [arXiv:0903.4158 [astro-ph.CO]].

[428] T. S. Koivisto and N. J. Nunes, "Inflation and dark energy from three-forms," Phys. Rev. D **80** (2009), 103509 doi:10.1103/PhysRevD.80.103509 [arXiv:0908.0920 [astro-ph.CO]].

[429] L. Amendola, M. Quartin, S. Tsujikawa and I. Waga, "Challenges for scaling cosmologies," Phys. Rev. D **74** (2006), 023525 doi:10.1103/PhysRevD.74.023525 [arXiv:astro-ph/0605488 [astro-ph]].

[430] W. Yang, M. Shahalam, B. Pal, S. Pan and A. Wang, "Constraints on quintessence scalar field models using cosmological observations," Phys. Rev. D **100**, no.2, 023522 (2019) doi:10.1103/PhysRevD.100.023522 [arXiv:1810.08586 [gr-qc]].

[431] A. Gómez-Valent, Z. Zheng, L. Amendola, C. Wetterich and V. Pettorino, "Coupled and uncoupled early dark energy, massive neutrinos, and the cosmological tensions," Phys. Rev. D **106**, no.10, 103522 (2022) doi:10.1103/PhysRevD.106.103522 [arXiv:2207.14487 [astro-ph.CO]].

[432] A. G. Riess, W. Yuan, L. M. Macri, D. Scolnic, D. Brout, S. Casertano, D. O. Jones, Y. Murakami, L. Breuval and T. G. Brink, *et al.* "A Comprehensive Measurement of the Local Value of the Hubble Constant with 1 km $s^{?1}$ $Mpc^{?1}$ Uncertainty from the Hubble Space Telescope and the SH0ES Team," Astrophys. J. Lett. **934**, no.1, L7 (2022) doi:10.3847/2041-8213/ac5c5b [arXiv:2112.04510 [astro-ph.CO]].

[433] M. Quartin, M. O. Calvao, S. E. Joras, R. R. R. Reis and I. Waga, "Dark Interactions and Cosmological Fine-Tuning," JCAP **05** (2008), 007 doi:10.1088/1475-7516/2008/05/007

[arXiv:0802.0546 [astro-ph]].

[434] L. Amendola, M. Baldi and C. Wetterich, "Quintessence cosmologies with a growing matter component," Phys. Rev. D **78** (2008), 023015 doi:10.1103/PhysRevD.78.023015 [arXiv:0706.3064 [astro-ph]].

[435] M. Baldi, V. Pettorino, L. Amendola and C. Wetterich, "Oscillating nonlinear large scale structure in growing neutrino quintessence," Mon. Not. Roy. Astron. Soc. **418** (2011), 214 doi:10.1111/j.1365-2966.2011.19477.x [arXiv:1106.2161 [astro-ph.CO]].

[436] E. J. Copeland, M. Sami and S. Tsujikawa, "Dynamics of dark energy," Int. J. Mod. Phys. D **15** (2006), 1753-1936 doi:10.1142/S021827180600942X [arXiv:hep-th/0603057 [hep-th]].

[437] D. F. Mota and J. D. Barrow, "Varying alpha in a more realistic Universe," Phys. Lett. B **581** (2004), 141-146 doi:10.1016/j.physletb.2003.12.016 [arXiv:astro-ph/0306047 [astro-ph]].

[438] J. Khoury and A. Weltman, "Chameleon cosmology," Phys. Rev. D **69** (2004), 044026 doi:10.1103/PhysRevD.69.044026 [arXiv:astro-ph/0309411 [astro-ph]].

[439] E. Komatsu *et al.* [WMAP], "Seven-Year Wilkinson Microwave Anisotropy Probe (WMAP) Observations: Cosmological Interpretation," Astrophys. J. Suppl. **192** (2011), 18 doi:10.1088/0067-0049/192/2/18 [arXiv:1001.4538 [astro-ph.CO]].

[440] W. Zimdahl and D. Pavon, "Interacting quintessence," Phys. Lett. B **521** (2001), 133-138 doi:10.1016/S0370-2693(01)01174-1 [arXiv:astro-ph/0105479 [astro-ph]].

[441] J. Valiviita, E. Majerotto and R. Maartens, "Instability in interacting dark energy and dark matter fluids," JCAP **07** (2008), 020 doi:10.1088/1475-7516/2008/07/020 [arXiv:0804.0232 [astro-ph]].

[442] G. Izquierdo and D. Pavon, "Limits on the parameters of the equation of state for interacting dark energy," Phys. Lett. B **688** (2010), 115-124 doi:10.1016/j.physletb.2010.03.087 [arXiv:1004.2360 [astro-ph.CO]].

[443] D. Pavon and B. Wang, "Le Chatelier-Braun principle in cosmological physics," Gen. Rel. Grav. **41** (2009), 1-5 doi:10.1007/s10714-008-0656-y [arXiv:0712.0565 [gr-qc]].

[444] J. Dunkley *et al.* [WMAP], "Five-Year Wilkinson Microwave Anisotropy Probe (WMAP) Observations: Likelihoods and Parameters from the WMAP data," Astrophys. J. Suppl. **180** (2009), 306-329 doi:10.1088/0067-0049/180/2/306 [arXiv:0803.0586 [astro-ph]].

[445] C. G. Boehmer, G. Caldera-Cabral, N. Chan, R. Lazkoz and R. Maartens, "Quintessence with quadratic coupling to dark matter," Phys. Rev. D **81** (2010),

083003 doi:10.1103/PhysRevD.81.083003 [arXiv:0911.3089 [gr-qc]].

[446] H. M. Sadjadi and M. Alimohammadi, "Cosmological coincidence problem in interactive dark energy models," Phys. Rev. D **74** (2006), 103007 doi:10.1103/PhysRevD.74.103007 [arXiv:gr-qc/0610080 [gr-qc]].

[447] Z. K. Guo, N. Ohta and S. Tsujikawa, "Probing the Coupling between Dark Components of the Universe," Phys. Rev. D **76** (2007), 023508 doi:10.1103/PhysRevD.76.023508 [arXiv:astro-ph/0702015 [astro-ph]].

[448] K. Y. Kim, H. W. Lee and Y. S. Myung, "Holographic interacting dark energy in the braneworld cosmology," Mod. Phys. Lett. A **22** (2007), 2631-2645 doi:10.1142/S0217732307025765 [arXiv:0706.2444 [gr-qc]].

[449] J. H. He and B. Wang, "Effects of the interaction between dark energy and dark matter on cosmological parameters," JCAP **06** (2008), 010 doi:10.1088/1475-7516/2008/06/010 [arXiv:0801.4233 [astro-ph]].

[450] S. Chen, B. Wang and J. Jing, "Dynamics of interacting dark energy model in Einstein and Loop Quantum Cosmology," Phys. Rev. D **78** (2008), 123503 doi:10.1103/PhysRevD.78.123503 [arXiv:0808.3482 [gr-qc]].

[451] S. Chen, B. Wang and J. Jing, "Dynamics of interacting dark energy model in Einstein and Loop Quantum Cosmology," Phys. Rev. D **78** (2008), 123503 doi:10.1103/PhysRevD.78.123503 [arXiv:0808.3482 [gr-qc]].

[452] M. Quartin, M. O. Calvao, S. E. Joras, R. R. R. Reis and I. Waga, "Dark Interactions and Cosmological Fine-Tuning," JCAP **05** (2008), 007 doi:10.1088/1475-7516/2008/05/007 [arXiv:0802.0546 [astro-ph]].

[453] S. H. Pereira and J. F. Jesus, "Can Dark Matter Decay in Dark Energy?," Phys. Rev. D **79** (2009), 043517 doi:10.1103/PhysRevD.79.043517 [arXiv:0811.0099 [astro-ph]].

[454] C. Quercellini, M. Bruni, A. Balbi and D. Pietrobon, "Late universe dynamics with scale-independent linear couplings in the dark sector," Phys. Rev. D **78** (2008), 063527 doi:10.1103/PhysRevD.78.063527 [arXiv:0803.1976 [astro-ph]].

[455] G. Caldera-Cabral, R. Maartens and L. A. Urena-Lopez, "Dynamics of interacting dark energy," Phys. Rev. D **79** (2009), 063518 doi:10.1103/PhysRevD.79.063518 [arXiv:0812.1827 [gr-qc]].

[456] C. G. Boehmer, G. Caldera-Cabral, R. Lazkoz and R. Maartens, "Dynamics of dark energy with a coupling to dark matter," Phys. Rev. D **78** (2008), 023505 doi:10.1103/PhysRevD.78.023505 [arXiv:0801.1565 [gr-qc]].

[457] J. Valiviita, R. Maartens and E. Majerotto, "Observational constraints on an interacting dark energy model," Mon. Not. Roy. Astron. Soc. **402** (2010), 2355-2368 doi:10.1111/j.1365-2966.2009.16115.x [arXiv:0907.4987 [astro-ph.CO]].

[458] C. G. Boehmer, G. Caldera-Cabral, N. Chan, R. Lazkoz and R. Maartens, "Quintessence with quadratic coupling to dark matter," Phys. Rev. D **81** (2010), 083003 doi:10.1103/PhysRevD.81.083003 [arXiv:0911.3089 [gr-qc]].

[459] C. G. Boehmer and J. Burnett, "Dark energy with dark spinors," Mod. Phys. Lett. A **25** (2010), 101-110 doi:10.1142/S0217732310032275 [arXiv:0906.1351 [gr-qc]].

[460] C. G. Boehmer and T. Harko, "Dark energy as a massive vector field," Eur. Phys. J. C **50** (2007), 423-429 doi:10.1140/epjc/s10052-007-0210-1 [arXiv:gr-qc/0701029 [gr-qc]].

[461] T. S. Koivisto and N. J. Nunes, "Inflation and dark energy from three-forms," Phys. Rev. D **80** (2009), 103509 doi:10.1103/PhysRevD.80.103509 [arXiv:0908.0920 [astro-ph.CO]].

[462] T. S. Koivisto and N. J. Nunes, "Three-form cosmology," Phys. Lett. B **685** (2010), 105-109 doi:10.1016/j.physletb.2010.01.051 [arXiv:0907.3883 [astro-ph.CO]].

[463] T. Ngampitipan and P. Wongjun, "Dynamics of three-form dark energy with dark matter couplings," JCAP **11** (2011), 036 doi:10.1088/1475-7516/2011/11/036 [arXiv:1108.0140 [hep-ph]].

[464] E. J. Copeland, M. Sami and S. Tsujikawa, "Dynamics of dark energy," Int. J. Mod. Phys. D **15** (2006), 1753-1936 doi:10.1142/S021827180600942X [arXiv:hep-th/0603057 [hep-th]].

[465] E. J. Copeland, A. R. Liddle and D. Wands, "Exponential potentials and cosmological scaling solutions," Phys. Rev. D **57** (1998), 4686-4690 doi:10.1103/PhysRevD.57.4686 [arXiv:gr-qc/9711068 [gr-qc]].

[466] R. R. Caldwell, "A Phantom menace?," Phys. Lett. B **545** (2002), 23-29 doi:10.1016/S0370-2693(02)02589-3 [arXiv:astro-ph/9908168 [astro-ph]].

[467] G. Leon and E. N. Saridakis, "Phantom dark energy with varying-mass dark matter particles: acceleration and cosmic coincidence problem," Phys. Lett. B **693** (2010), 1-10 doi:10.1016/j.physletb.2010.08.016 [arXiv:0904.1577 [gr-qc]].

[468] A. D. Rendall, "Cosmological models and center manifold theory," Gen. Rel. Grav. **34** (2002), 1277-1294 doi:10.1023/A:1019734703162 [arXiv:gr-qc/0112040 [gr-qc]].

[469] T. Ngampitipan and P. Wongjun, "Dynamics of three-form dark energy with dark matter couplings," JCAP **11** (2011), 036 doi:10.1088/1475-7516/2011/11/036

[arXiv:1108.0140 [hep-ph]].

[470] C. G. Boehmer, N. Chan and R. Lazkoz, "Dynamics of dark energy models and centre manifolds," Phys. Lett. B **714** (2012), 11-17 doi:10.1016/j.physletb.2012.06.064 [arXiv:1111.6247 [gr-qc]].

[471] S. Mishra and S. Chakraborty, Eur. Phys. J. C **79** (2019) no.4, 328 doi:10.1140/epjc/s10052-019-6839-8

[472] T. S. Koivisto and N. J. Nunes, "Three-form cosmology," Phys. Lett. B **685** (2010), 105-109 doi:10.1016/j.physletb.2010.01.051 [arXiv:0907.3883 [astro-ph.CO]].

[473] C. Armendariz-Picon, T. Damour and V. F. Mukhanov, "k - inflation," Phys. Lett. B **458** (1999), 209-218 doi:10.1016/S0370-2693(99)00603-6 [arXiv:hep-th/9904075 [hep-th]].

[474] Lawrence Perko, "Differential equations and Dynamical systems," Springer-Verlag, New York. Inc., Third edition.

[475] S. Mishra and S. Chakraborty, "Dynamical system analysis of Einstein–Skyrme model in a Kantowski–Sachs spacetime," Annals Phys. **406** (2019), 207-219 doi:10.1016/j.aop.2019.04.006 [arXiv:1812.01975 [physics.gen-ph]].

[476] S. Mishra and S. Chakraborty, "Stability and bifurcation analysis of interacting f(T) cosmology," Eur. Phys. J. C **79** (2019) no.4, 328 doi:10.1140/epjc/s10052-019-6839-8

[477] S. Mishra and S. Chakraborty, "A non-canonical scalar field cosmological model: Stability and bifurcation analysis," Mod. Phys. Lett. A **34** (2019) no.32, 1950261 doi:10.1142/S0217732319502614

[478] H. Zonunmawia, W. Khyllep, J. Dutta and L. Järv, "Cosmological dynamics of brane gravity: A global dynamical system perspective," Phys. Rev. D **98** (2018) no.8, 083532 doi:10.1103/PhysRevD.98.083532 [arXiv:1810.03816 [gr-qc]].

[479] W. Yang, N. Banerjee and S. Pan, "Constraining a dark matter and dark energy interaction scenario with a dynamical equation of state," Phys. Rev. D **95** (2017) no.12, 123527 doi:10.1103/PhysRevD.95.123527 [arXiv:1705.09278 [astro-ph.CO]].

[480] Steven Weinberg, "The cosmological constant problem," Rev. Mod. Phys. **61** (1989) no.1-23, 123527 doi:10.1103/RevModPhys.61.1 .

[481] E. J. Copeland, A. R. Liddle and D. Wands, "Exponential potentials and cosmological scaling solutions," Phys. Rev. D **57** (1998), 4686-4690 doi:10.1103/PhysRevD.57.4686 [arXiv:gr-qc/9711068 [gr-qc]].

[482] E. J. Copeland, M. Sami and S. Tsujikawa, "Dynamics of dark energy," Int. J. Mod. Phys. D **15** (2006), 1753-1936 doi:10.1142/S021827180600942X [arXiv:hep-th/0603057

[hep-th]].

[483] D. F. Mota and J. D. Barrow, "Varying alpha in a more realistic Universe," Phys. Lett. B **581** (2004), 141-146 doi:10.1016/j.physletb.2003.12.016 [arXiv:astro-ph/0306047 [astro-ph]].

[484] J. Khoury and A. Weltman, "Chameleon cosmology," Phys. Rev. D **69** (2004), 044026 doi:10.1103/PhysRevD.69.044026 [arXiv:astro-ph/0309411 [astro-ph]].

[485] T. Ngampitipan and P. Wongjun, JCAP **11** (2011), 036 doi:10.1088/1475-7516/2011/11/036 [arXiv:1108.0140 [hep-ph]].

[486] T. S. Koivisto and N. J. Nunes, "Coupled three-form dark energy," Phys. Rev. D **88** (2013) no.12, 123512 doi:10.1103/PhysRevD.88.123512 [arXiv:1212.2541 [astro-ph.CO]].

[487] N. Aghanim *et al.* [Planck], "Planck 2018 results. VI. Cosmological parameters," Astron. Astrophys. **641** (2020), A6 [erratum: Astron. Astrophys. **652** (2021), C4] doi:10.1051/0004-6361/201833910 [arXiv:1807.06209 [astro-ph.CO]].

[488] S. Mishra and S. Chakraborty, "Stability analysis of an interacting holographic dark energy model," Mod. Phys. Lett. A **34** (2019) no.19, 19 doi:10.1142/S0217732319501475 [arXiv:2005.06296 [gr-qc]].

[489] V. V. Kiselev, "Vector field as a quintessence partner," Class. Quant. Grav. **21** (2004), 3323-3336 doi:10.1088/0264-9381/21/13/014 [arXiv:gr-qc/0402095 [gr-qc]].

[490] C. Armendariz-Picon, "Could dark energy be vector-like?," JCAP **07** (2004), 007 doi:10.1088/1475-7516/2004/07/007 [arXiv:astro-ph/0405267 [astro-ph]].

[491] C. G. Boehmer and T. Harko, "Dark energy as a massive vector field," Eur. Phys. J. C **50** (2007), 423-429 doi:10.1140/epjc/s10052-007-0210-1 [arXiv:gr-qc/0701029 [gr-qc]].

[492] M. Novello, S. E. Perez Bergliaffa and J. Salim, "Non-linear electrodynamics and the acceleration of the universe," Phys. Rev. D **69** (2004), 127301 doi:10.1103/PhysRevD.69.127301 [arXiv:astro-ph/0312093 [astro-ph]].

[493] B. Himmetoglu, C. R. Contaldi and M. Peloso, "Instability of the ACW model, and problems with massive vectors during inflation," Phys. Rev. D **79** (2009), 063517 doi:10.1103/PhysRevD.79.063517 [arXiv:0812.1231 [astro-ph]].

[494] T. S. Koivisto, D. F. Mota and C. Pitrou, "Inflation from N-Forms and its stability," JHEP **09** (2009), 092 doi:10.1088/1126-6708/2009/09/092 [arXiv:0903.4158 [astro-ph.CO]].

[495] C. Germani and A. Kehagias, "P-nflation: generating cosmic Inflation with p-forms," JCAP **03** (2009), 028 doi:10.1088/1475-7516/2009/03/028 [arXiv:0902.3667 [astro-

ph.CO]].

[496] G. A. Rave-Franco, C. Escamilla-Rivera and J. Levi Said, "Dynamical complexity of the teleparallel gravity cosmology," Phys. Rev. D **103** (2021) no.8, 084017 doi:10.1103/PhysRevD.103.084017 [arXiv:2101.06347 [gr-qc]].

[497] A. G. Riess *et al.* [Supernova Search Team], "Observational evidence from supernovae for an accelerating universe and a cosmological constant," Astron. J. **116** (1998), 1009-1038 doi:10.1086/300499 [arXiv:astro-ph/9805201 [astro-ph]].

[498] S. Perlmutter *et al.* [Supernova Cosmology Project], "Measurements of Ω and Λ from 42 high redshift supernovae," Astrophys. J. **517** (1999), 565-586 doi:10.1086/307221 [arXiv:astro-ph/9812133 [astro-ph]].

[499] J. L. Feng, "Dark Matter Candidates from Particle Physics and Methods of Detection," Ann. Rev. Astron. Astrophys. **48** (2010), 495-545 doi:10.1146/annurev-astro-082708-101659 [arXiv:1003.0904 [astro-ph.CO]].

[500] M. Kowalski *et al.* [Supernova Cosmology Project], "Improved Cosmological Constraints from New, Old and Combined Supernova Datasets," Astrophys. J. **686** (2008), 749-778 doi:10.1086/589937 [arXiv:0804.4142 [astro-ph]].

[501] E. J. Copeland, A. R. Liddle and D. Wands, Phys. Rev. D **57** (1998), 4686-4690 doi:10.1103/PhysRevD.57.4686 [arXiv:gr-qc/9711068 [gr-qc]].

[502] L. Amendola, "Scaling solutions in general nonminimal coupling theories," Phys. Rev. D **60** (1999), 043501 doi:10.1103/PhysRevD.60.043501 [arXiv:astro-ph/9904120 [astro-ph]].

[503] C. Wetterich, "The Cosmon model for an asymptotically vanishing time dependent cosmological 'constant'," Astron. Astrophys. **301** (1995), 321-328 [arXiv:hep-th/9408025 [hep-th]].

[504] C. Wetterich, "The Cosmon model for an asymptotically vanishing time dependent cosmological 'constant'," Astron. Astrophys. **301** (1995), 321-328 [arXiv:hep-th/9408025 [hep-th]].

[505] V. V. Kiselev, "Vector field as a quintessence partner," Class. Quant. Grav. **21** (2004), 3323-3336 doi:10.1088/0264-9381/21/13/014 [arXiv:gr-qc/0402095 [gr-qc]].

[506] C. Armendariz-Picon, "Could dark energy be vector-like?," JCAP **07** (2004), 007 doi:10.1088/1475-7516/2004/07/007 [arXiv:astro-ph/0405267 [astro-ph]].

[507] C. G. Boehmer and T. Harko, "Dark energy as a massive vector field," Eur. Phys. J. C **50** (2007), 423-429 doi:10.1140/epjc/s10052-007-0210-1 [arXiv:gr-qc/0701029 [gr-qc]].

[508] B. Himmetoglu, C. R. Contaldi and M. Peloso, "Instability of the ACW model, and problems with massive vectors during inflation," Phys. Rev. D **79** (2009), 063517 doi:10.1103/PhysRevD.79.063517 [arXiv:0812.1231 [astro-ph]].

[509] T. S. Koivisto, D. F. Mota and C. Pitrou, "Inflation from N-Forms and its stability," JHEP **09** (2009), 092 doi:10.1088/1126-6708/2009/09/092 [arXiv:0903.4158 [astro-ph.CO]].

[510] L. Amendola, M. Quartin, S. Tsujikawa and I. Waga, "Challenges for scaling cosmologies," Phys. Rev. D **74** (2006), 023525 doi:10.1103/PhysRevD.74.023525 [arXiv:astro-ph/0605488 [astro-ph]].

[511] M. Quartin, M. O. Calvao, S. E. Joras, R. R. R. Reis and I. Waga, "Dark Interactions and Cosmological Fine-Tuning," JCAP **05** (2008), 007 doi:10.1088/1475-7516/2008/05/007 [arXiv:0802.0546 [astro-ph]].

[512] . Amendola, M. Baldi and C. Wetterich, "Quintessence cosmologies with a growing matter component," Phys. Rev. D **78** (2008), 023015 doi:10.1103/PhysRevD.78.023015 [arXiv:0706.3064 [astro-ph]].

[513] M. Baldi, V. Pettorino, L. Amendola and C. Wetterich, "Oscillating nonlinear large scale structure in growing neutrino quintessence," Mon. Not. Roy. Astron. Soc. **418** (2011), 214 doi:10.1111/j.1365-2966.2011.19477.x [arXiv:1106.2161 [astro-ph.CO]].

[514] E. Komatsu *et al.* [WMAP], "Seven-Year Wilkinson Microwave Anisotropy Probe (WMAP) Observations: Cosmological Interpretation," Astrophys. J. Suppl. **192** (2011), 18 doi:10.1088/0067-0049/192/2/18 [arXiv:1001.4538 [astro-ph.CO]].

[515] W. Zimdahl and D. Pavon, "Interacting quintessence," Phys. Lett. B **521** (2001), 133-138 doi:10.1016/S0370-2693(01)01174-1 [arXiv:astro-ph/0105479 [astro-ph]].

[516] J. Valiviita, E. Majerotto and R. Maartens, "Instability in interacting dark energy and dark matter fluids," JCAP **07** (2008), 020 doi:10.1088/1475-7516/2008/07/020 [arXiv:0804.0232 [astro-ph]].

[517] G. Izquierdo and D. Pavon, "Limits on the parameters of the equation of state for interacting dark energy," Phys. Lett. B **688** (2010), 115-124 doi:10.1016/j.physletb.2010.03.087 [arXiv:1004.2360 [astro-ph.CO]].

[518] D. Pavon and B. Wang, "Le Chatelier-Braun principle in cosmological physics," Gen. Rel. Grav. **41** (2009), 1-5 doi:10.1007/s10714-008-0656-y [arXiv:0712.0565 [gr-qc]].

[519] J. Dunkley *et al.* [WMAP], "Five-Year Wilkinson Microwave Anisotropy Probe (WMAP) Observations: Likelihoods and Parameters from the WMAP data," Astrophys. J. Suppl. **180** (2009), 306-329 doi:10.1088/0067-0049/180/2/306 [arXiv:0803.0586 [astro-ph]].

[520] C. G. Boehmer, G. Caldera-Cabral, N. Chan, R. Lazkoz and R. Maartens, "Quintessence with quadratic coupling to dark matter," Phys. Rev. D **81** (2010), 083003 doi:10.1103/PhysRevD.81.083003 [arXiv:0911.3089 [gr-qc]].

[521] H. M. Sadjadi and M. Alimohammadi, "Cosmological coincidence problem in interactive dark energy models," Phys. Rev. D **74** (2006), 103007 doi:10.1103/PhysRevD.74.103007 [arXiv:gr-qc/0610080 [gr-qc]].

[522] Z. K. Guo, N. Ohta and S. Tsujikawa, "Probing the Coupling between Dark Components of the Universe," Phys. Rev. D **76** (2007), 023508 doi:10.1103/PhysRevD.76.023508 [arXiv:astro-ph/0702015 [astro-ph]].

[523] K. Y. Kim, H. W. Lee and Y. S. Myung, "Holographic interacting dark energy in the braneworld cosmology," Mod. Phys. Lett. A **22** (2007), 2631-2645 doi:10.1142/S0217732307025765 [arXiv:0706.2444 [gr-qc]].

[524] J. H. He and B. Wang, "Effects of the interaction between dark energy and dark matter on cosmological parameters," JCAP **06** (2008), 010 doi:10.1088/1475-7516/2008/06/010 [arXiv:0801.4233 [astro-ph]].

[525] S. Chen, B. Wang and J. Jing, "Dynamics of interacting dark energy model in Einstein and Loop Quantum Cosmology," Phys. Rev. D **78** (2008), 123503 doi:10.1103/PhysRevD.78.123503 [arXiv:0808.3482 [gr-qc]].

[526] M. Quartin, M. O. Calvao, S. E. Joras, R. R. R. Reis and I. Waga, "Dark Interactions and Cosmological Fine-Tuning," JCAP **05** (2008), 007 doi:10.1088/1475-7516/2008/05/007 [arXiv:0802.0546 [astro-ph]].

[527] S. H. Pereira and J. F. Jesus, "Can Dark Matter Decay in Dark Energy?," Phys. Rev. D **79** (2009), 043517 doi:10.1103/PhysRevD.79.043517 [arXiv:0811.0099 [astro-ph]].

[528] C. Quercellini, M. Bruni, A. Balbi and D. Pietrobon, "Late universe dynamics with scale-independent linear couplings in the dark sector," Phys. Rev. D **78** (2008), 063527 doi:10.1103/PhysRevD.78.063527 [arXiv:0803.1976 [astro-ph]].

[529] G. Caldera-Cabral, R. Maartens and L. A. Urena-Lopez, "Dynamics of interacting dark energy," Phys. Rev. D **79** (2009), 063518 doi:10.1103/PhysRevD.79.063518 [arXiv:0812.1827 [gr-qc]].

[530] C. G. Boehmer, G. Caldera-Cabral, R. Lazkoz and R. Maartens, "Dynamics of dark energy with a coupling to dark matter," Phys. Rev. D **78** (2008), 023505 doi:10.1103/PhysRevD.78.023505 [arXiv:0801.1565 [gr-qc]].

[531] J. Valiviita, R. Maartens and E. Majerotto, "Observational constraints on an interacting dark energy model," Mon. Not. Roy. Astron. Soc. **402** (2010), 2355-2368 doi:10.1111/j.1365-2966.2009.16115.x [arXiv:0907.4987 [astro-ph.CO]].

[532] C. G. Boehmer, G. Caldera-Cabral, N. Chan, R. Lazkoz and R. Maartens, "Quintessence with quadratic coupling to dark matter," Phys. Rev. D **81** (2010), 083003 doi:10.1103/PhysRevD.81.083003 [arXiv:0911.3089 [gr-qc]].

[533] C. G. Boehmer and J. Burnett, "Dark energy with dark spinors," Mod. Phys. Lett. A **25** (2010), 101-110 doi:10.1142/S0217732310032275 [arXiv:0906.1351 [gr-qc]].

[534] T. S. Koivisto and N. J. Nunes, "Inflation and dark energy from three-forms," Phys. Rev. D **80** (2009), 103509 doi:10.1103/PhysRevD.80.103509 [arXiv:0908.0920 [astro-ph.CO]].

[535] T. S. Koivisto and N. J. Nunes, "Three-form cosmology," Phys. Lett. B **685** (2010), 105-109 doi:10.1016/j.physletb.2010.01.051 [arXiv:0907.3883 [astro-ph.CO]].

[536] T. Ngampitipan and P. Wongjun, "Dynamics of three-form dark energy with dark matter couplings," JCAP **11** (2011), 036 doi:10.1088/1475-7516/2011/11/036 [arXiv:1108.0140 [hep-ph]].

[537] E. J. Copeland, A. R. Liddle and D. Wands, "Exponential potentials and cosmological scaling solutions," Phys. Rev. D **57** (1998), 4686-4690 doi:10.1103/PhysRevD.57.4686 [arXiv:gr-qc/9711068 [gr-qc]].

[538] R. R. Caldwell, "A Phantom menace?," Phys. Lett. B **545** (2002), 23-29 doi:10.1016/S0370-2693(02)02589-3 [arXiv:astro-ph/9908168 [astro-ph]].

[539] G. Leon and E. N. Saridakis, "Phantom dark energy with varying-mass dark matter particles: acceleration and cosmic coincidence problem," Phys. Lett. B **693** (2010), 1-10 doi:10.1016/j.physletb.2010.08.016 [arXiv:0904.1577 [gr-qc]].

[540] A. D. Rendall, "Cosmological models and center manifold theory," Gen. Rel. Grav. **34** (2002), 1277-1294 doi:10.1023/A:1019734703162 [arXiv:gr-qc/0112040 [gr-qc]].

[541] C. G. Boehmer, N. Chan and R. Lazkoz, "Dynamics of dark energy models and centre manifolds," Phys. Lett. B **714** (2012), 11-17 doi:10.1016/j.physletb.2012.06.064 [arXiv:1111.6247 [gr-qc]].

[542] S. Mishra and S. Chakraborty, "Stability and bifurcation analysis of interacting f(T) cosmology," Eur. Phys. J. C **79** (2019) no.4, 328 doi:10.1140/epjc/s10052-019-6839-8

[543] C. Armendariz-Picon, T. Damour and V. F. Mukhanov, "k - inflation," Phys. Lett. B **458** (1999), 209-218 doi:10.1016/S0370-2693(99)00603-6 [arXiv:hep-th/9904075 [hep-th]].

[544] S. Mishra and S. Chakraborty, "Dynamical system analysis of Einstein–Skyrme model in a Kantowski–Sachs spacetime," Annals Phys. **406** (2019), 207-219 doi:10.1016/j.aop.2019.04.006 [arXiv:1812.01975 [physics.gen-ph]].

[545] S. Mishra and S. Chakraborty, "A non-canonical scalar field cosmological model: Stability and bifurcation analysis," Mod. Phys. Lett. A **34** (2019) no.32, 1950261 doi:10.1142/S0217732319502614

[546] H. Zonunmawia, W. Khyllep, J. Dutta and L. Järv, "Cosmological dynamics of brane gravity: A global dynamical system perspective," Phys. Rev. D **98** (2018) no.8, 083532 doi:10.1103/PhysRevD.98.083532 [arXiv:1810.03816 [gr-qc]].

[547] W. Yang, N. Banerjee and S. Pan, "Constraining a dark matter and dark energy interaction scenario with a dynamical equation of state," Phys. Rev. D **95** (2017) no.12, 123527 doi:10.1103/PhysRevD.95.123527 [arXiv:1705.09278 [astro-ph.CO]].

[548] E. J. Copeland, A. R. Liddle and D. Wands, "Exponential potentials and cosmological scaling solutions," Phys. Rev. D **57** (1998), 4686-4690 doi:10.1103/PhysRevD.57.4686 [arXiv:gr-qc/9711068 [gr-qc]].

[549] D. F. Mota and J. D. Barrow, "Varying alpha in a more realistic Universe," Phys. Lett. B **581** (2004), 141-146 doi:10.1016/j.physletb.2003.12.016 [arXiv:astro-ph/0306047 [astro-ph]].

[550] N. Aghanim *et al.* [Planck], "Planck 2018 results. VI. Cosmological parameters," Astron. Astrophys. **641** (2020), A6 [erratum: Astron. Astrophys. **652** (2021), C4] doi:10.1051/0004-6361/201833910 [arXiv:1807.06209 [astro-ph.CO]].

[551] Bhandari, Animesh and Borah, Debajit and Mukherjee, Saikat, "Characterizations of weaving K-frames," Proc. Japan Acad. Ser. A Math. Sci., **96** (2020).

[552] S. Pal and S. Chakraborty, "Dynamical system analysis of a three fluid cosmological model: an invariant manifold approach," Eur. Phys. J. C **79** (2019) no.4, 362 doi:10.1140/epjc/s10052-019-6875-4 [arXiv:2002.07588 [gr-qc]].

[553] S. Pal and S. Chakraborty, "Dynamical system analysis of a Dirac-Born-Infeld model: a center manifold perspective," Gen. Rel. Grav. **51** (2019) no.9, 124 doi:10.1007/s10714-019-2608-0 [arXiv:2103.02715 [gr-qc]].

[554] H. Mohseni Sadjadi, "On cosmic acceleration in four dimensional Einstein-Gauss-Bonnet gravity," Phys. Dark Univ. **30** (2020), 100728 doi:10.1016/j.dark.2020.100728 [arXiv:2005.10024 [gr-qc]].

[555] S. Pal, S. Mishra and S. Chakraborty, "Dynamical system analysis of a non-minimally coupled scalar field," Int. J. Mod. Phys. D **28** (2019) no.15, 1950173 doi:10.1142/S0218271819501736

[556] David J. Mulryne and Johannes Noller and Nelson J. Nunes, "Three-form inflation and non-Gaussianity," Journal of Cosmology and Astroparticle Physics **12** (2012)

[557] A. De Felice, K. Karwan and P. Wongjun, "Stability of the 3-form field during inflation," Phys. Rev. D **85** (2012), 123545 doi:10.1103/PhysRevD.85.123545 [arXiv:1202.0896 [hep-ph]].

[558] A. De Felice, K. Karwan and P. Wongjun, "Reheating in 3-form inflation," Phys. Rev. D **86** (2012), 103526 doi:10.1103/PhysRevD.86.103526 [arXiv:1209.5156 [astro-ph.CO]].

[559] T. S. Koivisto and N. J. Nunes, "Coupled three-form dark energy," Phys. Rev. D **88** (2013) no.12, 123512 doi:10.1103/PhysRevD.88.123512 [arXiv:1212.2541 [astro-ph.CO]].

[560] C. G. Boehmer, N. Chan and R. Lazkoz, "Dynamics of dark energy models and centre manifolds," Phys. Lett. B **714** (2012), 11-17 doi:10.1016/j.physletb.2012.06.064 [arXiv:1111.6247 [gr-qc]].

[561] C. G. Boehmer, N. Tamanini and M. Wright, "Interacting quintessence from a variational approach Part I: algebraic couplings," Phys. Rev. D **91** (2015) no.12, 123002 doi:10.1103/PhysRevD.91.123002 [arXiv:1501.06540 [gr-qc]].

[562] T. S. Koivisto, D. F. Mota and C. Pitrou, "Inflation from N-Forms and its stability," JHEP **09** (2009), 092 doi:10.1088/1126-6708/2009/09/092 [arXiv:0903.4158 [astro-ph.CO]].

[563] A. G. Riess *et al.* [Supernova Search Team], "Observational evidence from supernovae for an accelerating universe and a cosmological constant," Astron. J. **116** (1998), 1009-1038 doi:10.1086/300499 [arXiv:astro-ph/9805201 [astro-ph]].

[564] S. Perlmutter *et al.* [Supernova Cosmology Project], "Measurements of Ω and Λ from 42 high redshift supernovae," Astrophys. J. **517** (1999), 565-586 doi:10.1086/307221 [arXiv:astro-ph/9812133 [astro-ph]].

[565] J. L. Feng, "Dark Matter Candidates from Particle Physics and Methods of Detection," Ann. Rev. Astron. Astrophys. **48** (2010), 495-545 doi:10.1146/annurev-astro-082708-101659 [arXiv:1003.0904 [astro-ph.CO]].

[566] M. Kowalski *et al.* [Supernova Cosmology Project], "Improved Cosmological Constraints from New, Old and Combined Supernova Datasets," Astrophys. J. **686** (2008), 749-778 doi:10.1086/589937 [arXiv:0804.4142 [astro-ph]].

[567] E. J. Copeland, A. R. Liddle and D. Wands, "Exponential potentials and cosmological scaling solutions," Phys. Rev. D **57** (1998), 4686-4690 doi:10.1103/PhysRevD.57.4686 [arXiv:gr-qc/9711068 [gr-qc]].

[568] L. Amendola, "Scaling solutions in general nonminimal coupling theories," Phys. Rev. D **60** (1999), 043501 doi:10.1103/PhysRevD.60.043501 [arXiv:astro-ph/9904120 [astro-ph]].

[569] C. Wetterich, "The Cosmon model for an asymptotically vanishing time dependent cosmological 'constant'," Astron. Astrophys. **301** (1995), 321-328 [arXiv:hep-th/9408025 [hep-th]].

[570] C. G. Boehmer, G. Caldera-Cabral, R. Lazkoz and R. Maartens, "Dynamics of dark energy with a coupling to dark matter," Phys. Rev. D **78** (2008), 023505 doi:10.1103/PhysRevD.78.023505 [arXiv:0801.1565 [gr-qc]].

[571] V. V. Kiselev, "Vector field as a quintessence partner," Class. Quant. Grav. **21** (2004), 3323-3336 doi:10.1088/0264-9381/21/13/014 [arXiv:gr-qc/0402095 [gr-qc]].

[572] C. Armendariz-Picon, "Could dark energy be vector-like?," JCAP **07** (2004), 007 doi:10.1088/1475-7516/2004/07/007 [arXiv:astro-ph/0405267 [astro-ph]].

[573] C. G. Boehmer and T. Harko, "Dark energy as a massive vector field," Eur. Phys. J. C **50** (2007), 423-429 doi:10.1140/epjc/s10052-007-0210-1 [arXiv:gr-qc/0701029 [gr-qc]].

[574] B. Himmetoglu, C. R. Contaldi and M. Peloso, "Instability of the ACW model, and problems with massive vectors during inflation," Phys. Rev. D **79** (2009), 063517 doi:10.1103/PhysRevD.79.063517 [arXiv:0812.1231 [astro-ph]].

[575] T. S. Koivisto, D. F. Mota and C. Pitrou, "Inflation from N-Forms and its stability," JHEP **09** (2009), 092 doi:10.1088/1126-6708/2009/09/092 [arXiv:0903.4158 [astro-ph.CO]].

[576] L. Amendola, M. Quartin, S. Tsujikawa and I. Waga, "Challenges for scaling cosmologies," Phys. Rev. D **74** (2006), 023525 doi:10.1103/PhysRevD.74.023525 [arXiv:astro-ph/0605488 [astro-ph]].

[577] M. Quartin, M. O. Calvao, S. E. Joras, R. R. R. Reis and I. Waga, "Dark Interactions and Cosmological Fine-Tuning," JCAP **05** (2008), 007 doi:10.1088/1475-7516/2008/05/007 [arXiv:0802.0546 [astro-ph]].

[578] L. Amendola, M. Baldi and C. Wetterich, "Quintessence cosmologies with a growing matter component," Phys. Rev. D **78** (2008), 023015 doi:10.1103/PhysRevD.78.023015 [arXiv:0706.3064 [astro-ph]].

[579] M. Baldi, V. Pettorino, L. Amendola and C. Wetterich, "Oscillating nonlinear large scale structure in growing neutrino quintessence," Mon. Not. Roy. Astron. Soc. **418** (2011), 214 doi:10.1111/j.1365-2966.2011.19477.x [arXiv:1106.2161 [astro-ph.CO]].

[580] E. J. Copeland, M. Sami and S. Tsujikawa, "Dynamics of dark energy," Int. J. Mod. Phys. D **15** (2006), 1753-1936 doi:10.1142/S021827180600942X [arXiv:hep-th/0603057 [hep-th]].

[581] J. Khoury and A. Weltman, "Chameleon cosmology," Phys. Rev. D **69** (2004), 044026 doi:10.1103/PhysRevD.69.044026 [arXiv:astro-ph/0309411 [astro-ph]].

[582] E. Komatsu *et al.* [WMAP], "Seven-Year Wilkinson Microwave Anisotropy Probe (WMAP) Observations: Cosmological Interpretation," Astrophys. J. Suppl. **192** (2011), 18 doi:10.1088/0067-0049/192/2/18 [arXiv:1001.4538 [astro-ph.CO]].

[583] W. Zimdahl and D. Pavon, "Interacting quintessence," Phys. Lett. B **521** (2001), 133-138 doi:10.1016/S0370-2693(01)01174-1 [arXiv:astro-ph/0105479 [astro-ph]].

[584] J. Valiviita, E. Majerotto and R. Maartens, "Instability in interacting dark energy and dark matter fluids," JCAP **07** (2008), 020 doi:10.1088/1475-7516/2008/07/020 [arXiv:0804.0232 [astro-ph]].

[585] G. Izquierdo and D. Pavon, "Limits on the parameters of the equation of state for interacting dark energy," Phys. Lett. B **688** (2010), 115-124 doi:10.1016/j.physletb.2010.03.087 [arXiv:1004.2360 [astro-ph.CO]].

[586] D. Pavon and B. Wang, "Le Chatelier-Braun principle in cosmological physics," Gen. Rel. Grav. **41** (2009), 1-5 doi:10.1007/s10714-008-0656-y [arXiv:0712.0565 [gr-qc]].

[587] J. Dunkley *et al.* [WMAP], "Five-Year Wilkinson Microwave Anisotropy Probe (WMAP) Observations: Likelihoods and Parameters from the WMAP data," Astrophys. J. Suppl. **180** (2009), 306-329 doi:10.1088/0067-0049/180/2/306 [arXiv:0803.0586 [astro-ph]].

[588] C. G. Boehmer, G. Caldera-Cabral, N. Chan, R. Lazkoz and R. Maartens, "Quintessence with quadratic coupling to dark matter," Phys. Rev. D **81** (2010), 083003 doi:10.1103/PhysRevD.81.083003 [arXiv:0911.3089 [gr-qc]].

[589] H. M. Sadjadi and M. Alimohammadi, "Cosmological coincidence problem in interactive dark energy models," Phys. Rev. D **74** (2006), 103007 doi:10.1103/PhysRevD.74.103007 [arXiv:gr-qc/0610080 [gr-qc]].

[590] Z. K. Guo, N. Ohta and S. Tsujikawa, "Probing the Coupling between Dark Components of the Universe," Phys. Rev. D **76** (2007), 023508 doi:10.1103/PhysRevD.76.023508 [arXiv:astro-ph/0702015 [astro-ph]].

[591] K. Y. Kim, H. W. Lee and Y. S. Myung, "Holographic interacting dark energy in the braneworld cosmology," Mod. Phys. Lett. A **22** (2007), 2631-2645 doi:10.1142/S0217732307025765 [arXiv:0706.2444 [gr-qc]].

[592] J. H. He and B. Wang, "Effects of the interaction between dark energy and dark matter on cosmological parameters," JCAP **06** (2008), 010 doi:10.1088/1475-7516/2008/06/010 [arXiv:0801.4233 [astro-ph]].

[593] S. Chen, B. Wang and J. Jing, "Dynamics of interacting dark energy model in Einstein and Loop Quantum Cosmology," Phys. Rev. D **78** (2008), 123503 doi:10.1103/PhysRevD.78.123503 [arXiv:0808.3482 [gr-qc]].

[594] M. Quartin, M. O. Calvao, S. E. Joras, R. R. R. Reis and I. Waga, "Dark Interactions and Cosmological Fine-Tuning," JCAP **05** (2008), 007 doi:10.1088/1475-7516/2008/05/007

[595] S. H. Pereira and J. F. Jesus, "Can Dark Matter Decay in Dark Energy?," Phys. Rev. D **79** (2009), 043517 doi:10.1103/PhysRevD.79.043517 [arXiv:0811.0099 [astro-ph]].

[596] C. Quercellini, M. Bruni, A. Balbi and D. Pietrobon, "Late universe dynamics with scale-independent linear couplings in the dark sector," Phys. Rev. D **78** (2008), 063527 doi:10.1103/PhysRevD.78.063527 [arXiv:0803.1976 [astro-ph]].

[597] G. Caldera-Cabral, R. Maartens and L. A. Urena-Lopez, "Dynamics of interacting dark energy," Phys. Rev. D **79** (2009), 063518 doi:10.1103/PhysRevD.79.063518 [arXiv:0812.1827 [gr-qc]].

[598] C. G. Boehmer, G. Caldera-Cabral, R. Lazkoz and R. Maartens, "Dynamics of dark energy with a coupling to dark matter," Phys. Rev. D **78** (2008), 023505 doi:10.1103/PhysRevD.78.023505 [arXiv:0801.1565 [gr-qc]].

[599] J. Valiviita, R. Maartens and E. Majerotto, "Observational constraints on an interacting dark energy model," Mon. Not. Roy. Astron. Soc. **402** (2010), 2355-2368 doi:10.1111/j.1365-2966.2009.16115.x [arXiv:0907.4987 [astro-ph.CO]].

[600] C. G. Boehmer, G. Caldera-Cabral, N. Chan, R. Lazkoz and R. Maartens, "Quintessence with quadratic coupling to dark matter," Phys. Rev. D **81** (2010), 083003 doi:10.1103/PhysRevD.81.083003 [arXiv:0911.3089 [gr-qc]].

[601] C. G. Boehmer and J. Burnett, "Dark energy with dark spinors," Mod. Phys. Lett. A **25** (2010), 101-110 doi:10.1142/S0217732310032275 [arXiv:0906.1351 [gr-qc]].

[602] T. S. Koivisto and N. J. Nunes, "Inflation and dark energy from three-forms," Phys. Rev. D **80** (2009), 103509 doi:10.1103/PhysRevD.80.103509 [arXiv:0908.0920 [astro-ph.CO]].

[603] T. S. Koivisto and N. J. Nunes, "Three-form cosmology," Phys. Lett. B **685** (2010), 105-109 doi:10.1016/j.physletb.2010.01.051 [arXiv:0907.3883 [astro-ph.CO]].

[604] T. Ngampitipan and P. Wongjun, "Dynamics of three-form dark energy with dark matter couplings," JCAP **11** (2011), 036 doi:10.1088/1475-7516/2011/11/036 [arXiv:1108.0140 [hep-ph]].

[605] E. J. Copeland, A. R. Liddle and D. Wands, "Exponential potentials and cosmological scaling solutions," Phys. Rev. D **57** (1998), 4686-4690 doi:10.1103/PhysRevD.57.4686

[arXiv:gr-qc/9711068 [gr-qc]].

[606] R. R. Caldwell, "A Phantom menace?," Phys. Lett. B **545** (2002), 23-29 doi:10.1016/S0370-2693(02)02589-3 [arXiv:astro-ph/9908168 [astro-ph]].

[607] G. Leon and E. N. Saridakis, "Phantom dark energy with varying-mass dark matter particles: acceleration and cosmic coincidence problem," Phys. Lett. B **693** (2010), 1-10 doi:10.1016/j.physletb.2010.08.016 [arXiv:0904.1577 [gr-qc]].

[608] A. D. Rendall, "Cosmological models and center manifold theory," Gen. Rel. Grav. **34** (2002), 1277-1294 doi:10.1023/A:1019734703162 [arXiv:gr-qc/0112040 [gr-qc]].

[609] C. G. Boehmer, N. Chan and R. Lazkoz, "Dynamics of dark energy models and centre manifolds," Phys. Lett. B **714** (2012), 11-17 doi:10.1016/j.physletb.2012.06.064 [arXiv:1111.6247 [gr-qc]].

[610] C. Armendariz-Picon, T. Damour and V. F. Mukhanov, "k - inflation," Phys. Lett. B **458** (1999), 209-218 doi:10.1016/S0370-2693(99)00603-6 [arXiv:hep-th/9904075 [hep-th]].

[611] S. Mishra and S. Chakraborty, "A non-canonical scalar field cosmological model: Stability and bifurcation analysis," Mod. Phys. Lett. A **34** (2019) no.32, 1950261 doi:10.1142/S0217732319502614

[612] H. Zonunmawia, W. Khyllep, J. Dutta and L. Järv, "Cosmological dynamics of brane gravity: A global dynamical system perspective," Phys. Rev. D **98** (2018) no.8, 083532 doi:10.1103/PhysRevD.98.083532 [arXiv:1810.03816 [gr-qc]].

[613] W. Yang, N. Banerjee and S. Pan, "Constraining a dark matter and dark energy interaction scenario with a dynamical equation of state," Phys. Rev. D **95** (2017) no.12, 123527 doi:10.1103/PhysRevD.95.123527 [arXiv:1705.09278 [astro-ph.CO]].

[614] Weinberg, Steven, "The cosmological constant problem," Rev. Mod. Phys. **61** (1989) no.23, doi:10.1103/RevModPhys.61.1

[615] E. J. Copeland, A. R. Liddle and D. Wands, "Exponential potentials and cosmological scaling solutions," Phys. Rev. D **57** (1998), 4686-4690 doi:10.1103/PhysRevD.57.4686 [arXiv:gr-qc/9711068 [gr-qc]].

[616] D. F. Mota and J. D. Barrow, "Varying alpha in a more realistic Universe," Phys. Lett. B **581** (2004), 141-146 doi:10.1016/j.physletb.2003.12.016 [arXiv:astro-ph/0306047 [astro-ph]].

[617] N. Aghanim *et al.* [Planck], "Planck 2018 results. VI. Cosmological parameters," Astron. Astrophys. **641** (2020), A6 [erratum: Astron. Astrophys. **652** (2021), C4] doi:10.1051/0004-6361/201833910 [arXiv:1807.06209 [astro-ph.CO]].

[618] A. De Felice, K. Karwan and P. Wongjun, "Stability of the 3-form field during inflation," Phys. Rev. D **85** (2012), 123545 doi:10.1103/PhysRevD.85.123545 [arXiv:1202.0896 [hep-ph]].

[619] A. De Felice, K. Karwan and P. Wongjun, "Reheating in 3-form inflation," Phys. Rev. D **86** (2012), 103526 doi:10.1103/PhysRevD.86.103526 [arXiv:1209.5156 [astro-ph.CO]].

[620] T. S. Koivisto and N. J. Nunes, "Coupled three-form dark energy," Phys. Rev. D **88** (2013) no.12, 123512 doi:10.1103/PhysRevD.88.123512 [arXiv:1212.2541 [astro-ph.CO]].

[621] C. G. Boehmer, N. Chan and R. Lazkoz, "Dynamics of dark energy models and centre manifolds," Phys. Lett. B **714** (2012), 11-17 doi:10.1016/j.physletb.2012.06.064 [arXiv:1111.6247 [gr-qc]].

[622] C. G. Boehmer, N. Tamanini and M. Wright, "Interacting quintessence from a variational approach Part I: algebraic couplings," Phys. Rev. D **91** (2015) no.12, 123002 doi:10.1103/PhysRevD.91.123002 [arXiv:1501.06540 [gr-qc]].

[623] T. S. Koivisto, D. F. Mota and C. Pitrou, "Inflation from N-Forms and its stability," JHEP **09** (2009), 092 doi:10.1088/1126-6708/2009/09/092 [arXiv:0903.4158 [astro-ph.CO]].

[624] S. Mishra and S. Chakraborty, "Dynamical system analysis of Einstein–Skyrme model in a Kantowski–Sachs spacetime," Annals Phys. **406** (2019), 207-219 doi:10.1016/j.aop.2019.04.006 [arXiv:1812.01975 [physics.gen-ph]].

[625] S. Mishra and S. Chakraborty, "Dynamical system analysis of quintom dark energy model," Eur. Phys. J. C **78** (2018) no.11, 917 doi:10.1140/epjc/s10052-018-6405-9 [arXiv:1811.08279 [gr-qc]].

[626] S. Pal and S. Chakraborty, "Dynamical system analysis of Hessence scalar field in teleparallel gravity: Invariant manifold technique," Int. J. Mod. Phys. A **34** (2019) no.28, 1950156 doi:10.1142/S0217751X19501562

[627] S. K. Biswas and S. Chakraborty, "Interacting dark energy model in the brane scenario: A Dynamical System Analysis," Int. J. Geom. Meth. Mod. Phys. **16** (2019) no.08, 1950115 doi:10.1142/S0219887819501159 [arXiv:1701.02584 [physics.gen-ph]].

[628] S. K. Biswas, S. Chakraborty, J. Dutta and S. Chakraborty, "Dynamical analysis of an interacting dark energy model in the framework of a particle creation mechanism," Phys. Rev. D **95** (2017) no.10, 103009 doi:10.1103/PhysRevD.95.103009 [arXiv:1604.07636 [gr-qc]].

[629] S. K. Biswas and S. Chakraborty, "Interacting Dark Energy in $f(T)$ cosmology : A Dynamical System analysis," Int. J. Mod. Phys. D **24** (2015) no.07, 1550046 doi:10.1142/S0218271815500467 [arXiv:1504.02431 [gr-qc]].

[630] S. K. Biswas and S. Chakraborty, "Dynamical systems analysis of an interacting dark energy model in the brane scenario," Gen. Rel. Grav. **47** (2015), 22 doi:10.1007/s10714-015-1866-8 [arXiv:1502.06913 [gr-qc]].

[631] N. Mahata and S. Chakraborty, "A Dynamical System Analysis of Three Fluid cosmological Model," [arXiv:1512.07017 [gr-qc]].

[632] N. Mahata and S. Chakraborty, "A dynamical system analysis of holographic dark energy models with different IR cutoff," Mod. Phys. Lett. A **30** (2015) no.27, 1550134 doi:10.1142/S0217732315501345 [arXiv:1511.07955 [gr-qc]].

[633] N. Mahata and S. Chakraborty, Mod. Phys. Lett. A **30** (2015) no.02, 1550009 doi:10.1142/S0217732315500091 [arXiv:1501.04441 [gr-qc]].

[634] N. Mahata and S. Chakraborty, "Dynamical System Analysis for a phantom model," Gen. Rel. Grav. **46** (2014), 1721 doi:10.1007/s10714-014-1721-3 [arXiv:1312.7644 [gr-qc]].

[635] N. Mahata and S. Chakraborty, "Dilatonic Scalar Field: A Dynamical System Analysis," [arXiv:1305.1702 [gr-qc]].

[636] S. Chakraborty, S. Mishra and S. Chakraborty, "Dynamical system analysis of three-form field dark energy model with baryonic matter," Eur. Phys. J. C **80** (2020) no.9, 852 doi:10.1140/epjc/s10052-020-8427-3

[637] S. Chakraborty, S. Mishra and S. Chakraborty, "A dynamical system analysis of cosmic evolution with coupled phantom dark energy with dark matter," Int. J. Mod. Phys. D **31** (2022) no.01, 2150129 doi:10.1142/S0218271821501297 [arXiv:2011.09842 [gr-qc]].

[638] G. Mandal, S. Chakraborty, S. Mishra and S. K. Biswas, "A study of interacting scalar field model from the perspective of the dynamical systems theory," Phys. Dark Univ. **40** (2023), 101210 doi:10.1016/j.dark.2023.101210 [arXiv:2101.04496 [gr-qc]].

[639] S. Chakraborty, S. Mishra and S. Chakraborty, "Dynamical system analysis of self-interacting three-form field cosmological model: stability and bifurcation," Eur. Phys. J. C **81** (2021) no.5, 439 doi:10.1140/epjc/s10052-021-09221-6

[640] A. G. Riess *et al.* [Supernova Search Team], "Observational evidence from supernovae for an accelerating universe and a cosmological constant," Astron. J. **116** (1998), 1009-1038 doi:10.1086/300499 [arXiv:astro-ph/9805201 [astro-ph]].

[641] C. Deffayet, G. R. Dvali and G. Gabadadze, "Accelerated universe from gravity leaking to extra dimensions," Phys. Rev. D **65** (2002), 044023 doi:10.1103/PhysRevD.65.044023 [arXiv:astro-ph/0105068 [astro-ph]].

[642] G. Leon and E. N. Saridakis, "Phantom dark energy with varying-mass dark matter particles: acceleration and cosmic coincidence problem," Phys. Lett. B **693** (2010), 1-10

doi:10.1016/j.physletb.2010.08.016 [arXiv:0904.1577 [gr-qc]].

[643] M. Doran and C. Wetterich, "Quintessence and the cosmological constant," Nucl. Phys. B Proc. Suppl. **124** (2003), 57-62 doi:10.1016/S0920-5632(03)02077-2 [arXiv:astro-ph/0205267 [astro-ph]].

[644] R. R. Caldwell, R. Dave and P. J. Steinhardt, "Cosmological imprint of an energy component with general equation of state," Phys. Rev. Lett. **80** (1998), 1582-1585 doi:10.1103/PhysRevLett.80.1582 [arXiv:astro-ph/9708069 [astro-ph]].

[645] A. R. Liddle and R. J. Scherrer, "A Classification of scalar field potentials with cosmological scaling solutions," Phys. Rev. D **59** (1999), 023509 doi:10.1103/PhysRevD.59.023509 [arXiv:astro-ph/9809272 [astro-ph]].

[646] R. R. Caldwell, M. Kamionkowski and N. N. Weinberg, "Phantom energy and cosmic doomsday," Phys. Rev. Lett. **91** (2003), 071301 doi:10.1103/PhysRevLett.91.071301 [arXiv:astro-ph/0302506 [astro-ph]].

[647] V. K. Onemli and R. P. Woodard, Phys. Rev. D **70** (2004), 107301 doi:10.1103/PhysRevD.70.107301 [arXiv:gr-qc/0406098 [gr-qc]].

[648] S. Nojiri, S. D. Odintsov and S. Tsujikawa, Phys. Rev. D **71** (2005), 063004 doi:10.1103/PhysRevD.71.063004 [arXiv:hep-th/0501025 [hep-th]].

[649] E. N. Saridakis, "Quintom evolution in power-law potentials," Nucl. Phys. B **830** (2010), 374-389 doi:10.1016/j.nuclphysb.2010.01.005 [arXiv:0903.3840 [astro-ph.CO]].

[650] M. R. Setare and E. N. Saridakis, "Braneworld models with a non-minimally coupled phantom bulk field: A Simple way to obtain the -1-crossing at late times," JCAP **03** (2009), 002 doi:10.1088/1475-7516/2009/03/002 [arXiv:0811.4253 [hep-th]].

[651] Shilnikov, LP and Shilnikov, Andrey, "Shilnikov Bifurcation," Schopedia (2007), https://www.researchgate.net/publication/220580167.

[652] Banerjee, Ankan and Ghosh, Manojit and Pal, Pinaki, "Transitions in overstable rotating magnetoconvection," Phys. Rev. E **102** (2020), doi:10.1103/PhysRevE.102.013107.

[653] S. Perlmutter *et al.* [Supernova Cosmology Project], "Measurements of Ω and Λ from 42 high redshift supernovae," Astrophys. J. **517** (1999), 565-586 doi:10.1086/307221 [arXiv:astro-ph/9812133 [astro-ph]].

[654] D. N. Spergel *et al.* [WMAP], "First year Wilkinson Microwave Anisotropy Probe (WMAP) observations: Determination of cosmological parameters," Astrophys. J. Suppl. **148** (2003), 175-194 doi:10.1086/377226 [arXiv:astro-ph/0302209 [astro-ph]].

[655] S. W. Allen, R. W. Schmidt, H. Ebeling, A. C. Fabian and L. van Speybroeck, "Constraints on dark energy from Chandra observations of the largest relaxed galaxy clusters," Mon. Not. Roy. Astron. Soc. **353** (2004), 457 doi:10.1111/j.1365-2966.2004.08080.x [arXiv:astro-ph/0405340 [astro-ph]].

[656] A. G. Riess *et al.* [Supernova Search Team], "Type Ia supernova discoveries at z > 1 from the Hubble Space Telescope: Evidence for past deceleration and constraints on dark energy evolution," Astrophys. J. **607** (2004), 665-687 doi:10.1086/383612 [arXiv:astro-ph/0402512 [astro-ph]].

[657] B. Feng, X. L. Wang and X. M. Zhang, "Dark energy constraints from the cosmic age and supernova," Phys. Lett. B **607** (2005), 35-41 doi:10.1016/j.physletb.2004.12.071 [arXiv:astro-ph/0404224 [astro-ph]].

[658] Z. K. Guo, Y. S. Piao, X. M. Zhang and Y. Z. Zhang, "Cosmological evolution of a quintom model of dark energy," Phys. Lett. B **608** (2005), 177-182 doi:10.1016/j.physletb.2005.01.017 [arXiv:astro-ph/0410654 [astro-ph]].

[659] B. Feng, M. Li, Y. S. Piao and X. Zhang, "Oscillating quintom and the recurrent universe," Phys. Lett. B **634** (2006), 101-105 doi:10.1016/j.physletb.2006.01.066 [arXiv:astro-ph/0407432 [astro-ph]].

[660] R. R. Caldwell, M. Kamionkowski and N. N. Weinberg, "Phantom energy and cosmic doomsday," Phys. Rev. Lett. **91** (2003), 071301 doi:10.1103/PhysRevLett.91.071301 [arXiv:astro-ph/0302506 [astro-ph]].

[661] Y. H. Wei, "Big rip in SO(1,1) phantom universe," [arXiv:gr-qc/0502077 [gr-qc]].

[662] A. Vikman, "Can dark energy evolve to the phantom?," Phys. Rev. D **71** (2005), 023515 doi:10.1103/PhysRevD.71.023515 [arXiv:astro-ph/0407107 [astro-ph]].

[663] S. Nojiri and S. D. Odintsov, "Inhomogeneous equation of state of the universe: Phantom era, future singularity and crossing the phantom barrier," Phys. Rev. D **72** (2005), 023003 doi:10.1103/PhysRevD.72.023003 [arXiv:hep-th/0505215 [hep-th]].

[664] E. N. Saridakis, "Phantom evolution in power-law potentials," Nucl. Phys. B **819** (2009), 116-126 doi:10.1016/j.nuclphysb.2009.04.011 [arXiv:0902.3978 [gr-qc]].

[665] M. R. Setare and E. N. Saridakis, "Braneworld models with a non-minimally coupled phantom bulk field: A Simple way to obtain the -1-crossing at late times," JCAP **03** (2009), 002 doi:10.1088/1475-7516/2009/03/002 [arXiv:0811.4253 [hep-th]].

[666] S. Weinberg, "The Cosmological Constant Problem," Rev. Mod. Phys. **61** (1989), 1-23 doi:10.1103/RevModPhys.61.1

[667] L. Amendola, M. Quartin, S. Tsujikawa and I. Waga, "Challenges for scaling cosmologies," Phys. Rev. D **74** (2006), 023525 doi:10.1103/PhysRevD.74.023525

[arXiv:astro-ph/0605488 [astro-ph]].

[668] X. m. Chen, Y. g. Gong and E. N. Saridakis, "Phase-space analysis of interacting phantom cosmology," JCAP **04** (2009), 001 doi:10.1088/1475-7516/2009/04/001 [arXiv:0812.1117 [gr-qc]].

[669] N. J. Nunes and D. F. Mota, "Structure formation in inhomogeneous dark energy models," Mon. Not. Roy. Astron. Soc. **368** (2006), 751-758 doi:10.1111/j.1365-2966.2006.10166.x [arXiv:astro-ph/0409481 [astro-ph]].

[670] T. Clifton and J. D. Barrow, "The Ups and downs of cyclic universes," Phys. Rev. D **75** (2007), 043515 doi:10.1103/PhysRevD.75.043515 [arXiv:gr-qc/0701070 [gr-qc]].

[671] C. Xu, E. N. Saridakis and G. Leon, "Phase-Space analysis of Teleparallel Dark Energy," JCAP **07** (2012), 005 doi:10.1088/1475-7516/2012/07/005 [arXiv:1202.3781 [gr-qc]].

[672] C. Xu, E. N. Saridakis and G. Leon, "Phase-Space analysis of Teleparallel Dark Energy," JCAP **07** (2012), 005 doi:10.1088/1475-7516/2012/07/005 [arXiv:1202.3781 [gr-qc]].

[673] H. S. Zhang and Z. H. Zhu, "Interacting chaplygin gas," Phys. Rev. D **73** (2006), 043518 doi:10.1103/PhysRevD.73.043518 [arXiv:astro-ph/0509895 [astro-ph]].

[674] C. R. Fadragas and G. Leon, "Some remarks about non-minimally coupled scalar field models," Class. Quant. Grav. **31** (2014) no.19, 195011 doi:10.1088/0264-9381/31/19/195011 [arXiv:1405.2465 [gr-qc]].

[675] T. Gonzalez and I. Quiros, "Exact models with non-minimal interaction between dark matter and (either phantom or quintessence) dark energy," Class. Quant. Grav. **25** (2008), 175019 doi:10.1088/0264-9381/25/17/175019 [arXiv:0707.2089 [gr-qc]].

[676] G. W. Anderson and S. M. Carroll, "Dark matter with time dependent mass," doi:10.1142/9789814447263_0025 [arXiv:astro-ph/9711288 [astro-ph]].

[677] T. Damour, G. W. Gibbons and C. Gundlach, "Dark Matter, Time Varying G, and a Dilaton Field," Phys. Rev. Lett. **64** (1990), 123-126 doi:10.1103/PhysRevLett.64.123

[678] G. R. Farrar and P. J. E. Peebles, "Interacting dark matter and dark energy," Astrophys. J. **604** (2004), 1-11 doi:10.1086/381728 [arXiv:astro-ph/0307316 [astro-ph]].

[679] M. B. Hoffman, "Cosmological constraints on a dark matter - dark energy interaction," [arXiv:astro-ph/0307350 [astro-ph]].

[680] X. Zhang, "Coupled quintessence in a power-law case and the cosmic coincidence problem," Mod. Phys. Lett. A **20** (2005), 2575 doi:10.1142/S0217732305017597 [arXiv:astro-ph/0503072 [astro-ph]].

[681] M. S. Berger and H. Shojaei, "Interacting dark energy and the cosmic coincidence problem," Phys. Rev. D **73** (2006), 083528 doi:10.1103/PhysRevD.73.083528 [arXiv:gr-qc/0601086 [gr-qc]].

[682] L. Amendola and D. Tocchini-Valentini, "Baryon bias and structure formation in an accelerating universe," Phys. Rev. D **66** (2002), 043528 doi:10.1103/PhysRevD.66.043528 [arXiv:astro-ph/0111535 [astro-ph]].

[683] M. Pietroni, "Brane worlds and the cosmic coincidence problem," Phys. Rev. D **67** (2003), 103523 doi:10.1103/PhysRevD.67.103523 [arXiv:hep-ph/0203085 [hep-ph]].

[684] L. Amendola, G. Camargo Campos and R. Rosenfeld, "Consequences of dark matter-dark energy interaction on cosmological parameters derived from SNIa data," Phys. Rev. D **75** (2007), 083506 doi:10.1103/PhysRevD.75.083506 [arXiv:astro-ph/0610806 [astro-ph]].

[685] L. Amendola, "Coupled quintessence," Phys. Rev. D **62** (2000), 043511 doi:10.1103/PhysRevD.62.043511 [arXiv:astro-ph/9908023 [astro-ph]].

[686] D. Comelli, M. Pietroni and A. Riotto, "Dark energy and dark matter," Phys. Lett. B **571** (2003), 115-120 doi:10.1016/j.physletb.2003.05.006 [arXiv:hep-ph/0302080 [hep-ph]].

[687] U. Franca and R. Rosenfeld, "Age constraints and fine tuning in VAMP models," Phys. Rev. D **69** (2004), 063517 doi:10.1103/PhysRevD.69.063517 [arXiv:astro-ph/0308149 [astro-ph]].

[688] T. Gonzalez and I. Quiros, "Exact models with non-minimal interaction between dark matter and (either phantom or quintessence) dark energy," Class. Quant. Grav. **25** (2008), 175019 doi:10.1088/0264-9381/25/17/175019 [arXiv:0707.2089 [gr-qc]].

[689] M. Jamil and E. N. Saridakis, "New agegraphic dark energy in Horava-Lifshitz cosmology," JCAP **07** (2010), 028 doi:10.1088/1475-7516/2010/07/028 [arXiv:1003.5637 [physics.gen-ph]].

[690] M. R. Setare and M. Jamil, "Holographic dark energy with varying gravitational constant in Horava-Lifshitz cosmology," JCAP **02** (2010), 010 [erratum: JCAP **08** (2010), E01] doi:10.1088/1475-7516/2010/02/010 [arXiv:1001.1251 [hep-th]].

[691] A. P. Billyard, "The Asymptotic behavior of cosmological models containing matter and scalar fields," [arXiv:gr-qc/9908067 [gr-qc]].

[692] A. A. Coley, "Dynamical systems in cosmology," [arXiv:gr-qc/9910074 [gr-qc]].

[693] A. Ali, S. Dutta, E. N. Saridakis and A. A. Sen, "Horava-Lifshitz cosmology with generalized Chaplygin gas," Gen. Rel. Grav. **44** (2012), 657-683 doi:10.1007/s10714-011-

1298-z [arXiv:1004.2474 [astro-ph.CO]].

[694] S. Dutta and E. N. Saridakis, "Observational constraints on Horava-Lifshitz cosmology," JCAP **01** (2010), 013 doi:10.1088/1475-7516/2010/01/013 [arXiv:0911.1435 [hep-th]].

[695] G. Panotopoulos, "Cosmological evolution in brane-worlds with large transverse dimensions: Inflation and dark matter," [arXiv:hep-ph/0604152 [hep-ph]].

[696] E. N. Saridakis, "Aspects of Horava-Lifshitz cosmology," Int. J. Mod. Phys. D **20** (2011), 1485-1504 doi:10.1142/S0218271811019670 [arXiv:1101.0300 [astro-ph.CO]].

[697] M. Trodden and S. M. Carroll, "TASI lectures: Introduction to cosmology," [arXiv:astro-ph/0401547 [astro-ph]].

[698] G. Leon and C. R. Fadragas, "Cosmological dynamical systems," LAP Lambert Academic Publishing, 2012, ISBN 978-3-8473-0233-9 [arXiv:1412.5701 [gr-qc]].

[699] S. Mishra and S. Chakraborty, "Dynamical system analysis of Einstein–Skyrme model in a Kantowski–Sachs spacetime," Annals Phys. **406** (2019), 207-219 doi:10.1016/j.aop.2019.04.006 [arXiv:1812.01975 [physics.gen-ph]].

[700] H. Matsui, F. Takahashi and T. Terada, "Non-singular bouncing cosmology with positive spatial curvature and flat scalar potential," Phys. Lett. B **795** (2019), 152-159 doi:10.1016/j.physletb.2019.06.013 [arXiv:1904.12312 [gr-qc]].

[701] E. N. Saridakis, "Theoretical Limits on the Equation-of-State Parameter of Phantom Cosmology," Phys. Lett. B **676** (2009), 7-11 doi:10.1016/j.physletb.2009.04.065 [arXiv:0811.1333 [hep-th]].

[702] P. Bari and K. Bhattacharya, "Evolution of scalar and vector cosmological perturbations through a bounce in metric $f(R)$ gravity in flat FLRW spacetime," JCAP **11** (2019), 019 doi:10.1088/1475-7516/2019/11/019 [arXiv:1907.11607 [gr-qc]].

[703] S. Chakraborty, S. Mishra and S. Chakraborty, "A dynamical system analysis of cosmic evolution with coupled phantom dark energy with dark matter," Int. J. Mod. Phys. D **31** (2022) no.01, 2150129 doi:10.1142/S0218271821501297 [arXiv:2011.09842 [gr-qc]].

[704] G. Mandal, S. Chakraborty, S. Mishra and S. K. Biswas, "A study of interacting scalar field model from the perspective of the dynamical systems theory," Phys. Dark Univ. **40** (2023), 101210 doi:10.1016/j.dark.2023.101210 [arXiv:2101.04496 [gr-qc]].

[705] A. Savaş Arapoğlu and A. Emrah Yükselci, "Dynamical System Analysis of Quintessence Models with Exponential Potential - Revisited," Mod. Phys. Lett. A **34** (2019) no.09, 1950069 doi:10.1142/S021773231950069X [arXiv:1711.03824 [gr-qc]].

[706] N. Roy and N. Banerjee, "Quintessence Scalar Field: A Dynamical Systems Study," Eur. Phys. J. Plus **129** (2014), 162 doi:10.1140/epjp/i2014-14162-7 [arXiv:1402.6821

[gr-qc]].

[707] S. S. Singh and C. Sonia, "Dynamical system perspective of cosmological models minimally coupled with scalar field," Adv. High Energy Phys. **2020** (2020), 1805350 doi:10.1155/2020/1805350 [arXiv:1906.11947 [gr-qc]].

[708] S. Mishra, "Dynamics around nonhyperbolic equilibrium and bifurcation analysis of various cosmological models."

[709] S. Chakraborty, S. Mishra and S. Chakraborty, "A dynamical system analysis of cosmic evolution with coupled phantom dark energy with dark matter," Int. J. Mod. Phys. D **31** (2022) no.01, 2150129 doi:10.1142/S0218271821501297 [arXiv:2011.09842 [gr-qc]].

[710] B. Ratra and P. J. E. Peebles, "Cosmological Consequences of a Rolling Homogeneous Scalar Field," Phys. Rev. D **37** (1988), 3406 doi:10.1103/PhysRevD.37.3406

[711] S. Dodelson, M. Kaplinghat and E. Stewart, "Solving the Coincidence Problem : Tracking Oscillating Energy," Phys. Rev. Lett. **85** (2000), 5276-5279 doi:10.1103/PhysRevLett.85.5276 [arXiv:astro-ph/0002360 [astro-ph]].

[712] L. A. Urena-Lopez and T. Matos, "A New cosmological tracker solution for quintessence," Phys. Rev. D **62** (2000), 081302 doi:10.1103/PhysRevD.62.081302 [arXiv:astro-ph/0003364 [astro-ph]].

[713] P. Brax and J. Martin, "Quintessence and supergravity," Phys. Lett. B **468** (1999), 40-45 doi:10.1016/S0370-2693(99)01209-5 [arXiv:astro-ph/9905040 [astro-ph]].

[714] P. J. Steinhardt, L. M. Wang and I. Zlatev, "Cosmological tracking solutions," Phys. Rev. D **59** (1999), 123504 doi:10.1103/PhysRevD.59.123504 [arXiv:astro-ph/9812313 [astro-ph]].

[715] J. A. Frieman, C. T. Hill, A. Stebbins and I. Waga, "Cosmology with ultralight pseudo Nambu-Goldstone bosons," Phys. Rev. Lett. **75** (1995), 2077-2080 doi:10.1103/PhysRevLett.75.2077 [arXiv:astro-ph/9505060 [astro-ph]].

[716] A. Moss, D. Scott and J. P. Zibin, "No evidence for anomalously low variance circles on the sky," JCAP **04** (2011), 033 doi:10.1088/1475-7516/2011/04/033 [arXiv:1012.1305 [astro-ph.CO]].

[717] D. L. Jow and D. Scott, "Re-evaluating evidence for Hawking points in the CMB," JCAP **03** (2020), 021 doi:10.1088/1475-7516/2020/03/021 [arXiv:1909.09672 [astro-ph.CO]].

[718] N. Aghanim *et al.* [Planck], "Planck 2018 results. VI. Cosmological parameters," Astron. Astrophys. **641** (2020), A6 [erratum: Astron. Astrophys. **652** (2021), C4]

doi:10.1051/0004-6361/201833910 [arXiv:1807.06209 [astro-ph.CO]].

[719] Kardashev, Nicolai S, "Optimistic cosmological model," Astron. Astrophys. **243** (1990).

[720] M. P. Dabrowski, "Oscillating Friedman cosmology," Annals Phys. **248** (1996), 199-219 doi:10.1006/aphy.1996.0057 [arXiv:gr-qc/9503017 [gr-qc]].

[721] P. W. Graham, B. Horn, S. Kachru, S. Rajendran and G. Torroba, "A Simple Harmonic Universe," JHEP **02** (2014), 029 doi:10.1007/JHEP02(2014)029 [arXiv:1109.0282 [hep-th]].

[722] P. W. Graham, B. Horn, S. Rajendran and G. Torroba, "Exploring eternal stability with the simple harmonic universe," JHEP **08** (2014), 163 doi:10.1007/JHEP08(2014)163 [arXiv:1405.0282 [hep-th]].

[723] M. P. Dabrowski, "Oscillating Friedman cosmology," Annals Phys. **248** (1996), 199-219 doi:10.1006/aphy.1996.0057 [arXiv:gr-qc/9503017 [gr-qc]].

[724] P. W. Graham, B. Horn, S. Rajendran and G. Torroba, "Exploring eternal stability with the simple harmonic universe," JHEP **08** (2014), 163 doi:10.1007/JHEP08(2014)163 [arXiv:1405.0282 [hep-th]].

[725] M. Bouhmadi-López, J. Marto, J. Morais and C. M. Silva, "Cosmic infinity: A dynamical system approach," JCAP **03** (2017), 042 doi:10.1088/1475-7516/2017/03/042 [arXiv:1611.03100 [gr-qc]].

[726] Harry Gingold, "Approximation of unbounded functions via compactification," Journal of Approximation Theory **131** (2004), doi:https://doi.org/10.1016/j.jat.2004.08.001 .

[727] G. Leon and F. O. F. Silva, "Generalized scalar field cosmologies: a global dynamical systems formulation," Class. Quant. Grav. **38** (2021) no.1, 015004 doi:10.1088/1361-6382/abc095 [arXiv:2007.11990 [gr-qc]].

[728] Uri Elias and Harry Gingold, "Critical points at infinity and blow up of solutions of autonomous polynomial differential systems via compactification," Journal of Mathematical Analysis and Applications **318** (2006) no.1, 015004 doi:https://doi.org/10.1016/j.jmaa.2005.06.002.

[729] Lawrence Perko, "Differential equations and Dynamical systems," Springer-Verlag, New York. Inc., Third edition.

[730] U. Alam, V. Sahni and A. A. Starobinsky, "The Case for dynamical dark energy revisited," JCAP **06** (2004), 008 doi:10.1088/1475-7516/2004/06/008 [arXiv:astro-ph/0403687 [astro-ph]].

[731] A. A. Starobinsky, "Future and origin of our universe: Modern view," Grav. Cosmol. **6** (2000), 157-163 [arXiv:astro-ph/9912054 [astro-ph]].

[732] P. P. Dechant, A. N. Lasenby and M. P. Hobson, "An Anisotropic, non-singular early universe model leading to a realistic cosmology," Phys. Rev. D **79** (2009), 043524 doi:10.1103/PhysRevD.79.043524 [arXiv:0809.4335 [gr-qc]].

[733] A. S. Agrawal, S. Mishra, S. K. Tripathy and B. Mishra, "Bouncing cosmological models in a functional form of F(R) gravity," [arXiv:2210.09726 [gr-qc]].

[734] A. S. Agrawal, F. Tello-Ortiz, B. Mishra and S. K. Tripathy, "Bouncing Cosmology in Extended Gravity and Its Reconstruction as Dark Energy Model," Fortsch. Phys. **70** (2022) no.1, 2100065 doi:10.1002/prop.202100065 [arXiv:2111.02894 [gr-qc]].

[735] J. K. Singh, K. Bamba, R. Nagpal and S. K. J. Pacif, "Bouncing cosmology in $f(R,T)$ gravity," Phys. Rev. D **97** (2018) no.12, 123536 doi:10.1103/PhysRevD.97.123536 [arXiv:1807.01157 [gr-qc]].

[736] A. Ijjas and P. J. Steinhardt, "Bouncing Cosmology made simple," Class. Quant. Grav. **35** (2018) no.13, 135004 doi:10.1088/1361-6382/aac482 [arXiv:1803.01961 [astro-ph.CO]].

[737] R. Brandenberger and P. Peter, Found. Phys. **47** (2017) no.6, 797-850 doi:10.1007/s10701-016-0057-0 [arXiv:1603.05834 [hep-th]].

[738] D. Battefeld and P. Peter, "A Critical Review of Classical Bouncing Cosmologies," Phys. Rept. **571** (2015), 1-66 doi:10.1016/j.physrep.2014.12.004 [arXiv:1406.2790 [astro-ph.CO]].

[739] S. Bahamonde, C. G. Böhmer, S. Carloni, E. J. Copeland, W. Fang and N. Tamanini, "Dynamical systems applied to cosmology: dark energy and modified gravity," Phys. Rept. **775-777**, 1-122 (2018) doi:10.1016/j.physrep.2018.09.001 [arXiv:1712.03107 [gr-qc]].

[740] Starobinskii, A. A., "On a nonsingular isotropic cosmological model," Soviet Astronomy Letters **4** (1978), 82-84.

[741] G. León Torres, "Qualitative analysis and characterization of two cosmologies including scalar fields," [arXiv:1412.5665 [gr-qc]].

[742] B. Ratra and P. J. E. Peebles, "Cosmological Consequences of a Rolling Homogeneous Scalar Field," Phys. Rev. D **37** (1988), 3406 doi:10.1103/PhysRevD.37.3406.

[743] S. Mishra and S. Chakraborty, Eur. Phys. J. C **79** (2019) no.4, 328 doi:10.1140/epjc/s10052-019-6839-8.

[744] T. Patil, S. Panda, M. Sharma and Ruchika, "Dynamics of interacting scalar field model in the realm of chiral cosmology," Eur. Phys. J. C **83** (2023) no.2, 131

doi:10.1140/epjc/s10052-023-11259-7 [arXiv:2205.14946 [gr-qc]].

[745] F. Okamatsu, T. Sekiguchi and T. Takahashi, "H_0 tension without CMB data: Beyond the ΛCDM," Phys. Rev. D **104** (2021) no.2, 023523 doi:10.1103/PhysRevD.104.023523 [arXiv:2105.12312 [astro-ph.CO]].

[746] A. Del Popolo and M. Le Delliou, "Small scale problems of the ΛCDM model: a short review," Galaxies **5** (2017) no.1, 17 doi:10.3390/galaxies5010017 [arXiv:1606.07790 [astro-ph.CO]].

[747] H. A. P. Macedo, L. S. Brito, J. F. Jesus and M. E. S. Alves, "Cosmological constraints on $\Lambda(t)$CDM models," Eur. Phys. J. C **83** (2023) no.12, 1144 doi:10.1140/epjc/s10052-023-12321-0 [arXiv:2305.18591 [astro-ph.CO]].

[748] V. Sahni, "Dark matter and dark energy," Lect. Notes Phys. **653** (2004), 141-180 doi:10.1007/b99562 [arXiv:astro-ph/0403324 [astro-ph]].

[749] S. Bahamonde, C. G. Böhmer, S. Carloni, E. J. Copeland, W. Fang and N. Tamanini, "Dynamical systems applied to cosmology: dark energy and modified gravity," Phys. Rept. **775-777**, 1-122 (2018) doi:10.1016/j.physrep.2018.09.001 [arXiv:1712.03107 [gr-qc]].

[750] A. A. Coley, "Dynamical systems in cosmology," [arXiv:gr-qc/9910074 [gr-qc]].

[751] A. Sangwan, A. Tripathi and H. K. Jassal, "Observational constraints on quintessence models of dark energy," [arXiv:1804.09350 [astro-ph.CO]].

[752] J. C. H. Liu, "A quintessence dynamical dark energy model from ratio gravity," Eur. Phys. J. C **82**, no.2, 165 (2022) doi:10.1140/epjc/s10052-022-10134-1 [arXiv:2202.12241 [gr-qc]].

[753] A. Bouali, H. Chaudhary, A. Mehrotra and S. K. J. Pacif, "Model-Independent Study for a Quintessence Model of Dark Energy: Analysis and Observational Constraints," Fortsch. Phys. **71**, no.12, 2300086 (2023) doi:10.1002/prop.202300086 [arXiv:2304.02652 [gr-qc]].

[754] A. Savaş Arapoğlu and A. Emrah Yükselci, "Dynamical System Analysis of Quintessence Models with Exponential Potential - Revisited," Mod. Phys. Lett. A **34**, no.09, 1950069 (2019) doi:10.1142/S021773231950069X [arXiv:1711.03824 [gr-qc]].

[755] G. K. Goswami, A. Pradhan and A. Beesham, "A Dark Energy Quintessence Model of the Universe," Mod. Phys. Lett. A **35**, no.04, 2050002 (2019) doi:10.1142/S0217732320500029 [arXiv:1905.10801 [gr-qc]].

[756] V. K. Oikonomou, "Autonomous dynamical system approach for inflationary Gauss–Bonnet modified gravity," Int. J. Mod. Phys. D **27**, no.05, 1850059 (2018)

doi:10.1142/S0218271818500591 [arXiv:1711.03389 [gr-qc]].

[757] S. D. Odintsov and V. K. Oikonomou, "Autonomous dynamical system approach for $f(R)$ gravity," Phys. Rev. D **96**, no.10, 104049 (2017) doi:10.1103/PhysRevD.96.104049 [arXiv:1711.02230 [gr-qc]].

[758] S. Chakraborty, S. Mishra and S. Chakraborty, "A dynamical system analysis of cosmic evolution with coupled phantom dark energy with dark matter," Int. J. Mod. Phys. D **31**, no.01, 2150129 (2022) doi:10.1142/S0218271821501297 [arXiv:2011.09842 [gr-qc]].

[759] A. Jawad and A. M. Sultan, "Analyzing stability of five-dimensional Einstein Chern–Simons gravity through dynamical systems," Phys. Dark Univ. **38**, 101127 (2022) doi:10.1016/j.dark.2022.101127

[760] S. Capozziello, R. D'Agostino and O. Luongo, "The phase-space view of non-local gravity cosmology," Phys. Lett. B **834**, 137475 (2022) doi:10.1016/j.physletb.2022.137475 [arXiv:2207.01276 [gr-qc]].

[761] G. Acquaviva and N. Katirci, "Dynamical analysis of logarithmic energy–momentum squared gravity," Phys. Dark Univ. **38**, 101128 (2022) doi:10.1016/j.dark.2022.101128 [arXiv:2203.01234 [gr-qc]].

[762] A. Alho, W. C. Lim and C. Uggla, "Cosmological global dynamical systems analysis," Class. Quant. Grav. **39**, no.14, 145010 (2022) doi:10.1088/1361-6382/ac7769 [arXiv:2201.07596 [gr-qc]].

[763] F. Humieja and M. Szydłowski, "Bifurcations in Ratra–Peebles quintessence models and their extensions," Eur. Phys. J. C **79**, no.9, 794 (2019) doi:10.1140/epjc/s10052-019-7299-x [arXiv:1901.06578 [gr-qc]].

[764] C. J. Feng, X. Z. Li and L. Y. Liu, "Bifurcation and global dynamical behavior of the f(T) theory," Mod. Phys. Lett. A **29**, no.07, 1450033 (2014) doi:10.1142/S0217732314500333 [arXiv:1403.4328 [astro-ph.CO]].

[765] N. Roy and N. Banerjee, "Quintessence Scalar Field: A Dynamical Systems Study," Eur. Phys. J. Plus **129**, 162 (2014) doi:10.1140/epjp/i2014-14162-7 [arXiv:1402.6821 [gr-qc]].

[766] M. Biswas and N. Bairagi, "On the dynamic consistency of a two-species competitive discrete system with toxicity: Local and global analysis," Journal of Computational and Applied Mathematics **363**, 145-155 (2020).

[767] P. Saha and N. Bairagi, "On the Dynamics of a Discrete Predator?Prey Model," Springer International Publishing, 219-232 (2018).